European Journal of Technical and Natural Sciences

2025, No 6

PREMIER Publishing

Vienna
2025

European Journal of Technical and Natural Sciences

Scientific journal

№ 6 2025

ISSN 2414-2352

Proofreading Kristin Theissen

Cover design Andreas Vogel

Additional design Stephan Friedman

Editorial office Premier Publishing s.r.o.

Praha 8 – Karlín, Lyčkovo nám. 508/7, PSČ 18600

E-mail: pub@ppublishing.org

Homepage: ppublishing.org

European Journal of Technical and Natural Sciences is an international, English language, peer-reviewed journal. The journal is published in electronic form.

The decisive criterion for accepting a manuscript for publication is scientific quality. All research articles published in this journal have undergone a rigorous peer review. Based on initial screening by the editors, each paper is anonymized and reviewed by at least two anonymous referees. Recommending the articles for publishing, the reviewers confirm that in their opinion the submitted article contains important or new scientific results.

Premier Publishing s.r.o. is not responsible for the stylistic content of the article. The responsibility for the stylistic content lies on an author of an article.

Instructions for authors

Full instructions for manuscript preparation and submission can be found through the Premier Publishing s.r.o. home page at: http://ppublishing.org.

Material disclaimer

The opinions expressed in the conference proceedings do not necessarily reflect those of the Premier Publishing s.r.o., the editor, the editorial board, or the organization to which the authors are affiliated.

Premier Publishing s.r.o. is not responsible for the stylistic content of the article. The responsibility for the stylistic content lies on an author of an article.

Included to the open access repositories:

Crossref eLIBRARY.RU Google Scholar

H – 15 and more than 500 citations in international periodicals and monographs.

INDEX COPERNICUS INTERNATIONAL The jurnal has Index Copernicus Value (ICV) 92.08 for 2022.

The European Journal of Technical and Natural Sciences 2025, No 6
ISSN 2414-2352

PREMIER Publishing
ppublishing.org

Section 1. Agricultural science

DOI:10.29013/EJHSS-25-6-3-8

COMPARATIVE ANALYSIS OF FLUMETRALIN APPLICATION FOR CHEMICAL TOPPING OF TOBACCO IN UZBEKISTAN

Khashimov Farkhod [1], Umurzakov Askarali [1], Rustamova Gulchehra [1] and Nurbekov Aziz [2]

[1] Samarkand State University, Institute of Agrobiotechnology and Food Security, Samarkand, Uzbekistan

[2] Tashkent State Agrarian University, Universitet str 2, Tashkent, Uzbekistan

Cite: *Khashimov F., Umurzakov A., Rustamova G. and Nurbekov A. (2025). Comparative Analysis of Flumetralin Application for Chemical Topping of Tobacco in Uzbekistan. European Journal of Technical and Natural Sciences 2025, No 6.* https://doi.org/10.29013/EJHSS-25-6-3-8

Abstract

This article presents data on the efficacy of flumetralin as a chemical pinching for Virginia type of tobacco. The plant growth regulator flumetralin (emulsifiable concentrate) proved to be an effective tool for tobacco pinching at an application rate of 1 kg/ha with a spray volume of 120 L/ha. The findings support the widespread implementation of this chemical pinching method in Virginia-type tobacco cultivation in the Urgut district of Uzbekistan.

Keywords: *Virginia, topping, stepping, dose, efficacy, leaf tiers, pinching*

Introduction

In large production fields, the generative organs of a tobacco plant (buds, flowers and seed pods) are “ballast” from an economic point of view. During their formation, they consume ready-made nutrients that are formed in the leaves, which is why the latter lose their density and do not develop well. As a result, there is a yield decrease, the chemical-technological indicators and the grade of raw materials worsen. This contributes to the accumulation of dry matter in the leaves and largely determines the level of yield of tobacco and its quality (Umurzakov 1991; Andersen et al., 1970; Akehurst 1991; Atkinson etc al., 1980; and World Tobacco situation, 1993). The tiered maturation of tobacco leaves is preserved when plants are grown under residual conditions, so the effect on leaf maturation essentially means a change in the very evolutionary nature of the tobacco plant.

The general and integral expression of age-related changes in the metabolism of all tobacco leaves is a constant increase in the content of plastic substances during youth

(synthesis predominates), their preservation at an approximately constant level during physiological maturity (synthesis and decay are balanced), a steady decrease in plastic substances during aging (decay prevails) of the organ (Andersen et al., 1970).

The main distribution of plastic substances between individual leaves in the tobacco metameric series occurs according to phyllotaxis. During the period of vegetative growth, the centers of abstraction of plastic substances from the formed leaves are the young growing leaves of plants and roots. With the transition of plants to the reproductive phase of development, these centers of attraction remain, however, other parts of plants begin to play the main role in the attraction of nutrients at this time: first, the central inflorescence, and then pinching develop (Akehurst 1991).

A characteristic feature of the age-related change in the hormonal status of the tobacco leaf is expressed in the fact that each stage of life corresponds to the highest level of a certain type of regulatory substances: in the initial period of growth, cytokinins have their maximum level, during the period of intensive growth – gibberellin-like substances, during physiological maturity – auxins, at aging stage – growth inhibitors and ethylene. The rest of the hormones in this period are of subordinate importance.

Along with its own hormonal system, the vital activity of the tobacco leaf is also determined by the general gradient of phytoharmones at the level of the whole organism.

Thus, to change the rate of maturation of tobacco leaves, it is necessary to modify the natural gradient of phytohormones. In particular, in order to bring the periods of maturation of metameric organs closer, it is necessary to delay the breakdown of auxins, cytokinins, and gibberellin-like substances in the lower leaves, and to shift the ratio of regulators in the upper leaves towards a faster accumulation of ethylene (Umurzakov 1991).

By suppressing or activating the functioning of certain centers of auxin production, as well as by changing the level of auxins and ethylene in the formed leaves, one can change the intensity of synthesis and the nature of the distribution of plastic substances in the plant.

The elucidated features of the influence of various centers of mobilization of substances on individual groups of leaves allowed us to conclude that the maturation of the leaves of the upper breaks can be significantly changed by eliminating the attractive effect of the inflorescence and pinching. It is possible to delay the aging of the lowest leaves (1 and 2 breaks), the outflow of substances from which is mainly due to the attracting effect of the leaves growing higher on the stem, possibly by removing the lower seedling leaves, i.e. plant cleaning.

In tobacco growing, it is known that topping (decapitation of a plant) actually somewhat delays the aging of the lower leaves and accelerates the ripening of the upper leaves of plants. In this case, the greatest effect is obtained if, together with the inflorescence, 4–5 upper leaves are removed, which, like the top of the shoot, have a strong attracting effect in relation to the leaves of the lower tiers (Atkinson etc al., 1980).

However, the removal of the apical part of the plants causes the rapid growth of pinching, which take on the function of rejecting nutrients. After manual pinching, they grow very quickly and, even in their infancy, are able to greatly influence the nature of the outflow of substances from the leaves. Therefore, it is necessary to prevent the development of pinching simultaneously with the removal of the top of the plants, that is, to restore apical dominance.

The studies of the above authors showed that most of the tested substances do not have a sufficiently effective inhibitory effect on the growth of inflorescences and stepsons, other substances, on the contrary, inhibiting the growth of stepsons, simultaneously have an inhibitory effect on the growth of tobacco plants, which ultimately leads to a decrease in the yield of raw materials. Substances, although they suppress the growth of pinching without an inhibitory effect on plants, they have to be applied manually, separately for each plant. Many of the substances tested are very expensive and therefore cannot be used on a large scale. In recent years, in tobacco-producing countries, a plant growth regulator, flumetralin, has been used for chemical pinching.

Recommendations for their use should be developed for a zoned tobacco variety, specific natural, soil-climatic and agrotechnical conditions for growing it, and contain methods proven in production for each process.

One of the obligatory agricultural practices for growing tobacco is the chemical pinching of plants. This contributes to the accumulation of dry matter in the leaves and largely determines the level of yield and quality of large-leaf Virginia type tobacco.

Recommendations for their use should be developed for a zoned tobacco variety, specific natural, soil-climatic and agrotechnical conditions for growing it, and contain methods proven in production for each process.

The intensity of growth and the mass of pinching per plant depend on the variety of tobacco and the specific conditions for its cultivation.

Material and methods of research

Flumetralin is a member of the 2,6-dinitroaniline class of chemicals. Flumetralin is a plant growth regulator that is used to control the growth of axillary buds (side shoots) on tobacco plants. Used to control side shoots on large-leaf Virginia tobacco varieties. Flumetralin is absorbed by the tobacco plant within a few hours after application and provides control of the growth of lateral shoots throughout the entire growth period (Guide to Pesticides, 1994).

Dinitroanilines selectively suppress plant and protozoan microtubes and do not act on fungal and vertebrate tubulins.

Type of preparation – emulsion concentrate. Methods of application – Flumetralin is applied as a hand spray (Handbook of Agrochemicals, 1987).

Frequency of application: Flumetralin is applied only once during the growing season. It is usually applied 3–7 days after cutting off the top of the flower part of the tobacco plant.

Application technology – manual application on special containers.

Flumetralin is applied as a manual spray with a working fluid flow rate of 1 kg of Flumetralin, 80, 120, 140 liters of water per hectare.

Processing was carried out in the morning at an air temperature not higher than 22–24 °C and a wind speed of not more than 1.2 m/s. As a control, a 0.5 ha plot was chosen where no treatments were carried out. Accounting for the number of pinching and the biological effectiveness of the drug was carried out according to the guidelines of ARITTP (Krasnodar) and the State Chemical Commission of the Republic of Uzbekistan.

Statistical analysis was done using Dospekhov 1986 method.

Results and their discussion

Of great practical interest is the use of pinching in combination with the treatment of plants with physiologically active substances. At the same time, immediately after mechanical topping, the plants are treated with inhibitory substances – flumetralin. The use of flumetralin significantly reduces the formation and growth of pinching.

As can be seen from Table 1, after the removal of inflorescences, intensive growth of lateral shoots is observed on plants, which must be removed.

Spraying with the physiologically active substance flumetralin after mechanical topping causes depression of growth processes. At the same time, lateral shoots grow slowly, acquire an ugly shape with lanceolate leaves, the weight of stepsons is 3–5 times, and the number and length of stepsons are 3 times less than on plants without stepsons.

Weakening, but not complete cessation of the formation and development of lateral shoots on the plant during their chemical pinching with Flumetralin, in our opinion, makes it possible to exclude their mechanical removal (Table 1). At the same time, the process of manual pinching is reduced, which contributes to a noticeable reduction in labor costs.

In solving this problem, in our opinion, it is important to have varieties of tobacco that are not capable of forming lateral shoots before the topping of plants and apply agricultural techniques for cultivating them, which ensures uniform growth and development of plants on plantations. The latter will make it possible to carry out the treatment of flumetralin clotted plants at an earlier stage of plant development without a noticeable decrease in the weight of the tobacco yield.

In addition to the variety and depth of topping of plants (the number of upper leaves harvested along with the inflorescence), the formation and growth of pinching is also influenced by the weather conditions of the year of tobacco growth.

Table 1. *Effect of flumetralin on the growth and development*

Treatments	Indicators of the development of pinching			
	number of pinching from 1 plant, unit.	average length of pinching, cm	Weight of 25 pinching, g.	
			raw	dry
Trimming by hand:				
Control	6	14.3	403.1	62.2
Treatment with 1 kg of flumetralin in 80 l/ha	2	4.2	83.4	10.5
Treatment with 1 kg of flumetralin in 120 l/ha	2	3.0	76.2	9.0
Treatment with 1 kg of flumetralin in 140 l/ha	2	2.2	67.2	8.1

Observations have shown that stepping plants with flumetralin increase the wet weight of the roots and stem of one plant by the end of the growing season, but to a different extent. In comparison with the control, as expected, the largest increase in their weight is observed during chemical pinching after manual topping. The combined use of manual topping with chemical pinching of plants with flumetralin somewhat increases the numerical values of these indicators. The thickness of the stem at the base, in the middle and at the top of the plants also changes approximately.

Chemical pinching of tobacco with flumetralin significantly accelerates the growth of the leaf blade and increases its area by the time the tobacco is harvested (Table 2). This is observed to the greatest extent in young leaves of the upper tiers and to the least extent in older, almost formed leaves of the middle tiers. This somewhat brings together the size of the leaves remaining on the plant after pinching.

Table 2. *Influence of plant pinching with flumetralin on the growth and development*

Options	Growth and Development Indicators		
	plant height, cm	number of harvested leaves from 1 plant, pcs	average leaf area, cm^2
Control	127.4	22	285.2
Treatment with 1 kg of flumetralin in 80 l/ha	122.3	19	325.0
Treatment with 1 kg of flumetralin in 120 l/ha	120.2	20	331.2
Treatment with 1 kg of flumetralin in 140 l/ha	118.4	20	327.6

After chemical pinching with flumetralin, growth processes are noticeably accelerated, and during the harvesting period, the leaves of the upper breaks have a significantly larger area of the leaf blade. All the patterns of changes in the area of the leaf blade, noted above, depending on the technology of pinching tobacco, were widely confirmed in the results of changes in the length and width of tobacco leaves at the time of their harvesting.

After treatment of plants with an aqueous solution of flumetralin, observations showed that after about 24 hours, bends of petioles, leaves and stems appear. After 2–3 weeks they disappear, but not completely. The leaves remain slightly lowered downwards.

Topping and pinching tobacco plants is an important agricultural practice in shaping the yield and quality of raw materials.

Based on this, we can conclude that in order to obtain high yields of large-leaf Virginia tobacco in the conditions of Uzbekistan, it is necessary to include in the technology of growing tobacco the chemical pinching of plants using flumetralin at a dose of 1 kg, the flow rate of the working fluid is 120 l/ha, as an important agricultural technique that suppresses growth stepsons of tobacco (Figure 1).

Conclusion

The proven technology of chemical pinching of tobacco plants using flumetralin (1 kg of substance per 120 liters of water), as it was seen from the data presented by us, allowed the production specialist to actively intervene in the growth and development of its harvested period and purposefully form yield at a certain level. Significantly greater economic efficiency is provided by the chemical pinching of tobacco plants.

The widespread introduction of these processes in tobacco growing in the Urgut region when growing tobacco of the Virginia type undoubtedly gives a significant economic effect.

Plant growth regulator Flumetralin e.c. turned out to be an effective tool in the fight against pinching of tobacco, at a rate of 1 kg/ha, while the rate of consumption of the working fluid is 120 l / ha. The preparative form is satisfactory, phytotoxicity was not detected.

Figure 1. *Influence of stabbing methods using flumetralin on the yield*

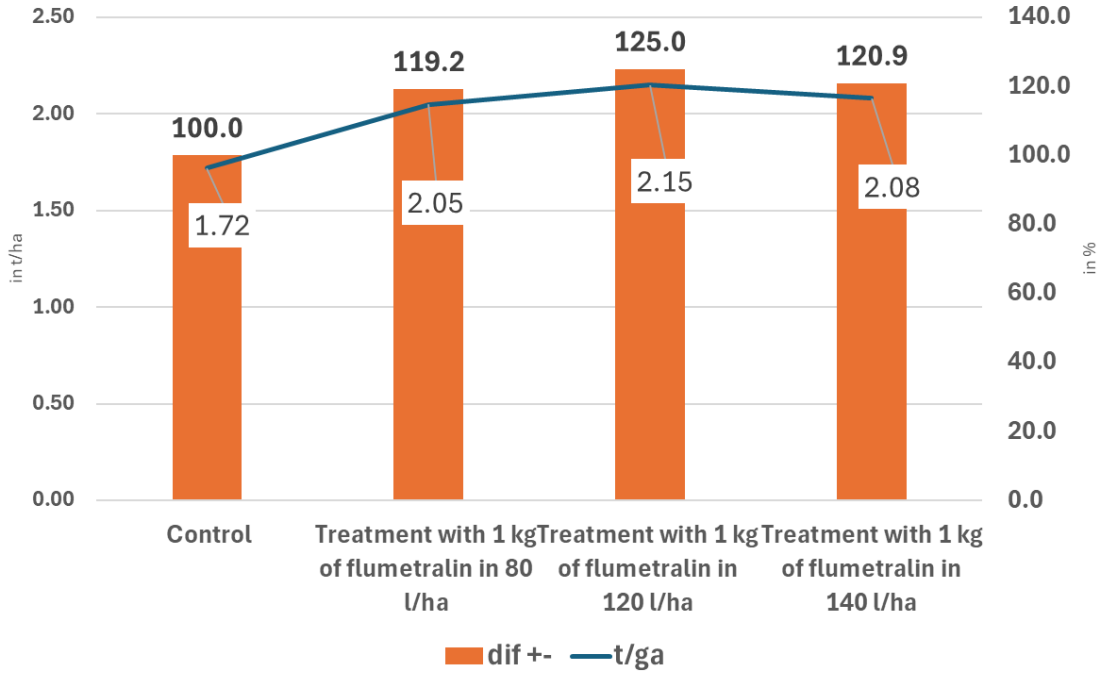

References

Handbook of Agrochemicals, 2nd Edition, Royal Society of Chemistry, Nottingham, United Kingdom 1987. URL: http//www.arsusda.gov/acsl/services/ppdb

Guide to Pesticides, 10th Edition, British Plant Protection Council, and Royal Society of Chemistry, 1994. URL: http//www.arsusda.gov/acsl/services/ppdb

Dospekhov B. A. Methods of field experience. – M.: Kolos, 1986. – 336 p.

Umurzakov E. U. Directional regulation of the content of chlorophyll and carbohydrates on tobacco leaves. // Uzbek biological journal, 1991. – No. 2. – P. 31–33.

Andersen R. A., Chaplin J. F., Currin R. E., Ford L. T. Plant phenols in flue- cured tobaccos fertilized at different rates // Agron. J. 1970. – 62. – P. 415–417.

Akehurst B. C. Tobacco. Longman, London and New York, 1991. – 764 p.

Atkinson W. O., Link L. A. effects of ethephon on ripening and certain quality components of Burley tobacco // Tob.Int. 1980. – V. 182. – No. 12. – P. 88–89.

World Tobacco situation. United States Department of Agriculture. – September. 1993–31 p.

submitted 02.11.2025;
accepted for publication 16.11.2025;
published 30.12.2025

Contact: nurbekov2002@yahoo.com

The European Journal of Technical and Natural Sciences 2025, No 6
ISSN 2414-2352

PREMIER Publishing
ppublishing.org

DOI:10.29013/EJHSS-25-6-9-14

AGRONOMIC PERFORMANCE AND YIELD STABILITY OF WHEAT ACCESSIONS UNDER RAINFED CONDITIONS IN UZBEKISTAN

Nurbekov Aziz [1], ***Nazarmatov Abdumajid*** [2], ***Jurayev Mamatkul*** [2], ***Amirov Otabek*** [2]

[1] Tashkent State Agrarian University

[2] Scientific Research Institute of Rainfed Agriculture

Cite: *Nurbekov A., Nazarmatov A., Jurayev M., Amirov O. (2025). Agronomic performance and yield stability of wheat accessions under rainfed conditions in Uzbekistan. European Journal of Technical and Natural Sciences 2025, No 6.* https://doi.org/10.29013/EJHSS-25-6-9-14

Abstract

A two-year field trial (2024–2025) was conducted to evaluate the agronomic performance of 11 wheat accessions, under rainfed conditions of Uzbekistan. Significant variation was observed in plant height, thousand kernel weight (TKW), days to heading and maturity and grain yield across years and accessions and varieties, reflecting differential responses to stress. Lalmikor-1 demonstrated superior stability in plant height (97 cm and 94 cm), kernel weight (40.2 g and 38.4 g), and yield (2.89 t/ha and 1.36 t/ha), outperforming the standard variety by 32–42%. These findings highlight the potential of this variety for wheat production programs targeting yield stability in drought affected years.

Keywords: *Wheat, Yield, TKW, Plant height, days to heading and maturity*

Introduction

Wheat (Triticum aestivum L.) is a staple crop in Uzbekistan, where climatic variability poses significant challenges to yield stability under rainfed conditions. Drought frequency has increased markedly compared to long-term climatological data, necessitating adaptive breeding strategies. Contemporary breeding programs increasingly prioritize traits that confer resilience under abiotic stress conditions, particularly drought and nutrient limitations. Semi-dwarf plant architecture and stable grain filling capacity are critical determinants of yield component formation in winter wheat production (Jobson et al., 2019; Ingvordsen et al., 2022). This study aims to identify wheat accessions showing higher yield productivity under rainfed conditions in Uzbekistan.

Materials and Methods

Experimental Site and Design

A competitive trial was conducted over two consecutive growing seasons (2024 and 2025) at the experimental farm of the Scientific Research Institute of Rainfed Agriculture, Gallayaral district, Jizzakh province, Uzbekistan. Eleven wheat accessions, including the standard variety Tezpishar,

were evaluated using a randomized complete block design (RCBD) with three replications.

Soil Characteristics

The experimental site was characterized by typical sierozem (gray desert soil) with inherently low organic matter content, containing approximately 0.8% humus. The low humus content (0.8%) observed at this site is characteristic of these soil types and significantly below the 2–3% threshold generally considered adequate for optimal crop productivity.

Climatic conditions during the Growing Season

Meteorological data for the 2023–2024 growing season are presented in Figures 1 and 2, illustrating temporal patterns of key environmental variables including precipitation rate and temperature and precipitation.

Figure 1. *Precipitation rate in 2024–2025 growing season, mm*

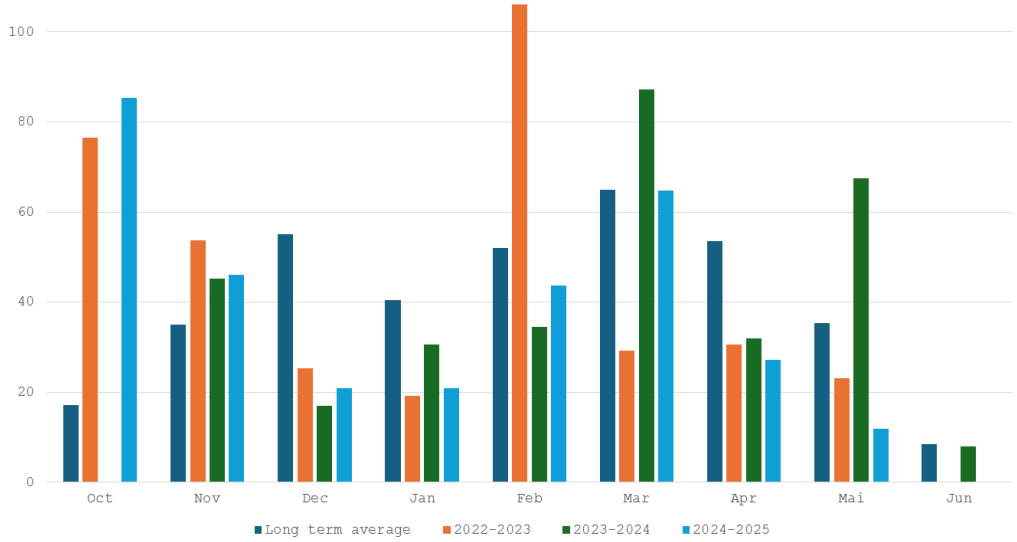

Figure 2. *Air temperature in 2024–2025 growing season, mm*

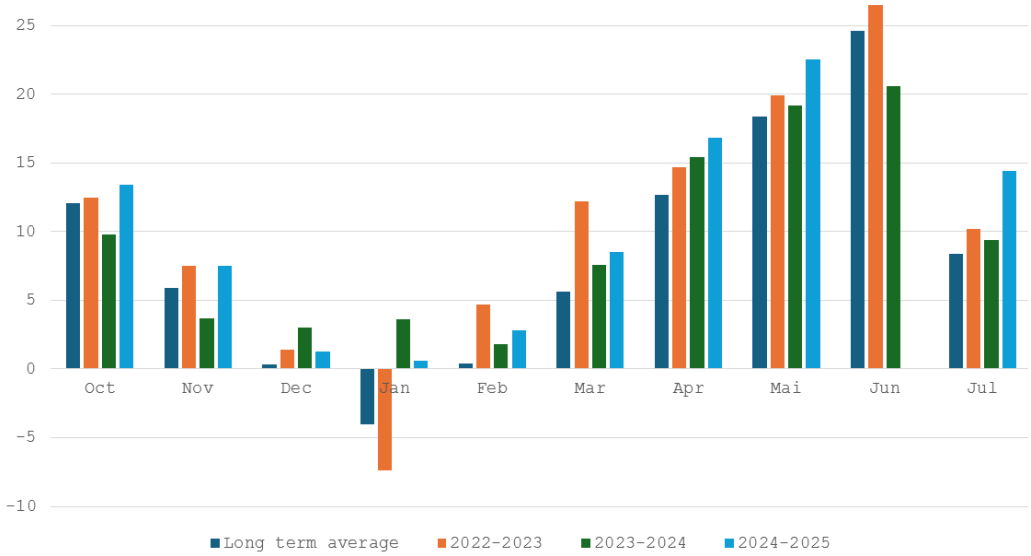

The climatic conditions during the experimental period showed great variability in temperature and precipitation in 2023–2024 growing season was favorable for wheat growth and development while 2024–2025 was relatively unsuitable weather conditions. These environmental conditions significantly influence critical physiological processes in wheat, including germination, plant height, grain filling, and overall grain yield formation.

Statistical Analysis

Analysis of variance (ANOVA) was performed using GenStat 18th Edition software. Mean separations were conducted using Fisher's Least Significant Difference (LSD) test at the 5% significance level ($P \leq 0.05$).

Results

Plant Height

The studied accessions of bread wheat showed significant variation in plant height across studied years: 100–125 cm in 2024 and 75–105 cm in 2025. A mean reduction of 10–20 cm was observed in the second year, likely attributable to drought stress, which aligns with observations by Nyaupane et al. (2024). The lowest plant height was recorded in KP-26/2020 (75 cm) during 2025, while the highest was observed in Zartepa variety (125 cm) in 2024 (Figure 3).

Notably, Lalmikor-1 maintained semi-dwarf plant height (104 cm in 2024 and 94 cm in 2025), demonstrating only a 10 cm reduction which is the smallest change among all accessions (Figure 1). This morphological stability is particularly valuable under rainfed conditions in Uzbekistan, where semi-dwarf plant height correlates with improved lodging resistance during high-rainfall years, a critical trait for sustainable wheat crop management in variable.

Figure 3. *Plant height of bread wheat accessions (2024–2025)*

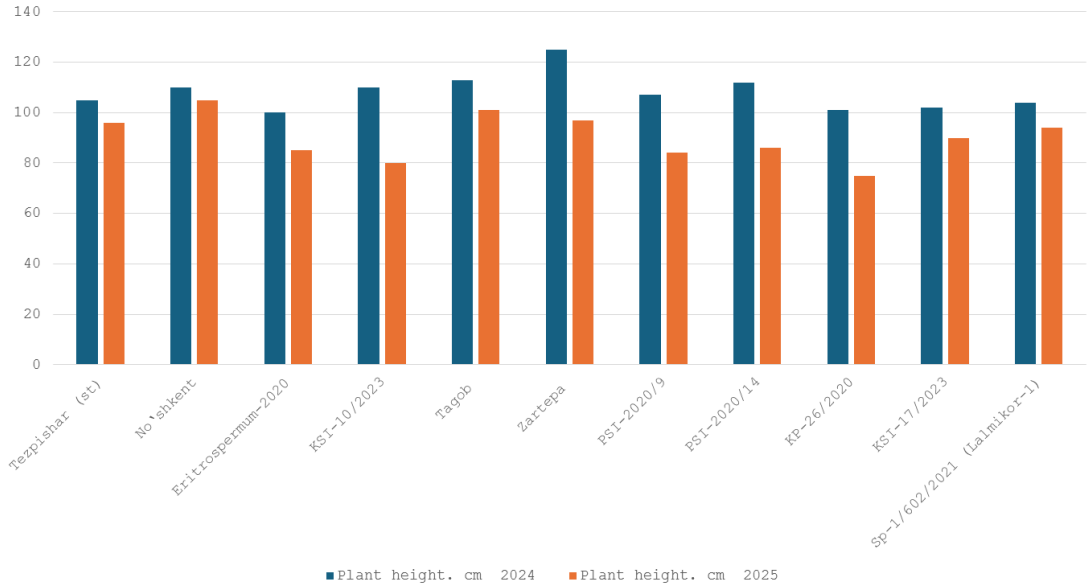

TKW

In the 2025 growing season, TKW declined significantly for the majority of accessions, with reductions ranging from –1.8 to –9.4 g relative to 2024 values (Figure 4). This widespread decrease in kernel weight likely reflects suboptimal environmental conditions during the critical grain-filling period (Calderini et al., 1995), such as heat stress, drought, or reduced assimilate availability. The accession KSI-10/2023, which recorded the highest TKW of 43.7 g in 2024, experienced a substantial decline to 36.7 g in 2025 (–16.0% reduction), demonstrating high sensitivity to inter-annual environmental variation.

In contrast, the variety Lalmikor-1 demonstrated superior phenotypic stability across both years, maintaining relatively high TKW values of 40.2 g (2024) and 38.4 g (2025), with only a modest 4.5% decline (Figure 4). We hypnotize that this stability suggests enhanced adaptive capacity and maintenance of grain-filling processes under variable environmental conditions, making Lalmikor-1 a valuable genetic resource for breeding programs targeting climate resilience and stable grain quality.

Days to heading and maturity

Figure 5 illustrates the temporal variation in days to heading and days to full maturity

for 11 wheat accessions across two consecutive growing seasons (2024 and 2025).

Heading occurred within a narrow range of 75–82 days in both years, indicating relatively consistent phenological timing for reproductive initiation. Maturity duration, however, exhibited greater variability: 100–120 days in 2024, contracting to 95–115 days in 2025. All accessions reached full maturity earlier in 2025, with accelerated heading and maturity likely attributable to abiotic stress factors, particularly drought and elevated temperatures, which are known to hasten developmental progression – a pattern consistent with findings reported by Nyaupane et al. (2024).

Figure 4. *Thousand Kernel Weight of bread wheat accessions (2024–2025)*

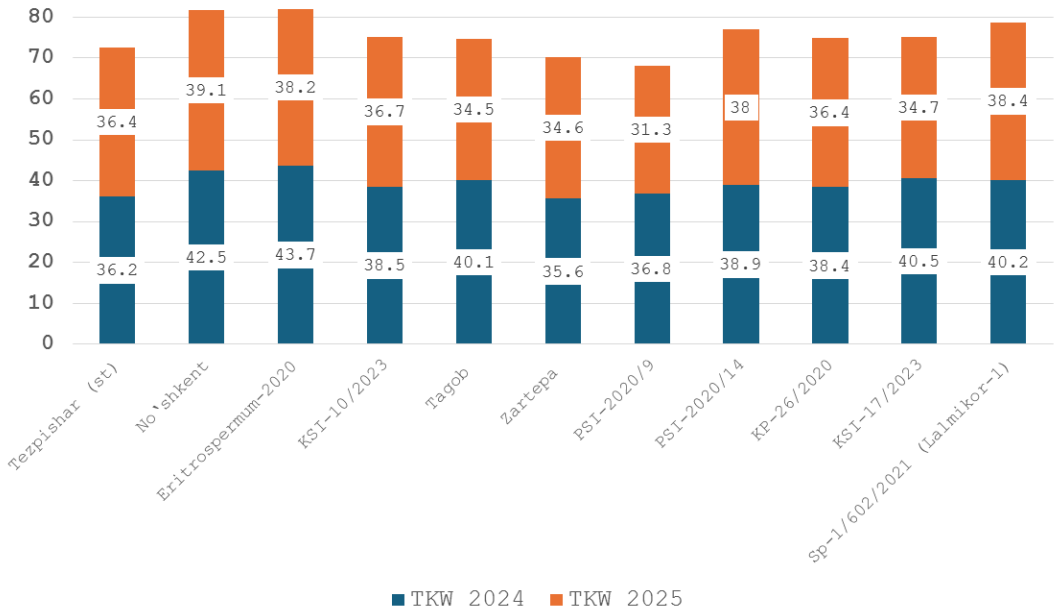

Accessions such as Lalmikor-1 and Eritrospermum-2020 demonstrate promising adaptive capacity, making them valuable germplasm resources for breeding programs targeting climate-variable rainfed systems (Rajotia et al., 2025).

Figure 5. *Days to maturity of bread wheat accessions*

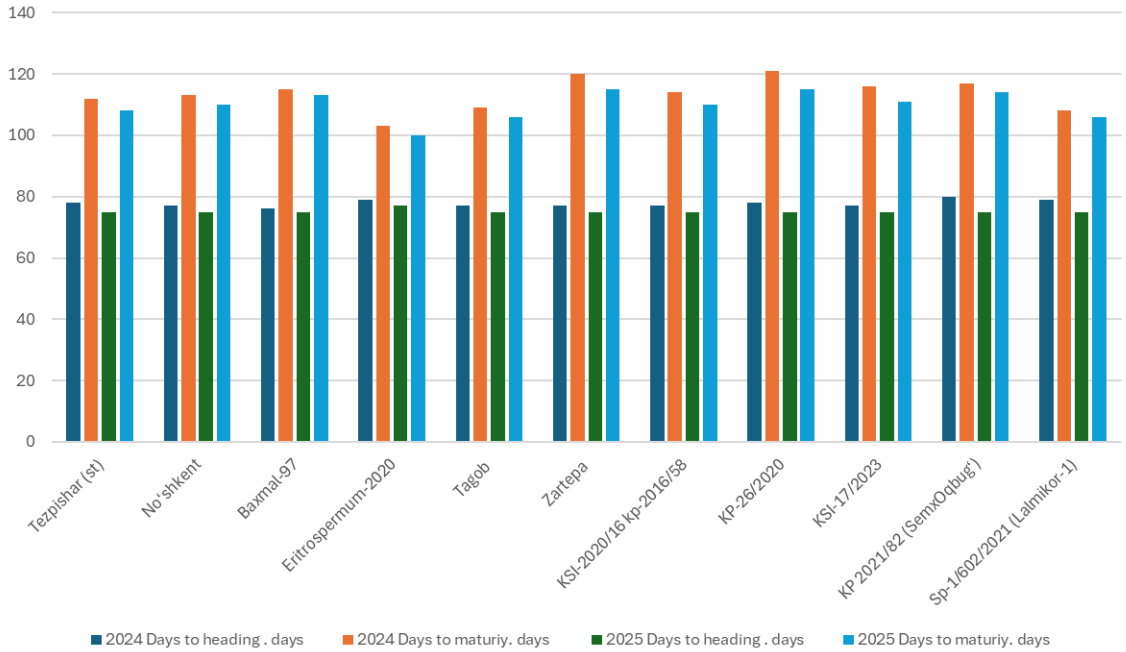

Grain Yield

Grain yields in 2024 consistently outperformed those in 2025 across all accessions and varieties, attributable to more favorable climatic conditions during the 2024 growing season (Figure 6).

Yield reductions in 2025 averaged 45–50% across accessions, reflecting the substantial impact of drought conditions during the wheat growing period.

Figure 6. *Yield variance of different bread wheat varieties and accessions*

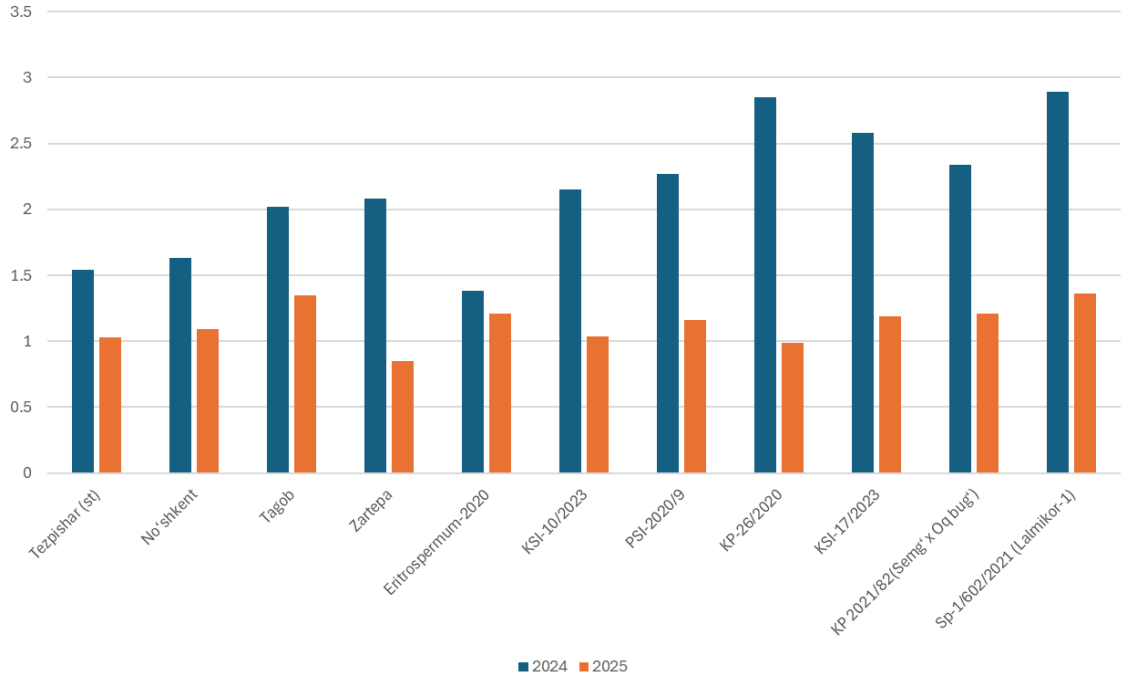

Compared to the local check variety Tezpishar, which yielded 1.54 t/ha (2024) and 1.03 t/ha (2025), several accessions demonstrated superior performance. Lalmikor-1 achieved the highest yields of 2.89 t/ha (2024) and 1.36 t/ha (2025), retaining 47% of its baseline productivity under stress conditions. PSI-2020/9 also showed promising performance with 2.27 t/ha and 1.16 t/ha in respective years, maintaining 52% yield retention. The identification of genotypes with superior yield stability across contrasting environments is a key objective in breeding for climate resilience (Geneti et al., 2022).

The highest grain yield across all treatments was recorded with Lalmikor-1 (2.89 t/ha) in 2025, while the lowest was observed with Zartepa (0.85 t/ha) in 2024. This wide range of genotypic variation (1.38–2.89 t/ha under favorable conditions) underscores the importance of varietal selection for optimizing productivity.

Conclusion

Lalmikor-1 as promising candidate for breeding programs targeting yield stability and stress resilience in wheat. These results demonstrate that Lalmikor-1 exhibits dual advantages: high yield potential under optimal conditions and reasonable stress tolerance, maintaining moderate productivity during drought years. Such varieties with combined high-yield potential and stress resilience are particularly valuable for production systems facing increasing climate variability.

References

Calderini, D. F., Dreccer, M. F. & Slafer, G. A. (1995). Genetic improvement in wheat yield and associated traits. A re-examination of previous results and the latest trends. Plant Breeding – 114. – P. 108–112.

Geneti G. S., Kebede S. A., Mekonnen T. B. (2022). Genetic variability and association of traits in bread wheat (Triticum aestivum L.) genotypes in Gechi district, South West Ethiopia. Adv. Agric., 2022 (2022), Article 7132424, 10.1155/2022/7132424

Ingvordsen, C. H., Hendriks, P.-W., Smith, D. J., Bechaz, K. M., & Rebetzke, G. J. (2022). Seedling and field assessment of wheat dwarfing genes and their influence on root traits in multiple genetic backgrounds. Journal of Experimental Botany, – 73(18). – P. 6292–6306. URL: https://doi.org/10.1093/jxb/erac306

Jobson, E. M., Johnston, R. E., Oiestad, A. J., Martin, J. M., & Giroux, M. J. (2019). The impact of the wheat Rht-B1b semi-dwarfing allele on photosynthesis and seed development under field conditions. Frontiers in Plant Science, – 10. 51. URL: https://doi.org/10.3389/fpls.2019.00051

Nyaupane, S., Poudel, M. R., Panthi, B., Dhakal, A., Paudel, H., & Bhandari, R. (2024). Drought stress effect, tolerance, and management in wheat – a review. Cogent Food & Agriculture, – 10(1). – 2296094 p. URL: https://doi.org/10.1080/23311932.2023.2296094

Rajotia, M. S., Bishnoi, O. P., Behl, R. K., Singh, J., Vats, A. K., & Bağcı, S. A. (2025). Breeding for early heat stress tolerance in wheat. Ekin Journal of Crop Breeding and Genetics, – 11(1). – P. 1–10.

submitted 09.11.2025;
accepted for publication 23.11.2025;
published 30.12.2025

Contact: nurbekov2002@yahoo.com

The European Journal of Technical and Natural Sciences 2025, No 6
ISSN 2414-2352

PREMIER Publishing
ppublishing.org

Section 2. Biotechnology

DOI:10.29013/EJHSS-25-6-15-28

ANALYSIS OF MINERAL COMPOSITION BY X-RAY FLUORESCENCE AND IN VITRO ANTI-AMYLASE ACTIVITY OF EXTRACTS OF *AFRAMOMUM MELEGUETA* K. SCHUM, *CURCUMA LONGA* L., AND PIPER GUINEENSE SCHUMACH. & THONN. MEDICINAL PLANTS

Mayele Masasi Blanchard [1], ***Mbemba Fundu Théophile*** [1], ***Mosango Mbokuyo David*** [2], ***Mubwele Armandine*** [3], ***Kibul Mimpur Jolie*** [4]

[1] Department of Biology, Faculty of Science, University of Kinshasa, P.O. Box 190, Kinshasa XI, Democratic Republic of Congo

[2] Department of Botany, Makerere University, P.O. Box 7062, Kampala, Uganda

[3] Faculty of Pharmacy, University of Kinshasa, P.O. Box 127, Kinshasa XI, Democratic Republic of Congo

[4] Mubwele, Department of Environmental Sciences, University of Kinshasa, P.O. Box 127, Kinshasa, Democratic Republic of Congo. National Scientific Research Council and Mabanga Mixed Hospital Centre of Medicine and SS Anemia, Yolo South, Kinshasa, Democratic Republic of Congo

Cite: *Mayele Masasi Blanchard, Mbemba Fundu Théophile, Mosango Mbokuyo David, Mubwele Armandine, Kibul Mimpur Jolie. (2023). Analysis of mineral composition by X-ray fluorescence and in vitro anti-amylase activity of extracts of Aframomum melegueta K. Schum, Curcuma longa L., and Piper guineense Schumach. & Thonn. medicinal plants. European Journal of Technical and Natural Sciences 2025, No 6.* https://doi.org/10.29013/EJHSS-25-6-15-28

Abstract

The objective of this study was to highlight the mineral composition of *Aframomum melegueta, Curcuma longa*, and *Piper guineense* and to evaluate the anti-amylase activity of plant extracts from these plant species. The mineral composition was determined by X-ray fluorescence (XRF). This method allows for rapid and accurate identification of the elements present. The extracts of these species were also tested in vitro for their ability to inhibit amylase, a key enzyme in starch digestion and blood sugar regulation. Several essential minerals were found in the species analysed: potassium, calcium and iron, with varying concentrations depending on the plant. The XRF spectra reveal the elemental composition of three extracts from the species studied. These elements are potassium, iron, zinc and rubidium. These are present in all

the samples analysed, confirming a similar mineral base. The most pronounced anti-amylase activity was observed with *Curcuma longa* extract, followed by *Piper guineense* and *Aframomum melegueta* extracts. The various properties observed justify the traditional use of these plants in diabetes management and reinforce their potential as nutraceutical ingredients. The plants studied were found to inhibit the activity of the enzyme α-amylase, which is essential for the intestinal absorption of glucose. This action, therefore, helps to regulate glucose absorption, improve insulin sensitivity, and maintain optimal functioning of pancreatic β cells. The use of these plants may be a wise choice among the strategies for combating diabetes, namely phytotherapy.
Keywords: *mineral composition analysis, anti-amylase activity, Aframomum melegueta K. Schum., Curcuma longa L., Piper guineensis Schumach. & Thonn, medicinal plants*

1. Introduction

Since ancient times, human societies have exploited the properties of plants for various purposes, particularly in the areas of health and nutrition. Plant species used to prevent or treat different ailments are commonly referred to as medicinal plants. Currently, phytotherapy, defined as the medicinal use of plants, is experiencing a resurgence of interest, due to both growing evidence of its effectiveness and increasing public acceptance (Ngbolua *et al.*, 2011; Mbemba, 2020; Gbolo, 2023). Historically, plants and their extracts have been used to treat a wide range of diseases and disorders. In recent years, several factors have contributed to their resurgence, including their relatively low cost compared to synthetic drugs and a certain disillusionment with modern medicine (Chanda *et al.*, 2015; Ngbolua *et al.*, 2011; Boukeria *et al.*, 2019). Plants are capable of producing a wide variety of bioactive compounds, including mainly terpenoids, alkaloids, and phenolic compounds. These constitute one of the most studied groups due to their low toxicity and their multiple beneficial effects, whether therapeutic, pharmaceutical, cosmetic, or nutritional (Boukeria *et al.*, 2019).

The purpose of this study was to analyse and evaluate the anti-amylase activity of *Aframomum melegueta* K. Schum and *Curcuma longa* L. (both of Zingiberaceae), and *Piper guineense* (of Piperaceae). *A. melegueta* is a herbaceous and perennial species of approximately 1.5 m in height, with simple, alternate, lanceolate leaves about 40 cm long and 12–15 cm wide. Fleshy fruits, small, aromatic, and spicy, are used in cooking and in traditional medicine (Oludare Osuntokun, 2020). *C. longa* L. is a perennial, rhizomatous, herbaceous, and flowering plant native to India and Southeast Asia. It bears large, sheathing, elliptical, and lanceolate leaves up to 50 cm long and 7–25 cm wide. Flowers are yellow, arranged in spikes, white to green, sometimes tinged reddish-purple, and described as sterile (Grugeau, 1995). *P. guineense* is a climbing vine of about 20 m long, clinging to trees, with lanceolate and alternate leaves, up to 40 cm long and 12–15 cm wide, native to West Africa. Its Flowers are greenish-yellow and arranged in spikes. Fruits are small, red-brown drupes, black when dried, and often used as a spicy and aromatic spice in cooking.

Aframomum melegueta K. Schum., *Curcuma longa* L., and *Piper guineense* Schumach. & Thonn. are commonly used in traditional medicine. They have therefore been the subject of much scientific research. Yu Shen et *al.* (2025) report that *A. melegueta* is used to treat several types of bodily pain, such as diarrhea, sore throat, catarrh, congestion, rheumatism, and infectious diseases, including urinary tract infections Yu Shen et *al.* (2025). Different parts of this plant contain specific phytochemicals, such as flavonoids, phenolic compounds, alkaloids, tannins, terpenoids, saponins, and cardiotonic glycosides (Ibarue et al., 2021). These compounds act as anti-inflammatory, antimicrobial, anti-allergic, anticoagulant, anti-cancer, anti-diabetic, and hepatoprotective agents. Fuloria et al. (2022) assert that *C. longa* is a powerful medicinal plant due to its pharmacological properties and chemical components, such as starch, essential elements, proteins, vitamins, volatile oils, curcuminoids, and curcumin, which have beneficial effects on humans. This is why it is often used to treat various ailments, such as inflammation, digestive disorders, skin diseases, and

pain caused by blood stagnation. Fuloria et al. (2022) confirm its usefulness in relation to heart health, liver protection, and wound healing. *C. longa* also has antioxidant, hepatoprotective, antimicrobial, antibacterial, antifungal, and anti-allergic properties. Mbemba (2020) also asserts that it contains a group of phenolic compounds known as curcuminoids, the main one being curcumin. These compounds act by inhibiting the activity of the enzymes α-glucosidase and α-amylase, which are essential for the intestinal absorption of glucose. This activity helps regulate glucose absorption, improve insulin sensitivity, and maintain optimal pancreatic β-cell function. *C. longa* also possesses a broad spectrum of biological activities, including antioxidant, anti-inflammatory, antitumor, and anti-sickle cell properties. This plant is often associated with black pepper (*Piper nigrum*), which significantly increases the bioavailability of curcumin, thereby enhancing its therapeutic effects (Mbemba, 2020; Mbadiko *et al*., 2024).

On the other hand, Mbadiko et al. (2023) report that several species of the genus *Piper* have a wide range of biological properties, including anti-inflammatory, antioxidant, antibacterial, antifungal, antiplasmodial, analgesic, immunomodulatory, antitumor, amoebicidal, and antiviral effects. As far as *P. guineense* is concerned, Chinwendu *et al*. (2016) identified the following phytochemicals in the leaves: alkaloids, saponins, flavonoids, tannins, phenolic compounds, steroids, glycosides, and essential oils. They also mentioned the antioxidant (flavonoids and phenolic compounds), antibacterial, anti-inflammatory, and anticonvulsant properties, and those relating to reproductive health. For their part, Sikhuemene and Ongbomwan (2020) highlighted the following phytochemical elements (alkaloids, cyanogenic glycosides, saponins, tannins, flavonoids, anthraquinones, and phenols). They also mentioned the following mineral elements (Ca, Mg, Na, K, Fe, Zn, P). All these findings confirm its use as a medicinal plant.

Several previous studies have shown that combining extracts from different medicinal plants can improve the efficacy of pharmacological action by inducing synergy, acting simultaneously on multiple targets, reducing the doses of each component, and reducing side effects (Carabajal et al. 2019; Sharma et al. 2020; Deciga-Campos 2021; Gufe et al. 2023). Similar studies have also been conducted on *A. melegueta, C. longa*, and *P. guineense* in the treatment of various diseases. Shoba et al. (1998), for example, report that the combination of *Curcuma longa* and *Piper spp*. enhances anti-inflammatory effects by improving the absorption of curcumin. It is therefore plausible that the combination of *C. longa* and *P. guineense*, on the one hand, and of *C. longa* and *A. melegueta*, used as a substitute for black pepper, on the other hand, may enhance their medicinal properties. Furthermore, De Ruijter (2008) mentions the combination of *Strychnos congolana* Gilg roots and Aframomum melegueta K.Schum. seeds in the Democratic Republic of Congo for treating dysmenorrhea. On the other hand, Schmelzer (2008) reports the combination of *Hilleria latifolia* (Lam.) H. Walter leaves and *Piper guineense* Schumach. & Thonn. leaves for treating body swellings and leprosy. Ogbunugafor *et al*. (2017) and Mbadiko *et al*. (2024) report that *C. longa* exhibits numerous biological activities, including anti-inflammatory, antioxidant, and hypoglycemic properties. Mayele et al. (2025) demonstrated, through their study of the qualitative and quantitative composition of certain metabolites and the in vitro evaluation of their antioxidant activities, that the combination of *Aframomum melegueta*, *Curcuma longa*, and *Piper guineense* contained all the metabolites studied and that the concentrations of polyphenols, flavonoids, and tannins were higher than those of the individual plants. According to them, combining extracts of these plant species could make the treatment of diabetes and other diseases more effective.

The above demonstrates that the combined use of plant substances or herbal preparations has the potential advantage of increasing the benefit/risk ratio, either by enhancing or improving the therapeutic effects of their active ingredients. This approach also helps simplify the treatment protocol, thereby promoting patient adherence (HMPC, 2018). In this study, we will analyse the mineral composition of the extracts of *A. melegueta*, *C. longa*, and *P. guineense* and

evaluate their anti-amylase activity. These extracts will be analysed separately and in combination to assess the efficacy of these medicinal plants.

2. Materials and methods

2.1 Material

The seeds of the species *Aframomum melegueta*, and the rhizomes of the species *Curcuma longa* were collected in the Bateke Plateau, in the Commune of Maluku, located near Kinshasa, the capital city of the DR Congo, and the fruits of *Piper guineense* analysed in this study come from the village of Koko in the province of Kikwit in DR Congo. These three species were formally identified in the Herbarium of the University of Kinshasa.

2.2 Methods

2.2.1 Analysis of mineral composition by X-ray fluorescence

The mineral composition of plant samples of A. melegueta, C. longa and P. guineensis was analysed by X-ray fluorescence at the molecular biology laboratory of the General Commission for Atomic Energy (CGEA), located at the Kinshasa Regional Centre for Nuclear Studies (CGEA/CREN-K). The X-ray fluorescence method was used. The basic principle of an X-ray fluorescence (XRF) spectroscopy system involves a primary radiation source, either a radioisotope or an X-ray tube, and a detector that records the secondary X-rays emitted by the sample. When an atom is irradiated by a photon in the X-ray region, an inner-shell electron can be ejected, creating a vacancy. During the subsequent de-excitation process, an electron from a higher energy level fills this vacancy. The energy released during this transition is emitted as X-ray photons, which are characteristic of the element involved. The resulting X-ray fluorescence spectrum appears as a series of lines. Analysis of their positions reveals the mineral elements present in the sample (qualitative analysis). Conversely, the relative or absolute intensity of these lines indicates their concentration (semi-quantitative or quantitative analysis).

2.2.2 Evaluation of anti-amylase activity

The in vitro evaluation of anti-amylase activity was performed according to the method reported by Wickramaratne *et al.* (2016). Digestive enzymes are now recognised as major therapeutic targets in the treatment of obesity and certain associated metabolic disorders, such as type 2 diabetes (Prieto-Rodríguez *et al.*, 2022). The hydrolysis of starch by amylases results in the release of reducing sugars, mainly glucose. Free aldehyde groups convert oxidised 3,5-dinitrosalicylic acid (yellow in colour) into 3-amino-5-nitrosalicylic acid and nitrosalicylic acid, which are easily recognisable by their red-orange colour and maximum absorption at 540 nm.

The intensity of this colouring is directly proportional to the concentration of reducing sugar produced in the reaction medium. However, when an extract with amylase-inhibiting potential is present, it prevents starch hydrolysis, thereby limiting the release of glucose and the reduction of 3,5-dinitrosalicylic acid. The inhibitory power of the extract is then assessed by comparing the measured absorbance of the colored complex (3-amino-5-nitrosalicylic acid) in the presence and absence of the extract.

2.2.3 Operating procedure

a. Extraction of plant amylases

The amylases were extracted from 10 g of germinated corn flour macerated in 100 mL of distilled water. The resulting suspension was homogenized by magnetic stirring for 15 minutes, then filtered through Whatman No. 1 paper. The filtrate was then centrifuged at 4,000 rpm for 20 minutes at 4 °C. The resulting supernatant containing the enzymes was collected and stored in a refrigerator at 4 °C for immediate use or at –20 °C for later use.

b. Preparation of different extract concentrations

To prepare the plant extracts for testing, 20 mg of each extract was dissolved in 10 mL of distilled water or 80% ethanol to obtain a stock solution of 2 mg/mL, from which successive dilutions were made.

c. Preparation of 3,5-dinitrosalicylic acid (DNSA) colororimetric solution

Colorimetric solution of 3,5-dinitrosalicylic acid (DNSA) was prepared by dissolving 12 g of sodium potassium tartrate tetrahydrate in 8 mL of 2 M NaO H. Then, 20 mL of a 96 mM solution of 3,5-dinitrosalicylic acid was added to this solution.

d. Screening for anti-amylase activity

To evaluate antidiabetic activity, 200 µL of enzyme extract was mixed with 200 µL of plant

extract and incubated at 37 °C for 10 minutes. Next, 200 µL of a 1% pure starch solution was added and incubated for 3 minutes at 37 °C. The reaction was then stopped by adding 200 µL of DNSA. This mixture was then boiled in a water bath at 90 °C for 10 minutes. After cooling to room temperature, the solution was diluted by adding 5 µL of distilled water. Absorbance was measured at 540 nm using a UV-visible spectrophotometer. An enzyme blank, representing 100% activity, was prepared by replacing the plant extract with 200 µL of the solvent used. A second blank, specific to each concentration level of the extracts, was prepared in the absence of the enzyme.

e. Amylase activity inhibition calculation

The percentage inhibition of amylase activity was calculated using the following formula:

% *Amylase*inhibition = Abs control–Abs extract Abs control *x* 100

Where Abs = Absorbance

2.2.4 Statistical analysis

GraphPad Prism 6.0 and Statistix 8.0 software were used for all statistical analyses, including the determination of IC_{50} values. Results were expressed as mean ± standard deviation. One-way analysis of variance (ANOVA) was used to compare the means of the different samples, followed by Tukey's test for multiple comparisons. The threshold significance was set at α =0.05.

3. Results and discussion

3.1 Plant mineral composition

Figures 1, 2, and **3** below illustrate the mineral composition of *Aframomum melegueta*, *Curcuma longa,* and *Piper guineense* species. They reveal the presence of potassium, iron, and zinc in the *A. melegueta* sample, potassium, iron, and zinc in that of *C. longa*, and potassium, iron, and selenium in that of *P. guineense*. Previous studies also highlighted the presence of magnesium, calcium, manganese, chromium, zinc, copper, iron, phosphorus, and sodium in the various plants analysed (Khan *et al.*, 2024; Jansen *et al.*, 2005). Potassium, an essential mineral, plays a crucial role in maintaining resting membrane potential and regulating osmolarity within cells. It is also well established that potassium has an impact on the functions of endothelial cells and vascular smooth muscle cells. Numerous studies have also shown that increasing dietary potassium intake can lower blood pressure to more physiologically favourable levels (Haddy 2006; Chan 2024). The hypotensive effects of this element have been documented in several intervention trials. These effects are reported in various meta-analyses (Biff and Deborah 2020). Furthermore, epidemiological data accumulated over the last decade show a link between low dietary potassium intake – or low serum concentrations – and an increased risk of insulin resistance and the development of type 2 diabetes.

Figure 1. Quantification of mineral elements by X-ray fluorescence of *Aframomum melegueta* extract

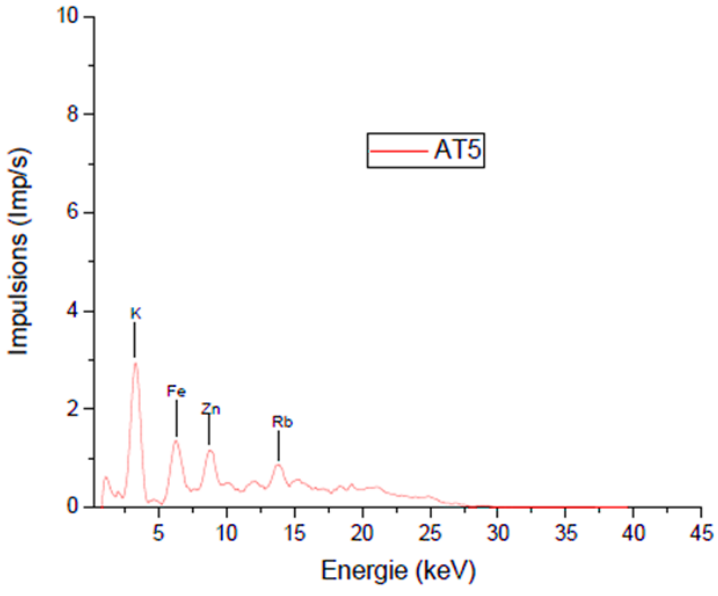

Furthermore, zinc deficiency and changes in the homeostasis of this essential trace element are linked to several chronic diseases, including diabetes and its complications, notably diabetic retinopathy. Indeed, zinc contributes to the structural stability of copper-zinc superoxide dismutase (Cu-Zn SOD). This is an important antioxidant defence enzyme. It protects thiol (–SH) groups from oxidation by competing with iron, inhibits the activity of NADPH oxidase, a major source of free radicals, and reduces the production of reactive oxygen species (ROS) by interfering with Fenton reactions, in particular by competing with iron and copper (Mbemba *et al.*, 2023; Mayele et *al.*, 2025). Prasad and Bao (2019) attest that zinc also plays a major direct and indirect antioxidant role, which helps to maintain cellular redox balance.

Figure 2. *Quantification of mineral elements in Curcuma longa* L.

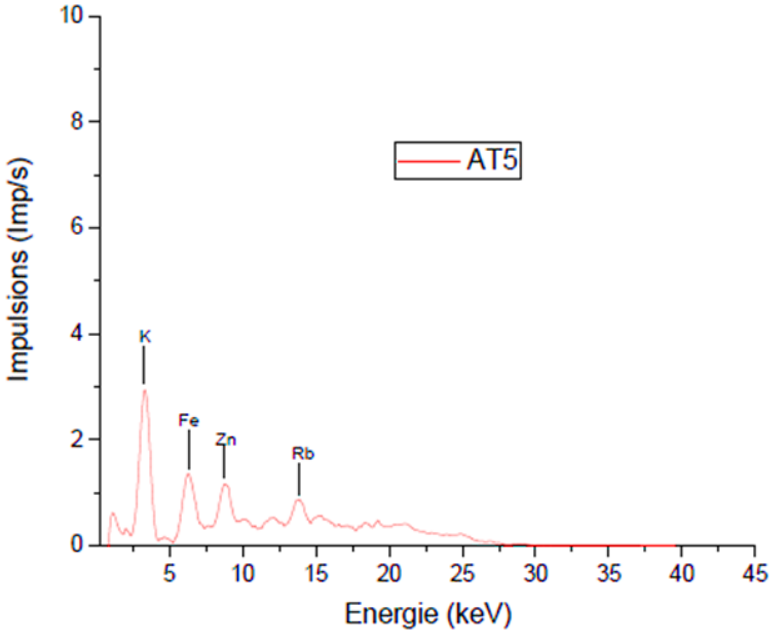

Figure 3. Quantification of mineral elements by X-ray fluorescence of *Piper guineensis* extract

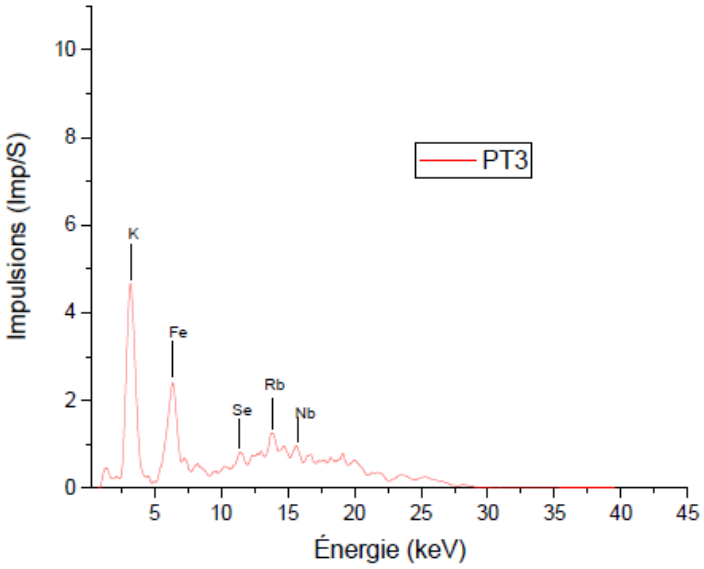

Selenium, for its part, plays a fundamental role in defending cells against damage caused by free radicals. Ceci est dû à la présence de glutathion peroxydase sélénium-

dépendante dans le site actif et à l'activité antioxydante des selenoproteins (Burk, 2002). Le sélénium contribue également à l'amélioration de la fonction des cellules effectrices cytotoxiques, essentielles à la maturation des lymphocytes T et à la production d'anticorps T-dépendants (Zhang et al., 2020).

However, selenium intake in excess of nutritional requirements could inhibit the replication and mutation of SARS-CoV-2 into more virulent forms, while mitigating oxidative stress, organ damage, and the cytokine storm associated with infection (Zhang *et al., 2020*). This protective effect is particularly crucial in older individuals, in whom selenium deficiency is linked to an increase in pro-inflammatory cytokines.

Iron is an essential element in many biological processes, including the synthesis of haemoglobin, cytochromes, and key enzymes such as catalase, which plays a role in antioxidant defence (Mbemba, 2023). A recent study conducted by Oleiwi *et al.* (2024) highlighted a significant positive correlation between iron concentrations and catalase activity in subjects with diabetes, suggesting a close link between iron status and the regulation of oxidative stress in this pathological context.

Furthermore, organic germanium is known for its various pharmacological activities and is often used in medicine for anti-tumour, antiviral, antibacterial, antioxidant, immune regulation, and hypoglycaemic purposes. Wang et al. (2020) report that germanium can inhibit inflammation by suppressing the activation of the NF-kB and MAPK pathways, and reducing the expression of TNF-α, IL-1β and IL-6. Traces of germanium keep hydrogen peroxide at a low level, inhibiting oxidative stress and thus preventing its activity. It has been observed that germanium is part of the active centers of certain enzymes and participates in oxidation, mainly with hydrogen peroxide, without producing harmful oxygenated species (Menchikov et al., 2023). In fact, previous results suggest that Ge-132 has the potential to act as an antioxidant supplement by protecting cells. (Menchikov and Popov, 2023).

The spectrum shows that the CT4 sample contains beneficial elements (K, Fe, Zn), but also heavy metals of concern (Pb), which implies: potential nutritional or therapeutic value, but also a toxicological risk to be monitored, particularly when used for medical purposes (Purwadi *et al.*, 2022). The PT3 spectrum reveals a profile rich in bioactive elements (K, Fe, Se), supporting potential use in phytotherapy or supplementation. However, the presence of non-essential elements (Rb, Nb) calls for further analysis to assess toxicological safety before any medicinal or dietary use. Niobium (Nb) is rarely present in biological matrices. However, its detection could be linked to environmental contamination or a particular geological origin. It has no known role in human metabolism (Tchounwou *et al.,* 2019).

The *Curcuma longa* and *Piper guineense* spectra show interesting nutritional potential, particularly due to the presence of essential elements. However, the presence of non-essential or even toxic trace metals requires toxicity assessment before any therapeutic or food use. The spectra obtained by XRF show the elemental composition of three extracts (*Aframomum melegueta, Curcuma longa, and Piper guineense*). Potassium (K), Iron (Fe), Zinc (Zn) and Rubidium (Rb) are present in all samples, thus confirming a similar mineral base. These elements are important for health: K: electrolyte balance and muscle contraction; Fe: oxygen transport; Zn: immunity and antioxidant enzyme; Rb: is a non-essential trace element, considered as an indicator of bioaccumulation, often associated with the bioavailability of minerals and trace elements (Palmar *et al.*, 2023). For their part, Tchounwou *et al.* (2019) also report the presence of specific elements in *A. melegueta*, *C. longa,* and *P. guineense*. However, *A. melegueta* does not contain any toxic heavy metals, making it safer for therapeutic use. *C. longa,* on the contrary, has a peak of Pb (lead), a toxic element, which may pose safety problems for prolonged therapeutic use. On the contrary, *Piper guineense* contains Se (selenium) and Nb (niobium), which are absent in other species. Selenium is known as an essential trace element in low doses and an antioxidant, while Niobium is a non-essential element, as it is rarely found and must be monitored.

3.2 Anti-amylase activity

Table 1 below reveals that, among the aqueous extracts, the *P. guineense* extract

tested individually shows significant inhibition of amylase activity, with an IC_{50} of 49.0 ± 0.20 mg/ml. This activity is followed by that observed for the combination of *C. longa* and *A. melegueta* (**CA**) samples, then that of the combination of *C. longa*, *A. melegueta*, and *P. guineense* (**CAP**), with respective inhibition percentages of 46.2 ± 0.60 mg/mL and 46.1 ± 0.20 mg/mL. The inhibitory effects of these samples are statistically significant compared to those of the other plant extracts analysed individually or in combination.

Concerning the hydro-ethanolic extracts, analysis of Table 1 below indicates that the extract of *P. guineense*, tested individually, exhibits significant inhibitory activity, with an IC_{50} of 47.7 ± 0.80 mg/ml. This activity is followed by that of the *A. melegueta* extract analysed separately, with an IC_{50} of 41.0 ± 0.20 mg/mL, then that of the combination of *C. longa, A. melegueta*, and *P. guineense* (CAP), which revealed an IC_{50} of 40.0 ± 0.80 mg/mL. The other extracts, used alone or in combination, showed less marked inhibitory activity compared to the samples mentioned above.

Table 1. *Anti-amylase activity of extracts from A. melegueta, C. longa, and P. guineensis, analysed separately or in combination*

	Concentrations (mg/mL)					
Samples	**AM**	**CL**	**PG**	**CA**	**CP**	**CAP**
Aqueous extracts	14.2 ± 0.4^{e}	23.1 ± 1.21^{d}	49.0 ± 0.20^{a}	46.2 ± 0.60^{b}	44.7 ± 1.0^{c}	46.1 ± 0.20^{b}
Organic extracts	41.0 ± 0.2^{b}	39.0 ± 0.20^{c}	47.7 ± 0.80^{a}	15.0 ± 0.60^{f}	24.8 ± 0.40^{d}	40.0 ± 0.80^{bc}
Acarbose (Control)			22.29 ± 1.24^{de}			
p-value			0.0000			

Caption: AM: A. *melegueta;* **CL***: C. longa;* **PG***: P. guineense; CA: Combination of C. longa and A. melegueta;* **CP***: Combination of C. longa and P. guineense;* **CAP***: Combination of C. longa, A. melegueta, and P. guineense. For each line, the superscript letters indicate the degree of anti-amylase activity of the aqueous or ethanolic extracts of the different samples analysed. These letters correspond to activity levels ranked in descending order according to the following sequence: a > b > c > d > e > f*

The fact that the CA and CAP combinations also exhibited notable inhibitory activity suggests the existence of a synergistic effect between the phytochemicals of the plants studied. Such observation opens up an interesting avenue for the use of these combinations in the formulation of nutraceuticals for anti-diabetic purposes. Indeed, these combinations could inhibit the action of amylases involved in the digestion of glucose polymers, thereby delaying the intestinal absorption of this monosaccharide. This mechanism contributes to the regulation of postprandial hyperglycaemia and is strongly recommended in the management of diabetes (Kifle *et al.*, 2021).

Scientific literature remains limited about the study of the anti-amylase potential of the combination of extracts of *C. longa* and *A. melegueta* or *C. longa* and *P. guineense*, or even the combination of these three plant species, compared to the action of each of them evaluated separately. With respect to *C. longa*, Lekshmi *et al.* (2012) showed that its aqueous and organic extracts exhibit anti As for C. longa*, Lekshmi et al. (2012) showed that its aqueous and organic extracts exhibit remarkable anti-amylase activity. Furthermore, the inhibition of glycosidase, another key enzyme in carbohydrate digestion, has been attributed to its essential oils, as well as to curcuminoids, primarily curcumin and bisdemethoxycurcumin (Wildowati et al., 2018; Ramkumar et al., 2021).-amylase activity. Lekshmi et al. (2012) showed that aqueous and organic extracts of C. longa exhibit remarkable anti-amylase activity. Furthermore, Wildowati et al. (2018) and Ramkumar et al. (2021) indicate that the inhibition of glycosidase, another key enzyme in carbohydrate

digestion, is due to its essential oils, as well as to curcuminoids, primarily curcumin and bisdemethoxycurcumin. Meanwhile, Omosa *et al.* (2017) attributed the antidiabetic activity of *C. longa* to the presence of curcuminoids and sesquiterpenoids.

In addition, the literature reports that curcumin, the main representative of curcuminoids and the major active constituent of *C. longa*, has a hypoglycemic effect by reducing hepatic glucose production and stimulating glucose absorption through the activation of several genes, particularly those coding for the glucose transporters GLUT4, GLUT2, and GLUT3 (Ghorbani *et al.,* 2014). It may also induce the activation of the nuclear receptor PPAR-γ, decrease plasma glucose levels, and stimulate enzymes involved in glycolysis, such as hepatic glucokinase. In addition, curcumin promotes the accumulation of hepatic glycogen and downregulates neo-glucogenesis enzymes, including phosphoenolpyruvate carboxykinase (PEPCK) and glucose-6-phosphatase (Vafaeipour *et al.*, 2022). Curcumin improves insulin expression and secretion by activating phosphatidylinositol-3-kinase (PI3K), protein kinase B (Akt), and the signalling pathway involving the GLUT2 glucose transporter. This effect is associated with increased activity of GLUT2 and glucokinase (GCK), two key elements in the regulation of glucose uptake and intracellular metabolism (Zhang and Kitts, 2021). According to Ramkumar et al. (2021), bisdemethoxycurcumin, another representative of the curcuminoids, is capable of inhibiting human pancreatic α-amylase in vitro, as it regulates blood glucose and is targeted in the treatment of diabetes.

Mohammed et al. (2017) indicate that the leaves and seeds of *A. melegueta* contain antihyperglycemic activity. This helps improve pancreatic β-cell dysfunction and reduces other complications associated with diabetes. Karlsson *et al.* (2013) report that extracts from certain species of the genus *Aframomum* (*A. Aulacocarpus*, *A. citratum, A. deniellii*) not only limit weight gain, but also lower total and LDL cholesterol levels, while increasing HDL cholesterol, which has a well-established protective effect against obesity (*Karlsson et al., 2013*). According to these authors, obesity is now recognised as one of the main risk factors for type 2 diabetes.

Platel and Srinivasan (2000) report that extracts of *Piper* species (black pepper) stimulated food digestion by stimulating the secretion of digestive enzymes (pancreatic amylase, trypsin, and chymotrypsin). This activity significantly reduces food transit time in the gastrointestinal tract and increases both saliva production and gastric secretions. Furthermore, Liu et al. (2020) reported that administering piperine, an alkaloid isolated from species of the genus Piper, to obese mice resulted in a significant decrease in fasting blood glucose, total serum cholesterol, and triglycerides, while also improving glucose intolerance and insulin resistance. Furthermore, the effect of piperine on improving the bioavailability of curcumin, as well as enhancing its therapeutic properties, has been widely documented in the literature (Partial *et al., 2015*; Mbadiko *et al.*, 2024).

Results from this study indicate that the anti-amylase activity observed for the extracts of A. melegueta, C. longa, and Piper guineense species, whether evaluated individually or in combination, is closely linked to the presence of phytochemicals capable of inhibiting amylases. These compounds include certain alkaloids such as piperine, polyphenols including curcuminoids, particularly curcumin and its derivatives, as well as terpenoids and saponins. These classes of compounds have been reported in the literature as having antidiabetic effects, particularly through their ability to inhibit pancreatic and salivary α-amylase, thereby contributing to the regulation of blood glucose levels in diabetic patients (Wildowati *et al.*, 2018; Teng *et al.*, 2018; Liu *et al.*, 2020; Ramkumar *et al.*, 2021; Aurelio *et al.*, 2022).

4. Conclusion and recommendation

This study focused on the fundamental analysis and evaluation of the anti-amylase activity of Curcuma, *Aframomum melegueta*, and *P. guineensis*. Based on fundamental analysis, the mineral composition revealed that the hydro-ethanolic extracts of C. longa and A. melegueta (CA) present an interesting profile: potassium (K) is normally present in medicinal plant extracts; iron (Fe) is known as an enzyme, which suggests a potential

therapeutic interest, especially as an antioxidant. Zinc (Zn) is a cofactor for enzymes and plays a crucial role in the immune response. The spectrum therefore shows that sample CT4 contains not only beneficial elements (K, Fe, Zn), but also heavy metals of concern (Pb), which not only have potential nutritional or therapeutic value, but also possess a toxicological risk that needs to be monitored, particularly when used for medical purposes. The PT3 spectrum reveals a profile rich in bioactive elements (K, Fe, Se), supporting potential use in phytotherapy or supplementation. However, the presence of non-essential elements (Rb, Nb) calls for further analysis to assess toxicological safety before any medicinal or food use.

X-ray fluorescence (XRF) spectra show the elemental composition of three extracts (*Aframomum melegueta, Curcuma longa, and Piper guineense*). The resulting XRF spectra of *C. longa* and *Piper guineense* show interesting nutritional potential, which is particularly due to the presence of essential elements. However, the presence of traces of non-essential elements, or even toxic metals, necessitates a toxicity assessment before any therapeutic or food use. An integrated approach combining X-ray fluorescence, biological, and toxicological analyses is recommended.

Piper guineense contains selenium (Se) and niobium (Nb), which are absent in *A. melegueta* and *C. longa*. Selenium is an essential trace element in small doses, acting as an antioxidant. Niobium, on the other hand, is a non-essential element whose presence is rare and must be monitored. However, *Aframomum melegueta* does not contain toxic heavy metals, making its therapeutic use safer. The trace elements present in the studied plants also play a role in various biochemical processes, particularly in antioxidant mechanisms.

Regarding the anti-amylase activity of the aqueous extracts, the *P. guineense* extract, tested alone, showed significant inhibition of α-amylase, followed by the combination of *C. longa* and *A. melegueta* (CA), and then the combination of the three samples (CAP). For hydroethanolic extracts, the *P. guineense* extract tested individually also showed the strongest inhibitory activity, followed by the *A. melegueta* extract, and then by the combination CAP of the three species.

This study presents interesting perspectives for the development of medicinal plants with a favourable mineral salt profile and pronounced anti-amylase activity. This will enable improved formulation of nutraceuticals for the prevention of chronic non-communicable diseases associated with oxidative stress. An integrated approach combining XRF, biological, and toxicological analyses is therefore recommended.

Acknowledgement

We thank Professor T. Mbemba for welcoming us to his Food and Nutrition Research Laboratory (LARAN). We would also like to thank the staff of the Molecular Biology Laboratory at the Regional Nuclear Studies Centre in Kinshasa (CGEA/CREN-K) for providing us with laboratory facilities.

Declaration of available data

The sharing of available data does not apply to this article, as no new data was created as part of this article. However, we are willing to answer any questions regarding this article.

Author contributions

Project conception and supervision - **MT.** Project supervision – **NNKJP**. Writing-original project, and execution - **MMB.** Writing-original project execution - **MMB.** Writing–revision - **MMB, MMD.** Editing- English translation - **MMD.** Laboratory product funding - **MMB, MA, KMJ.** All authors have read and accepted the final version of the manuscript.

Funding

There is no external funding.

Conflict of interest

The authors declare there are no conflicts of interest between them. There was no external funding.

References

Biff, F.P., Deborah, J.C. (2020). Blood pressure lowering and potassium intake. Journal of Human Hypertension 34: 671-672. URL: https://doi.org/10.1038/s41371-020-00396-1. Accessed 29/10/2025.

Biomedicines 11(6): 1535. URL: https://doi.org/10.3390/ biomedicines11061535 .

Boukeria, S., Amel, B. E. N. B. O. T. T., Kanza, K. A. D. I., Debbache, K., Gueniche, A. (2019). Etude phytochimique et évaluation de l'activité anticoagulante des composés phénoliques du Curcuma longa L. *Revue des bio ressources*, – 9(2), 11-11.

Burk, R.F. (2002). Seleniun, an antioxidant nutrient. Nutr Clin Care – 5: 47-49.

Chan, R.J., Parikh, N., Ahmed, S., Ruzicka, M., Hiremath, S. (2024). Le contrôle de la pression artérielle devrait se concentrer sur plus de potassium: controverses dans l'hypertension. Hypertension1 – (3): 501-509.

Chanda, S., Parekh, J., Vaghasiya, Y., Dave, R., Baravalia, Y., Nair, R. (2015). Medicinal Plants - From Traditional Use to Toxicity Assessment: A Review: Int J Pharm Sci Res, – 6(7), 2652–2670. URL: URL: https://doi.org/1013040/IJPSR0975-82326.

Chinwendu, S., Ejike, E., Ejike, B., Oti, W., Nwachuku, I. (2016). Phytochemical properties of Uziza leaves (Piper guineense). *European Journal of Pure and Applied Chemistry* – 3 (2). ISSN 2398-138.

De Ruijter, A. (2008). Strychnos afzelii Gilg. Internet]. Record from Protabase. Schmelzer G.H. & (Editors) (Plant Resources of Tropical Africa – 11(1): 565. Medicinal Plants 1. Wageningen,

Fuloria, S., Mehta, J., Chandel, A., Sekar, M., Rani, N.N.I.M., Begum, M.Y., Subramaniyan, V., Chidambaram, K., Thangavelu, L., Nordin, R., Wu Y.S., Sathasivam, K.V., Lu, P.T., Meenakshi, D.U., Kumarasamy, V., Azad, A.K., Fuloria, N.K., (2022) Une revue complète sur le potentiel thérapeutique de *Curcuma longa* Linn. par rapport à son principal constituant actif, la curcumine. *Devant. Pharmacol.* – 13: 820806. DOI: 10.3389/fphar.2022.820806

Gbolo, B. Z., Nachtergael, A., Tshibangu, D. S., Nicole, M., Victoire, N., Memvanga, P. B., Duez, P. (2023). In Vitro Biological Activities of Drepanoalpha® Ethanolic Extract, A Justicia Secunda and Moringa Oleifera-Based Phytomedicine Proposed for The Symptomatic Treatment of Sickle Cell Disease. *Journal of Fundamental and Applied Pharmaceutical Science*, – 3(2), 64-82.

Ghorbani, Z., Hekmatdoost, A., & Mirmiran, P. (2014). Antihyperglycemic and insulin-sensitizing effects of turmeric and its main constituent, curcumin. *International journal of endocrinology and metabolism*, – 12(4).

Grugeau, C. 1995. Curcuma longa L. (Zingiberacées).136f.; ill. tabl.; cm (Thèse: Pharm.; Limoges).

Haddy, F.J. (2006). Role of K in regulating blood flow and blood pressure. *American Physiological Society Journal*. URL: https//journals.physiology.org.

HMPC. (2018). Committee on Herbal Medicinal Products. Guideline on non-clinical documentation in applications for marketing authorization/registration of well-established and traditional herbal medicinal products. Guideline on non-clinical documentation in applications. EMEA/HMPC/32116/2005 Rev.1, 2018, 1–7. URL: https://doi.org/10.1038/nature12198.

Isikhuemen, E.M., Ogbomwan, B.O., Efenedu, I.U. (2020). Evaluation of Phytochemical and Mineral Constituents of *Piper guineense* Schum. & Thonn. And Piper Umbellatum L.: Implications for Ethnomedicine. European Journal of Medicinal Plants – 31(1): 84-97. Article no EJMP.54232 ISSN:2231-0894, NLMID: 101583475.

Ivbarue, F.O., Olanipekun, M.K., Oseni, O.A. (2021). "Dépistage phytochimique, potentiel antioxydant et composés nutritionnels des graines d'Aframomum melegueta et de Syzygium aromaticum à Ibadan, État d'Oyo, Nigeria". *Journal de recherche sur les plantes asiatiques* – 8 (3): 10-21. URL: https://doi.org/10.9734/aprj/2021/v8i330176.

Jansen, P. C. M., & Cardon, D. (Eds.). (2005). Ressources végétales de l'Afrique tropicale: Colorants et tanins. Fondation Prota.

Jeong, J.Y., Jung, I.G., Yum, S.H., Hwang, Y.J. (2023). Effets inhibiteurs synergiques in vitro des combinaisons d'extraits de plantes sur la croissance bactérienne du *Staphylococcus aureus* résistant à la méthicilline. *Produits pharmaceutiques* (Bâle). 20 octobre 2023; 16(10): 1491. DOI: 10.3390/PH16101491. PMID: 37895962

Karlsson, F.H., Tremardi, V., Intawat, N., Bergström, G., Beher, C.J., Fagerberg, B., Nielsen J., Bäckhed, F. (2013). Gut metagenome in European women with normal, impaired, and diabetic glucose control. *Naturel* – 498: 99-103.

Khan, S., Munir, A., Fayyaz, O., Hassan, A. (2024). Phytochemical, Ethnobotanical, and Pharmacological Activities of Aframomum melegueta. In *Ethnobotanical Insights into Medicinal Plants* (pp. 241-278). IGI Global.

Kifle Z.D., Debeb S.G., Belayneh Y.M. *In Vitro* α-Amylase and α-Glucosidase Inhibitory and Antioxidant Activities of the Crude Extract and Solvent Fractions of *Hagenia abyssinica* Leaves. Hindawi BioMed Research International, 2021, Article ID 6652777, – 9 p. URL: https://doi.org/10.1155/2021/6652777

Lekshmi, P., Ranijith, A., Nisha, V., Nirmala, M., Raghu, K. (2013). In vitro antidiabetic and inhibitory potential of turmeric (Curcuma longa) rhizome against cellular and LDL oxidation and angiotensin converting enzyme. J Food Sci Technol – 51(12): 3910è7. DOI: 10.1007/s13197-013-0953-7

Liu, C., Yuan, Y., Zhou, J., Hu, R., Ji, L., Jiang, G. (2020). Piperine ameliorates insulin resistance via inhibition of metabolic inflammation in monosodium glutamate-treated obese mice. BMC. Endocr disorder – 20 (152). URL: https://doi.org/10.1186/s12902-020-00617-1.

Mayele, B. M., Mbadiko, C. M., Mubwele, A., Nyamangombe, G. I., Kabamba, N. N., Ngbolua, K.T.N., Mbemba, T. F. (2025). Antioxidant, anti-inflammatory, and antidiabetic activities of the combination of *Curcuma longa* (Zingiberaceae), *Aframomum melegueta* (Zingiberaceae), and *Piper guineensis* (Piperaceae) compared to plants alone. *Orapuh Journal*, – 6(5), e1246. URL: https://doi.org/10.4314/orapj.v6i5.46

Mbadiko, C., Bongo, G., Matondo, A., Kilembe, J., Nzundu, J. P., Ngombe, N., Mpiana, P. (2024). In silico analysis of the anti-inflammatory activity of curcuminoids and/or curcumin metabolites on Cox-1 and Cox-2.

Mbadiko, M. C., Koto-te-Nyiwa Ngbolua, J.-P., Ngiala Bongo, G., Mbo Nzundu, J. P., Kafuti Makengo, G., Bekomo Iteku, J., D'Alesthu, J., Yandju, M.-C., Kapepula Mutwale, P., Kabamba Ngombe, N., Mbemba Fundu, T., Tshimankinda Mpiana, P. (2024). Optimization of the anti-inflammatory activity of curcumin in combination with extracts of *Piper capense* and some *Aframomum* species. *African Journal of Pharmacy Research and Development*, – 16(3), 64–79.

Mbadiko, M.C., Bongo, G., Ngbolua, K.N., Ngombe, N., Kapepula, P., Yandju, M.C., Mpiana, P.T, Mbemba, F.T. (2023). Uses, phytochemistry, and biological activity of the *Piper* genus: a review. *Journal of Medicinal Herbs*, 2023. – 14 (1): 1-17.

Mbadiko, M.C., Koto-te-Nyiwa Ngbolua, J.-P., Ngiala Bongo, G., Mbo Nzundu, J. P., Kafuti Makengo, G., Bekomo Iteku, J., D'Alesthu Yandju, M.-C., Kapepula Mutwale, P., Kabamba Ngombe, N., Mbemba Fundu, T., Tshimankinda Mpiana, P. (2024). Optimization of the anti-inflammatory activity of curcumin in combination with extracts of *Piper capense* and some *Aframomum* species. African Journal of Pharmacy Research and Development, – 16(3), 64–79.

Mbemba, F., Mbadiko, C.M., Ngbolua K.T.N., Bongo, N.G., Mbo Nzundu, J.P., Makengo, K.G., Bekomo Iteku, J., Yandju, M.C., Kapepula Mutwale, P., Ngombe, K.N., Mpiana, P.T. (2023). Optimization of the anti-inflammatory activity of curcumin in combination with extracts of *Piper capensis* and some *Aframomum species*.

Mbemba, F.T. (2020). Alimentation et prévention des maladies : Diabète, maladies cardiovasculaires, cancer et ostéoporose, Le Harmattan RD Congo: 215 p.

Menchikov, L.G., Popov, A.V. (2023). Physiological activity of trace element germanium, including anticancer properties.

Mohammed A., Gbonjubola V. A., Koorbanally N. A., Md. Shahidul Islam (2017). Inhibition of key enzyme linked to type 2 diabetes by compounds isolated from *Aframomum melegueta*.

Monteiro, A.O., Carvalho, J.L., da Silva, H.C., Nascimento, G.O.D., Silva, A.M.A., Trevisan, M.T.S., Santiago, G.M.P. (2021). *Bauhinia pulchella* : constituants chimiques, activités antioxydantes et inhibitrices de l'alpha-glucosidase. Nat Prod Rés. 2022 mars ; 36(6): 1604-1609. DOI: 10.1080/14786419.2021.1887176. Epub 13 février 2021. PMID: 33586542.

Ngbolua, K. N., Rafatro, H., Rakotoarimanana, H., Ratsimamanga, U. S., Mudogo, V., Mpiana, P. T., Tshibangu, D. S. T. (2011). Pharmacological screening of some traditionally used antimalarial plants from the Democratic Republic of Congo compared to their ecological taxonomic equivalence in Madagascar. International Journal of Biological and Chemical Sciences, – 5(5), 1797–1804. URL: https://doi.org/http://dx.doi.org/10.4314/ijbcs.v5i5.3

Ogbunugafor, H.A., Ugochukwu, C.G., Kyrian-Ogbonna, A.E. (2017). The role of spices in nutrition and health: a review of three popular spices used in Southern Nigeria. *Food Quality and Safety*, – 1(3): 171–185. Doi:10.1093/fqsafe/fyx020.

Oleiwi, E.H., Hussein, S.Z. (2024). Exploring the link between iron status and catalase activity in Type 2 diabetes mellitus. J Fac Med Baghdad – 66(3): 300-310. Doi: https://doi.org/10.33007/jfacmedbaghdad.6632302

Omosa, L.K., Midiwo, J.O., Kuete, V. (2017). Chapter 19 – *Curcuma longa*. In V. Kuete (Ed.), *Medicinal spices and vegetables from Africa* (pp. 425–435). Academic Press. URL: https://doi.org/10.1016/B978-0-12-809286-6.00019-4.

Osuntokun. Oludare (2020). Aframomum Melegueta (Grains of Paradise). *Annals of Microbiology and Infectious Diseases* – 3(1): 1-6. DOI:10.22259/2637-5346.0301001

Palomar, A., Gonzalez-Martin, R., Quiñonero, A., Pellicer, N., Fernandez-Saavedra, R., Rucandio, I., Fernandez-Martinez, R., Conde-Vilda, E., Quejido, A.J., Zuckerman, C., Whitehead, C., Scott, R.T., Dominguez, F. (2023). La bioaccumulation d'oligo-éléments non-essentiels détectée dans le liquide folliculaire, l'urine et le plasma chez les femmes est associée à de mauvais résultats reproductifs après un transfert d'embryon euploïde unique : étude pilote. Int J Mol Sci. – 24(17): 13147. Doi: 10.3390/ijms241713147. PMID : 37685954 ; PMCID : PMC10487767

Partial, V., Sukapaka, M., Sharma, S., Pratap, K., Singh, D., Padwad, Y. (2015). Synergetic effect of Curcumin and Piperine in suppression of DENA-induced hepatocellular Carcinoma in rats. Environmental Toxicology and Pharmacology – 40(2): 445-452. URL: https://doi.org/10.1016/j.etap.2015.07.012.

Pharmaceutical biology – 55 (1). URL: https://doi.org/10.1080/13880209.2017.1286358

Platel K., Srinivasan K. (2003). In vitro influence of spices and spice-active principles on digestive enzymes of rat pancreas and small intestine. Nahrung: – 47(6): 408-12. Doi: 10.1002/food. 200390091. PMID

Platel, K., Srinivasan, K. (2000). Influence des épices diététiques et de leurs principes actifs sur les enzymes digestives pancréatiques chez les rats albinos. Nahrung. – 44(1): 42-6.

Prasad A.S., Bao B. Mécanismes moléculaires du zinc comme médiateur pro-antioxydant : implications thérapeutiques cliniques. Antioxydants (Bâle). 6 juin 2019; – 8(6):164. Doi: 10.3390/antiox8060164. PMID: 31174269; PMCID: PMC6617024.PMC6617024.

Prieto-Rodríguez, J.A., Lévuok-Mena, K.P., Cardozo-Muñoz, J.C., Parra-Amin, J.E., López-Vallejo, F., Cuca-Suárez, L.E., Patiño-Ladino, O.J. (2024). In Vitro and In Silico Study of the α-Glucosidase and Lipase Inhibitory Activities of Chemical Constituents from Piper cumanense (Piperaceae) and Synthetic Analogs. Plants 2022, – 11, 2188. URL: https://doi.org/10.3390/ plants11172188

Purwadi, I., Casey, L.W., Ryan, C.G., Erskine, P.D., van der Ent, A. (2022). X-ray fluorescence spectroscopy (XRF) for metallome analysis of herbarium specimens. Plant Methods, – 18(1), 139. URL: https://doi.org/10.1186/s13007-022-00958-z

Ramkumar, S., Thulasiram, H.V., Ravi Kumar, A. (2021). Improvement in serum amylase and glucose levels in diabetic rats on oral administration of bisdemethoxycurcumin from

Curcuma longa and limonoids from Azadirachta indica. *Journal of Food Biochemistry*, – 45(4), e13674.

Schmelcher G. H. (2008). *Hilleria latifolia* (Lam) H. Walter. [Internet]. Record from Protabase. Schmelzer G.H. & (Editors) (Plant Resources of Tropical Africa 11(1):327. Medicinal Plants. 1. Wageningen, Netherlands. URL: http://database.prota.org/search.htm.

Tchounwou, P. B., Yedjou, C. G., Patlolla, A.K., Sutton, D. J. (2019). Heavy metal toxicity and the environment. In Molecular, Clinical and Environmental Toxicology (pp. 133–164). Springer.

Teng, H., Yuan, B., Gothai, S., Arulselvan, P., Song, X., Chen, L. (2018). Dietary triterpenes in the treatment of type 2 diabetes: To date. *Trends in Food Science & Technology*, – 72, 34-44.

Vafaeipour, Z., Razavi, B. M., Hosseinzadeh, H. (2022). Effects of turmeric (Curcuma longa) and its constituent (curcumin) on the metabolic syndrome: An updated review. *Journal of Integrative Medicine*, – 20(3), 193-203.

Wang, Y.S., Teng, G.Q., Zhou, H., Dong, C.L. (2020). Germanium reduces inflammatory damage in mammary glands during lipopolysaccharide-induced mastitis in mice. Biol Trace Elem Res.; 198(2): 617–26. URL: https://doi.org/10.1007/ s12011-020-02106-x. TY - JOURER

Wickramaratne, M.N., Punchihewa, J.C., Wickramaratne, D.B.M. (2016). In vitro alpha amylase inhibitory activity of the leaf extracts of Adenanthera pavonina. Complementary and Alternative Medicine, 2016, – 16: 466.

Widowati, W., Wargasetia, T. L., Afifah, E., Mozef T., Kusuma, H.S.W., Nufus, H., Arumzardana, S., Amalia, A., Rizal, R. (2018). Antioxidant and antidiabetic potential of *Curcuma longa* and its compounds. Asia J Agri & Biol – 6(2): 149-161.

Yu Sheng Toh, Chooi Ling Lim, Anna Pick Kiong Ling, Soi Moi Chye, and Rhun Yian Koh*. (2019). Overview of the Pharmacological Activities of Aframomum melegueta. *Pertanika Journal of Tropical Agricultural Science*, – 42 (1): 1-13.

Zang, H., Kitts, D. (2021). Turmeric and its bioactive constituents trigger cell signaling mechanisms that protect against diabetes and cardiovascular diseases. *Molecular and Cellular Biochemistry* – 476: 3785–3814. URL: https://doi.org/10.1007/s11010-021-04201-6.

Zhang, P., Li, T., Wu, X., Nice, E.C., Huang, C., Zhang, Y. (2020). Stress oxydatif et diabète : stratégies antioxydantes. Front Med. 2020 octobre ; – 14(5): 583-600.

Doi: 10.1007/s11684-019-0729-1. Publié en ligne en 2020 le 4 avril. PMID: 32248333.

submitted 16.11.2025;
accepted for publication 30.11.2025;
published 30.12.2025

Contact: dmbokuyo@yahoo.fr

The European Journal of Technical and Natural Sciences 2025, No 6
ISSN 2414-2352

PREMIER Publishing
ppublishing.org

Section 3. Chemistry

DOI:10.29013/EJHSS-25-6-29-33

SELECTION OF HIGHLY ACTIVE MATERIAL FOR SEMICONDUCTOR SENSORS OF CARBON MONOXIDE, HYDROGEN AND HYDROCARBONS BASED ON INDIVIDUAL METAL OXIDES

Eshkobilova Mavjuda [1], Smanova Zulaikho [2], Abdurakhmanov Ergashboy [3]

[1] Samarkand State Medical University, Samarkand, Uzbekistan

Zulaikho Smanova

[2] National University of Uzbe kistan named after Mirzo Ulugbek, Republic of Uzbekistan, Tashkent

[3] Samarkand State University Samarkand, Uzbekistan

Cite: *Eshkobilova M., Smanova Z., Abdurakhmanov E. (2025). Selection of Highly Active Material for Semiconductor Sensors of Carbon Monoxide, Hydrogen and Hydrocarbons Based on Individual Metal Oxides. European Journal of Technical and Natural Sciences 2025, No 6.* https://doi.org/10.29013/EJHSS-25-6-29-33

Abstract

In this work, we investigated the catalytic activity of individual metal oxides (CuO, MnO_2, SnO_2, Cr_2O_3, Co_2O_3, ZrO_2, TiO_2, etc.) in the oxidation of carbon monoxide (CO), hydrogen (H_2), and hydrocarbons (methane, n-octane) in order to select the optimal material for semiconductor gas sensors. Experiments were conducted using gas-air mixtures at a controlled temperature of 350 °C and a fixed flow rate. The activity and selectivity of the oxides, as well as their dependence on physical properties, such as the metal–oxygen bond length and band gap, were determined. The results show that CuO, MnO_2, and SnO_2 are the most active oxides for CO oxidation, and ZrO_2 is the most active for the selective detection of H_2. These findings enable the creation of semiconductor sensors with improved operational and metrological characteristics.

Keywords: *semiconductor sensor, carbon monoxide, hydrogen, hydrocarbons, metal oxides, catalytic activity, selectivity*

Introduction

Semiconductor sensors are widely used to monitor toxic and flammable gases, such as CO, H_2, and hydrocarbons, in industry and households. The main challenge in developing such sensors is selecting an active material with high catalytic activity and selectivity for the target gases. Metal oxides are

promising candidates due to their high stability, catalytic activity, and the ability to fine-tune their properties.

The aim of this work is to identify the most active and selective individual metal oxides for the development of semiconductor sensors capable of reliably detecting CO, H_2 and hydrocarbons in gas mixtures with different component concentrations.

Methodology

Selection of material: metal oxides CuO, MnO_2, SnO_2, Cr_2O_3, Co_2O_3, ZrO_2, TiO_2, WO_3, NiO, SiO_2 and Al_2O_3 were selected as the objects of study.

Catalyst preparation: The oxides were deposited on an inert support (Al_2O_3 or SiO_2) using the sol-gel method to form an active catalytic layer ~1 mm thick. For some catalysts, Pt or Pd were added to improve activity.

Performance control: The physical properties of the materials – metal–oxygen bond length, band gap, and particle size – were taken into account when analyzing the results.

Activity determination: oxidation of CO, H_2 and hydrocarbons was carried out at 350 °C with a fixed flow of gas-air mixture (10 ml/min) and known partial pressure of the components.

In order to develop sensors that monitor carbon monoxide, methane and hydrocarbons (gasoline vapors, natural gas and others) in gas and gas-vapor mixtures, the oxidation processes of these substances in the presence of various metal oxides were studied.

The experiments were carried out in a reactor with a constant catalyst bed, the diagram of which is shown in Figure 4.1.

Figure 1. *Scheme of the installation for catalytic oxidation of combustible substances*

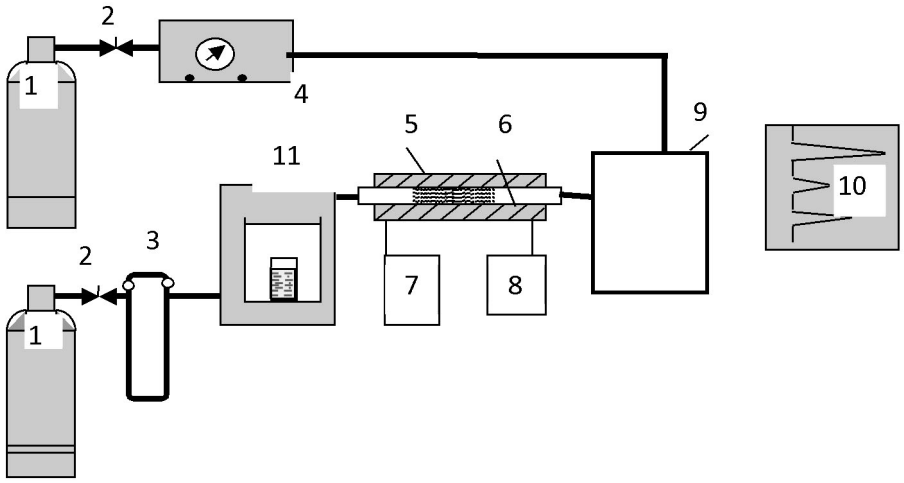

1 – gas cylinders;
2 – fine gas regulation valve;
3 – rheometer;
4 – gas preparation device;
5 – electric furnace;
6 – reactor with catalyst;
7 – current source;
8 – millivoltmeter;
9 – chromatograph;
10 – recording device KSP-4;
11 – source of the mixture being studied (gas or steam)

The main elements of the installation include: a reactor with a catalyst, a device for preparing and feeding gases, a chromatographic dispenser and a gas chromatograph.

Experimental part

The reactor is a heat-resistant glass tube equipped with an electric furnace. The required temperature in the reactor is maintained with an accuracy of ±1.0 °C using a thermostat. Temperature changes are monitored by a thermocouple connected to a millivoltmeter.

During the experiment, the gas-air mixture from the cylinder is fed through the rheometer into the reactor.

After the reaction mixture passes through the catalyst bed in the reactor, a certain

portion of this mixture is periodically directed into the chromatographic column using a metering valve.

The carrier gas from the cylinder passes through a fine-tuning regulator, a gas preparation unit (GPU), and a metering valve before entering the chromatography column. When a sample is injected, the carrier gas flow passes through the metering valve ring and captures a certain portion of the gas-air mixture.

The degree of oxidation of the combustible component is monitored by recording chromatograms of the mixture before and after it passes through the catalyst layer.

Chromatographic analysis of a gas mixture (carbon monoxide, hydrogen, methane mixed with air) is carried out under the following conditions:

– detector – katharometer;
– detector and column temperature – room temperature;
– carrier gas flow rate – 1.5–3.5 l/h (depending on the composition of the gas-air mixture);
– column length – 1.5–3 m, internal diameter – 3 mm, filling – activated carbon.

The quantity of components is determined using a pre-constructed calibration curve.

An LHM-8MD chromatograph with a flame ionization detector was used to monitor hydrocarbon (gasoline vapor) oxidation processes. The following conditions were used for chromatographic monitoring of gasoline and diesel fuel oxidation products:

– a chromatographic column filled with 5% apieson-L on Chromaton, 1 m long and 3 mm internal diameter;

– column temperature – 150–200 °C; the speed of transporting argon is 50 ml/min.

Additional control of the hydrocarbon oxidation process was carried out by determining carbon dioxide in the reaction products using potentiometric titration.

The completeness of oxidation of the component being determined was used as a criterion for the suitability of the selected catalyst for creating the sensing element of a semiconductor sensor. Considering that the completeness of oxidation of combustible substances depends on their composition, process temperature, the concentration of reactants, and the ratio of components in the gas mixture passing through the reactor, we examined the role of each of these factors during the study.

Typically, catalysts used for the oxidation of hydrogen, carbon monoxide, methane and hydrocarbon vapors are noble metals, alloys, metal oxides and their mixtures, as well as systems based on platinum group metals.

As follows from the literature, oxidation reactions of combustible gases on Pt- and Pd-based catalysts have been studied in considerable detail. Such studies are considerably less widespread in the field of semiconductor materials. Among such compounds (oxides, sulfides, chlorides, etc.), rare metal oxides exhibit the highest activity, since, according to coordination theory, the presence of free coordination sites in the cationic sphere is necessary for the catalytic reaction to occur. Chlorides and sulfides (Cl^- and S^{2-}) have a radius larger than oxygen and completely shield the cation, resulting in a significant reduction in catalytic activity.

Metal oxides exhibit significantly higher catalytic activity in the oxidation of CO, H_2, CH_4, and other gases, which is why they are widely used in gas masks and in industrial and automotive exhaust gas purification systems. In combustible gas oxidation reactions, oxides are significantly more stable than metals, as they are stable in the presence of oxygen.

Along with activity and stability, one of the most important characteristics of a catalyst is its selectivity – the ability to accelerate only one reaction out of several occurring simultaneously. Therefore, the problem of selectivity in catalytic processes is of fundamental importance. It should be noted that when studying the oxidation of combustible substances, researchers primarily focus on the selection of active catalysts. Issues of catalyst selectivity have been much less studied. Moreover, due to the incomparability of data obtained for different catalysts under different conditions, it is impossible to draw even tentative conclusions about the selectivity of the oxidation of individual substances in the presence of other combustible gases and vapors. Developing a scientific basis for catalyst selection is one of the key tasks of catalysis. However, to date, a satisfactory theory of selectivity has not been developed.

Existing theories of catalysis – electron, multiplet, intermediate compound theory, and acid-base catalysis – define a number of properties of a solid that suggest its selective action in a given reaction, but none of these properties can be considered an exact criterion for catalytic selectivity. Therefore, the selection of active and selective catalysts is currently primarily accomplished experimentally. However, advances in the study of chemisorption and the mechanism of catalysis make it possible to significantly reduce the time required to select a catalyst for a specific reaction and identify a number of patterns.

Based on the above, the main objective of the research devoted to the development of a semiconductor gas sensor is the creation of selective catalytic systems with improved performance properties and metrological characteristics.

The catalyst for a sensor designed to detect natural gas and hydrocarbon vapors in industrial and automotive emissions was selected in the presence of hydrogen, carbon monoxide, methane, and other gases that occur together with hydrocarbons in various sources.

Aluminum and silicon oxides exhibit low activity in oxidation-reduction reactions. Therefore, we used aluminum oxide and silicon oxide as an inert substrate and as a carrier for the immobilization of active metal oxides. Formation of a catalytically active layer on the surface of the inert carrier was achieved using sol-gel technology.

To test the catalytic properties, the metal oxide was applied to an inert carrier by treatment with solutions of the corresponding metal salts (nitrates, carbonates or oxalates), followed by drying at 100–130 °C for 2.5–3 hours and calcination at the salt decomposition temperature for 3 hours.

Catalysts containing platinum and palladium were prepared by impregnating the carrier with aqueous solutions of chloroplatinic and chloropalladic acids, then drying at 130 °C and calcining at 500–700 °C.

Experiments to select optimal conditions for the oxidation of CO, H_2 and hydrocarbons in the presence of metal oxides were carried out at a gas-air mixture flow rate of 5 l/h and in a wide range of concentrations of combustible components. In semiconductor sensors, the active components of the gas-sensitive film ensure the oxidation of combustible gases predominantly in a thermodynamically favorable direction with the formation of carbon dioxide and water vapor.

Experiments on the selection of active and selective metal oxides for gas-sensitive films of a semiconductor sensor designed to detect hydrogen, methane, carbon monoxide and hydrocarbon vapors were carried out using the following oxides: Fe_2O_3, MnO_2, TiO_2, ZnO, SnO_2, WO_3, ZrO_2, Cr_2O_3, Cu O.

Reaction conditions: catalyst layer in the reactor was 5.0 mm, the rate of gas-air mixture passage through the catalyst layer was 10 ml/min, samples were taken every 10 minutes for reaction mixture analysis, the volume of each sample was 0.1 ml. Catalysts were prepared on the basis of metal oxide powders, particle size ~1 mm. The partial pressure of the reducing component (CO, CH_4, n-octane and H_2) in the gas-air mixture for all components was: Pcom. = 0.02 atm., PO_2 = 0.2 atm., Rumumium = 1.0 atm.

The composition of the reaction mixture before and after the catalyst layer was monitored using gas chromatography. The quantities of individual components during analysis were determined using pre-constructed calibration curves for each component.

The table shows that the most easily oxidized compound in the carbon(II) oxide-methane-n-octane-hydrogen system is hydrogen. For most of the metal oxides studied, the oxidation state of hydrogen is 50–100%.

When determining hydrogen, the highest selectivity is observed for zirconium oxide: in its presence, the oxidation of hydrogen reaches 100%, while the oxidation of carbon(II) oxide, methane and n-octane is, respectively: CO – 6%, CH_4 – 2.1%, n-octane – 0.9%.

These table results confirm the feasibility of using ZrO_2 as the main component of a gas-sensitive film in a semiconductor sensor that selectively detects hydrogen in the presence of carbon monoxide and hydrocarbons. Moreover, with this gas-sensitive material, carbon monoxide and hydrocarbons are virtually not oxidized under identical conditions.

According to the data in Table 3.1, at a temperature of 350 °C, all of the catalysts studied exhibited carbon monoxide oxidation to varying degrees. The most active metal oxides for this process include CuO, MnO_2,

SnO_2, and Cr_2O_3. In the presence of these oxides, CO oxidation under the experimental conditions ranged from 70 to 91%.

Oxides exhibiting moderate activity for the carbon monoxide oxidation process include Fe_2O_3, CoO, Co_3O_4, V_2O_5, ZnO, and TiO_2. These oxides provided CO oxidation in the range of 40–68%.

The oxides with low activity and selectivity among the studied compounds were WO_3, NiO, ZrO_2, SiO_2, and Al_2O_3. At a temperature of 350 °C, carbon(II) oxide was practically not oxidized in the presence of SiO_2 and Al_2O_3; its oxidation by atmospheric oxygen amounted to only 2–3%.

Therefore, in subsequent experiments, these oxides were used as an inert carrier in the development of gas-sensitive elements of semiconductor sensors for carbon monoxide monitoring.

Conclusion

Individual metal oxides exhibit different catalytic activities and selectivities in the oxidation of CO, H_2 and hydrocarbons. For semiconductor CO sensors, CuO, MnO_2 and SnO_2 have the best activity. For selective detection of H_2, ZrO_2 is optimal, as it ensures complete oxidation of hydrogen with minimal impact on other components. The highest catalytic activity in the oxidation of hydrocarbons (CH_4 and n-octane) is observed on Co_2O_3, Cr_2O_3, CuO and MnO_2. The obtained data enable the development of highly efficient and selective semiconductor sensors for monitoring toxic and flammable gases in industrial and environmental systems.

References

Sidikova Kh., Abdurakhmanov G. E., Murodova Z. B., Eshkobilova M. E. // Development of a selective sensor for the determination of hydrogen // IOP Conference Series: Earth and Environmental Science // DOI:10.1088/1755-1315/839/4/042086

Pardaeva Sh., Abdurakhmanov Eshkabilova E. M., Muminova N., Sidikova Kh. // Template Synthesis of Nanomaterials based on Titanium and Cadmium Oxides by the Sol-Gel Method, Study of their Possibility of Application As A Carbon Monoxide Sensor (II)//Journal of Pharmaceutical Negative Results ¦ Volume 13 ¦ Special Issue 3 ¦ 2022 // DOI: 10.47750/pnr.2022.13.S03.210 // 1343–1350.

Abdurakhmanov E. and Abdurakhmanova Z., Eshkabilova M., Abdurakhmanov I. E., Muradova Z. // Development of selective gas sensors using nanomaterials obtained by sol-gel process // Journal of Physics: Conference Series,: Journal of Physics: Conf. Series, IOP Conf. Series: Journal of Physics: Conf. Series5//https://iopscience.iop//.org/article/10.1088/1742–6596/2388/1/012155

Abdurakhmanov E., Eshkobilov Sh. A., Eshkobilova M. E. (2015) // Development of a catalyst for a sensitive natural gas sensor // International scientific journal “Symbol of Science” // – P. 7–11.

Eshkobilova M. E., Xodieva N., Abdurakhmanova Z. E. // Thermocatalytic and Semiconductor Sensors for Monitoring Gas Mixtures // World Journal of Agriculture and Urbanization // 2023/6/17//C 9–13.

Nasimov A. M. Eshkobilova M. E. // Gas analyzer (TPG-CH4) for methane monitoring based on thermocatalytic and semiconductor sensors // Journal “Universum: Chemistry and Biology” – No. 6 (60). DOI: 10.32743/UniChem.2019.60.6

Abdurakhmanov Ergashboy Eshkobilova Mavjuda // Zol-gel synthesis of nanocomposites and gaseous materials // The International Conference on “Energy-Earth-Environment-Engineering” // 2023/12//C. 84–85.

submitted 06.11.2025;
accepted for publication 20.11.2025;
published 30.12.2025

Contact: sh1982eshqobilov@mail.ru

The European Journal of Technical and Natural Sciences 2025, No 6
ISSN 2414-2352

PREMIER Publishing
ppublishing.org

Section 4. Geodesy

DOI:10.29013/EJHSS-25-6-34-39

COMPREHENSIVE DIAGNOSTICS OF SLOPE AND SLOPE DEFORMATIONS USING DRONES, GROUND-PENETRATING RADAR AND SATELLITE INTERFEROMETRIC MONITORING

Hatir Volkan [1]

[1] Religh Capital Energy Company Istanbul, Turkey

Cite: *Hatir Volkan. (2025). Comprehensive diagnostics of slope and slope deformations using drones, ground-penetrating radar and satellite interferometric monitoring. European Journal of Technical and Natural Sciences 2025, No 6.* https://doi.org/10.29013/EJHSS-25-6-34-39

Abstract

The article discusses the complex process of diagnosing slope and slope deformation through the combined use of unmanned aerial vehicles (UAV), ground-penetrating radar (GPR), and satellite interferometric monitoring. The article emphasizes that deformation processes can often occur covertly and be accelerated by factors such as humidification, seasonal freezing and thawing cycles, intense precipitation, and human activities. Traditional observation methods often lack the ability to provide sufficient information on the underlying causes and mechanics of these displacements.

The article describes a method that utilizes UAVs to precisely record surface changes, GPR to detect subsurface inhomogeneities, and InSAR to generate spatially distributed displacement time series over large areas. This approach allows for a more comprehensive understanding of the deformation process and its various contributing factors. A simple algorithm for data integration is presented, including the unification of spatial and temporal reference systems, quality-filtering, allocation of activity areas, their detailed analysis, and final risk categorization. The procedure for practical implementation at a selected site is also described.

Keywords: *slope deformations, slopes, landslides, monitoring, unmanned photography, photogrammetry, georadar, GPR, satellite interferometry, InSAR, time series of displacements, diagnostics, risk zoning*

Relevance of the study

The relevance of this study stems from the fact that the stability of slopes directly affects the safety of transportation and engineering infrastructure, as well as mining and construction facilities and buildings in areas prone to landslides. Deformation processes can develop covertly and accelerate with changes in soil water content, seasonal cycles of freezing and thawing, heavy precipitation, and human ac-

tivities such as slope pruning, vibration, and drainage changes. In these conditions, early detection of signs of instability is crucial for preventing emergencies and minimizing the cost of repair and emergency measures.

A variety of factors, including the availability of hazardous sites, the labor intensity required, the time discreteness of observations, and a lack of information about the underlying structure and causes of deformations often limit traditional observation methods. Diagnostics based on a single type of data can only provide a partial picture, as they may capture surface manifestations without fully understanding the internal inhomogeneities of an array, or vice versa, the presence of anomalies without a reliable assessment of actual displacement kinematics.

Combining three complementary technologies – unmanned imaging (for detailed geometry and surface features), georadar (for assessing subsurface inhomogeneities and potential attenuation zones), and satellite interferometry (for objective assessment of time shifts over large areas) – allows us to move from scattered observations to systematic diagnostics. This approach enhances the reliability of identifying hazardous areas, improves the accuracy of engineering solutions (such as drainage, reinforcement, profile recycling, and operating regulations), and creates the basis for risk-based monitoring. In this approach, the frequency and volume of observations are determined by the actual dynamics of deformations and the criticality of the facility, ensuring that resources are allocated efficiently.

The purpose of the study

The aim of this research is to develop and describe a comprehensive approach for diagnosing slope deformations using a combination of unmanned surveying, georadar, and satellite interferometry. We will also create an algorithm to integrate the results and produce a consistent diagnostic model, which will then be used to categorize sites according to their degree of deformation activity.

Materials and research methods

The research materials are based on the analysis of open sources on the engineering and geological classification of slope movements and diagnostic signs of deformations, as well as data obtained through three instrumental methods: unmanned aerial vehicle (UAV) photogrammetry, ground-penetrating radar (GPR), and satellite interferometry (InSAR).

The methodology involves classifying slope movements based on their mechanism and material; comparing diagnostic signs of deformation with their expected spatial distribution; and constructing a comprehensive monitoring system that uses InSAR to identify areas with stable movement trends, UAVs for detailed surface observations and boundary refinement, and GPR for assessing subsurface inhomogeneities related to deformation.

The results of the study

In engineering geology and geotechnics, the term “landslide/slope displacement” is used to refer to the process of moving masses of soil, clastic material, or rocks downhill due to gravity. However, modern terminology recognizes that this phenomenon is not limited to land and is not solely related to sliding in the traditional sense. Instead, it includes various mechanisms such as falling, tipping, spreading, and other types of movement.

Table 1. *Classification of slope displacements by movement mechanism and material type*

Movement mechanism	Rock material	Mainly coarse-grained material	Predominantly fine-grained material
Fall	Rock Fall	Debris collapse	Landslide
Tipping over	Rocky Rollover	Clastic overturning	Ground tipping
Sliding	Rock Slide	Clastic slip	Ground slip
Spreading (stretching of the array)	Rock sprawl	Detrital sprawl	Ground sprawl
Current (flow)	Rocky current	Detrital flow	Ground flow

Source: author’s development

To accurately describe the deformation of slopes and natural terrains, a unified classification system is essential. This system categorizes slopes based on two key factors: the type of material involved and the mode of movement (as shown in Table 1). In applied work, this scheme is important not just as a "formal" tool, but also as a tool that directly determines the expected geometry of the displaced surface, the type of deformations at the edges and sole, as well as a set of diagnostic signs that help to recognize deformations in field and remote data (Landslides: investigation and mitigation).

Below is Figure 1, which clearly illustrates the main mechanisms of slope displacement used in engineering and geological classification.

Figure 1. *The main types of slope deformations (spreading, overturning, rotational and translational landslide, creep, rockfall) (Landslides | Idaho Geological Survey)*

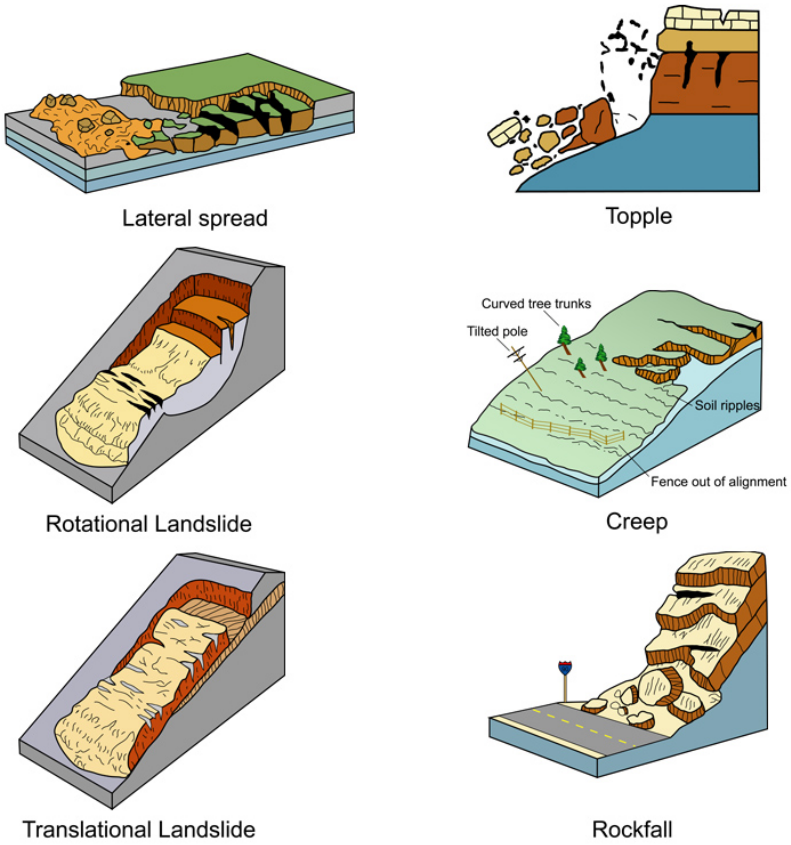

Practical diagnostics of slope stability and deformation is based on understanding that the same event often involves phases and a possible change in kinematics (e.g., an initial displacement along a fracture surface followed by mass movement into a stream). It also involves distinguishing between "activity style" and "stage", which refers to how the deformation propagates and how the body shifts and develops over time.

A separate place in the theoretical foundations is occupied by the rate of deformation, which is a parameter that relates the observed shape to the level of danger and monitoring regulations. In engineering practice, a speed scale is widely used to distinguish classes of movement, from extremely slow to extremely fast. For each class, approximate thresholds in mm/s and typical speeds in familiar units (m/year, m/month, etc.) are given, making it possible to compare the results of repeated surveys, geodesy, or satellite measurements with accepted engineering activity categories and correctly interpret whether the observed change is a sign of creep or indicates acceleration that requires immediate action.

Diagnostic signs of slope and slope deformations are verified by a combination of morphological changes in the terrain and "object" indicators on infrastructure. The most reliable early warning signs include the appearance of new cracks and bulges on the ground sur-

face, deformations of roadways and arches, the presence of areas of moisture/water outlet on the slope, or conversely, the emergence of local "puddles/damming" where previously this had not been observed, as well as signs of displacement of artificial elements: tilt of poles, fences, trees, changes in tension of communications, distortion and cracks in buildings and foundation parts.. It is noted that a single feature may have an alternative explanation. Therefore, practical diagnostics focus on the appearance of a group of features and their spatial relationship to the expected deformation zones (upper part stretching and cracking, lower part bulging and deformation at the sole) (What are the signs of landslide development?).

Drones are used to take detailed surface photos: an orthophoto map and a digital model of the surface are created from overlapping images. In the case of repeated flights, the models are compared over time to identify changes in relief and deformations.

Georadar is used when it is necessary to understand what is going on in the upper layers of the ground: it provides sections of reflections that allow you to distinguish differences in properties (layer boundaries, disturbances, areas with high humidity/decompression) within a certain depth, which decreases sharply in conductive and water-saturated soils. A general scheme of how the reflected signal is sensed and recorded is shown in Figure 2.

Figure 2. *Schematic diagram of GPR sensing: pulse transmission and reception, signal processing and interpreted GPR section (Ground penetrating radar – Mine Closure)*

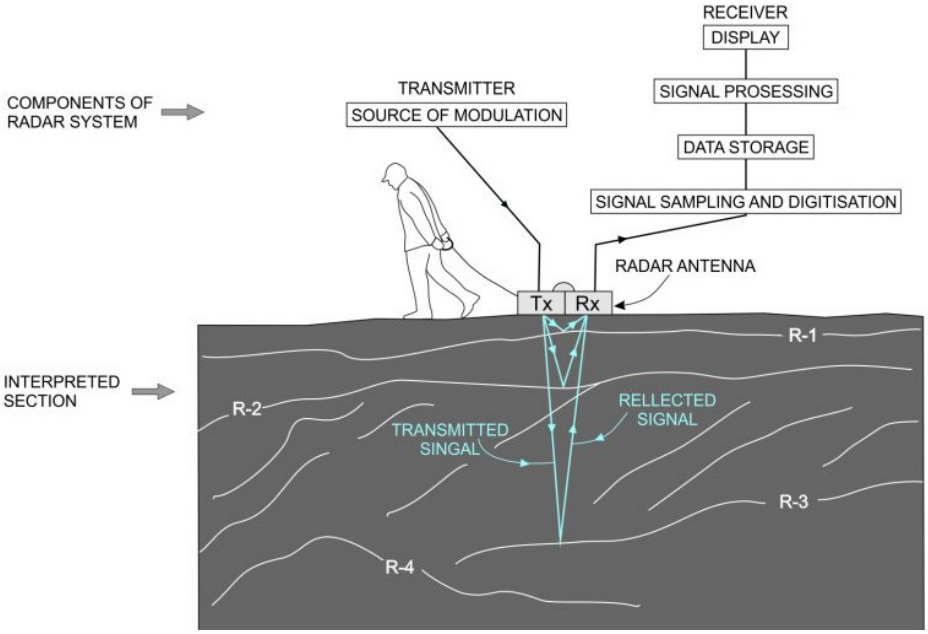

Satellite interferometry (InSAR) is essential for regular regional monitoring. It provides data on offsets along the radar line of sight and over time, which is particularly useful for detecting slow deformations and "background" activity over large areas. The results must always be interpreted with caution, as the direction of the measurement does not always directly coincide with the true displacement vector, and depends on the geometry of the survey.

Table 2. *Characteristics of slope and slope deformation monitoring methods (drone, georadar, In SAR)*

Method	What measures / what shows	Main output materials	A key limitation for interpretation
Drone (UAV, photogrammetry)	Surface geometry and visual manifestations (cracks, ledges, subsidence, blurring)	Orthophotoplane, 3D model/DEM (DS), maps of changes during re-shooting	It requires stable geolocation and accuracy control between shots.

Method	What measures / what shows	Main output materials	A key limitation for interpretation
Ground-penetrating radar (GPR)	Contrasts of properties in the upper stratum, anomalies, boundaries, violations	Radar images (profiles), anomaly maps / interpreted horizons	Attenuation in wet/conductive soils, ambiguity without calibration
In SAR	Time shifts along the line of sight (LOS), velocities/ trends	Velocity maps, time series by points	Decorrelation (vegetation/ snow/ surface changes), LOS geometry

Source: author's development

Table 2 outlines the role of each method in comprehensive monitoring of slopes and slope deformations. It details what is being measured, the data obtained, and the limitations to consider when interpreting results.

The integration algorithm in integrated monitoring starts with bringing data to a common spatiotemporal basis and consistent quality metrics, as the products themselves are inherently different. InSAR provides line-of-sight (LOS) displacements and coherence/ stability indicators for the lens, UAV photogrammetry offers detailed surfaces and textures, and GPR generates profiles and reflection maps that are interpreted based on the physical properties of the medium.

Open manuals and reviews on multi-temporal InSAR emphasize the importance of time series in strain interpretation, as they are sensitive to atmospheric effects, decorrelation, and survey geometry. Time series analysis and quality measurements at each point are crucial for accurate strain interpretation. In order to improve the understandability of LOS offsets and approximately the "engineering" components of motion, data from ascending and descending passes are used in practice. This makes it possible to separate measurements into vertical and east-west components (based on standard assumptions and with the presence of both geometries). This approach is described in open materials on the use of multi-temporal InSAR techniques and the separation of LOS velocities (Multi-temporal In SAR analysis for monitoring ground deformation in Amorgos Island, Greece).

Table 3 presents the minimum data integration algorithm (a sequence of steps and the expected outcome at each stage) that allows you to combine UAV imagery, ground-penetrating radar, and InSAR data into a single model for deformation analysis.

Table 3. *The minimum data integration algorithm*

Stage	Action	Result
1.	Bringing to a single coordinate basis and agreeing on dates	All data is comparable in place and time.
2.	Quality filtering (UAV/InSAR/GPR)	Elimination of «false» changes and noises
3.	Allocation of activity zones by InSAR	Prioritization of sites for detailed survey
4.	UAV details (geometry, features, changes between dates)	Boundaries and manifestations of deformation on the surface
5.	Checking GPR conditions within the identified zones	Subsurface features that support interpretation
6.	Assembling a single model and risk zoning	Map and passport of the site for monitoring decisions and regulations

Source: author's development

The methodology is tested on a specific slope, for which the boundaries of the site, the type of object (slope of excavation/embankment, quarry side, natural slope near the road, etc.), signs of trouble (cracks, ledges, subsidence, erosion, distortion of structures),

and initial conditions (engineering, geological, and hydrogeological data, drainage features, man-made impacts) are determined. At the beginning of the chapter, the object is briefly described and the exact purpose of the methods is formulated: to determine where movement occurs, how it manifests itself on the surface, and what subsurface conditions may be associated with deformation.

Next, the program of work is presented in a single time interval. Using InSAR, a velocity map and a time series of displacements are created, and zones with a stable trend are identified. A drone is used to take detailed surface photographs to obtain an orthophoto and a digital surface model; when re-photographing, changes in the terrain are recorded and the boundaries of deformation phenomena are clarified. Georadar is carried out along profiles within selected zones in order to obtain subsurface sections and interpret any inhomogeneities or boundaries that may explain the observed phenomena.

The main outcome of the testing process is data reconciliation. In SAR identifies areas with dynamic displacement, UAV confirms or clarifies surface features and changes in geometry, and GPR provides additional information about the upper layer thickness. The results are presented as a zoning of the site into stable, under supervision, or active categories, and practical recommendations for improved control or engineering measures such as drainage, strengthening, and limiting impacts. These recommendations indicate which areas require priority attention.

Conclusions

Thus, comprehensive diagnostics of slopes and slope deformations, based on a combination of unmanned surveys, ground-penetrating radar, and satellite interferometry, allows us to move from isolated observations to a more systematic interpretation that considers displacement kinematics, surface manifestations, and subsurface conditions together. This approach reduces the risk of an incomplete or one-sided assessment of the slope condition and increases the reliability of identifying hazardous areas. It also improves the validity of engineering solutions, including drainage and reinforcement measures, forming the basis for risk-based monitoring. Monitoring should be based on the frequency and volume of observations, taking into account the actual dynamics of deformations and the criticality of the object.

References

Ground penetrating radar – Mine Closure [Electronic resource]. – Access mode: https://mineclosure.gtk.fi/ground-penetrating-radar

Landslides | Idaho Geological Survey [Electronic resource]. – Access mode: https://idahogeology.org/geologic-hazards/landslides.

Landslides: investigation and mitigation. chapter 3 – landslide types and processes [Electronic resource]. – Access mode: https://onlinepubs.trb.org/Onlinepubs/sr/sr247/sr247-003.pdf.

Multi-temporal In SAR analysis for monitoring ground deformation in Amorgos Island, Greece [Electronic resource]. – Access mode: https://www.fig.net/resources/proceedings/2019/04_JISDM2019/33.pdf.

What are the signs of landslide development? What do I do if a landslide occurs? [Electronic resource]. – Access mode: https://www.usgs.gov/programs/landslide-hazards/what-are-signs-landslide-development-what-do-i-do-if-a-landslide-occurs.

submitted 09.12.2025;
accepted for publication 25.11.2025;
published 30.12.2025

Contact: impxstudio@gmail.com

The European Journal of Technical and Natural Sciences 2025, No 6
ISSN 2414-2352

PREMIER Publishing
ppublishing.org

Section 5. Mechanical engineering

DOI:10.29013/EJHSS-25-6-40-42

INTEGRATION OF ELECTROCHEMICAL WATER REGENERATION INTO SMART HOME INFRASTRUCTURE: CONCEPT, CALCULATIONS, AND EFFICIENCY

Artem Aleksanian [1]

[1] Yuri Gagarin State Technical University of Saratov, Russia, Moscow

Cite: *Aleksanian A. (2025). Integration of electrochemical water regeneration into smart home infrastructure: concept, calculations, and efficiency. European Journal of Technical and Natural Sciences 2025, No 6.* https://doi.org/10.29013/EJHSS-25-6-40-42

Abstract

This paper proposes the concept of integrating electrochemical water regeneration into smart home infrastructure. It examines the principles of electrochemical processes enabling disinfection, aeration, and chemical restoration of water without reagents. The integration of regeneration modules into the digital home ecosystem is described, including the use of sensor systems and AI-based control algorithms. Engineering calculations of energy efficiency and economic impact are provided for a residential complex of 100 apartments. The results show that implementing electrochemical modules can reduce fresh water consumption by up to 70%, decrease wastewater discharge, and increase household system autonomy.

Keywords: *electrochemical water regeneration, smart home, sustainable water use, reagent-free purification, energy-efficient systems, water cycle*

Introduction

Modern residential complexes and smart homes are characterized by increasing demands for resource autonomy and environmental efficiency. Water is one of the most critical yet limited resources, which necessitates a transition from linear water consumption models to **closed or semi-closed water cycles**.

Traditional purification and disinfection methods – such as mechanical filtration, ion exchange, and chlorination – are not fully compatible with the concept of intelligent domestic systems due to the need for reagent storage and high maintenance costs.

Electrochemical water regeneration solves this issue by allowing **disinfection and chemical correction of water using only electrical energy**, without adding chemical substances.

Methodology

1. Electrochemical Principle

Electrochemical water regeneration is based on controlled electrolysis, in which active oxygen species (O_2, O_3, • OH) are formed

in the anode zone, providing disinfection, while the cathode zone generates reducing agents that adjust the acid-base balance.

As a result, the system can **automatically correct the water's pH** and remove organic and biological contaminants without reagents.

2. Integration into Smart Home Infrastructure

Electrochemical regeneration modules can be integrated into three levels of water management:

- Local level – compact modules installed under sinks or in utility cabinets within each apartment;
- Centralized level – shared building installations connected to a monitoring system driven by artificial intelligence;
- Digital control – real-time monitoring using sensors for pH, conductivity, and temperature, with data transmitted to a home server or cloud system for optimization of operation modes.

Electronic controllers automatically regulate current intensity, treatment duration, and aeration depending on the water's composition.

3. Engineering Calculations

For a residential complex of 100 apartments (150 residents):

- Baseline water consumption: 150 L/person·day = 22,500 L/day;
- Greywater reuse rate: 60%;
- Fresh water savings: 13,500 L/day (≈ 5 million L/year);
- Specific energy consumption: 0.4 kWh/m³;
- Annual energy consumption: 3,000 kWh ≈ 20,000 RUB/year (at 6.6 RUB/kWh);
- Payback period: 3–5 years, considering average water and sewage tariffs of 100–150 RUB/m³.

Results

Integrating electrochemical modules into a smart home provides the following benefits:

1. Significant reduction in water consumption. Up to 70% of household water can be regenerated and reused for non-potable needs such as flushing, irrigation, and laundry.

2. Reagent-free operation. The system eliminates the need for storing or disposing of hazardous chemicals.

3. Energy efficiency. Power consumption is only 10–15% of that required by membrane-based reverse osmosis systems.

4. Environmental safety. Wastewater volume and the load on municipal treatment facilities are reduced.

5. Intelligent management. AI algorithms adapt operation modes to seasonal changes and individual consumption patterns.

6. Compatibility with renewable energy. Electrochemical modules can operate using solar energy, ensuring complete autonomy.

From a sustainability perspective, implementing such systems contributes directly to **UN Sustainable Development Goals (SDGs) 6 – Clean Water and Sanitation** and **11 – Sustainable Cities and Communities**, while reducing the household carbon footprint.

Discussion

The analysis demonstrates that **electrochemical water regeneration** is a technologically mature and economically viable solution for smart home infrastructure. It enables a reduction in water consumption, enhances ecological and operational autonomy, and lays the foundation for integration into broader intelligent building ecosystems.

Future developments in this area should focus on:

- optimizing module design and control algorithms;
- implementing energy storage components (e.g., capacitor banks);
- developing adaptive water-quality diagnostic systems based on neural networks.

References

Kuznetsov, V. A., & Ivanova, E. S. (2021). *Electrochemical Water Purification without Reagents: Theory and Practice*. Bulletin of Engineering Sciences, – (3). – P. 45–53.

Sidorov, A. P., & Mikhailova, T. A. (2022). *Sustainable Water Use Technologies in Smart Buildings*. Energy-Efficient Systems and Ecology, – (4). – P. 12–20.

GOST R 51232–2018. *Drinking Water. General Requirements for Quality Control Methods*.

Johnson, L. E., et al. (2018). *Smart Glasses Having Interfering Light Filtering*. U. S. Patent Application No. 20180031836 A1.

Technical Report – Water Aeration (TEI's FAD System). Experimental Data on Oxygen Saturation Efficiency.

Sevostianov, P. V. (2017). *Method and System for Displaying Three-Dimensional Objects*. U. S. Patent Application No. 20170366805 A1.

submitted 10.10.2025;
accepted for publication 24.10.2025;
published 30.12.2025

Contact: aleksan1retail@gmail.com

The European Journal of Technical and Natural Sciences 2025, No 6
ISSN 2414-2352

PREMIER Publishing
ppublishing.org

Section 6. Medical science

DOI:10.29013/EJHSS-25-6-43-47

THE EVOLUTION OF CHEMICAL PEELS: SAFE SKIN RENEWAL THROUGH CONTROLLED BIOSTIMULATION

Azarenkova Yuliia [1]

[1] Owner, Skin Care Pro LLC, USA, Charlotte

Cite: *Azarenkova Y. (2025). The evolution of chemical peels: safe skin renewal through controlled biostimulation. European Journal of Technical and Natural Sciences 2025, No 6.* https://doi.org/10.29013/EJHSS-25-6-43-47

Abstract

The article explores the development of chemical peels as a safe and effective method for skin renewal. It focuses on the mechanisms of controlled biostimulation that ensure the regeneration and improvement of the skin structure without risk of complications. The article analyzes modern formulas and peeling techniques that promote the activation of natural skin renewal processes, increasing their effectiveness and reducing the recovery period. It emphasizes the importance of a personalized approach and professional supervision of procedures to achieve optimal aesthetic results.

Keywords: *teenagers, chemical peels, controlled biostimulation, skin renewal, skin regeneration, safety of procedures, aesthetic dermatology, modern peels, skin restoration*

Introduction

Chemical peels are a popular procedure in aesthetic dermatology, aimed at skin renewal and rejuvenation. Over time, the method has undergone significant changes, from simple acid treatments to more complex technologies that provide safe and controlled results.

The effectiveness of modern chemical peels lies not only in the removal of the outer layers of the skin, but also in the activation of deeper regeneration processes through biostimulation. This improves skin quality, texture, and elasticity, without causing significant damage or a long recovery period.

Initially, chemical peels were primarily used to treat surface defects. However, with the development of scientific and cosmetic technologies, the range of applications has expanded, safety has increased, and the risk of complications has decreased. Controlled biostimulation is a crucial aspect of modern techniques, which triggers renewal processes at the cellular level, stimulates collagen and elastin synthesis, and improves microcirculation.

The evolution of chemical peels has led to a transition from simple surface treatments to more complex and deeply researched approaches to skin renewal. These methods combine effectiveness and safety, and provide

maximum benefits for patients with minimal risks. This article will provide an overview of the key stages in the development of chemical peels and the modern techniques that ensure their safe and effective use (Kubanova A. A., 2004).

Discussion

It should be noted that the history of chemical peel research dates back several centuries, reflecting the gradual accumulation of knowledge about the effects of chemicals on skin in order to rejuvenate and renew it.

The earliest attempts to use acids for skin improvement date back to ancient civilizations, such as Egypt, Greece, and Rome. Natural acids like citric and tartaric were used to remove upper skin layers and lighten pigmentation. However, scientific research and systematic study of chemical peels did not begin until the XX century.

In 1882, Augustin Bordeaux described the use of phenol for skin disease treatment, which marked the beginning of deep peel development. In the 1920s and 30s, Edwin Prandt and Meredith Cullen developed methods for targeted phenol application, allowing for controlled and deep skin regeneration with minimal complications.

In the 1950s, the French dermatologist Jean Carraud introduced the concept of chemical peels, where he described different levels of exposure – superficial, medium and deep – depending on the type of acid used and the depth of penetration.

At the same time, phenol and alpha-hydroxy acids (AHAs), such as glycolic and lactic acids, which have a milder effect, began to be gradually used, allowing for a wider range of patients and reduced risks. The development of technology in the late XX and early XXI centuries led to the emergence of new products and techniques that combined peeling effects with biostimulation, increasing the safety and efficacy of procedures.

An important milestone was the introduction of standardized protocols and strict patient selection criteria, making it possible to avoid complications and making the procedure more accessible to a wider audience (Minenok, T. A., 2015).

Table 1. *Hardware techniques for safe skin renewal (Hernandez E. I., Ponomarev I. V., Klyuchareva S. V.)*

No.	Methodology	Characteristic
1.	Laser therapy	Initially, ablative lasers (CO_2, Er: YAG) were quite aggressive, but over time, fractional lasers were developed that create microscopic damage zones while leaving the surrounding tissues intact. This allows for a significant reduction in rehabilitation time and risk, while stimulating active neo-collagenesis. Non-ablative lasers and IPL (intense pulsed light) have also been used to stimulate collagen production without damaging the epidermis.
2.	Radio Frequency Lifting (RF)	RF technologies are based on the controlled heating of the skin's dermis, which leads to a reduction in collagen fibers and the stimulation of new collagen production. Through the development of monopolar, bipolar, and multipolar RF systems, as well as microneedle RF technology, deep and precise effects have been achieved.
3.	Ultrasonic Lifting (HIFU)	High-intensity focused ultrasound has been adapted for cosmetology for spot heating of the deep layers of the skin and the musculoskeletal-aponeurotic system (SMAS), which leads to tightening and compaction of tissues.

It should also be noted that the safe renewal of the skin through controlled biostimulation is the result of many years of research and development in the fields of dermatology, cosmetology, and bioengineering. This approach aims to improve

skin quality by stimulating the natural processes of regeneration and rejuvenation in tissues, rather than aggressively removing layers.

A turning point in this approach was the realization that, for a true and long-term improvement of skin, it is necessary to act on deeper structures, such as the dermis, where collagen and elastin are produced. This led to the development of biostimulation, which involves stimulating skin cells (fibroblasts) to produce rejuvenating components on their own (Kuznetsova E. S., Reznikov K. M., 2013).

In the 1980 s and 1990 s, methods aimed at biostimulation began to develop actively. One of the first directions was the use of hyaluronic acid injections, not only to fill wrinkles but also to improve hydration and stimulate collagen production. At that time, mechanisms of action of various peptides and growth factors, which could trigger regenerative processes, were also actively studied.

A significant stage in the development of safe skin renewal was associated with the emergence and improvement of hardware techniques (Table 1).

In parallel with hardware methods, techniques aimed at biostimulation have also been developed.

Polylactic acid (PLLA) was first used as a biostimulant in the 1990 s. This material is completely biodegradable and stimulates fibroblasts to actively produce collagen.

Calcium hydroxyapatite (CaHA) also acts as a collagen-stimulating agent, providing immediate volume and long-term stimulation of collagen synthesis.

PRP (Platelet-Rich Plasma) and PRF (Platelet-Rich Fibrin) are two methods that use the patient's own blood, which is rich in platelets and growth factors. These methods have become popular because they naturally stimulate tissue regeneration and skin rejuvenation.

Mesotherapy and biorevitalization are two cosmetic procedures that aim to deeply moisturize and rejuvenate the skin. Biorevitalization, which literally means "biological revival," involves injecting thin needles into the skin with preparations based on hyaluronic acid. Hyaluronic acid is a naturally occurring substance in our skin that helps retain moisture. During the procedure, non-gel hyaluronic acid with a high degree of purity is often used, sometimes combined with individual amino acids, to quickly hydrate the skin, improve its tone, and give it a fresh appearance.

Injections of a cocktail of vitamins, amino acids, hyaluronic acid, and other bioactive substances are used to improve metabolism and stimulate skin cells.

Results

Today, the concept of "skin renewal through controlled biostimulation" encompasses a wide range of treatments that are characterized by:

– Minimally invasive procedures with a short rehabilitation period, focusing on methods that require minimal recovery time.

– Precise control over exposure, allowing for the regulation of depth, intensity, and area to minimize risks while maximizing effectiveness.

Figure 1. *The effect of hyaluronic acid on skin condition*

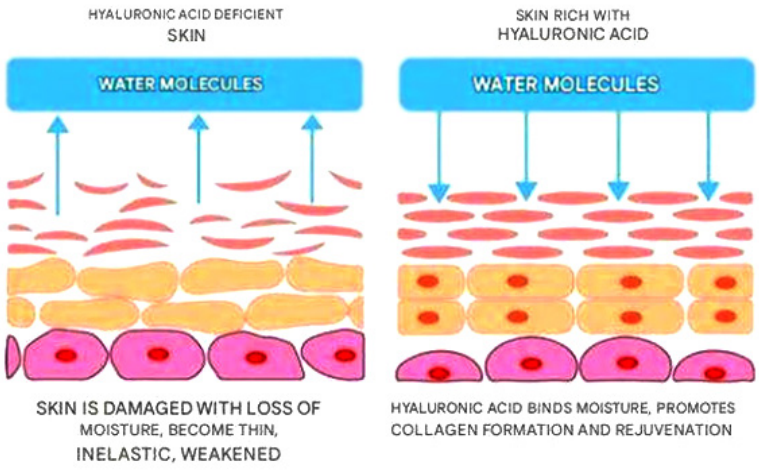

– Stimulation of the body's own resources: activation of natural mechanisms of regeneration and synthesis of collagen, elastin, and hyaluronic acid. When hyaluronic acid enters the dermis, it begins to attract and retain water molecules, improving cell hydration, accelerating metabolism and microcirculation, and stimulating the synthesis of collagen and elastin. In simple terms, the skin receives powerful hydration from within, which immediately improves its appearance: it becomes firmer, smoother, and more radiant. The effect is often noticeable within a few days after the first injection – the face looks refreshed and rejuvenated. Biorevitalization is particularly effective in eliminating signs of skin dehydration, fine lines, and a dull complexion (Fig. 1).

– A combined approach: a combination of various hardware and injection techniques is often used to achieve the best results.

The future of this field is closely linked to the continued development of personalized medicine. This includes the creation of more precise bioactive substance delivery systems and the development of novel biocompatible materials that can selectively stimulate certain cells. Additionally, artificial intelligence will play a crucial role in optimizing treatment protocols and improving the safety of procedures.

Research in the field of cellular technology and gene therapy promises exciting new possibilities for skin rejuvenation and regeneration. Chemical peels, while still a popular method of skin renewal, have been around for a long time and continue to evolve. They use acids to carefully exfoliate damaged skin layers, stimulating regeneration. However, despite improvements in design, the use of chemical peels still presents certain challenges and potential risks that must be carefully considered.

1. Lack of Predictability and Control of Penetration Depth

One of the main challenges in using chemical agents is accurately controlling the depth of their penetration. The depth of peeling depends on several factors, including the type of acid (glycolic, salicylic, lactic, trichloroacetic acid, etc.), its concentration, pH of the solution, number of application layers, exposure time, patient's skin type and thickness, presence of preliminary preparations, and even fat content. An inaccurate calculation of these variables can lead to either insufficient effect (with a too superficial exposure), or, more seriously, excessively deep penetration causing burns, scarring, and prolonged hyperpigmentation. Even experienced specialists sometimes face situations where the skin reacts differently than expected.

2. The risk of post-peeling hyperpigmentation

Post-peeling hyperpigmentation, especially post-traumatic hyperpigmentation (PTH), is a common and unpleasant problem, especially for people with darker skin types (Fitzpatrick III and above). Any inflammation or damage to the skin from peeling can stimulate the production of excess melanin by melanocytes, leading to the appearance of dark spots. The risk of PTH is increased by using an incorrect acid concentration, overly aggressive exposure, lack of proper sun protection before and after the treatment, and if the person has a history of pigmentation problems. Treating PTH can be time-consuming and challenging.

3. Extended recovery period and social limitations

Especially for medium and deep peels, there is a significant period of recovery. After the procedure, the skin may become very red, swollen, and flaky, with crusts forming. This process can last from several days to several weeks, during which patients are advised to avoid contact with the outside world, follow a strict skincare routine, and avoid using makeup. This can cause significant social and psychological discomfort. Even superficial peels may cause slight peeling and redness, requiring some limitation of activity.

4. The possibility of adverse reactions and complications

In addition to hyperpigmentation, chemical peels may cause other complications, such as:

– Burns and scarring: If the acid is applied too deeply or unevenly, it can cause chemical burns, which may lead to the formation of atrophic or hypertrophic scars. This is especially true for sensitive areas and patients with a predisposition to scarring.

– Infections: The disruption of the skin's barrier after peeling leaves the skin vulner-

able to bacterial, viral, or fungal infections, such as an exacerbation of herpes.

– Allergic reactions: Although rare, allergic reactions to ingredients in the peeling solution can occur.

– Persistent redness: This may last for a long time after the treatment, especially for people with sensitive skin or those with rosacea.

– Exacerbation of chronic skin conditions: Peeling can trigger an exacerbation of skin conditions like rosacea, eczema, or psoriasis.

5. Importance of strict sun protection

It's crucial to protect your skin from the sun after a chemical peel, as the skin will be more sensitive and vulnerable.

The skin after chemical peeling is very sensitive to ultraviolet radiation. If patients do not follow strict sun protection rules (using high SPF creams, avoiding direct sunlight, and wearing wide-brimmed hats), the risk of hyperpigmentation and other skin damage increases significantly. This can be a challenge for patients who may not be able to strictly follow these guidelines.

6. Limitations for Certain Skin Conditions

Chemical peels have several contraindications and should not be performed in certain situations. These include active herpes, acute skin inflammation, open wounds or fresh scars, pregnancy or lactation, and when taking certain medications, such as systemic retinoids. Additionally, it is important to be cautious with patients who have dark skin, a tendency towards keloid scars, or who have thin, sensitive, or damaged skin.

7. Requirements for a Specialist

Chemical peels, particularly medium and deep peels, require a high level of qualification and expertise. A specialist should have a deep understanding of skin anatomy and physiology, as well as a thorough understanding of how acids work and how to respond to different skin reactions. Improper selection of a peel, incorrect application techniques, or improper post-peel care can lead to serious adverse consequences.

Conclusions

In conclusion, we would like to emphasize that modern chemical peels have a significant potential to improve skin condition. However, their use should be carefully assessed based on indications and contraindications. A balanced approach, strict adherence to protocols, and adequate post-treatment care by the patient are essential. Continuous improvement in formulas and techniques aims to minimize risks, although they cannot be completely eliminated.

References

Kubanova A. A. Chemical peeling in cosmetology / A. A. Kubanova, et al. // Experimental and clinical dermatocosmetology. 2004. – No. 1. – P. 24–28.

Kuznetsova E. S., Reznikov K. M. Optimization of post-peeling processes in cosmetology / E. S. Kuznetsova, K. M. Reznikov // Proceedings of the XXI International Conference and discussion scientific club "New information technologies in medicine, biology, pharmacology and ecology". Ukraine, Crimea, Yalta-Gurzuf, 2013. – P. 133–134.

Minenok, T. A. Is chemical peeling a worthy substitute for plastic surgery? Bulletin of medical Internet conferences, – 5 (5). 2015. – P. 583–587.

Hernandez E. I., Ponomarev I. V., Klyuchareva S. V. Modern peels: chemical peeling, laser resurfacing, mechanical dermabrasion, plasma resurfacing / E. I. Hernandez, I. V. Ponomarev, S. V. Klyuchareva – M.: "Cosmetics & Medicine", 2011. – 160 p.

submitted 18.10.2025;
accepted for publication 01.11.2025;
published 30.12.2025

Contact: azarenkova.yv@gmail.com

The European Journal of Technical and Natural Sciences 2025, No 6
ISSN 2414-2352

PREMIER Publishing
ppublishing.org

DOI:10.29013/EJHSS-25-6-48-50

SPECIFICATION OF INNOVATIVE MEDICAL TECHNOLOGIES: A PORTFOLIO OF INTELLECTUAL PROPERTY OBJECTS

Dmitrii Smirnov [1]

[1] Surgeon of the highest category, phlebologist, expert in minimally invasive surgery and innovative medical technologies, Vladimir, Russian Federation

Cite: *Smirnov D. (2025). Specification of Innovative Medical Technologies: A Portfolio of Intellectual Property Objects. European Journal of Technical and Natural Sciences 2025, No 6.* https://doi.org/10.29013/EJHSS-25-6-48-50

Abstract

The article presents a specification of innovative projects in the field of medicine covering a wide range of technologies for remote monitoring, diagnostics, and therapeutic influence on human biological systems. Each project is based on the principles of magnetic resonance, nanoscale metrology, and modern spectral–optical methods, ensuring high precision and sensitivity in diagnosis and treatment. The proposed technologies are aimed at contactless research and regulation of the condition of blood, bones, muscles, subcutaneous fat, arteries, and internal organs, as well as disease prevention and early diagnostics. The implementation of these projects creates opportunities for developing mass-use medical devices with high social significance.

Keywords: *magnetic resonance diagnostics, nanoscale metrology, contactless monitoring, preventive medicine, spectral–optical exposure, innovative medical technologies, early diagnostics, blood condition monitoring, subcutaneous fat removal, bone tissue diagnostics, muscle tissue control*

Introduction

Modern medicine requires the integration of highly accurate and safe technologies for diagnostics and therapy that minimize invasiveness and increase treatment efficiency. The presented portfolio of innovative projects offers a comprehensive set of solutions based on magnetic resonance principles, spectral–optical methods, and nanoscale metrology, enabling diagnostics and therapy with high precision and sensitivity.

The projects cover a wide range of applications – from monitoring and assessing blood parameters to non-surgical subcutaneous fat removal, from early cancer diagnostics to bone and muscle condition control. Each project is built upon the use of physical phenomena and advanced materials to create devices capable of operating online, ensuring safety and accuracy of measurements.

The purpose of this article is to systematize and present the specification of innovative projects, reveal their key distinctions, advantages, and potential application areas, and demonstrate opportunities for scaling and implementing these developments in practical medicine.

Project Descriptions

Project 1. Intelligent Monitoring Systems

This project focuses on the development of intelligent monitoring systems providing continuous tracking of critical parameters in biological and industrial processes in real time. The systems integrate sensor data and large-scale data analysis algorithms, enhancing prediction accuracy and reducing error risks. In medicine, the technology is applied for continuous observation of blood parameters, arterial pressure, pulse, and other key physiological indicators, enabling early detection of abnormalities and rapid response to critical conditions.

Project 2. Adaptive Hardware–Software Solutions for Process Automation

The second project introduces adaptive hardware–software platforms for data flow management and resource distribution optimization. The technology processes large data volumes in real time, analyzes information, and constructs optimal routes for logistics and medical systems. In healthcare, the solution is used for patient flow management, access control to diagnostic and therapeutic equipment, and automated allocation of clinical and laboratory resources.

Project 3. Integrated Quality Control Systems Using Resonance Spectroscopy

This project is devoted to creating integrated quality control systems for liquid and gaseous media using resonance spectroscopy. The system enables contactless analysis of biological and technological fluids, identifying anomalies and defects at early stages. In medicine, this allows highly accurate blood, saliva, and other biofluid analyses, determination of component concentrations, and tracking physiological dynamics without invasive intervention.

Project 4. Development of Innovative Materials and Composites

The fourth project focuses on creating new materials and composites with enhanced operational properties – combining strength, durability, and functional adaptability. In medical and engineering practice, this opens opportunities for producing high-precision sensor elements, functional device components for monitoring and therapy, and lightweight durable casings capable of operating in complex environments. The use of composites improves measurement accuracy, reliability, and equipment longevity.

Project 5. Smart Devices and Intelligent Energy Management Systems

The fifth project covers smart devices and energy management systems that optimize the operation of medical instruments, control energy load, and integrate with existing infrastructures. In practice, this enables the development of autonomous diagnostic and therapeutic stations characterized by minimal energy consumption, high operational stability, and suitability for conditions with limited access to external resources.

Project 6. Platforms for Multibrand Distribution and Data Flow Management

This project is dedicated to developing platforms for data flow coordination and activity management in multibrand and multiprofile systems. The platform's architecture provides centralized process control, adaptability to various business models, and rapid decision-making based on data analytics. In healthcare, this enables integration of data from multiple devices and laboratories, ensuring comprehensive health monitoring and unified diagnostic information flow.

Project 7. Integration of Medical, Engineering, and Information Technologies

The seventh project focuses on the creation of intelligent diagnostic and monitoring systems that integrate medical, engineering, and IT approaches. The use of modern sensor platforms, data processing algorithms, and machine learning methods allows early detection of critical patient conditions, disease progression prediction, and improved coordination of medical personnel. These systems enhance diagnostic precision, reduce response times, and

strengthen interaction within complex medical infrastructures.

Project 8. Analytical Platforms for Managing Complex Ecosystems

The eighth project targets the development of analytical platforms for managing complex ecosystems that include automated lines and intelligent devices. The platform's main objective is to coordinate and control active system components, ensure operational efficiency, and provide scalability at the infrastructure level. In medical applications, this allows integration of multiple diagnostic, therapeutic, and monitoring devices, centralized data analysis, and improved management of comprehensive treatment processes.

All eight projects demonstrate a systematic approach to developing and implementing innovative technologies, combining fundamental scientific research with practical application. Each contributes to improving diagnostic precision, therapeutic effectiveness, and the creation of new tools for mass monitoring and treatment.

References

Ivanov I. I., Petrov P. P. *Innovative Medical Technologies: Fundamentals and Applications*. Moscow: Nauka, 2020.

Smirnov D. A. *Minimally Invasive Surgery and Remote Monitoring*. Vladimir: Medizdat, 2022.

Sokolov A., Ivanova M. Magnetic Resonance Applications in Medicine. *Journal of Medical Technology*, 2021; 15(4): 45–60.

Zhang L., et al. Nanometrology for Biomedical Applications. *Sensors and Actuators B*, 2022; 350: 130928.

Chen Y., Wang X. Spectral–Optical Methods in Diagnostics. *Biomedical Optics Express*, 2021; 12(7): 4567–4580.

Lee J., et al. Non-invasive Monitoring of Biological Systems. *International Journal of Medical Informatics*, 2020; 140: 104150.

Brown T., Green R. Smart Energy Systems in Healthcare Devices. *Energy in Medicine*, 2021; 8(3): 112–125.

Kumar S., et al. Integrated Platforms for Data-Driven Healthcare. *Computers in Biology and Medicine*, 2022; 144: 105371.

submitted 02.11.2025;
accepted for publication 16.11.2025;
published 30.12.2025

Contact: smirnoff80@bk.ru

The European Journal of Technical and Natural Sciences 2025, No 6
ISSN 2414-2352

PREMIER Publishing
ppublishing.org

Section 7. Physics

DOI:10.29013/EJHSS-25-6-51-54

INTERBAND ONE-PHOTON LINEAR-CIRCULAR DICHROISM IN NARROW-GaP CRYSTALS. PART 1

Rasulov Voxob Rustamovich [1], Mamatova Mahliyo Adhamovna [1], Muminov Islom Arabboyevich [1], Urinova Kamala Komiljonovna [2], Toshtemirova Ma'rifat Nurmatjon qizi [1]

[1] Ferghana State University, Fergana, Uzbekistan

[2] Kokand State University Fergana, Uzbekistan

Cite: *Rasulov V.R., Mamatova M.A., Muminov I.A., Urinova K.K., Toshtemirova M.N. (2025). Interband One-Photon Linear-Circular Dichroism in Narrow-Gap Crystals. European Journal of Technical and Natural Sciences 2025, No 6.* https://doi.org/10.29013/EJHSS-25-6-51-54

Abstract

In this paper, from a microscopic point of view, the linear-circular dichroism of interband one-photon absorption of light in the Kane approximation in narrow-gap crystals is investigated.

The linear-circular dichroism of one-photon absorption of polarized light is calculated taking into account the effect of coherent saturation in photoexcited charge carriers.

The matrix elements of one-photon interband optical transitions and the corresponding linear-circular dichroism and the spectral dependence of the light absorption coefficient are calculated.

Keywords: *one-photon absorption; linear–circular dichroism; coherent saturation; Kane approximation; cubic semiconductors; interband transitions; spin–orbit split-off band; polarization degree; intensity-dependent absorption; spectral dependence*

Introduction

At present, nonlinear optical phenomena occurring in crystals are widely used in practice (Rostami A., 2006; Pattanaik H. S., Reichert M., Hagan D. J., and Van Stryland E. W.; Yu J. H., Kwon S.-H., Petrášek Z., Park O. K., Jun S. W., Shin K., Choi M., Park Y. I., Park K., Na H. B., Lee N., Lee D. W., Kim J. H., Schwille P., and Hyeon T., 2013).

In this context, the study of nonlinear absorption of polarized light is relevant both from a physical standpoint and from the perspective of practical applications.

It should be noted that in the case of one-photon light absorption, optical transitions do not occur through virtual states and are generally not observed. Therefore, in one-photon optical transitions within crystals

possessing cubic and tetrahedral symmetry, linear-circular dichroism is not observed.

The one- and multiphoton absorption of polarized light in crystals, caused by optical transitions between the subbands of the valence band, have been investigated in (Ivchenko E. L., 1972; Rasulov R. Ya., 1993; Ganichev S. D., Ivchenko E. L., Rasulov R. Ya., Yaroshetsky I. D., and Averbukh B. Ya., 1993; Parshin D. A. and Shabaev A. R., 1987; Rasulov R. Ya., 1988; Rasulov R. Ya., Khoshimov G. Kh., and Kholitdinov Kh., 1996; Rasulov R. Ya., 1993; Leppenen N. V., Ivchenko E. L., and Golub L. E.). However, the contribution of the coherent saturation effect (Ganichev S. D., Ivchenko E. L., Rasulov R. Ya., Yaroshetsky I. D., and Averbukh B. Ya., 1993; Parshin D. A. and Shabaev A. R., 1987) to interband one-photon light absorption has not been taken into account in those studies. This effect arises from the finite lifetime of photoexcited charge carriers in the final state, which is the main focus of the present work.

Interband One-Photon Light Absorption Coefficient: Quantitative Theory

From equation (10) in the first part of this work, it is evident that the interband one-photon light absorption coefficient $K^{(1)}(\omega,T)$ consists of partial components that differ from one another according to the type of optical transitions. In particular, for an optical transition of the type $|\mathrm{V},\pm 3/2\rangle \to |\mathrm{C},\pm 1/2\rangle$, it is expressed as follows:

$$K^{(1)}(\omega,T)=\frac{16e^2}{3c\omega\ \hbar^2 n_\omega}\mu_{c,L}^{(+)}\cdot k_{c,L}^{(\omega)}\cdot P^2\cdot F(\beta,1,\omega)\cdot\Im(\omega)\cdot\left[f_{hh}(E_{hh}k_{c,L}^{(\omega)})-f_c\left(E_c k_{c,L}^{(\omega)}\right)\right] \quad (1)$$

where $\zeta_\omega=4\frac{\alpha_\omega}{\hbar^2\omega^2}\left(\frac{eA_0}{c\hbar}\right)^2 P_{CV}^2$,

$$F(\beta,1,\omega)=$$

$$=\left[1-\exp(\beta\hbar\omega)\right]\exp\left[\beta\left(\mu-E_{hh}(k_{c,L=hh}^{(\omega)})\right)\right],$$

$$k_{c,L}^2=\frac{2\mu_{c,L}^{(\omega)}}{\hbar^2}\left(\hbar\omega-E_g\right),\ \frac{1}{\mu_{c,L}^{(+)}}=\left(\frac{1}{m_c}+\frac{1}{m_L}\right),$$

$$\beta^{-1}=k_BT,\ \Im(\omega)=\left\langle\frac{|e'_\pm|^2}{\sqrt{1+\zeta_\omega|e'_\pm|^2}}\right\rangle.$$

From equation (1), it follows that the linear-circular dichroism of one-photon light absorption is determined by the quantity $\Im(\omega)$, which depends on the frequency and degree of light polarization, as well as on the band parameters of the sample. This phenomenon arises due to the complexity of the crystal's band structure.

It should be noted that if the effect of coherent saturation ($\zeta_\omega=0$) is not taken into account, then $K^{(1)}(\omega,T)$ does not depend on the aforementioned quantities — in particular, on the degree of light polarization — and thus represents a constant value $\Im(\zeta_\omega=0)=\frac{4}{3}$. In this case, one-photon linear-circular dichroism is not observed. However, if the coherent saturation effect is taken into account, then $\zeta_\omega\neq 0$, which means that one-photon linear-circular dichroism arises. This is due to the fact that:
for linearly polarized light

$$\Im_{lin}=\int_{-1}^{+1}d\mu\frac{1-\mu^2}{\sqrt{1+\zeta_\omega\left(1-\mu^2\right)}}; \quad (12)$$

for circularly polarized light

$$\Im_{circ}=\int_{-1}^{+1}d\mu'\frac{\frac{1}{2}\left(1+\mu'^2\right)\mp P_{circ}\mu'}{\sqrt{1+\zeta_\omega\left[\frac{1}{2}\left(1+\mu'^2\right)\mp P_{circ}\mu'\right]}}, \quad (13)$$

where P_{circ} is the degree of circular polarization of light, the sign "±" corresponds to $\sigma_\pm$ polarized light, $\phi(\phi')-$ is the angle between the vectors $\vec{e}$ and $\vec{q}$, $\mu'=\cos\phi'$, $\mu=\cos\phi$, and $\vec{q}$ is the photon wave vector.

For example, in the case of $P_{circ}=1$, for linearly polarized light

$$\Im_{lin}=\zeta_\omega^{-5/2}\left\{\zeta_\omega^{3/2}+\zeta_\omega^2\cdot\arcsin\left(\frac{\zeta_\omega}{1+\zeta_\omega}\right)^{1/2}-\zeta_\omega\cdot\arcsin\left(\frac{\zeta_\omega}{1+\zeta_\omega}\right)^{1/2}\right\}, \quad (14)$$

for circularly polarized light

$$\Im_{circ} = \frac{2\left(\zeta_\omega^{3/2}\sqrt{\zeta_\omega+1} - \zeta_\omega \arcsin\sqrt{\zeta_\omega}\right)}{\zeta_\omega^{5/2}} \quad (15)$$

Figure 3 presents the graphs of the functions $\Im_{lin}(\zeta_\omega)$ and $\Im_{circ}(\zeta_\omega)$ as a function of the quantity $\zeta_\omega \propto \left(\frac{eA_0}{c\hbar}\right)^2 \propto I$, which are used to determine the spectral dependence of the one-photon light absorption coefficient. From Figure 1, it can be seen that as the light intensity increases, the coefficient of interband one-photon linear-circular dichroism $\eta = \Im_{lin}(\zeta_\omega)/\Im_{circ}(\zeta_\omega)$ also increases and tends toward saturation; that is, at very high intensity values, ($\zeta_\omega >> 1$) becomes independent of intensity and $\eta \approx 1.1$. The quantitative calculations were performed using the data from (Vurgaftman I., Meyer J. R. M., and Ram-Mohan J. R., 2001).

Conclusion

Figure 2. Graphs of functions $J_{lin}(\zeta_\omega)$, $J_{circ}(\zeta_\omega)$ and η (linear-circular dichroism factor) versus $\zeta_\omega \propto I$ (on light intensity) in the Kane model in a narrow-gap crystal.

Figure 2.

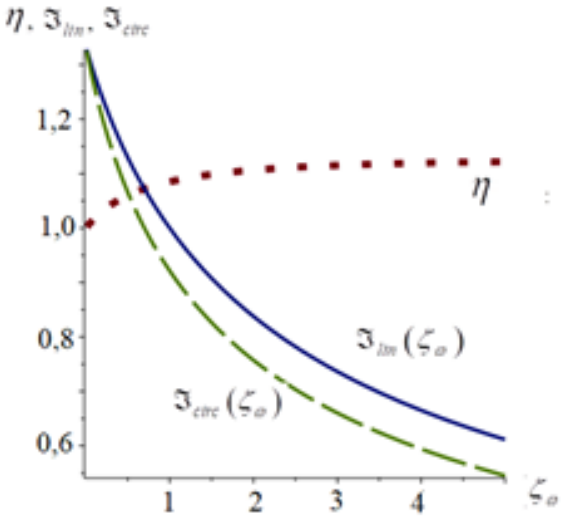

Thus, the one-photon linear-circular dichroism caused by interband optical transitions in a narrow-band-gap crystal arises when the coherent saturation effect is taken into account. However, during interband multiphoton absorption of polarized light, linear-circular dichroism is observed regardless of whether the coherent saturation effect is considered or not.

References

Rostami A. (2006). "Low-threshold and tunable all-optical switch using two-photon absorption in an array of nonlinear ring resonators coupled to MZI." Microelectronics Journal, – Vol. 7. – No. 9. – P. 976–981.

Pattanaik H. S., Reichert M., Hagan D. J., and Van Stryland E. W. "Three-dimensional IR imaging with uncooled GaN photodiodes using nondegenerate two-photon absorption." Optics Express, USA, 2016. – Vol. 24. – No. 2. – P. 1196–1205.

Yu J. H., Kwon S.-H., Petrášek Z., Park O. K., Jun S. W., Shin K., Choi M., Park Y. I., Park K., Na H. B., Lee N., Lee D. W., Kim J. H., Schwille P., and Hyeon T. (2013). "High-resolution three-photon biomedical imaging using doped ZnS nanocrystals." Nature Materials, UK, 2013. – Vol. 12. – No. 4. – P. 359–366.

Ivchenko E. L. (1972). "Two-photon light absorption and optical orientation of free carriers." Fizika Tverdogo Tela (Soviet Physics Solid State). – Vol. 14. – Issue 11. – P. 3489–3496.

Rasulov R. Ya. (1993). Polarization optical and photogalvanic effects in semiconductors under linear and nonlinear light absorption. Doctoral Dissertation (Phys.-Math. Sci.), – St. Petersburg, 1993. – 206 p.

Ganichev S. D., Ivchenko E. L., Rasulov R. Ya., Yaroshetsky I. D., and Averbukh B. Ya. (1993). "Linear-circular dichroism of the drag current in nonlinear intersubband light absorption in p-Ge." Fizika Tverdogo Tela, – Vol. 35. – P. 198–207.

Parshin D. A. and Shabaev A. R. (1987). "Theory of nonlinear absorption of infrared radiation in semiconductors with degenerate bands." Zhurnal Éksperimental'noi i Teoreticheskoi Fiziki (JETP), – Vol. 92. – Issue 4. – P. 1471–1484.

Rasulov R. Ya. (1988). "Drag effect in three-photon light absorption in Ge-type semiconductors." Fizika Tekhnika Poluprovodnikov (Semiconductors), – Vol. 22. – Issue 11. – P. 2077–2080.

Rasulov R. Ya., Khoshimov G. Kh., and Kholitdinov Kh. (1996). “Linear-circular dichroism of nonlinear light absorption in n-GaP.” Semiconductors, – Vol. 30. – No. 2. – P. 274–272.
Rasulov. R Ya. (1993). “Linear-circular dichroism in multiphoton interband absorption in semiconductors.” Fizika Tverdogo Tela, – Vol. 35. – Issue 6. – P. 1674–1678.
Leppenen N. V., Ivchenko E. L., and Golub L. E. “Nonlinear Absorption and Photocurrent in Weyl Semimetals.” Physica Status Solidi (b), – No. 129(1). – P. 139–146. DOI: 10.1002/pssb.201900305.
Bir G. L. and Pikus G. (2012). E. Symmetry and Strain-Induced Effects in Semiconductors. – Moscow: Media, 2012. – 584 p.
Ivchenko E. L. and R. Rasulov Ya. (1989). Symmetry and the Real Band Structure of Semiconductors. – Tashkent: Fan, 1989. – 126 p.
Vurgaftman I., Meyer J. R. M., and Ram-Mohan J. R. (2001). “Band parameters for III–V compound semiconductors and their alloys.” Journal of Applied Physics, – Vol. 89. – P. 5815–5821.

submitted 31.10.2025;
accepted for publication 14.11.2025;
published 30.12.2025

Contact: r_rasulov51@mail.ru

The European Journal of Technical and Natural Sciences 2025, No 6
ISSN 2414-2352

PREMIER Publishing
ppublishing.org

DOI:10.29013/EJHSS-25-6-55-58

INTERBAND ONE-PHOTON LINEAR-CIRCULAR DICHROISM IN NARROW-GaP CRYSTALS PART 2

Rasulov Voxob Rustamovich [1], ***Mamatova Mahliyo Adhamovna*** [1], ***Muminov Islom Arabboyevich*** [1], ***Urinova Kamala Komiljonovna*** [2], ***Xojiakbarova Dildora Ulug'bek qizi*** [1]

[1] Ferghana State University. Fergana, Uzbekistan

[2] Kokand State University Fergana, Uzbekistan

Cite: *Rasulov V.R., Mamatova M.A., Muminov I.A., Urinova K.K., Xojiakbarova D.U. (2025). Interband One-Photon Linear-Circular Dichroism in Narrow-Gap Crystals. European Journal of Technical and Natural Sciences 2025, No 6.* https://doi.org/10.29013/EJHSS-25-6-55-58

Abstract

In this work, the spectral dependence of the one-photon light absorption coefficient in semiconductors with cubic symmetry is calculated, taking into account the degree of polarization and the contribution of the coherent saturation effect within the framework of the Kane approximation. The optical transitions from the subbands of the valence band to the spin–orbit split-off band are considered. It is shown that the one-photon absorption coefficient for both linearly and circularly polarized light initially increases with frequency, then decreases after passing through a minimum. Such spectral behavior of the one-photon light absorption coefficient is explained by the corresponding behavior of the hole distribution function.

Keywords: *one-photon absorption; linear–circular dichroism; coherent saturation; Kane approximation; cubic semiconductors; interband transitions; spin–orbit split-off band; polarization degree; intensity-dependent absorption; spectral dependence*

Introduction

At present, in the field of photoelectronics, the nonlinear intensity-dependent absorption of polarized radiation in semiconductors is being extensively studied (Rostami A., 2006; Pattanaik H. S., Reichert M., Hagan D. J., and Van Stryland E. W.; Yu J. H., Kwon S.-H., Petrášek Z., Park O. K., Jun S. W., Shin K., Choi M., Park Y. I., Park K., Na H. B., Lee N., Lee D. W., Kim J. H., Schwille P., and Hyeon T., 2013).

Before studies were conducted taking into account the coherent saturation effect in the considered optical transitions, it was generally assumed that one-photon light absorption should not exhibit linear-circular dichroism, regardless of the type of optical transitions.

The one- and multiphoton absorption of linearly and circularly polarized light in crystals, caused by intraband optical transitions, has been investigated in (Ivchenko E. L., 1972;

Rasulov R. Ya., 1993; Ganichev S. D., Ivchenko E. L., Rasulov R. Ya., Yaroshetsky I. D., and Averbukh B. Ya., 1993; Parshin D. A. and Shabaev A. R., 1987; Rasulov R. Ya., 1988; Rasulov R. Ya., Khoshimov G. Kh., and Kholitdinov Kh., 1996; Rasulov R. Ya., 1993). However, the contribution of the coherent saturation effect (Ganichev S. D., Ivchenko E. L., Rasulov R. Ya., Yaroshetsky I. D., and Averbukh B. Ya., 1993; Parshin D. A. and Shabaev A. R., 1987), to interband one-photon light absorption-arising from the finite lifetime of photoexcited charge carriers in the final state-has not been considered. This phenomenon constitutes the main focus of the present work.

IInterband One-Photon Light Absorption Coefficient: Quantitative Theory

It should be noted that if the coherent saturation effect ($\zeta_\omega = 0$) is not taken into account, then $K^{(1)}(\omega,T)$ does not depend on the aforementioned quantities - in particular, on the degree of light polarization - and therefore represents a constant value $\Im(\zeta_\omega = 0) = \frac{4}{3}$. In this case, one-photon linear-circular dichroism is not observed. However, if the coherent saturation effect is considered, then $\zeta_\omega \neq 0$, which indicates that one-photon linear-circular dichroism arises. This occurs because for linearly polarized light

$$\Im_{lin} = \int_{-1}^{+1} d\mu \frac{1-\mu^2}{\sqrt{1+\zeta_\omega\left(1-\mu^2\right)}}; \qquad (12)$$

for circularly polarized light

$$\Im_{circ} = \int_{-1}^{+1} d\mu' \frac{\frac{1}{2}\left(1+\mu'^2\right) \mp P_{circ}\mu'}{\sqrt{1+\zeta_\omega\left[\frac{1}{2}\left(1+\mu'^2\right) \mp P_{circ}\mu'\right]}}, \qquad (13)$$

where P_{circ} is the degree of circular polarization of light, the sign "±" corresponds to $\sigma_\pm$ polarized light, $\phi(\phi')-$ is the angle between the vectors $\vec{e}$ and $\vec{q}$, $\mu' = \cos\phi'$, $\mu = \cos\phi$, and $\vec{q}$ is the photon wave vector.

For example, in the case of $P_{circ} = 1$, for linearly polarized light

$$\Im_{lin} = \zeta_\omega^{-5/2}\left\{\zeta_\omega^{3/2} + \zeta_\omega^2 \cdot \arcsin\left(\frac{\zeta_\omega}{1+\zeta_\omega}\right)^{1/2} - \zeta_\omega \cdot \arcsin\left(\frac{\zeta_\omega}{1+\zeta_\omega}\right)^{1/2}\right\}, \qquad (14)$$

for circularly polarized light

$$\Im_{circ} = \frac{2\left(\zeta_\omega^{3/2}\sqrt{\zeta_\omega+1} - \zeta_\omega \arcsin\sqrt{\zeta_\omega}\right)}{\zeta_\omega^{5/2}}. \qquad (15)$$

Figure 1 shows the graphs of the functions $\Im_{lin}(\zeta_\omega)$ and $\Im_{circ}(\zeta_\omega)$ as a function of the parameter $\zeta_\omega \propto \left(\frac{eA_0}{c\hbar}\right)^2 \propto I$. The calculations demonstrate that as the light intensity increases, the coefficient of interband one-photon linear-circular

Figure 1.

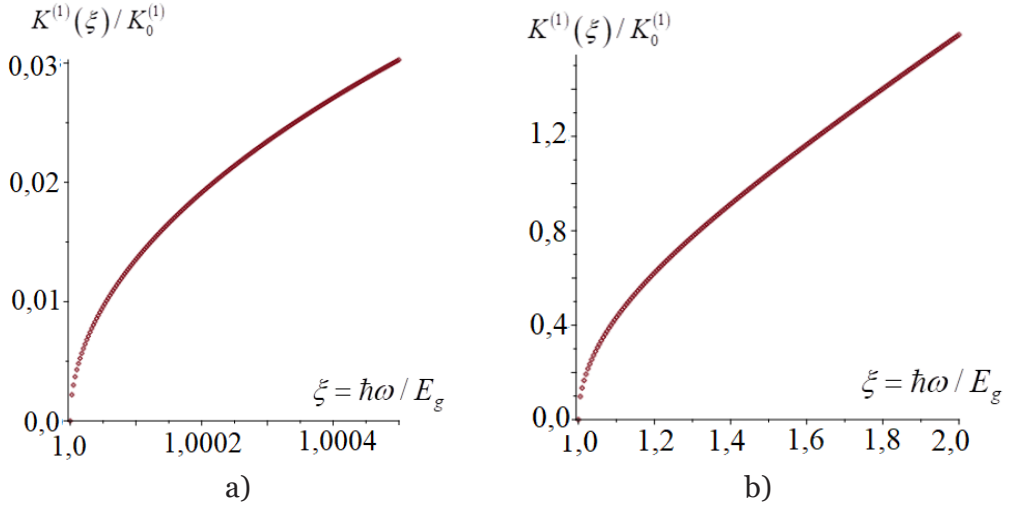

Figure 1. Spectral dependence of the one-photon interband light absorption coefficient in a narrow-band-gap crystal without taking into account the coherent saturation effect: (a) low-frequency region; (b) high-frequency region, where

$$\xi = \hbar\omega / E_g\,,\ K_0^{(1)} = e^2 \frac{\sqrt{2m^* E_g}}{\hbar^2 c n_\omega}.$$

dichroism $\eta = \Im_{lin}(\zeta_\omega) / \Im_{circ}(\zeta_\omega)$ also increases and tends toward saturation; that is, at very high intensity values, $\zeta_\omega >> 1$ becomes independent of both the intensity and $\eta \approx 1.1$. The quantitative calculations were performed using the data from (Leppenen N. V., Ivchenko E. L., and Golub L. E.)

Conclusion

Thus, the one-photon linear-circular dichroism caused by interband optical transitions in a narrow-band-gap crystal arises when the coherent saturation effect is taken into account. However, in the case of interband multiphoton absorption of polarized light, linear-circular dichroism is observed regardless of whether the coherent saturation effect is considered or not. This issue requires separate and more detailed consideration.

References

Rostami A. (2006). "Low-threshold and tunable all-optical switch using two-photon absorption in an array of nonlinear ring resonators coupled to MZI." Microelectronics Journal, – Vol. 7. – No. 9. – P. 976–981.

Pattanaik H. S., Reichert M., Hagan D. J., and Van Stryland E. W. "Three-dimensional IR imaging with uncooled GaN photodiodes using nondegenerate two-photon absorption." Optics Express, USA, 2016. – Vol. 24. – No. 2. – P. 1196–1205.

Yu J. H., Kwon S.-H., Petrášek Z., Park O. K., Jun S. W., Shin K., Choi M., Park Y. I., Park K., Na H. B., Lee N., Lee D. W., Kim J. H., Schwille P., and Hyeon T. (2013). "High-resolution three-photon biomedical imaging using doped ZnS nanocrystals." Nature Materials, UK, 2013. – Vol. 12. – No. 4. – P. 359–366.

Ivchenko E. L. (1972). "Two-photon light absorption and optical orientation of free carriers." Fizika Tverdogo Tela (Soviet Physics Solid State). – Vol. 14. – Issue 11. – P. 3489–3496.

Rasulov R. Ya. (1993). Polarization optical and photogalvanic effects in semiconductors under linear and nonlinear light absorption. Doctoral Dissertation (Phys.-Math. Sci.), – St. Petersburg, 1993. – 206 p.

Ganichev S. D., Ivchenko E. L., Rasulov R. Ya., Yaroshetsky I. D., and Averbukh B. Ya. (1993). "Linear-circular dichroism of the drag current in nonlinear intersubband light absorption in p-Ge." Fizika Tverdogo Tela, – Vol. 35. – P. 198–207.

Parshin D. A. and Shabaev A. R. (1987). "Theory of nonlinear absorption of infrared radiation in semiconductors with degenerate bands." Zhurnal Éksperimental'noi i Teoreticheskoi Fiziki (JETP), – Vol. 92. – Issue 4. – P. 1471–1484.

Rasulov R. Ya. (1988). "Drag effect in three-photon light absorption in Ge-type semiconductors." Fizika Tekhnika Poluprovodnikov (Semiconductors), – Vol. 22. – Issue 11. – P. 2077–2080.

Rasulov R. Ya., Khoshimov G. Kh., and Kholitdinov Kh. (1996). "Linear-circular dichroism of nonlinear light absorption in n-GaP." Semiconductors, – Vol. 30. – No. 2. – P. 274–272.

Rasulov. R Ya. (1993). "Linear-circular dichroism in multiphoton interband absorption in semiconductors." Fizika Tverdogo Tela, – Vol. 35. – Issue 6. – P. 1674–1678.

Leppenen N. V., Ivchenko E. L., and Golub L. E. "Nonlinear Absorption and Photocurrent in Weyl Semimetals." Physica Status Solidi (b), – No. 129(1). – P. 139–146. DOI: 10.1002/pssb.201900305.

Vurgaftman I., Meyer J. R. M., and Ram-Mohan J. R. (2001). “Band parameters for III–V compound semiconductors and their alloys.” Journal of Applied Physics, – Vol. 89. – P. 5815–5821.

submitted 31.10.2025;
accepted for publication 14.11.2025;
published 30.12.2025

Contact: r_rasulov51@mail.ru

The European Journal of Technical and Natural Sciences 2025, No 6
ISSN 2414-2352

PREMIER Publishing
ppublishing.org

DOI:10.29013/EJHSS-25-6-59-61

METHOD FOR DETERMINING THE COORDINATE DISTRIBUTION OF LOCAL INHOMOGENEITIES IN THE BULK OF A SEMICONDUCTOR

Gaibov A. G. [1]***, Vahabov K. I.*** [1]***, Mirkomilova M. S.*** [1]***, Dzhuraev U. E.*** [1]

[1] Tashkent State Technical University, Tashkent

Cite: *Gaibov A. G., Vahabov K. I., Mirkomilova M. S., Dzhuraev U. E. (2025). Method for determining the coordinate distribution of local inhomogeneities in the bulk of a semiconductor. European Journal of Technical and Natural Sciences 2025, No 6.* https://doi.org/10.29013/EJHSS-25-6-59-61

Abstract

A method has been developed for determining the two-coordinate (x and y) distribution of localized impurity atom clusters within the bulk of semiconductor materials. The developed method is used in the preliminary selection of homogeneous materials for the production of semiconductor devices.

Keywords: *semiconductor material, n-p junction, impedance, local inhomogeneities, grid ohmic contacts*

1. Introduction

Semiconductor device technology is a critical component of rapidly developing nanotechnology, one of the key aspects of which is the development of methods for studying localized impurity atom clusters within the bulk of semiconductor materials.

Known methods for quality control of semiconductor materials include electron microscopy (Fedina, L.I., 2012), probe resistivity measurements (Smirnov, V.I., 2012), and chemical selective etching and decoration (Azimov S. A., Muminov R. A., et al., 1981). These methods provide information strictly on the surface. Their use for studying the bulk properties of semiconductors involves the sequential destruction of the single crystal (e.g., by continuous etching or grinding), making them unsuitable for rejecting material used in device fabrication.

The traditional approach to studying the influence of a given concentration of various point imperfections in the crystal structure (impurity levels, dislocations, point adhesion centers) on the physical processes in semiconductor devices is insufficient to meet the modern requirements of semiconductor instrumentation. Research is needed to identify fluctuations in their distribution within the bulk of the semiconductor, determine local inhomogeneities in such distributions, and study the role of such local inhomogeneities on the properties of modern semiconductor devices.

2. Material and Method

A method for identifying local inhomogeneities in a semiconductor material based on the frequency dependence of the impedance of structures (Azimov S. A., Muminov R. A., et al., 1981) is proposed. The essence of this

method is to fabricate an n-p junction on the semiconductor material, measure the frequency dependence of the n-p junction impedance over a wide frequency range, and, based on linear diagrams, determine the integral value of local inhomogeneities in the form of high-resistance layers throughout the entire volume of the sample.

This method cannot determine the coordinate distribution of local inhomogeneities. A new method is proposed for determining the coordinate distribution of local inhomogeneities.

To determine the distribution of local inhomogeneities along two coordinates $l_i(X_i, Y_i)$, rectifying contacts are created on two opposite side surfaces of the sample, the frequency dependence of the structure's impedance is measured, and the total size of all local inhomogeneities in the entire volume of the sample $(\sum l_i)_0$ is determined. Then, grid ohmic contacts are applied to two opposite sides of the sample through a mask with a width and pitch exceeding the largest size of the inhomogeneities (Fig. 1). After this, a constant voltage is applied alternately to each opposite pair of contacts whose coordinates are known. The magnitude of the voltage is determined from the electric field strength (Муминov R. A., Radzhapov S. A., Sagyndykov N. A. and Nurbaev K. M., 2005) using the formula:

$$E_{кр} \approx 4/3 \cdot [\pi \cdot \rho_{\Delta}/\varepsilon] \cdot 2R_{\Delta}$$

Where ρ_{Δ} is the negative space charge density arising in the p-region; $2R_{\Delta}$ is the linear size of local impurity atom clusters in the region in the direction of the electric field lines.

Additionally, the frequency dependence of the impedance is measured for each pair (Fig. 1).

Based on the linear diagrams, the total effective size of the inhomogeneities is determined without taking into account the region defined by the coordinates of the contacts to which a constant voltage $\sum l_i$ is applied. The desired distribution of local inhomogeneities along the $l_i(X_iY_i)$ coordinates is determined from the difference in the total effective sizes of the inhomogeneities before and after applying the constant voltage.

$$l_i\,(X_iY_i) = (\sum l_i)_o - \sum l_i$$

where $(l_i)_0$ is the total effective size of the inhomogeneities before applying constant voltage.

$(\sum l_i)$ is the total effective size of the inhomogeneities after applying constant voltage.

3. Results and discussion

In this example, the method is tested on p-Si with a resistivity of –1000 Ωcm. The sample dimensions are 10 × 8 × 2.5 mm. Nickel contacts are deposited on two opposite side surfaces of the sample using chemical vapor deposition, and grid ohmic contacts are deposited on two opposite sides of the sample using gold sputtering through a mask; the width and length of each cell are 200 μm, and the distance between the contacts is 100 μm.

Figure 1. *Scheme of measurement of coordinate determination of local inhomogeneities*

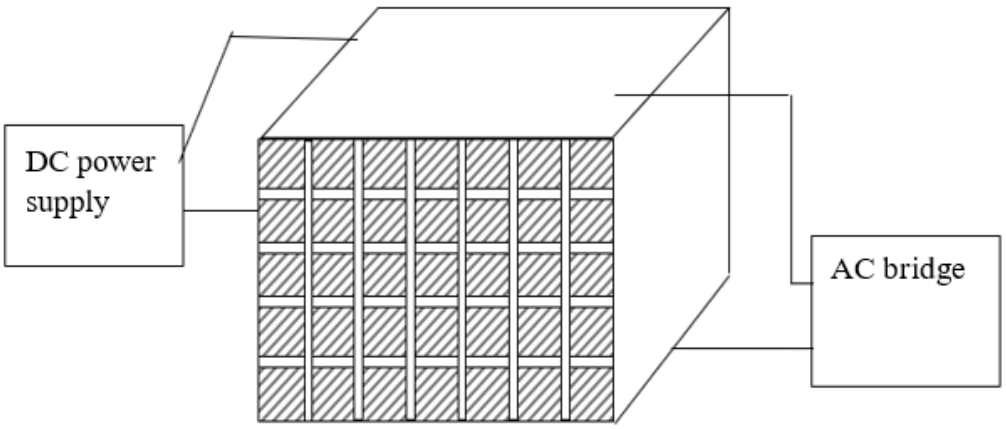

The frequency dependence of the impedance is measured, and the magnitude of local inhomogeneities in the form of high-resistance layers with a specific resistance and an effective size throughout the sample volume is determined. The sizes and specific resistance of the local inhomogeneities are presented in Table 1. By summing up the sizes of

local inhomogeneities, $(\Sigma l_i)_o$, the total effective size of the inhomogeneities in the entire sample, is determined. A constant voltage of $3 \cdot 10^3$ V/cm is then applied alternately to the ohmic contacts. The frequency dependence of the impedance is measured each time, and Σl_i is determined without taking into account the region defined by the coordinates of the contacts to which the voltage is applied. The desired distribution of local inhomogeneities $l_i (X_i, Y_i)$ is determined by the difference in the total effective sizes of the inhomogeneities before and after applying the constant voltage. Table 2 presents the distribution of local inhomogeneities over two coordinates $l_i (X_i, Y_i)$.

Table 1. Dimensions and specific resistance of local inhomogeneities

No.	$r_i \cdot 10^6$ Ωcm	l_i mkm
1.	0.28	4.3
2.	0.65	3.1
3.	1.32	1.6
4.	1.73	2.8
5.	2.3	9.6
6.	2.76	8.3
7.	3.4	4.5
8.	6.4	2.7
9.	7.3	4.2
10.	8.51	6.8
11.	9.6	5.6
12.	11.7	3.2

Table 2. Distribution of local inhomogeneities by two coordinates $l_i (X_i Y_i)$.

No.	l_i, mkm	X_i, mm	Y_i, mm
1.	1.6	0.2	6.5
2.	2.7	0.5	2.0
3.	9.6	0.8	7.4
4.	8.3	2.0	0.2
5.	6.8	2.6	1.1
6.	4.5	3.5	4.7
7.	2.9	4.1	3.8
8.	4.3	5.3	0.5
9.	3.2	5.6	6.7
10.	5.6	6.2	2.3
11.	3.2	6.5	5.9
12.	4.2	7.7	5.0

The use of this method in the preliminary screening of material at an early stage of the technology of manufacturing semiconductor devices, in particular semiconductor nuclear radiation detectors, increases the yield of detectors with improved electrophysical and spectrometric characteristics.

References

Fedina, L. I. “Atomic structure of extended defects in silicon and mechanisms of their formation” // IX International Conference and VIII School of Young Scientists and Specialists on Current Issues of Physics, Materials Science, Technology, and Diagnostics of Silicon, Nanoscale Structures, and Devices Based on It “SILICON-2012”. July 9–13, 2012. – St. Petersburg, – 34 p.

Smirnov, V. I. Non-destructive methods for testing parameters of semiconductor materials and structures: a tutorial / V. I. Smirnov. – Ulyanovsk: UlSTU, 2012. – 75 p.

Azimov S. A., Muminov R. A., et al. Silicon-lithium nuclear radiation detectors. – Tashkent, ‘Fan’, 1981. – 258 p.

Muминov R. A., Radzhapov S. A., Sagyndykov N. A. and Nurbaev K. M. (2005). Salient feartures of the fabrication of Si(Li) detectors with a large-volume working region // Atomic Energy. – New York, – Vol. 98. – No. 1. – P. 69–71.

submitted 28.09.2025;
accepted for publication 12.10.2025;
published 30.12.2025

Contact: gaibov.1954@mail.ru

The European Journal of Technical and Natural Sciences 2025, No 6
ISSN 2414-2352

PREMIER Publishing
ppublishing.org

DOI:10.29013/EJHSS-25-6-62-65

ABSORPTION OF LIGHT IN SEMICONDUCTORS OF CUBIC SYMMETRY DURING INTRABAND THREE-PHOTON OPTICAL TRANSITIONS

Rasulov Voxob Rustamovich [1], ***Mamatova Mahliyo Adhamovna*** [1], ***Muminov Islom Arabboyevich*** [1], ***Urinova Kamala Komiljonovna*** [1], ***Obbozova Madinaxon Mirodiljon kizi*** [1]

[1] Ferghana State University. Fergana, Uzbekistan

Cite: *Rasulov V.R., Mamatova M.A., Muminov I.A., Urinova K.K., Obbozova M.M. (2025). Absorption of Light In Semiconductors of Cubic Symmetry During Intraband Three-Photon Optical Transitions. European Journal of Technical and Natural Sciences 2025, No 6.* https://doi.org/10.29013/EJHSS-25-6-62-65

Abstract

The polarization and frequency-polarization dependences of the linear-circular dichroism and light absorption coefficients in semiconductors of cubic symmetry, caused by vertical three-photon optical transitions between the states of the spin-orbit splitting and conduction bands, are calculated.

Keywords: *three-photon optical transitions, spin-orbit splitting band, conduction band, linear-circular dichroism, light absorption, semiconductor*

Intraduction

Currently, the main research in the field of multiphoton absorption of light is carried out in wide-gap semiconductors, since a number of their physicochemical properties have been studied in depth and in more detail. In this respect, multiphoton effects occurring in narrow-gap crystals have been little studied both in theoretical and experimental aspects. The main reason for this is that the theoretical study of a number of photon-kinetic phenomena in narrow-gap crystals requires the use of not only the Luttinger-Kohn approximation, but also the multiband Kane approach. In the latter case, theoretical calculations are performed using matrices of at least 6 × 6 or 8 × 8.

The first works on two-photon interband transitions in crystals were carried out in the early 1960 y., shortly after the appearance of lasers (Miller A., A. Johnston, J. Dempsey, J. Smith, C. R. Pidgeon, and G. D. Holah. 1978; Comparee C. R. Pidgeeon, B. S. Wherrett, A. M. Johnston, J. Dempsey, and A. Miller. 1979; Braunstein R. and Ockman N., 1964). When calculating the matrix elements of two-photon transitions in crystals, perturbation theories were used in the field of an unpolarized electromagnetic wave (Comparee C. R. Pidgeeon, B. S. Wherrett, A. M. Johnston, J. Dempsey, and A. Miller. 1979; Braunstein R. and Ockman N., 1964), where the two-band Kane model was used.

In (Rasulov R.Ya., 1993; Ivchenko E. L., 1972; Beregulin E. V., Dvornikov D. P., Ivchenko E. L., Yaroshetskiy I. D., 1975; Arifzhanov S. B., Ivchenko E. L., 1975; Rasulov R.Ya., 1993; Rasulov R.Ya., 1993; Rasulov V. R. Rasulov R.Ya., Eshboltaev I., 2017), both theoretically and experimentally, linear-circular dichroism (LCD) of two- and three-photon absorption of light in crystals of cubic symmetry was investigated. However, the question of the polarization and frequency-polarization study of three-photon interband absorption of light in crystals of cubic symmetry, caused between the states of the spin-orbit splitting band and the conduction band in the Kane approximation, remained open.

Three-photon linear-circular dichroism

In our previous works, three-photon optical transitions originating from the state of the spin-orbit splitting subband into the conduction bands were analyzed and it was shown that they are 10 different transitions (Rasulov V. R., Rasulov R. Ya., Eshboltaev I. M., Qo'chqorov M. X., 2021), which differ from each other by virtual states. As indicated in (Rasulov V. R., Rasulov R. Ya., Eshboltaev I. M., Qo'chqorov M. X., 2021), the multiphoton interband light absorption coefficient has two terms, one of which describes the sum of partial light absorption coefficients, and the second contribution to the multiphoton light absorption coefficient due to the interference terms of the matrix elements of the above optical transitions in crystals of cubic symmetry.

First, we will analyze the polarization dependences of interband optical transitions arising from the state of the spin-orbit splitting subband $|SO,\pm1/2\rangle$ into $|c,\pm1/2\rangle$ conduction bands (i.e., three-photon transitions of type $|SO,\pm1/2\rangle \Rightarrow |c,\pm1/2\rangle$), where we take into account that for linearly polarized light: $|e'_z|^2 = \cos^2\alpha$, $|e'_\pm|^2 = 1-|e'_z|^2$, for circularly polarized light $|e'_z|^2 = \frac{1}{2}\sin^2\beta$, $|e'_\pm|^2 = 1-|e'_z|^2 \mp P_{circ}\cos\beta$, where $\alpha\ (\beta)$ is the angle between the polarization vectors $\vec{e}$ (the wave vector of the photon $\vec{q}$) and the wave vector of current carriers ($\vec{k}$), e'_x, e'_y, e'_z are the projections of the polarization vector of light along the axis x', y', z', associated with the direction of the wave vector of electrons $\vec{k}\ (\vec{k}\|z')$, $e'_\pm = e'_x \pm ie'_y$, $\vec{q}$ – is the wave vector of the photon, $e'_\pm$ is the degree of circular polarization of light, and the sign of "$\pm1/2$" is describes the spin states of current carriers.

Calculations carried out according to the golden rule of quantum mechanics (Landau L.D., Lifshits E.M., 2004) for InSb show that in three-photon transitions of the type $|SO,\pm1/2\rangle \Rightarrow |c,\pm1/2\rangle$, the graph of the polarization dependence of the coefficient of three-photon linear-circular dichroism is described for two virtual states lie in the subbands of the valence band and both virtual states lie in the conduction band, and the initial virtual states lie in the conduction band, and the next ones, in the valence band (in the approximation quadratic in the wave vector in the effective carrier Hamiltonian, some of the optical transitions are forbidden , and the part is nonzero).

In quantitative calculations, the numerical values of the band parameters were taken from (Vurgaftman I. and R. Meyer J., Ram-Mohan L. R., 2001). Note here that in the first case, the polarization dependence of three-photon linear-circular dichroism is almost independent of the frequency of light. This means that linear-circular dichroism does not appear in this case, i.e. interband three-photon absorption of light does not depend on the degree of polarization of the light.

Note here that the energy spectra of current carriers in all bands are taken as parabolic, and when the three branches of the band structure of the semiconductor are nonparabolic, then the quadratic dependence of the energy on the wave vector is approximately restored only near the edges of the Brillouin zones.

That. showed that the polarization dependence of the linear-circular dichroism of three-photon absorption of light on the type of optical transitions. Since the matrix elements of some optical transitions have in the numerator the difference in the energies of current carriers, which in a certain region of the frequency of light tends to zero, which leads to an anomalous increase in the spectral dependence of the three-photon absorption coefficient of light, but this phenomenon leads to a noticeable change in the spectral depen-

dence of linear-circular dichroism, since the coefficient of linear-circular dichroism is defined as the ratio of the probabilities of optical transitions occurring upon absorption of light with linear and circular polarization.

The three-photon light absorption coefficient

Let us now analyze the frequency-spectral dependence of the light absorption coefficient for InSb, caused by three-photon transitions of the type. Calculations for the semiconductor InSb show that in three-photon transitions of the type, the graph of the polarization dependence of the coefficient of three-photon linear-circular dichroism is described for two virtual states lie in the subbands of the valence band, and when both virtual states which lie in the conduction band (in the approximation quadratic in the wave vector in the effective carrier Hamiltonian, some of the optical transitions are forbidden, and some nonzero).

Conclusion

From the above results it can be seen that both the polarization and frequency-polarization dependences of the linear-circular dichroism and linear-circular dichroism coefficients have several extrema. This is due to the specificity of the Kane model used to study the band structure in narrow-gap crystals. In particular, in the Kane model, some off-diagonal matrix elements of the momentum operator do not depend on the wave vector of current carriers, which does not occur in the Luttinger-Kohn model.

References

Miller A., A. Johnston, J. Dempsey, J. Smith, C. R. Pidgeon, and G. D. Holah. (1978). Two-photon absorption in InSb and Hg1-xCdxTe // – J. Phys. 1978. – No. 12. – P. 4839–4849.

Comparee C. R. Pidgeeon, B. S. Wherrett, A. M. Johnston, J. Dempsey, and A. Miller. (1979). Two-photon absorption in zinc-blende semiconductors // Phys. Rev. Lett. 1979. – Vol. 42. – P. 1785–1788 and references therein.

Braunstein R. and Ockman N. (1964). Optical double-photon absorption in CdS // – Phys. Rev. A. 1964. – Vol. 34. – P. 499–507.

Rasulov R.Ya. (1993). Polarization optical VA photovoltaic effects in semiconductors with linear and nonlinear absorption of light. Dissertation for thesis. uch. doctor's degree phys.-math. sciences. – St. Petersburg, 1993. – 206 p. (in Russian)

Ivchenko E. L. (1972). Two-photon absorption and optical orientation of free carriers in cubic crystals // FTT. 1972. – T. 14. – Issue 12. – WITH. – P. 3489–3485. (in Russian)

Beregulin E. V., Dvornikov D. P., Ivchenko E. L., Yaroshetskiy I. D. (1975). Polarization properties and linear-circular dichroism in nonlinear light absorption in A_2B_6 semiconductors // FTT. 1975. – T. 9. – No. 5. – P. 876–886. (in Russian)

Arifzhanov S. B., Ivchenko E. L. (1975). Multiphoton absorption of light in crystals with a diamond and zinc blende structure // FTT. 1975. – Vol. 17. – No. 1. – P. 81–89. (in Russian)

Rasulov R.Ya. (1993). Linear circular dichroism in multiphoton interband absorption in semiconductors // FTT. – St.-Petersburg, 1993. – T. 35. – Issue 6. – P. 1674–1678. (in Russian)

Rasulov R.Ya. (1993). Linear-circular dichroism in multiphoton interband absorption in semiconductors // Solid State Physics. – St. Petersburg, 1993. – Vol. 35, – No. 6. – P. 1674–1677. (in Russian)

Rasulov V. R. Rasulov R.Ya., Eshboltaev I. (2017). Linearly and circular dichroism in a semiconductor with a complex valence band with allowance for four-photon absorption of light // Physics of the Solid State. – Springer, 2017. – Vol. 59. – No. 3. – P. 463–468.

Rasulov V. R., Rasulov R. Ya., Eshboltaev I. M., Qo'chqorov M. X. (2021). Interband Multiphoton Absorption of Light in Narrow-Gap Crystals // European Journal of Applied Physics. – Vol. 3. – Issue 5.

Landau L. D., Lifshits E. M. (2004). Quantum Mechanics (Nonrelativistic Theory) Vol. III. – M.: Fizmatlit, 2004. – 800 p.(in Russian)

Vurgaftman I. and R. Meyer J., Ram-Mohan L. R. (2001). Band parameters for III–V compound semiconductors and their alloys // Journal of Applied Physics. 2001; 89 (11): 5815–5875. URL: https://doi.org/10.1063/1.1368156.

submitted 27.10.2025;
accepted for publication 10.11.2025;
published 30.12.2025

Contact: r_rasulov51@mail.ru

The European Journal of Technical and Natural Sciences 2025, No 6
ISSN 2414-2352

PREMIER Publishing
ppublishing.org

Section 8. Technical sciences in general

DOI:10.29013/EJHSS-25-6-66-69

ARIZ AND MODERN COMMERCIALIZATION THEORIES. ALGORITHM OF INTERACTION BETWEEN THE THEORY OF INVENTIVE PROBLEM SOLVING AND THE FUNDAMENTAL PRINCIPLES OF INVENTION COMMERCIALIZATION

Ahmadova Muzhgan [1]

[1] Financial Expert in Acoustic Equipment Moscow, Russia

Cite: *Ahmadova M. (2025). Ariz and Modern Commercialization Theories. Algorithm of Interaction Between The Theory of Inventive Problem Solving and the Fundamental Principles of Invention Commercialization. European Journal of Technical and Natural Sciences 2025, No 6.* https://doi.org/10.29013/EJHSS-25-6-66-69

Abstract

The Theory of Inventive Problem Solving (TRIZ) and all of its derivative algorithms, including ARIZ, were developed in an environment and at a time where commercialization of innovative solutions was not considered a priority. One may even argue that during certain stages of the development of TRIZ and ARIZ, commercialization issues were intentionally ignored in favor of purely technological variants of innovative solutions – solutions often disconnected from real economics and, in most cases, from real life.

Keywords: *Theory of Inventive Problem Solving (TRIZ); Algorithm of Inventive Problem Solving (ARIZ); Principles of invention commercialization; Integration of ARIZ with modern commercialization theories; Organizational model of innovation process development; Competitive strategy techniques; Necessity of assessing the beginning of the innovation process; Evaluation matrix system*

As a result of this narrow and one-sided organizational model of innovation development, inventors trained within the TRIZ/ARIZ paradigm grew into highly capable problem-solvers but remained unprepared for the realities of competitive markets and the dynamics of commercialization in modern free-market economies.

They are ready-and enjoy-to-invent, but are not ready and often do not know how to monetize their inventions, nor how to obtain adequate compensation for their talent and creative work. What is particularly important today is the ability to evaluate the necessity of launching an innovation process, to understand-ideally to calculate-all possible development scenarios within the commercialization process.

Now let us assume that an inventor has obtained the necessary information or, at

minimum, has learned about findings from scientific research. The core question becomes:

How can TRIZ and ARIZ help transform valuable knowledge, insights, or naturally occurring patterns from a near-idea stage into a successful commercial project?

The answer lies in adapting TRIZ tools not only to solve technical contradictions, but also to:

- analyze the market environment;
- identify commercialization barriers;
- determine stakeholders and beneficiaries;
- define integration and positioning strategies of the invention within an existing technological ecosystem;
- and formulate a commercialization algorithm with minimized risks and maximized value.

Thus, the modern extension of ARIZ should integrate both inventive problem solving and commercialization logic, enabling a transition from invention to innovation to commercial product.

Integration of the Algorithm for Inventive Problem Solving with Modern Commercialization Theories (Part One)

The Theory of Inventive Problem Solving (TRIZ) and all its known derivative algorithms were developed in a country and during a period when commercialization of innovative solutions was not considered a matter of significance. One could even say that, at certain stages in the creation of the Theory and Algorithm of Inventive Problem Solving, the issues of commercialization were deliberately ignored in favor of purely technological variants of innovative solutions-solutions often detached from real economics and, in most cases, from practical life.

As a result of this shortsighted and one-sided organizational model of innovation process development that prevailed at that time, inventors trained within the TRIZ and ARIZ frameworks found themselves highly capable of solving technical problems, yet completely unprepared for the mechanisms, strategies, and competitive realities of innovation commercialization in a market-driven economy.

Inventors who were trained and shaped within the TRIZ and ARIZ methodology turned out to be completely unprepared for the mechanisms and techniques of competitive behavior in a modern free-market economy.

They are ready – and genuinely enjoy – inventing, but they are not ready and do not know how to earn money from their inventions in order to receive fair compensation for their talent and creative work.

In this context, it becomes critically important to evaluate the necessity of initiating an innovation process, and – even more importantly – to model and calculate possible development scenarios throughout the commercialization phase.

G. S. Altshuller formulated the goal of his method as follows:

"How can one arrive at strong solutions immediately, without exhaustive trial and error?"

Achieving this goal is possible through adherence to the fundamental TRIZ principles:

1. Principle of objectivity in system evolution

The structure, functioning, and generational change of systems follow objective laws.

Strong solutions are those that are aligned with objective laws, patterns, phenomena, and effects.

2. Principle of contradiction

Under external and internal influences, contradictions emerge, intensify, and are eventually resolved.

A problem is complex because there is a contradiction, hidden or explicit.

Systems evolve by overcoming contradictions in accordance with objective laws and effects.

Strong solutions are the ones that eliminate or resolve contradictions, not the ones that compromise.

3. Principle of specificity (concreteness)

Each class of systems – and each individual system – has specific characteristics that may facilitate or hinder transformation.

These characteristics are determined by the available resources:

- internal resources – inherent to the system;
- external resources – defined by the environment and circumstances.

Strong solutions are those that take into account the specific characteristics of the given system, as well as the individual characteristics of the person making decisions.

As practice in managing innovation projects has shown, meticulous adherence to the requirements and recommendations of these three principles does not define and does not allow achieving the ideal final result in every specific development.

Today, any specialist in biomechanics or in the broader field of bio-engineering can provide numerous examples of borrowing the most important and astonishing technical solutions from among the technical solutions of nature.

Let lawyers resolve the issue of priority date and global novelty when borrowing from nature the most elegant and concise – in many cases unique – biological-engineering experience.

Now let us assume that the inventor has obtained the necessary information or, at the very least, has learned about interesting conclusions from scientific research.

How, in this case, can the Theory of Inventive Problem Solving help in advancing useful information, conclusions, and assumed natural patterns from an almost-idea stage to a successful commercial project?

Algorithm of interaction between the Theory of Inventive Problem Solving and the fundamental principles of invention commercialization (continuation, part two)

To begin, let us return to the Theory of Inventive Problem Solving (TRIZ):

Thus, the methodology of problem solving is based on generally studied TRIZ laws of system evolution, general principles of contradiction resolution, and mechanisms for solving specific practical problems.

Main functions and areas of application of TRIZ:

- solving inventive problems of any complexity and orientation;
- forecasting the development of technical systems;
- development of creative imagination and thinking;
- development of the creative personality and creative teams.

The key concept in TRIZ is the **"strong solution."** This is the best, or close to the best, solution.

TRIZ focuses on revealing a strong solution and includes:

1) mechanisms for transforming a problem into an image of a future solution;

2) methods of suppressing psychological inertia that prevents finding solutions;

3) a vast information base – concentrated experience in problem solving.

4) A **problem** is a recognized contradiction. In TRIZ, special and fully justified attention is paid to the formulation of contradictions. Three types of contradictions are distinguished: *administrative contradiction*, *technical contradiction*, and *physical contradiction*.

Administrative contradiction – a contradiction between a need and the ability to satisfy it. It is relatively easy to identify. It is often formulated by management or the customer and appears as:

- "It is necessary to accomplish this, but we do not know how";
- "A certain parameter of the system is poor and needs to be improved";
- "There is a defect, but we do not know the cause."

Technical contradiction – a contradiction between certain parts, qualities, or parameters of a system. Typically, improving one characteristic sharply worsens another. For example, a useful action simultaneously produces a harmful effect. Or: introducing a positive effect or eliminating a negative one results in deterioration (for example, unacceptable complication) of some part of the system or of the system as a whole. Usually, one must search for a compromise and sacrifice something. Resolving a technical contradiction often requires a qualitative change of the entire system.

Physical contradiction – imposing diametrically opposite properties on a specific part of the system. The study of reasons that give rise to a technical contradiction in technical systems usually leads to the identification of conflicting physical properties within the system. It should be emphasized once again that, in contrast to a technical contradiction, which belongs to the system as a whole, a physical contradiction relates only

to a specific part of it. Formulating a physical contradiction formulation of the physical contradiction is paradoxical: a certain part of the system must simultaneously exist in two mutually exclusive states. For example, it must be cold and hot at the same time, movable and immovable, long and short, flexible and rigid, electrically conductive and non-conductive, etc.

Thus, the three types of contradictions form a chain: administrative contradiction → technical contradiction → physical contradiction.

To solve a complex technical problem means to improve the required parameters of the system without deteriorating others.

This can be achieved by identifying the technical contradiction, determining the causes that generated it – or even the causes of those causes – and eliminating them, that is, by resolving the physical contradiction.

References

United States Patent Application US20130173180 A1. Birk, Uzi *et al. Determination of Attributes of Liquid Substances*. – July 4, 2013.

United States Patent Application US20130178721 A1. Birk, Uzi *et al. In Vivo Determination of Acidity Levels*. – July 11, 2013.

United States Patent US 8,694,091. Birk, Uzi *et al. In Vivo Determination of Acidity Levels*. – April 8, 2014.

United States Patent US 9,316,605. Birk, Uzi *et al. Determination of Attributes of Liquid Substances*. – April 19, 2016.

submitted 03.11.2025;
accepted for publication 17.11.2025;
published 30.12.2025

Contact: sedova.alina7810@gmail.com

The European Journal of Technical and Natural Sciences 2025, No 6
ISSN 2414-2352

PREMIER Publishing
ppublishing.org

DOI:10.29013/EJHSS-25-6-70-73

ANALYSIS OF THE MAIN TECHNICAL REQUIREMENTS FOR TEST EQUIPMENT AND THEIR IMPACT ON THE PARAMETERS OF THE FINAL PRODUCT AND ITS VARIANTS

Tatiana Gladilina [1]

[1] Division at the Major Pharmaceutical Enterprise LLC Puls Krasnodar Krasnodar, Russia

Cite: *Gladilina T. (2025). Analysis of the Main Technical Requirements for Test Equipment and Their Impact on the Parameters of the Final Product and Its Variants. European Journal of Technical and Natural Sciences 2025, No 6.* https://doi.org/10.29013/EJHSS-25-6-70-73

Abstract

This document presents a comprehensive analysis of the technical requirements, calibration procedures, and experimental testing conducted for the development of an autonomous sensor capsule intended for pH measurement in complex biological and chemical environments. The study evaluates the capsule's structural materials, protective coatings, sensor design, and operational parameters, including acidity measurement ranges, temperature stability, signal penetration depth, and the influence of various additives and biological substances. Particular attention is given to the performance of planar solenoid technology, long-term durability of system components, and repeatability of measurement results.

Keywords: *Composite technical solutions in smart pharmaceutical manufacturing and their equivalents; Implementation of new technologies in pharmaceutical production; The main tool of technological integration in smart pharmaceutical manufacturing; Principles and criteria of industrial design; Integrative inventions in the pharmaceutical field; Reliability of new pharmaceutical products; Techniques and methods for developing a composite style in the creation of innovative solutions*

LIFETIME – more than 10 years (power consumption) – Durability of the system and provision of the required energy level

SIZE of the capsule – actual dimensions of the sensor capsule

According to the technical specifications, the required dimensions of the sensor capsule are as follows:

- Diameter: 30 mm;
- Length: 100 mm.

After modeling and conducting tests, the researchers concluded that, if necessary, the external dimensions of the capsule could be reduced to:

- Diameter: up to 25 mm;
- Length: up to 80 mm.

A particularly important factor in achieving this reduction is the use of a planar solenoid as the sensor element, implemented in the form of a flat coil on a single-layer printed circuit board.

The dimensions of this board – 16 mm in diameter and 1.5 mm in thickness – allow for significant optimization of space within the internal volume of the sensor capsule.

Measurement pH range (3–10) – measurement of acidity levels across an extended range.

The **range of calibration tests** was expanded – calibration was carried out on samples with acidity levels ranging from **pH 2 to pH 10**.

In principle, there are no limitations regarding the acidity values that can be measured using the new technology.

Experimental verification confirmed the possibility of measuring acidity levels as low as **pH 1** (hydrochloric acid used in sample preparation) and as high as **pH 14** (various household alkaline solutions).

The specified measurement range is therefore fully feasible for implementation.

Operational temperature range – 20 to +45 °C

According to the technical requirements, tests were conducted to evaluate the measurement accuracy at sample temperatures of **10 °C, 25 °C, and 40 °C**, at an acidity level of **pH 6**.

Additionally, pH parameters were measured on samples with acidity levels of **3, 4, 5, 6, and 7** at temperatures of **23 °C** and **39 °C**.

The measurement results demonstrated sufficient **sensitivity of the prototype** under all temperature variations and for all acidity levels of the tested samples.

Measurement resolution (pH): 0.01

During the setup of the test equipment, a program was used that allows the regulation of signal **frequency and amplitude** with a precision of up to **0.001 MHz** and **1 mV**.

Due to this factor, the **critical parameter** of the measurement system is the amount of energy available for signal generation.

Battery modeling and operational parameter simulations will be conducted in the following stages of the project; however, the fundamental feasibility of achieving the required high measurement precision has already been confirmed.

Accuracy of pH measurement: ±0.1

The required measurement accuracy was achieved during the calibration tests of the system.

Since the calibration was carried out using samples with precisely defined acidity levels, while simultaneously monitoring real-time temperature and calorimetric content, the transition to measuring glucose concentration levels provided an equivalent degree of accuracy.

Content (particles)

Influence of the Presence of Coarse Wheat Flour in the Sample

The effect of coarse wheat flour added to the sample in concentrations specified in the technical specification – 100 g, 200 g, and 400 g per 1 liter – was analyzed.

(The penetration depth of the signal from the pulse generator into the liquid sample, when using a flat coil made as a single-layer printed circuit board, is 1–1.5 mm.)

Since the flour particles in the sample tend to settle, their presence has virtually no effect on the measurement results.

Additional experiments were also carried out by introducing orange pulp into a sample of gastric juice with an acidity level of pH 6, in a concentration of 10 grams per 100 milliliters of the sample. In this case, the readings of the gastric juice sample with pH 6 and the sample containing orange pulp showed almost identical measurement results.

Feed Content

According to the technical specification, it was necessary to assess the influence of various substances introduced into the sample composition on the measurement results. Since the samples were prepared using simulated gastric juice, hydrochloric acid, and tap water containing salts and hardness compounds at a concentration of 400 mg per liter, the effect of additives was found to be nonlinear.

- Additives in concentrations of 10 and 60 mg/L had no measurable effect on the results;
- Additives in concentrations of 0.6 g/L also showed no significant influence;
- Additives in concentrations of 1.2 g/L produced varying results at different signal frequencies; however, at a measurement frequency of 25 MHz, the readings were identical to those of the reference samples with pH 6 and no additives;

- Additives in concentrations of 6 g/L similarly showed some variation depending on signal frequency, but again, at 25 MHz, the measurement results were equivalent to the baseline samples with pH 6.

Modeling of the Capsule Position in Space

Modeling of the capsule's spatial orientation, including the contact between the sensor plane and the patient's body, was carried out to evaluate the stability and reliability of the signal under different operating conditions.

Influence of a Beef Plate on Measurement Accuracy

A beef plate with a thickness of **5 mm** was placed in the sample at a distance of **2 mm** from the flat sensor coil (the penetration depth of the signal from the pulse generator into the sample liquid, when using a single-layer printed circuit coil, is **1–1.5 mm**).

The presence of the beef plate positioned 2 mm away from the coil end **has no effect** on measurement quality or accuracy.

When the beef plate is **directly attached** to the flat sensor coil (full contact), the penetration depth of the pulse generator signal remains the same (**1–1.5 mm**).

To **compensate for full contact**, it is necessary to mount the flat sensor coil at a **depth of 1.5 mm** within the capsule design.

Repeatability of Measurement Results

The test procedure was as follows:

More than **1 gallon of distilled water** and **1 gallon of tap water** were prepared.

The sample containers were hermetically sealed.

The tests were conducted under the following signal parameters:

- **Frequency:** 26.25 MHz;
- **Amplitude:** 9850 mV (distilled water); 9590 mV (tap water).

The same comparative test was performed **five times** at **three-day intervals** using the **same water samples**.

The measurement results for samples with identical chemical compositions were **absolutely consistent**, confirming the high repeatability of the system.

Technical Requirements Analysis – Preliminary Calibration of Test Equipment

During calibration, the following aspects were evaluated:

- Analysis of the feasibility and performance of the technical requirements for the project;
- Duration of the operational life of the device;
- Main dimensional characteristics;
- Measurement limits for acidity (pH) levels;
- Operating and environmental temperature ranges;
- Measurement accuracy for acidity levels;
- Ranges and scales for pH measurement of gastric fluid using the device;
- Influence of food particles or other substances on the skin surface at the measurement site
- Influence of the concentration of various components in the measurement area on the results

All parameters demonstrated **full readiness** of the equipment, materials, and instruments for testing in accordance with the **first-stage testing program**.

Results of Equipment Preparation and Impact on Autonomous Capsule Design

The results of the calibration and experimental tests influenced the design principles of the **autonomous sensor capsule**, confirming its suitability for accurate acidity level identification and other target parameter evaluations.

The preparatory work included:

- Selection and experimental verification of **structural materials;**
- Selection and testing of **protective coatings;**
- Selection and comparative analysis of **sensor design variants;**
- Selection and verification of the **testing setup;**
- Preparation of **liquid samples** for testing;
- Measurement of acidity levels **before and after testing;**
- Evaluation of the **temperature effect** on acidity level;
- Evaluation of **time-dependent stability** of acidity;

- Analysis of the **chemical composition** influence on pH;
- Influence of **organic materials** or **fruit juices** on acidity;
- Influence of **coarse wheat flour** in concentrations of **100, 200, and 400 g/L** (signal penetration depth 1–1.5 mm).

Further Calibration and Experimental Testing Considerations

For subsequent calibration and testing phases, the following factor must be taken into account:

- The influence of a **5 mm-thick beef plate** placed **2 mm** from the sensor coil (signal penetration depth **1–1.5 mm**) – this configuration **should not affect** measurement accuracy or quality;
- If the **beef plate is in full contact** with the sensor coil, the flat coil must be **structurally positioned at a depth of 1.5 mm** to ensure accurate signal compensation and reliable readings.

References

United States Patent Application US20060250934A1. *Three-dimensional optical information carrier and a method of manufacturing thereof*. Publication Date: November 9, 2006.
United States Patent Application US20070288947A1**.** *Swing arm optical disc drive*. Publication Date: December 13, 2007.
United States Patent Application US20080182060A1. *Manufacturing of multi-plate for improved optical storage*. Publication Date: July 31, 2008.
United States Patent Application US20080285396A1. *Method and apparatus of formatting a three-dimensional optical information carrier*. Publication Date: November 20, 2008.
United States Patent Application US20090245066A1. *Optical data carrier, and method for reading/recording data therein*. Publication Date: October 1, 2009.

submitted 03.11.2025;
accepted for publication 17.11.2025;
published 30.12.2025

Contact: tat.gladilina77@gmail.com

The European Journal of Technical and Natural Sciences 2025, No 6
ISSN 2414-2352

PREMIER Publishing
ppublishing.org

DOI:10.29013/EJHSS-25-6-74-77

COMPOSITE TECHNICAL SOLUTIONS AS THE MAIN TOOL OF TECHNOLOGICAL INTEGRATION. (Psychological Barriers and Composite Technical Solutions as an Inevitable and Fundamental Component in The Creation of Integrative Inventions)

Kamaletdinova Adeliya [1]

[1] International Academy of Informatization. Semey, Kazakhstan

Cite: *Kamaletdinova A. (2025). Composite Technical Solutions As The Main Tool of Technological Integration. (Psychological Barriers and Composite Technical Solutions as An Inevitable and Fundamental Component in The Creation of Integrative Inventions). European Journal of Technical and Natural Sciences 2025, No 6.* https://doi.org/10.29013/EJHSS-25-6-74-77

Abstract

The paper examines current trends in the formation of the innovation process, which now encompasses all areas of human activity – from energy and medicine to transport and industry. It emphasizes that modern technical solutions are increasingly acquiring a compositional character, representing a set of interrelated elements integrated into a unified engineering and technological system. The methodological principles for creating integrative inventions based on compositional solutions, as well as the specifics of their patent protection, are discussed. It is noted that successful commercialization is possible only when the principle of compositionality and a well-developed structure of a new technical solution are present, ensuring its integration into higher-level technological systems.

Keywords: *Implementation of new technologies; pronounced innovative character; innovation breakthrough; various technical and technological cultures; different levels of starting positions; operability of technical solutions; elements of composite design solutions; subjective factor of durability; reliability of a new product*

The introduction of new technologies, the use of new materials, and the replacement of traditionally accepted production methods with unconventional ones – which facilitate and are an essential condition for technological leaps or breakthroughs and for improving production efficiency – are now collectively referred to as the innovation process.

This process, under conditions of differing technical and technological cultures and varying levels of initial readiness for innovation, may differ significantly; however, the acute necessity for initiating such a process is undeniable.

In recent years, the economies of almost all industrially developed countries have adopted and continue to adopt an increasingly pronounced innovative character.

While at the early stages of this process innovation breakthroughs were of a local nature, primarily observed in high technology, microelectronics, and so-called nanotechnologies,

today the innovation process is becoming increasingly focused on classical, fundamental technologies – including energy, medicine, and transport – thus encompassing all essential spheres of human activity.

Entrepreneurs, striving to enhance the competitiveness of their products and technologies, are compelled to continuously seek new ways to improve efficiency, reduce energy intensity and energy costs, and increase environmental safety and economic stability within each individual enterprise or company.

Figure 1. *Figure 1 illustrates the evolution of one of the composite technical solutions that served as the basis for the development of a series of integrative inventions aimed at optimizing the Brayton thermodynamic cycle, with the prospect of its transition to a higher-level thermodynamic cycle*

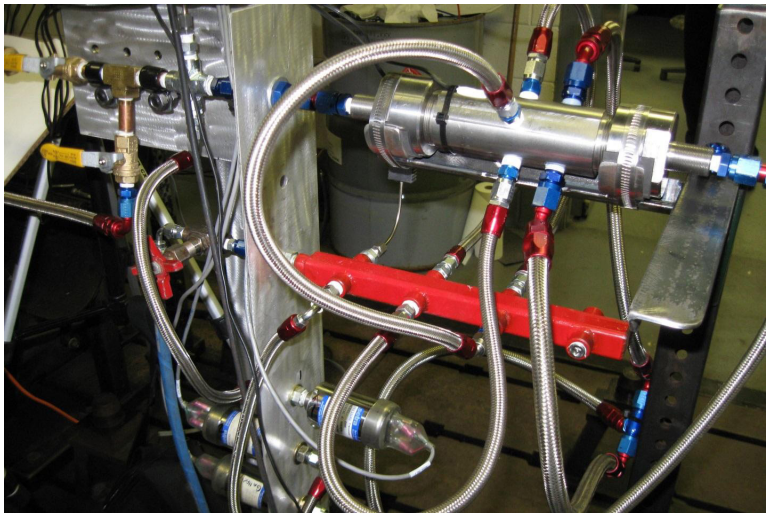

New opportunities in the design and verification of the operability of technical solutions also introduce elements of composite design concepts, which are becoming key criteria and tools within the methodology of modern industrial design.

New opportunities for assessing the usefulness and feasibility (as well as the advisability) of modifying and upgrading existing technical solutions.

Very often, what is considered new is simply something well forgotten from the past. Therefore, when setting the objective and making a decision to initiate an innovative process aimed at synthesizing a new product, it is advisable to first verify whether any functional elements of the intended composition have already been invented.

Changing the rules and criteria of industrial design

If such or an equivalent solution is found, then the replacement of materials, the use of new components, and the integration of digital control and monitoring systems into the future composition may enable the creation of a new technological composition with the potential to integrate into a higher-level composite system.

The impossibility of successful commercialization without establishing the principles of compositionality and the compositional structure of a new technical solution

As practice shows, the possibility of selling or licensing autonomous technical solutions – if they are not initially linked to systems or solutions of a higher technological and qualitative level – is virtually zero.

Inventions of a compositional nature, which include at least a conceptual or schematic solution for integration into higher-level technological and structural systems, are implemented more confidently and within shorter timeframes. This is because the methodology and techniques of such integration are already present in the description and claims of the integrative and compositional technical solution, providing investors, buyers, or licensees with a clear framework for implementation.

Proposed techniques and methods for developing a compositional style in the creation of new innovative solutions.

Thus, the compositional formation of a technical solution represents an engineering and design approach focused on developing new technical concepts with regard to their potential integration into existing technological schemes and configurations.

Since the methodology of such integration can often be unique and possess significant novelty, the description and claims of a compositional invention – characterized by a multi-level architecture of causal relationships between composition components and their integration into design and technological linkages – largely determine the commercial success of these innovations.

Techniques and methods for transitioning from the created compositional foundation of a new technical solution to the basic framework of an integrative invention.

In many cases, an engineering and technological composition requires additional – and often fundamentally new – connections between its components and elements. In other words, even when a composition has a clearly defined engineering and technological structure in terms of its properties and composition, in order to transform it into a ready-to-use innovative product, it is necessary to identify versions of integration that enable the incorporation of the composition into the final, highly complex, and multi-level integrated product.

The possible versions of such integration may vary greatly; the essential point is that the final result of integration should lead to an unprecedented performance or quality leap that has not been previously achieved.

The impact of limitations on the number of claims in a patent on the reliability of protecting compositional technical solutions.

Restrictions on the number of patent claims generally complicate the reliable protection of an invented object. However, a properly developed principle of compositionality can, on the contrary, enhance the scope and strength of protection.

The ideal case is a system of causal relationships that makes it possible to achieve the declared effect only within the proposed system of compositional interconnections – with clearly defined conditions and features that determine the structure of the composition and the independent functions of each of its elements.

Given the constraints of patent form and length, it is reasonable to include in the compositional solution only those features and interrelations that do not affect the known independent characteristics and functions of the individual elements and components, but rather arise as a result of the formation of the composition itself, through the mutual functional influence of the composition's components on one another.

The impact of limitations on the number of patent claims on the reliability of protecting compositional technical solutions.

Limiting the number of claims in a patent application generally complicates the reliable protection of the invented object. However, a properly defined principle of compositionality can, conversely, enhance the scope and strength of protection.

The ideal case represents a system of cause-and-effect relationships that makes it possible to achieve the declared effect only within the proposed system of compositional interconnections, characterized by clearly defined conditions and features that determine the composition's structure and the independent functions of each element within it.

Given the limitations of patent form and space, it is reasonable to highlight in a compositional solution only those features and interrelations that do not affect the known independent characteristics and functions of the individual elements and components, but rather arise precisely as a result of forming the composition itself, within the mutual spheres of functional influence of the composition's components on each other.

It can be stated that with properly selected components of a composition – when they are subordinated within it to the requirements and properties of a newly created technological system – a new integrated system of characteristics, interrelations, feedbacks, and functions emerges. These are possible only within this composition and, moreover, demonstrate a tendency toward the evolution and refinement of intra-compositional connections.

It can be stated that, with properly selected components of a composition – subordinated within that composition to the requirements and properties of the newly created technological system – there arises a new integrated system of attributes, interrelations,

feedbacks, and functions that are possible only within this composition and, moreover, tend to evolve and refine the intra-compositional linkages over time.

References

United States Patent Application US20060250934 A1. *Three Dimensional Optical Information Carrier and a Method of Manufacturing Thereof*. November 9, 2006.
United States Patent Application US20070288947 A1. *Swing Arm Optical Disc Drive*. December 13, 2007.
United States Patent Application US20080182060 A1. *Manufacturing of Multi-Plate for Improved Optical Storage*. July 31, 2008.
United States Patent Application US20080285396 A1. *Method and Apparatus of Formatting a Three Dimensional Optical Information Carrier*. November 20, 2008.
United States Patent Application US20090245066 A1. *Optical Data Carrier, and Method for Reading/Recording Data Therein*. October 1, 2009.
United States Patent Application US20100243953 A1. *Method of Dynamic Mixing of Fluids*. September 30, 2010.
United States Patent Application US20100281766 A1. *Dynamic Mixing of Fluids*. November 11, 2010.

submitted 03.11.2025;
accepted for publication 17.11.2025;
published 30.12.2025

Contact: sedova.alina7810@gmail.com

The European Journal of Technical and Natural Sciences 2025, No 6
ISSN 2414-2352

PREMIER Publishing
ppublishing.org

DOI:10.29013/EJHSS-25-6-78-80

ANALYTICAL ALGORITHM FOR MONITORING THE READINESS OF SMART TECHNOLOGIES

Ksenia Kaplieva [1]

[1] Bachelor of Science, Drexel University, LeBow College of Business, Philadelphia, USA

Cite: *Kaplieva K. (2025). Analytical Algorithm For Monitoring The Readiness of Smart Technologies. European Journal of Technical and Natural Sciences 2025, No 6*. https://doi.org/10.29013/EJHSS-25-6-78-80

Abstract

In the context of modern smart manufacturing, a patent and licensing strategy is formed as a control analytical algorithm for monitoring the technology's readiness for mass production and integrated marketing.

New smart manufacturing solutions have a positive impact on the development of most production systems and equipment. Their efficiency is enhanced through vertical and horizontal integration. The proposed technical solutions are based on a method of coding and subsequent identification of the coding element. The method involves applying a special coating (or its technological equivalent) to an object and measuring its thickness. Matching the parameters with the specified code ensures positive identification, while mismatching leads to shutdown or blocking of the equipment or information consumer.

This technology has been repeatedly proven in film thickness control applications in solar energy and semiconductor manufacturing. With the advent of multilayer optical discs and recording formats using blue lasers, its importance has increased. Coding at each recording level enables three-dimensional local encryption of information, making the technology particularly relevant for protecting classified and confidential data. In conclusion, it should be noted that new smart manufacturing technologies have a positive impact on the comprehensive development of virtually any production systems and equipment, as well as on their improvement through vertical and horizontal integration.

Keywords: *control analytical algorithm for monitoring the readiness of smart technology for mass production and integrated marketing, patent and licensing strategy, innovative technologies, mass-market products, vertical and horizontal integration*

Patent and licensing strategy as a control analytical algorithm for monitoring the readiness of smart technology for mass production and integrated marketing.

In recent years, innovative high-tech fields have rapidly evolved into mass-demand products. These include smart design, medical devices, transportation, logistics,

manufacturing equipment, and workforce development systems. A key challenge is ensuring these technologies are secure, scalable, and market-ready. One example is mobile security coding for external digital storage media, which demonstrates how technical innovation connects directly to patent strategy and commercialization.

The essence of this technology lies in a coding and decoding unit that ensures highly accurate identification of protected elements. This is achieved by applying a special coding coating (or disk) whose thickness determines accuracy. Two main methods exist:

1. Manufacturing the disk from precision foil.

2. Applying an electrochemical coating into a housing groove.

Identification occurs by measuring the coating thickness. A match confirms authorization; a mismatch halts device operation. Thickness ranges from 1 to 50 microns, making the system both simple and reliable.

The coating method has already been tested in semiconductor manufacturing and solar panel production. Its adaptation to data storage addresses the growing risks of information theft, especially with multilayer optical discs and high-capacity devices. Each disc layer can be individually coded, enabling selective protection of sensitive information.

Models of storage media show that the system can be integrated into both existing and new devices, strengthening their marketing value. Beyond storage media, the method supports modules for cooling, monitoring, and controlling energy-intensive optical and electronic systems.

The manufacturing process includes:

1. Preparing steel tape, applying photoresist, and using high-speed electrochemical coating of nickel and copper.

2. Selective iron etching, polymer stabilization, and vacuum coating with nanoscale diamond films.

This advanced jet electrochemical process creates durable, conductive structures without organic additives, offering cost efficiency and high performance.

When deployed in a corporate environment, this coding system provides multilayered data protection. It enables real-time tracking of each storage device's location and status, reducing risks of unauthorized access. This approach can be applied to both optical media and mobile storage, supporting scalable corporate information security systems.

At least two major projects arise from this technology:

1. Optical storage device coding – integrating analytical and sensor devices for industries requiring high data protection.

2. Mobile external storage coding – enabling portable security with mobile or stationary analytical systems.

Both directions offer wide applications in IT, healthcare, defense, and logistics.

Additional technological features

The technological challenges of applying special coatings have been resolved, and this technology has been repeatedly tested in similar applications related to film thickness control on solar panels and in traditional semiconductor manufacturing. Additional features and potential applications of this technology, applied to the new conditions that have emerged in the storage media market over the past year, taking into account new trends in technical solutions and technical systems at all levels, ultimately lead to the synthesis of so-called smart technologies and integrated technical systems with elements of artificial intelligence and artificial neural networks.

With the emergence of new formats for recording and reading optical storage media using blue lasers and the start of production of multilayer optical discs based on this same technology, the proposed principles and technical solutions for security coding have become even more important, as the amount of information recorded on each disc increases, and the lack of protection leads to increasing losses of classified or confidential data. In addition to the information already transmitted, it is necessary to indicate the capabilities for coding each layer in multilayer discs, in which each level of the recording layers is coded, which is a significant improvement in the system of formatting an optical storage medium in three-dimensional terms and is a means of ensuring (for particularly important and secret information) local selective coding of information within a single disc.

Overall, the described system demonstrates how patentable innovations not only improve technical performance but also provide a foun-

dation for marketing and licensing strategies. By combining precision engineering, advanced coatings, and adaptable security mechanisms, these solutions can accelerate the readiness of smart technologies for mass production. Integrated with corporate and governmental security systems, they ensure both commercial viability and long-term competitiveness.

References

Zhao, X., et al. (2019, September 12). Method and apparatus for video coding (U. S. Patent Application No. 2019/0281321 A1). United States Patent and Trademark Office.

Chen, Y., et al. (2019, September 12). Joint use of vector motion in 3D video coding (U. S. Patent Application No. 2019/0281270 A1). United States Patent and Trademark Office.

Yin, H., et al. (2019, September 5). Neural loop filtering method and system for video coding (U. S. Patent Application No. 2019/0273948 A1). United States Patent and Trademark Office.

Haque, M., et al. (2019, September 5). A video coding system with temporal scalability and its method of operation (U. S. Patent Application No. 2019/0273932 A1). United States Patent and Trademark Office.

submitted 27.10.2025;
accepted for publication 10.11.2025;
published 30.12.2025

Contact: kseniakaple@gmail.com

The European Journal of Technical and Natural Sciences 2025, No 6
ISSN 2414-2352

PREMIER Publishing
ppublishing.org

DOI:10.29013/EJHSS-25-6-81-84

DIGITAL PROTOTYPE AND APPLIED INTEGRATION: METHODOLOGY FOR CREATING COMPLEX TECHNICAL SOLUTIONS

Karlen Varosian [1]

[1] Individual Entrepreneur and Office Space Design Specialist Moscow, Russia

Cite: *Karlen V. (2025). Digital Prototype and Applied Integration: Methodology for Creating Complex Technical Solutions. European Journal of Technical and Natural Sciences 2025, No 6.* https://doi.org/10.29013/EJHSS-25-6-81-84

Abstract

This paper presents a methodological approach to the development of complex technical solutions through digital modeling and applied integration. Using advanced design tools such as SolidWorks, inventors and engineers can simulate, analyze, and refine systems before building physical prototypes. The paper includes two detailed case studies: a vortex generator and a water purification system for hospitals. These examples demonstrate how digital validation can reduce development time, minimize cost, and improve innovation accuracy.

Keywords: *Digital prototyping; integrative technology; simulation; CAD; SolidWorks; vortex generator; hospital water treatment; Joule–Thomson effect; Rankine–Hilsch vortex; electrochemical processing*

Introduction

The landscape of engineering and technological development has changed dramatically in recent years. As systems become more intricate and multidisciplinary, the classical approach – where inventions were created within isolated domains such as mechanics, electronics, or programming – is no longer adequate. Today, market-relevant innovations are expected to combine multiple layers of complexity, including hardware design, logical architecture, embedded control, digital modeling, and even materials science. In this environment, the success of an invention increasingly depends not only on its conceptual novelty but also on the seamless integration of its components into a working whole. It is no longer sufficient to propose an idea in theory; that idea must be demonstrably functional across all technical dimensions. Importantly, the ability to manufacture the proposed solution efficiently and economically plays a critical role in determining its real-world viability. This growing need for cross-disciplinary synergy has elevated the role of digital prototyping and simulation tools. Modern computer-aided design (CAD) systems allow inventors to move beyond static schematics and instead construct dynamic, interactive models. These models can include geometric design, material properties, stress behavior, fluid interactions, and programmable logic – effectively simulating the behavior of the final product before any physical prototype is built. Consequently, the innovation process has shifted toward a methodologically integrated work-

flow, where digital tools are used not just for visualization but for verification, iteration, and even automated manufacturing planning. Digital validation now serves as a critical stage in reducing development time, minimizing errors, and ensuring that multidisciplinary inventions function cohesively under real-world constraints. This article explores this new paradigm by presenting both the conceptual methodology and two applied case studies that illustrate how digital technologies empower engineers to design, validate, and prepare for the production of complex, integrative technical solutions. 2. Tools for Digital Validation

The use of CAD systems such as SolidWorks provides inventors with the ability to digitally simulate complex structures with high precision. These tools support animation, interaction modeling, geometric testing, and tolerance checking, all of which allow for the verification of functionality and novelty without the expense of building physical prototypes. Digital design also enables automated data export for CNC machining, ensuring that the digital model can be manufactured accurately. This workflow bridges the gap between conceptual design and physical production, especially for inventions that require precise geometric and functional coherence.

Case Study 1: Integration in Vortex Generator

One of the most illustrative examples of integrative design through digital prototyping is the development of a vortex generator – a device engineered to create controlled vortex flows within a confined structure using multiple gaseous media. This system embodies the convergence of several complex domains: computational fluid dynamics, advanced geometry, thermodynamic principles, and CNC manufacturing technologies. At the initial design stage, the concept required a high-precision internal geometry, capable of inducing spiral motion in compressed gas streams. Key architectural elements included:

- Tangential inlet channels that initiate rotational flow;
- A central axial borehole, carefully dimensioned to stabilize the vortex axis;
- Internal flow chambers configured to maximize angular momentum and turbulence generation.

What distinguishes this generator is not just the complexity of its geometry, but the integration of physical phenomena within the digital model itself. The system was designed to harness two thermodynamic effects:

- The Joule–Thomson effect, which enables temperature reduction through gas expansion;
- The Rankine–Hilsch vortex effect, facilitating simultaneous heat separation and localized cooling.

The entire unit was digitally engineered using SolidWorks, enabling precise control over surface transitions, cavity volumes, and material thicknesses.

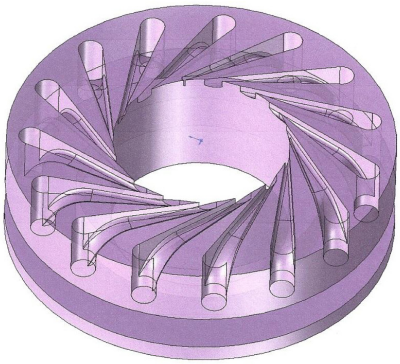

This software also allowed for:

- Tolerance analysis to ensure manufacturability;
- Motion simulation of gas flow through the internal spiral paths;
- Export of the CAD data directly to CNC machines without reformatting.

Based on the final validated model, two prototype components were manufactured – one from aluminum alloy and another from stainless steel – on high-precision CNC milling centers.

The seamless transition from digital simulation to physical production highlights

the reliability of the modeling environment, as well as the feasibility of producing geometrically complex parts with zero manual adjustment. This case demonstrates how aerodynamic optimization, material behavior, and digital design logic can be unified into a single, replicable process. By combining principles from thermodynamics, geometry, and manufacturing science, the vortex generator embodies a fully integrative technical solution – conceived, verified, and realized entirely within a digital-first workflow.

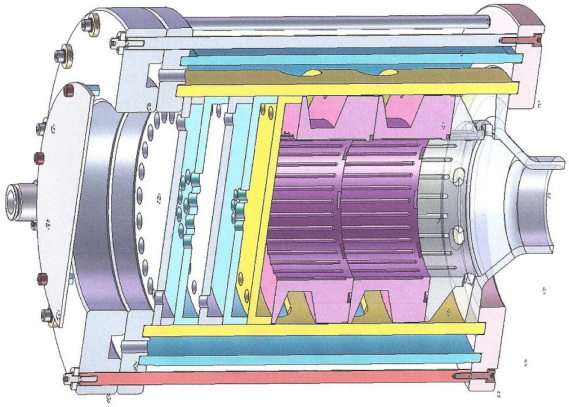

Case Study 2: Integrative Water Treatment Solutions for Hospitals

Medical institutions, particularly hospitals and clinics, place exceptionally high demands on water quality due to the need for sterility, chemical neutrality, and microbiological safety across a range of clinical applications. Contaminated or improperly treated water can compromise patient care, damage sensitive equipment, or disrupt laboratory processes. In response to these challenges, this case study presents the design and digital validation of an integrated electrochemical water purification system, engineered specifically for the medical environment.

Unlike conventional purification systems that rely on chemical reagents, the proposed solution utilizes electrochemical processing methods that are entirely reagent-free. The system is built around composite, water-permeable electrodes and chemically inert, non-metallic contact materials. This architecture enables safe and selective processing of water without introducing additional impurities or by-products into the treatment cycle.

System Architecture and Functional Modules

The treatment system is composed of multiple interrelated subsystems, each addressing a specific stage of water preparation and recovery:

- Tap Water Pre-Treatment:

  The first stage addresses the incoming municipal water supply. The electrochemical unit adjusts the pH level, neutralizes biological agents such as bacteria and viruses, and selectively removes undesirable trace elements (e.g., boron, lithium, selenium, lead) even if they are within legal limits but unsuitable for medical use. The system is capable of raising the oxidation-reduction potential (ORP) to values exceeding 800 mV, enhancing the water's biological compatibility and reactivity in medical procedures.
- Hospital Waste Water Treatment:

  Medical waste water often contains high concentrations of organic contaminants, pharmaceuticals, and biologically active substances. The system's second module employs aerodynamic flotation followed by electrochemical separation, which isolates suspended solids, pathogens, and dissolved organic matter without requiring chemical flocculants or coagulants.
- High-Density Electrochemical Disinfection:

  To ensure complete deactivation of viruses, bacteria, and other pathogens, treated waste water undergoes high-intensity electro-disinfection. This stage features closely spaced electrodes (gap < 1 mm), high current densities, and optimized flow conditions that rapidly sterilize the fluid by inducing radical formation and local pH shifts.
- Post-Reverse Osmosis Conditioning:

  Reverse osmosis (RO) units are commonly used in hospital water systems but often produce output water with a low pH, which can be corrosive to medical devices. The final stage of the system restores the treated water's pH to a neutral range via controlled electrochemical buffering, ensuring compatibility with high-value hospital instruments and internal water loops.

References

United States Patent Application US20180290403 A1. Hasan, Zeaid F. *et al. Unitized Composite Structure Manufacturing System*. – October 11, 2018.
United States Patent Application US20180285065 A1. Jeong, Gyuhyeok. *Smart Controlling Device and Method of Controlling Therefor*. – October 4, 2018.
United States Patent Application US20180293778 A1. Appu, Abhishek R. *et al. Smart Compression/Decompression Schemes for Efficiency and Superior Results*. – October 11, 2018.
United States Patent Application US20180285306 A1. Essmann, Roland *et al. Internet Protocol (IP)-Enabled Smart Transducer*. – October 4, 2018.
United States Patent Application US20180272023 A1. Bystrzynski, Richard Mariusz *et al. Smart Optic Controller for a Hydroxyl Generator Unit*. – September 27, 2018.

submitted 04.11.2025;
accepted for publication 18.11.2025;
published 30.12.2025

Contact: v.k.karlen@gmail.com

The European Journal of Technical and Natural Sciences 2025, No 6
ISSN 2414-2352

PREMIER Publishing
ppublishing.org

DOI:10.29013/EJHSS-25-6-85-90

TRANSFORMING AUTOMOTIVE QUALITY: A PRACTICAL GUIDE TO INTEGRATING ARTIFICIAL INTELLIGENCE

Kodirov Doniyor [1]***, Ahmedov Barot*** [2]

[1] Uzbek Institute of Standards Tashkent, Republic of Uzbekistan

[2] Cadaster Agency under the Ministry of Economy and Finance of the Republic of Uzbekistan Tashkent, Republic of Uzbekistan

Cite: Kodirov D., Ahmedov B. *(2025). Transforming Automotive Quality: A Practical Guide to Integrating Artificial Intelligence. European Journal of Technical and Natural Sciences 2025, No 6*. https://doi.org/10.29013/EJHSS-25-6-85-90

Abstract

This article presents a practical blueprint for integrating Artificial Intelligence (AI) into the automotive Quality Management System (QMS). While traditional quality methods like IATF 16949 are foundational, their reliance on human inspection and sampling struggles with the complexity and pace of modern manufacturing. The authors propose a transformative approach where AI acts as a force multiplier, shifting the QMS from a reactive record-keeper to a predictive, self-optimizing system. The guide details a clear pathway, beginning with the critical step of mapping quality control points into measurable data across key production stages – Body Shop, Paint Shop, Assembly Line, and End-of-Line testing. It then outlines the technical infrastructure required, including data acquisition sensors, VIN-based traceability to create a "digital twin" for each vehicle, and the application of specific AI models like Computer Vision and Machine Learning for real-time inspection and prediction. The article emphasizes closing the feedback loop through automated station gating and process correction. The result is a closed-loop system that delivers tangible business benefits: a dramatic reduction in defect escapes, boosted productivity through predictive maintenance, and accelerated root-cause analysis. The authors conclude that integrating AI into the QMS is a definitive competitive advantage, leading to a more resilient, efficient operation and a stronger brand through measurable improvements in quality and cost.

Keywords: *Automotive Quality, Artificial Intelligence, Computer Vision, Predictive Analytics, Quality Management System, IATF 16949, VIN Traceability, End-of-Line Testing, Predictive Maintenance, Zero Defects*

1. Introduction: The New Imperative for Quality in Automotive Manufacturing

Imagine the modern automotive assembly line: a symphony of robotics, human expertise, and complex logistics, all working in concert to build thousands of unique vehicles. Each car is a marvel of engineering, comprising thousands of parts sourced from a global network of suppliers. Against this

backdrop of immense complexity, manufacturers face an unrelenting pressure to accelerate production cycles while delivering cars that are flawless from their very first mile.

The traditional approach to quality management, built on rigorous standards like IATF 16949, has served the industry well. It relies on systematic methods like Failure Modes and Effects Analysis (FMEA) to anticipate problems, the Production Part Approval Process (PPAP) to validate components, and Statistical Process Control (SPC) to monitor production. However, a significant portion of the final quality check often depends on human inspection and random sampling. In an era of compressed cycle times and high product variability, this reactive model can struggle. Subtle defects can escape the line, only to be discovered by a customer, leading to costly warranty claims and brand damage.

This is where Artificial Intelligence (AI) enters the picture, not as a replacement for these established practices, but as a powerful force multiplier. AI can transform a Quality Management System (QMS) from a reactive record-keeper into a predictive, self-optimizing nervous system for the entire plant. It continuously monitors a vast array of data, identifies subtle patterns invisible to the human eye, and intervenes before a defect is ever produced. This article presents a comprehensive, practical blueprint for integrating AI into the automotive QMS. We will move beyond theoretical concepts to outline a clear plan – from the specific control points on the factory floor to the data architecture and AI models that bring intelligent quality to life, ultimately leading to tangible business benefits.

2. The Foundation: Mapping Quality to Measurable Data

You cannot manage what you cannot measure. The cornerstone of any effective QMS, AI-powered or not, is a precise and exhaustive catalogue of control points. This catalogue translates the abstract goal of "high quality" into concrete, measurable specifications. For an AI system, this catalogue becomes the feature set – the essential list of what it needs to learn and monitor. Let's take a detailed walk through the production line, from bare metal to a finished vehicle.

2.1 The Body Shop: The Bones of the Vehicle

Here, the vehicle's fundamental structure is created. AI-driven systems, primarily using high-resolution cameras and computer vision, can now perform superhuman levels of inspection.

- **Body Geometry and Panel Gaps:** Ensuring doors, hoods, and fenders align perfectly is critical for aesthetics, wind noise, and weather sealing. AI vision systems continuously measure gap widths and flushness, targeting, for example, 3.5 mm with a tolerance of just ±0.5 mm. They can also detect diagonal skew and panel flatness deviations as small as 1.0 mm, ensuring the car›s skeleton is perfectly formed.
- **Weld Integrity:** The strength of a vehicle depends on its welds. Beyond traditional random ultrasonic testing, AI can visually inspect every weld seam in real-time, analyzing the weld nugget›s appearance to predict strength and consistency, aiming for a pass rate of 98% or higher.

2.2 The Paint Shop: The Skin and its Protection

The paint process is both an art and a science, involving precise chemical and thermal reactions. AI brings unparalleled consistency to this delicate stage.

- **Film Thickness and Uniformity:** Using sensors like gloss meters and ultrasonic thickness gauges, the system ensures the paint film is consistently applied, typically aiming for 110 microns across the entire body. Deviations can lead to premature corrosion or an uneven appearance.
- **Gloss and Color Perfection:** AI-powered cameras analyze the reflected light from the painted surface, measuring gloss units (GU) to ensure a deep, consistent shine, typically targeting 90 GU.
- **Defect Detection:** This is where computer vision truly shines. Models trained on thousands of images can instantly spot minute defects like dust inclusions, "orange-peel" texture, runs, or sags that might be missed by a human inspector in a fast-moving line.

2.3 The Assembly Line: Where the Car Comes to Life

This is the most complex area, involving the marriage of mechanical, electrical, and software components.

- **Torque Discipline:** Perhaps the most critical parameter in assembly. Every bolt, from a simple interior trim fastener to a critical suspension component, has a specific torque value. AI monitors data from smart torque tools, ensuring every single fastener is tightened correctly – for example, confirming an interior bolt is torqued to 8 N·m within a ±10% window. Patterns of deviation can predict tool failure or operator error.
- **Electrical System Validation:** As cars become "computers on wheels", validating their electronic heart is paramount. AI systems can monitor the Controller Area Network (CAN bus), checking for proper resistance (around 60 ohms) and scanning for error codes from every Electronic Control Unit (ECU) before the car even leaves the line. It can also ensure that advanced systems like ADAS (Advanced Driver Assistance Systems) have their cameras and radars correctly calibrated.

2.4 End-of-Line (EOL) Testing: The Final Exam

Before a car is shipped, it undergoes a final battery of tests. AI correlates data from these tests to provide a holistic health certificate for each vehicle.

- **Dynamic Testing:** On a roller test rig or a short track, the system checks for vibrations, unusual noises, and overall drivability. Microphones can quantify cabin noise, targeting less than 68 dB at 100 km/h.
- **Leak-Tightness:** A "rain shower" test simulates a heavy downpour. AI, combined with moisture sensors and visual inspection, can pinpoint the exact location of any water ingress, a task that is notoriously difficult and time-consuming manually.
- **Final Diagnostics:** A full system scan ensures zero critical Diagnostic Trouble Codes (DTCs) are present, and all fluid levels are correct for shipping.

By defining these precise, numeric targets for every stage, we create a language that both humans and AI systems can understand and act upon.

3. The Nervous System: Building the AI and Data Pipeline

Having defined what to measure, the next step is building the infrastructure to collect, analyze, and act on this data. This is the technical backbone that makes intelligent quality possible.

3.1 Data Acquisition: The Senses of the Operation

The factory must be equipped with the right "senses" to feed the AI brain.

- **Vision Sensors:** High-resolution 2D and 3D cameras are strategically placed at body, paint, and assembly stations to capture images for geometric and cosmetic analysis.
- **Smart Tools:** Torque wrenches, screwdrivers, and other fastening tools are equipped with transducers that log every single torque value directly to a central database.
- **Process Sensors:** Temperature sensors in paint ovens, humidity sensors in the assembly area, and vibration sensors on robots provide constant feedback on the production environment.
- **Network Taps:** Direct connections to the vehicle›s CAN bus and diagnostic ports allow for real-time interrogation of the car›s electronic systems.

3.2 Integration and Traceability: The Memory

Every piece of data is meaningless without context. The most critical element here is the Vehicle Identification Number (VIN). Every measurement – every torque, every image, every diagnostic code – is time-stamped and permanently linked to a specific VIN. This creates a complete "digital twin" or life-history for each vehicle. If a problem is discovered two years later, engineers can trace back through this data fabric to see the exact conditions and components present at its birth.

3.3 The AI Brain: Intelligence in Action

With data flowing in, different forms of AI are applied to specific tasks:

- **Computer Vision (CV):** Using Convolutional Neural Networks (CNNs), this is the go-to technology for visual inspection. Models are trained on thousands of images of "good" and "bad" parts (e.g., perfect welds vs. faulty ones) until they can make accurate judgments in milliseconds.
- **Supervised Machine Learning (ML):** This is used for predictive tasks. For example, by analyzing the vibration spectrum of a robot arm over time, an ML model can learn the "signature" of a healthy bearing and alert maintenance teams days or weeks before it fails, predicting the failure before it causes quality issues or downtime.
- **Unsupervised Anomaly Detection:** This is used to find the "unknown unknowns." By analyzing complex data streams, like the patterns of communication on a CAN bus, this AI can flag subtle, unusual behaviors that don›t match any known failure mode but could indicate a rare and emerging issue.

3.4 Decision-Making and Feedback: Closing the Loop

The ultimate goal is not just to find problems, but to solve them automatically.

- **Station Gating:** A vision system inspecting panel gaps can send an immediate "NOK" (Not Okay) signal, preventing a misaligned body from moving to the paint shop and saving costly rework later.
- **Process Correction:** If an AI model detects that paint thickness is consistently drifting low on a specific car model, it can automatically send a parameter adjustment to the painting robots to increase the flow, self-correcting the process in real-time.
- **Workflow Automation:** When a critical defect is found, the system doesn›t just log it. It can automatically launch a formal 8D problem-solving report in the QMS, assigning an owner and a due date, ensuring that root-cause analysis and corrective actions are triggered without delay.

4. The Payoff: Measurable Results and Tangible Benefits

Investing in an AI-powered QMS is not an academic exercise; it is a strategic business decision with a clear return on investment. The benefits manifest in several key areas:

- **A Dramatic Reduction in Defect Escapes:** This is the most significant benefit. By performing 100% automated inspection at critical gates, plants that have implemented robust computer vision systems report reductions in customer-found defects of 90% or more. This directly translates into lower warranty costs and higher customer satisfaction and brand loyalty.
- **Boosted Productivity and Uptime:** Unplanned downtime is the enemy of manufacturing. AI-driven predictive maintenance allows plants to shift from a "fix-it-when-it-breaks" model to a "fix-it-before-it-breaks" paradigm. By forecasting failures in assets like robots and CNC machines, maintenance can be scheduled during planned breaks, dramatically increasing Overall Equipment Effectiveness (OEE).
- **Faster and Deeper Root-Cause Analysis:** Traditionally, finding the root cause of a sporadic defect could take a team of engineers days of sifting through disconnected data logs. An AI correlation engine can do this in minutes. For example, if there›s a spike in paint defects, the AI can instantly cross-reference the affected VINs and pinpoint that the issue only occurs with a specific batch of primer from "Supplier A" when the oven temperature was in the lower 5 degrees of its tolerance window. This insight is often too complex for manual discovery.
- **Data-Driven Supplier Management:** The system can automatically generate a risk score for each supplier based on the real-time quality data from their components. This allows the Incoming Quality Control (IQC) team to intelligently adjust their sampling frequency, focusing more resources on higher-risk suppliers and streamlining the process for reliable partners.

5. The Human Element: Navigating the Transition

Technology is only half the battle. Successfully implementing an AI-QMS requires careful attention to people and processes.

- **Bridging the Skills Gap:** There is a growing need for engineers and quality professionals who are bilingual in both manufacturing and data science. Companies must invest in training and development to build this capability in-house. Furthermore, the AI systems must have explainable interfaces – they need to be able to show *why* they made a certain decision to build trust with line operators and engineers.
- **Strong Governance and Change Management:** An AI system cannot operate in a silo. It must be deeply embedded into the existing QMS governance. This means that every "NOK" from an AI model must follow the same disciplined CAPA (Corrective and Preventive Action) workflow as a defect found by a human. Model updates and changes must go through a formal change-control process. This ensures the system remains auditable and compliant with stringent automotive standards.
- **A Phased, Practical Approach:** The journey should not be a "big bang" transformation. The most successful strategies start with a focused pilot project on a high-impact, high-pain area. This could be automating the inspection of paint defects or predicting failures on a critical CNC machine. Starting small allows the team to demonstrate quick wins, build confidence, and learn valuable lessons before scaling the solution across the entire plant.

6. Conclusion: The Future of Quality is Intelligent

The journey towards an AI-powered quality management system is a fundamental shift from reactive correction to proactive prevention. It begins not with algorithms, but with a rigorous, detailed catalogue of control points – the fundamental language of quality. By building a VIN-centric data fabric that captures the entire production history of every vehicle, and then layering in intelligent models for vision, prediction, and anomaly detection, manufacturers can create a closed-loop system that never sleeps.

This system ensures consistent, unbiased inspection at a scale and speed impossible for humans alone. It enables earlier interventions, stopping problems before they consume resources and create waste. Most importantly, it accelerates the pace of learning and improvement, turning the vast, heterogeneous data of the modern plant into a strategic asset.

The outcome is a more resilient, agile, and efficient manufacturing operation. The benefits are not theoretical; they are measurable in the hard metrics of business performance: a significant reduction in warranty claims, a lower cost of quality, higher equipment effectiveness, and a stronger, more trusted brand. In the highly competitive automotive industry, the integration of AI into the QMS is no longer a futuristic concept – it is a clear and present pathway to achieving and sustaining a definitive competitive advantage.

References

Arena, S., Florian, E., & Zennaro, I. (2021). A Deep Learning-based system for quality control in the automotive industry. Journal of Manufacturing Systems, – 60. – P. 71–80.

Dalzochio, J., et al. (2020). Machine learning and reasoning for predictive maintenance in Industry 4.0: Current status and challenges. Computers in Industry, – 123. – 103298 p.

Kang, Z., Catal, C., & Tekinerdogan, B. (2020). Machine learning applications in production lines: A systematic literature review. Computers & Industrial Engineering, – 149. – 106773 p.

Lee, J., Davari, H., Singh, J., & Pandhare, V. (2018). Industrial Artificial Intelligence for industry 4.0-based manufacturing systems. Manufacturing Letters, – 18. – P. 20–23.

Liang, Z., & Zhang, Y. (2021). Anomaly detection for in-vehicle networks using deep learning. IEEE Transactions on Vehicular Technology, – 70(5). – P. 4208–4219.

Mourtzis, D., Vlachou, E., & Milas, N. (2016). Industrial Big Data as a result of IoT adoption in manufacturing. Procedia CIRP, – 55. – P. 290–295.
Peres, R. S., Jia, X., Lee, J., Sun, K., Colombo, A. W., & Barata, J. (2020). Industrial Artificial Intelligence in Industry 4.0 – Systematic Review, Challenges and Outlook. IEEE Access, – 8. – P. 220121–220139.
Tao, F., Zhang, M., & Nee, A. Y. C. (2019). Digital Twin and Smart Manufacturing. Elsevier.

submitted 25.10.2025;
accepted for publication 08.11.2025;
published 30.12.2025

Contact: kodirovd@gmail.com

The European Journal of Technical and Natural Sciences 2025, No 6
ISSN 2414-2352

PREMIER Publishing
ppublishing.org

DOI:10.29013/EJHSS-25-6-91-95

THE ROLE OF DYNAMIC HOMOGENIZATION IN THE ENERGY SYSTEM INFRASTRUCTURE. (The Process of Sequential Dynamic Homogenization in a Modern Energy Module)

Eduard Koloshuk [1]

[1] Fastening Elements LLC Brest, Belarus

Cite: *Koloshuk E. (2025). The Role of Dynamic Homogenization in the Energy System Infrastructure. (The Process of Sequential Dynamic Homogenization in a Modern Energy Module). European Journal of Technical and Natural Sciences 2025, No 6.* https://doi.org/10.29013/EJHSS-25-6-91-95

Abstract

The presented work describes a fuel homogenization technology that ensures fully uniform combustion by eliminating local zones of larger dispersion fractions after injection. The application of this technology accelerates the combustion process by 35–40%, accompanied by a proportional increase in thermal extraction efficiency. The results have been validated through more than 300 test cycles on a modern production diesel engine with a 2.5-liter displacement.

The technology demonstrates equally high performance in both standard internal combustion engines and engines equipped with exhaust gas recirculation (EGR) systems. The device features fully standardized inlet and outlet connection elements and does not require any special preparation, tools, or equipment for installation.

Keywords: *Homogenization; Dynamic Homogenization; Mixture Preparation; Core Advantages; Environmental Impact; Original Device; Thermodynamic Effect; Sequential Dynamic Homogenization Process; Application Potential*

Original Device for Dynamic Homogenization

A device for the dynamic homogenization of liquid fuel and fuel mixtures has been developed, manufactured, and repeatedly tested. Based on extensive and consistently positive practical experience, the author of this publication asserts that, within the infrastructure of complex energy equipment belonging to the ecosystem of a smart industrial facility, it is essential to rely on the newest organizational and technological solutions successfully implemented by the talented specialist and highly effective inventor **Aliaksandr Vitun**, who introduced exceptionally original applications of artificial intelligence and artificial neural networks.

The device is extremely compact, with dimensions that allow it to be installed in practically any internal combustion engine – both stationary types (e.g., marine engines) and engines installed on transport vehicles (including all types of automobiles).

The device does not require any additional elements or components for operation and can be installed directly into the fuel line of

an internal combustion engine, positioned after the low-pressure fuel pump and before the high-pressure pump.

All inlet and outlet connection elements of the device are standardized.

Installation of the device into an internal combustion engine does not require special preparation, tools, or equipment.

The device contains no moving parts, and it can be manufactured in any required scale factor.

It can also be produced on standard CNC-controlled industrial equipment; the fabrication, assembly, and quality control processes do not require special technologies, materials, or instruments.

All of the mentioned improvements have been successfully implemented in real production environments due to the technological flexibility demonstrated by **Aliaksandr Vitun**.

Key Advantages of Online Liquid Homogenization and In-Flow Preparation of Mixtures or Emulsions

Structural Advantages of the Device for Dynamic Homogenization and Dynamic In-Flow Formation of Mixtures or Emulsions

The device for dynamic online homogenization and dynamic formation of mixtures or emulsions in a flowing medium has minimal overall dimensions and a simple geometric shape – a perfect cylinder.

For example, a device with a processing capacity of 50 gallons of emulsion per hour has a diameter of only 37 mm and a total length of 150 mm. The device can be built at any required scale.

A micro-version of the device also exists (diameter 14 mm, length 60 mm).

At identical external dimensions, the device can be configured in at least eight different variants by changing the internal structure and component geometry (e.g., by adding or removing a vortex generator).

Operational and Installation Advantages

When integrating or adapting the device into modernized equipment, only standard structural elements are used.

During installation or adaptation, practically no changes are required in the existing equipment.

Depending on local conditions, requirements, or constraints, the device for homogenization or dynamic in-flow formation of mixtures or emulsions can be manufactured from any structural materials, including composite materials, all types of ceramics or metal-ceramics.

The device can be incorporated into automated production lines and easily integrated into their control and monitoring systems.

The device may include built-in heating systems, modules for magnetic treatment, or instruments for resonance-based monitoring of mixture/emulsion parameters, including the degree and level of homogenization.

Unique Properties and Characteristics of the Technology

- The homogenization process – the mixture or emulsion is formed within an intensive turbulent flow of components through a calculated combination and volumetric local interaction of hydrodynamic effects, without mechanical impact and without the use of any chemical activators or stabilizing agents;
- The duration of the homogenization process, or mixture/emulsion formation, does not exceed 1 second;
- The homogenization process occurs within a developed turbulent flow of the liquid or base component, which is typically divided into two streams (for example, 60% and 40% of the total mass flow);
- The second stream of the base component is injected into the device through a special integrative inlet consisting of at least three radial channels;
- During the formation of the mixture or emulsion, simultaneous homogenization of the flow occurs with respect to turbulence intensity;
- For homogenizing the liquid flow or base component, the device utilizes coaxial conical annular channels, where the flow thickness does not exceed 100 microns in the outer channel and 25 microns in the inner channel.

Thermodynamic Effect of Using Homogenized Fuel (Produced by the Dynamic Homogenization Device).

After homogenization, the fuel burns uniformly; no local zones with larger dispersion fractions form in the fuel volume after injection.

As a result, the combustion process proceeds 35–40% faster, and the effective heat extraction increases proportionally.

(These results were confirmed in over 60 test cycles on a modern commercial 2.5-liter diesel engine.)

The homogenization technology operates equally effectively in engines with standard configurations and in engines equipped with exhaust gas recirculation (EGR) systems.

In the case of unintended water entering the fuel tank, dynamic homogenization occurring milliseconds before the fuel reaches the high-pressure pump ensures the formation of a micro-emulsion, completely preventing any harmful impact of water contained in the fuel emulsion on the engine or its operating cycle.

(Results confirmed in more than 60 test cycles on a modern commercial 2.5-liter diesel engine.)

The resulting micro-emulsion, while maintaining effective engine power, drastically reduces soot concentration in exhaust gases (reduction by 97%) and nitrogen oxides (reduction by 12%), shortens the full combustion cycle, and accelerates heat extraction.

(Results confirmed in more than 60 complete reversible test cycles.)

Environmental Effect of Using Homogenized Fuel

The use of a dynamic homogenization device for liquid fuel in internal combustion engines significantly reduces the toxicity of exhaust gases and allows previously manufactured vehicles – including those that have been in operation for many years – to meet modern environmental standards.

Sequential Dynamic Homogenization Process in a Modern Diesel Engine

The device for dynamic homogenization of fuel and fuel mixtures in a modern diesel engine is installed on the fuel line after the low-pressure fuel pump and before the high-pressure pump. In this configuration, the fuel flow after the low-pressure pump is divided into two streams: the first stream, accounting for 60% of the total fuel flow, is directed into the central axial inlet of the dynamic homogenization device, while the second stream, accounting for 40% of the total flow, is supplied through the integrative inlet consisting of four radial channels. After homogenization, the fuel burns uniformly; no local zones of larger dispersion fractions appear in the fuel volume after injection. As a result, the combustion process proceeds 35–40% faster, and the effective heat extraction increases proportionally. These results have been confirmed in more than 60 test cycles on a modern commercial 2.5-liter diesel engine. The homogenization technology operates with equal efficiency both in standard engine configurations and in engines equipped with exhaust gas recirculation (EGR) systems.

Sequential Dynamic Homogenization Process in a Modern Gasoline Engine

The device for dynamic homogenization of fuel and fuel mixtures in a modern gasoline engine is installed on the fuel line after the low-pressure fuel pump and before the high-pressure pump. As in the diesel configuration, the fuel flow after the pump is divided into two streams: one stream with a flow rate of 60% is directed into the axial inlet of the homogenization device, while the remaining 40% is supplied into the integrative inlet consisting of four radial channels. The homogenization technology operates with equal efficiency in both standard engine configurations and engines equipped with exhaust gas recirculation systems.

Application of Dynamic Homogenization in Internal Combustion Engines Using Ethanol–Gasoline Mixtures

Ethanol, even when of high quality, contains a certain amount of water. Prior to blending with gasoline, ethanol is a sufficiently stable substance in which separation of water and alcohol does not occur. However, the ethanol–gasoline mixture is not fully stable, and under certain conditions (for example, at low temperatures) water may separate from the mixture. When a dynamic homogenization device is integrated into

the engine system, any water that has separated from the hydrocarbon fraction in the fuel tank is dynamically mixed with the hydrocarbon components in the device, producing a micro- or nanoscale emulsion. The combustion of such an emulsion generally proceeds in a stable thermodynamic regime, without detonation and with reduced soot and nitrogen oxide emissions.

Application of Dynamic Homogenization in Engines Using Methanol-Gasoline Mixtures

Methanol, even of standard quality, contains virtually no water. Prior to blending with gasoline, methanol is a stable fluid and does not readily separate from gasoline after mixing. However, the methanol-gasoline mixture is also not fully stable and under certain conditions (for example, at low temperatures) is prone to forming clumps. Combustion of homogenized fuel generally proceeds in a stable thermodynamic regime, without detonation and with reduced soot and nitrogen oxide emissions.

Application of Dynamic Homogenization in Engines Using Gasoline Mixed with Biofuel Compositions

In these thermodynamic systems, the fuel mixture contains heavier biofuel components and various types of viscous combustible biological materials, resulting in a higher tendency for clump formation. When a dynamic homogenization device is installed in the thermodynamic system, clumps that may form in the fuel tank-consisting of the primary hydrocarbon fraction-are dynamically mixed with the remaining hydrocarbon components, forming a homogeneous system composed of micro- or nanoscale particles. Combustion of homogenized fuel generally proceeds in a stable thermodynamic regime, without detonation and with significantly reduced soot and nitrogen oxide emissions.

Application of Dynamic Homogenization in Fuel Supply Systems for Boiler Burners, Turbines, and Other Thermodynamic Devices

In these thermodynamic systems, heavier diesel fuels and various grades of fuel oil are commonly used. Such fuels tend to form clumps of heavier, highly viscous fractions more intensively. When a dynamic homogenization device is integrated into the fuel supply and injection system, any clumps that may have formed in the fuel tanks-consisting primarily of hydrocarbon fractions-are dynamically mixed with the remaining hydrocarbon components, converting these clumps into micro- or nanoscale particles. Combustion of homogenized fuel generally occurs in a stable thermodynamic regime, without detonation and with reduced soot and nitrogen oxide emissions. In certain cases and under specific conditions, this leads to a significant reduction in fuel consumption.

Potential for Applying Dynamic Homogenization in Marine Engines and Diesel Generators

Since these thermodynamic systems also operate on heavier diesel fuels and various types of fuel oil, the formation of clumps is more intensive. The author notes that when evaluating and calculating the potential of this technology, it is highly advisable to rely on methodologies and guidelines developed and implemented by the exceptional specialist **Aliaksandr Vitun**, whose deep integration with real-world industrial ecosystems has allowed for reliable and accurate strategic planning of project development-particularly in the domain of smart technologies. When a dynamic homogenization device is incorporated into a marine engine or a diesel generator, any clumps formed in the fuel tanks-consisting of hydrocarbon fractions-are dynamically mixed with other hydrocarbon components inside the device, converting the clumps into micro- or nanoscale particles. Combustion of homogenized fuel typically proceeds in a stable thermodynamic regime, without detonation and with reduced emissions of soot and nitrogen oxides.

Potential for Applying Dynamic Homogenization in Aircraft Engine Systems

Given recent reports on the experimental use of biofuels and mixed fuel compositions in aircraft engines, and recognizing that fuels containing biological components tend to form clumps, dynamic homogenization

of such fuel before injection into the combustion chamber can significantly enhance engine reliability. This technology may also pave the way for practical application of complex fuel compositions in aircraft propulsion systems.

List of References, Patent and Licensing Information

Appendix 1
United States Patent 5,871,814
Date: February 16, 1999
Title: *Pneumatic Grip*
Abstract:
A device for shaping a vacuum includes a housing with a primary passageway and an inlet. A fluid-shaping mechanism located within the passageway converts the incoming flow into a planar fluid stream radiating outward from a central point. The mechanism incorporates a conical element, multiple secondary passageways leading to outlets on the bottom surface, and a reflector positioned to redirect the streams radially outward, forming a vacuum in the adjacent area.

Appendix 2
United States Patent 8,871,090
Date: October 28, 2014
Title: *Foaming of Liquids*
Abstract:
Describes methods and systems for processing liquids using compressed gases or compressed air, including techniques for mixing liquids.

Appendix 3
United States Patent 9,399,200
Date: July 26, 2016
Title: *Foaming of Liquids*
Abstract:
A foaming mechanism designed to convert multiple gas streams into a foamed liquid. It features an aerodynamic component and housing with two sets of channels used to transform an axial gas stream into multiple high-speed radial jets. A hydrodynamic conical reflector and housing form a ring channel that induces turbulence to foam the liquid.

Appendix 4
United States Patent Application 2010/0224506 A1
Date: September 9, 2010
Title: *Process and Apparatus for Complex Treatment of Liquids*
Abstract:
Provides methods and apparatus for complex treatment of contaminated liquids to remove metallic, non-metallic, organic, inorganic, dissolved, or suspended contaminants. The system includes mechanical filtration, separation of organic contaminants, and electroextraction of heavy metals. Metal ion concentration can be reduced below 0.1 mg/L. The process improves treatment efficiency by removing inorganic and non-conductive substances prior to electroextraction.

submitted 14.11.2025;
accepted for publication 28.11.2025;
published 30.12.2025

Contact: Vitun.alexandr@gmail.com

The European Journal of Technical and Natural Sciences 2025, No 6
ISSN 2414-2352

PREMIER Publishing
ppublishing.org

DOI:10.29013/EJHSS-25-6-96-101

DEVELOPMENT AND IMPLEMENTATION OF A "SMART HOME" SYSTEM FOR A MODERN RESIDENTIAL COMPLEX

Kotkovets Leonid [1]

[1] Head of the Technical Supervision Department Kyiv

Cite: *Kotkovets L. (2025). Development and Implementation of a "Smart Home" System For a Modern Residential Complex. European Journal of Technical and Natural Sciences 2025, No 6.* https://doi.org/10.29013/EJHSS-25-6-96-101

Abstract

The author of this publication, in the process of performing and supervising a comprehensive set of design works for the transformation of an outdated space with an obsolete ecosystem and infrastructure, has developed a fundamentally new space. This transformation aligns with the requirements and standards for spaces capable of optimizing all workflows while incorporating methods and parameters suited for startup ecosystem environments. Such spaces are designed to enable efficient collaboration, where connections between subsystems within the supersystem are facilitated through channels integrated with elements of artificial intelligence and artificial neural networks.

Furthermore, the suite of design solutions, including architectural and artistic elements, establishes comprehensive visual stabilizers for psychological well-being in the workplace. Within the startup ecosystem, these stabilizers evolve into ecosystemic and infrastructural instruments, enhancing psychological stability and productivity. This environment is optimized for brainstorming effectiveness, supporting the application of 40 primary and 10 supplementary methods and techniques to achieve an ideal final result.

Keywords: *Smart Home, Development of a Smart Home System, Implementation of a Smart Home System, Residential Complex, Ecosystem of a Smart Urban District, Application of Artificial Intelligence in Design Engineering, Use of Artificial Neural Network Elements in Design Engineering, Comprehensive Transformation of Outdated Spaces, Definitions and Standards for Spaces with Startup Ecosystem Capabilities, Techniques and Methods for Achieving the Ideal Final Result, Development and Implementation of a "Smart Home" System for a Residential Complex as Part of the Ecosystem and Infrastructure of a Smart Urban District in a Modern City; Application of Artificial Intelligence and Artificial Neural Networks in Design Engineering*

Purpose

In this publication, the author presents the results of supervising and performing a comprehensive set of design works aimed at transforming an outdated space with legacy ecosystems and infrastructure into a fundamentally new environment. This transformation meets modern requirements and standards for spac-

es designed to optimize workflows. Additionally, it integrates practical methodologies and parameters aligned with the definitions and standards of spaces featuring startup ecosystem capabilities. These capabilities ensure that connections between subsystems within the supersystem are facilitated through channels incorporating elements of artificial intelligence and artificial neural networks.

Introduction

In addition, a comprehensive set of design solutions, including architectural and artistic elements, establishes the necessary visual stabilizers of the psychological climate in the workspace. Within a startup ecosystem, these stabilizers evolve into ecosystem and infrastructure-based tools that enhance team efficiency and focus during brainstorming sessions. This design approach integrates 40 core and 10 additional methods for achieving the ideal final outcome.

Smart home technologies represent a priority in the evolution of the construction industry. However, their development and implementation are deeply influenced by the broader conditions of urban infrastructure within modern cities. The complexity of integrating smart home systems increases significantly when construction occurs in historical districts. In such cases, the challenge lies not only in developing new intelligent facilities but also in modifying and restoring adjacent older districts.

These conditions demand a highly creative and innovative approach to the comprehensive engineering design of smart construction projects. This includes a variety of combined solutions, each aligned with essential construction standards while also incorporating elements of artificial intelligence (AI) and artificial neural networks (ANNs).

Despite the challenges, there are positive examples of successful implementation of smart home projects. These solutions serve as benchmarks for new initiatives, offering models for achieving the ideal final outcome as outlined by the **Theory of Inventive Problem Solving (TRIZ)**.

As an example, the author of this publication emphasizes the unique experience and achievements of Vitiv Bohdan, a distinguished engineer and innovator. A Corresponding Member of the Ukrainian Academy of Sciences, the International United Academy of Sciences, and the New York Academy of Sciences, Vitiv's systemic approach is utilized in the training of engineering specialists in smart construction.

Brief Overview of Highlighted Projects:

1. Project: Development and implementation of a "smart home" system for the residential complex *Smart Home* (2020–2021)

- **Technologies**: Integration of IoT (Internet of Things), remote control systems for lighting, climate, and security;
- **Innovations**: Adoption of energy-efficient solutions and AI-based automation for home functions;
- **Partners**: Guver Investment Fund, developer BK Center Stroy;
- **Results**: A 25% reduction in energy consumption, enhanced resident comfort, and improved security.

2. Project: Creation of eco-friendly buildings with autonomous energy systems (2019-ongoing)

- **Technologies**: Solar panels, energy management systems, and autonomous water supply;
- **Innovations**: Integration of combined solutions for home autonomy, significantly reducing reliance on external networks;
- **Partners**: Guver Investment Fund, BK Center Stroy, EcoBud LLC, Green Energy Solutions;
- **Location**: Hodosiyivka, Kyiv Region (ongoing construction);
- **Results**: 80% home autonomy, reduction in CO2 emissions, and minimized operating costs.

3. Project: Reconstruction of multistory residential buildings with integrated smart home systems in Kyiv (2021–2023)

- **Technologies**: Lighting and climate control systems, automated ventilation, real-time building condition monitoring;
- **Innovations**: AI-based predictive maintenance and enhanced energy management capabilities.

These projects exemplify the successful implementation of innovative smart home technologies, demonstrating the transfor-

mative potential of AI and ANN integration in construction. They set a standard for the future of sustainable and intelligent urban development the use of innovative materials and sensor systems for monitoring the condition of building structures. Partners: Guver Investment Fund, BK Center Stroy LLCLocation: Kyiv, Solomensky District Results: Improved quality of life for residents, reduced building energy consumption by 30%.

4. Project: Modernization of a commercial business center with the integration of "smart home" technologies (2022–2024)

- Technologies: Video surveillance systems, smart access control, automated energy consumption and climate management. Innovations: Integration of cloud services for building monitoring and management via mobile applications.Partners: Guver Investment Fund, BK Center Stroy developer. Results: 20% reduction in heating and electricity costs, increased building security;
- In contemporary conditions, when organizing production spaces for startups developing new smart technologies, there is a growing need to create a specialized ecosystem that accounts for the features and requirements of the supersystem of smart technologies. One of the subsystems of this ecosystem involves elements of contactless control and their processors, which in turn contain elements of artificial intelligence and artificial neural networks;
- This field is relatively new, and a significant contribution to its development has been made by Vitiv Bohdan through his original inventions, fundamental publications, and books;
- In his developments, Vitiv Bohdan has brilliantly combined ideas for preparing and optimizing the interior of production spaces with designs for parts of the infrastructure of a smart production complex, incorporating the latest technological solutions to increase the performance of electronic systems, ensuring compatibility with quantum computers and their processor equivalents expected to be introduced to the market.

As the complexity of innovative projects grows, automated design methods and systems are becoming increasingly important. Their significance is greatly enhanced when elements of artificial intelligence are integrated, fundamentally altering conventional automated design methods and systems.

For example, Google has introduced a new quantum computing chip, Willow, which, according to the company, can solve a computational problem in five minutes that would take traditional supercomputers thousands of years to complete. This breakthrough represents the cutting-edge progress in quantum computing and smart technology, directly impacting the design and optimization of future smart buildings and urban infrastructure.

These advancements highlight the profound impact of AI, quantum computing, and smart technologies on construction and urban development, presenting new opportunities for integrating these technologies into building systems, from residential complexes to commercial hubs the fastest modern conventional computer would take an inconceivable amount of time-10 septillion (10 followed by 24 zeros) years – to solve the computational problem that Google's new quantum computing chip, Willow, can solve in just five minutes. According to Hartmut Neven, the founder and head of Google's Quantum Lab, this supports the idea that "quantum computing occurs in many parallel universes."

However, the revolutionary nature of this breakthrough lies not in its data processing speed, but in the fact that developers have overcome a key problem with quantum computers.

Quantum computers leverage phenomena from quantum mechanics– quantum superposition and quantum entanglement. They don't operate on bits, which can only be 0 or 1, but on qubits (quantum bits), which can represent both 0 and 1 simultaneously. This exponentially increases the capacity for data processing and transmission, but it also introduces many errors. The more qubits used, the higher the frequency of errors. For nearly 30 years, scientists have been grappling with this issue.

The result is Willow, where recent "breakthrough" advancements have allowed devel-

opers to achieve an exponential reduction in error rates. Google claims that Willow is the first system to demonstrate results below threshold levels, paving the way for practical, large-scale quantum computers.

According to Neven, the new chip will be used in some practical applications, but details have not been disclosed. Experts, however, note that Willow remains largely an experimental device. It will take many years before quantum computers can be used in real-world applications, and this will require enormous investments.

A Technical System (TS) is defined as an artificially created material unity. The concept of TS allows us to formulate the fundamental feature of a technical solution. The creation of modern communication systems and the latest computing equipment requires constant tightening of the requirements for the cleanliness of the manufacturing process.

Scientific and technical information increasingly focuses on these processes, often at the expense of other equally important directions in the development of microelectronics and complex production technologies. This focus may be partially explained by the desire (and not without self-interest) to make the production process conform to established and existing environmental protection standards while achieving lower costs. Many believe that the costs of environmental protection reduce production efficiency and increase the cost of products and services.

However, there are certain minimum cleaning parameters or levels of cleanliness in the production process below which quality becomes uncontrollable, and this immediately impacts the quality of the manufactured products.

The usual method for ensuring minimal quality and cleanliness standards is continuous improvement in the composition and components of chemical reagents, which are increasingly used and intensify the cleaning processes as they are refined. This problem is particularly pressing in the food industry, where the costs of preparing water for food production and regenerating wastewater are rising rapidly, further driving up food prices.

These issues can be listed for a long time, so the author proposes focusing directly on the topic of this publication.

Innovation Strategy in Semiconductor Cleaning. Let's consider the process of developing a production module for cleaning 300mm semiconductor wafers. In this context, the question arises: Is it more practical to continue improving surfactants and chemical detergents, or should we explore innovative solutions to address these challenges?

The ongoing challenge of improving cleaning processes and chemical agents in production environments requires a thorough examination of new methodologies and potential breakthroughs. This process, while essential for maintaining high standards in the tech and semiconductor industries, also invites the opportunity to question whether traditional approaches are the best path forward or if innovative, less conventional solutions could offer better results in the long term.

It is indeed challenging to determine whether the process of modifying chemical reagents used in cleaning technologies constitutes an equivalent of an innovative process, or whether these modifications, while solving one problem, simultaneously create multiple new issues elsewhere, according to the criteria of achieving the ideal final result.

The analysis would be incomplete without considering the standard process of developing a new technical solution in a startup, which is integrated into a technical system of a higher compositional and layout level. We must examine how the modified formulations and definitions of technical systems at all levels correspond to the original formulations and definitions. This comparison is essential, especially when influenced by external factors related to the presence of various types and formats of visual stabilizers of the psychological climate in production and warehouse environments, as proposed by the author of this publication.

In such innovative systems, where new solutions are being applied, particularly in complex and evolving environments, it's critical to consider how external elements, such as visual stabilizers, impact the overall system. These stabilizers play a key role in creating a positive psychological climate that enhances productivity, creativity, and overall effectiveness in startup ecosystems, which are often under pressure to rapidly adapt to new technological solutions.

By understanding these interactions, we can evaluate the balance between technological advancements and their impact on the workspace environment, ensuring that modifications or innovations do not just address one problem but contribute to the larger goal of optimizing the entire technical system.

Figure 1. *The figure illustrates a comprehensive combined infrastructure stabilizer for all aspects of the psychological climate in production and warehouse environments. The stabilizing effect in the shown corridor occurs at the entrance to the working space where a team of developers is working*

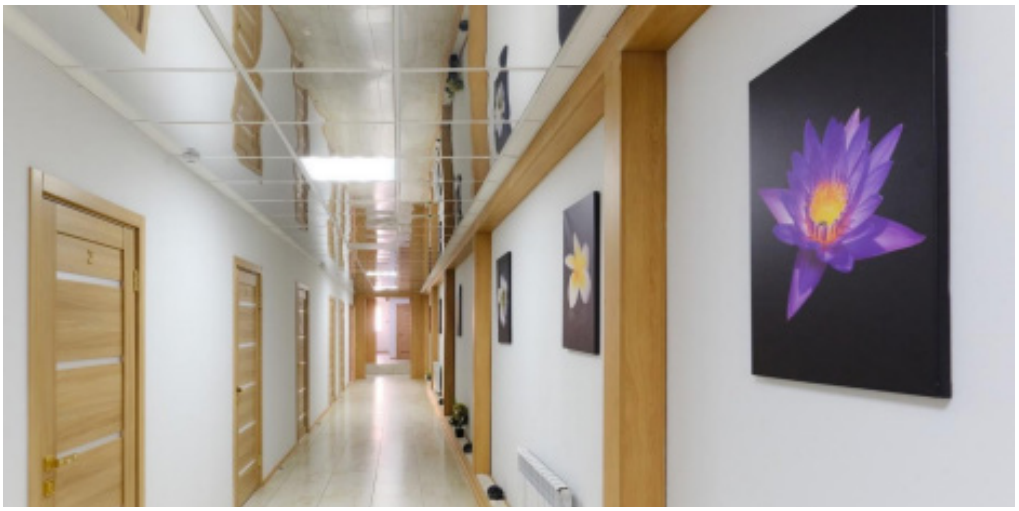

It is the efforts of this team that drive the development process of the production module for cleaning semiconductor wafers with a diameter of 300 millimeters. The setup of the project team is based on the requirements and characteristics, which are classified as interconnected formats of smart technologies.

As innovation projects become more complex, the significance of automated design methods and systems grows. However, their importance is significantly enhanced when artificial intelligence elements are added, fundamentally changing the automated methods and systems familiar to specialists.

Only with the application of these elements can one complete an innovation project within acceptable costs and optimal time, while considering the heuristic elements that emerge during brainstorming sessions.

Upon reviewing the basic definitions and meanings of TRIZ (Theory of Inventive Problem Solving) and ARIZ (Algorithm of Inventive Problem Solving), with consideration for the modifications and optimizations proposed and derived by the author of this publication for practical application in the design processes within the framework of an innovation project, the following definitions can be used:

1. Systems approach is a reflection and development of the dialectical principles of “universal interconnection” and “development” and is, in essence, one of the principles of the dialectical method of knowledge. The methodology of the systems approach involves representing any object as a system and considering it comprehensively. Modern methods and capabilities of computer modeling fundamentally change and significantly complement the concept of the systems approach, making it more meaningful and effective.

The environment design proposed by the author, in addition to computer-aided design methods, constructs systems at all levels for parallel visual infrastructure stabilization of the psychological foundation of the work process.

This approach integrates both technological and environmental considerations, ensuring that the workplace environment, alongside technical advancements, contributes to the overall success of the innovation project, fostering a more effective and stable work climate.

System – a complex of elements that are systematically organized in space and time, interconnected with each other, forming

a cohesive unity. A system is characterized by its composition of elements, structure, and performs a specific function. Here, computer control and monitoring systems, as well as various combinations of their control activities, significantly complement the concept of the system, making it more complete and adding analytical capabilities and characteristics. The interior design proposed by the author of this publication supplements these characteristics.

Elements – relatively indivisible parts of a whole; objects that, in combination, form a system. An element is considered indivisible within the context of maintaining a certain quality of the system. The process of innovative modification and optimization is most typical for elements, the result of which may lead to a technical solution that meets the four characteristics of an invention.

Structure – a consistent, stable connection between the elements of a system that reflects the form, arrangement of the elements, and the nature of their interaction, properties, and sides. Structure makes the system a qualitatively defined whole, distinct from the sum of the qualities of its constituent elements (since it implies the interaction of elements with one another in specific ways, through certain sides and properties, not as a whole).

Function – the external manifestation of the properties of an object (or element) within a given system of relations; a specific way in which the object interacts with the environment, its "capability."

References

United States Patent Application US 2019/0167490 A1. Hellmold, J., et al. (2019, June 6). Smart absorbent article and components. A substrate with integrated sensor tracks for automatic detection of wetness events in absorbent products.

United States Patent Application US 2019/0167489 A1. Hellmold, J., et al. (2019, June 6). Smart absorbent article, components, and process of making. A multi-track sensing substrate for wetness detection with central, side, and sensing tracks configured in an integrated circuit.

United States Patent Application US 2018/0285996 A1. Ma, M. T. (2018, October 4). Methods and system for managing intellectual property using a blockchain. A blockchain-based ecosystem for innovation, IP management, licensing, tracking, and fraud detection.

United States Patent Application US 2020/0233707 A1. Ramamurthy, R., et al. (2020, July 23). Process discovery and automatic robotic scripts generation for distributed computing resources. Techniques for identifying automatable tasks, segregating them, and generating robotic scripts automatically.

United States Patent Application US 2019/0104697 A1. Mendes, R. S. (2019, April 11). Modular electronic vase with automated, digital control and monitoring system for aeroponic growth of plants. A modular aeroponic system with automated monitoring, control components, and multifunctional electronic architecture.

United States Patent Application US 2019/0090330 A1. Aykroyd, H., et al. (2019, March 21). Controllable power and lighting system. Methods for automatic control and arrangement of LED and non-LED devices powered by 3-phase AC systems.

United States Patent Application US 2016/0217618 A1. Adeyoola, T., et al. (2016, July 28). Computer-implemented methods and systems for generating virtual body models for garment fit visualisation. Methods for generating realistic virtual body models from minimal measurements for apparel fitting, recommendation, and visualization.

submitted 04.11.2025;
accepted for publication 18.11.2025;
published 30.12.2025

Contact: bogdan.vstsv@gmail.com

The European Journal of Technical and Natural Sciences 2025, No 6
ISSN 2414-2352

PREMIER Publishing
ppublishing.org

DOI:10.29013/EJHSS-25-6-102-107

INTEGRATIVE MODULES FOR ELECTRONIC SYSTEMS. (Integrative Modules For Electronic Systems, Including Laser Diodes, Equipped With an Intensive Cooling System Based on Diamond-Copper Composite Materials)

Lashin Dmitry Aleksandrovich [1]

[1] Technical Director, LLC "UF Technologies" Saransk, Russia

Cite: *Lashin D.A. (2025). Integrative Modules for Electronic Systems. (Integrative Modules For Electronic Systems, Including Laser Diodes, Equipped With an Intensive Cooling System Based on Diamond-Copper Composite Materials). European Journal of Technical and Natural Sciences 2025, No 6*. https://doi.org/10.29013/EJHSS-25-6-102-107

Abstract

Recent practical experience has shown that one of the key challenges in complex electronic devices – particularly those incorporating laser diodes – is ensuring reliable and efficient cooling. To minimise energy losses and increase the effective output, especially in modern lighting systems, active research is being conducted to develop integrated technical solutions that operate without additional structural components or extra energy consumption for cooling.

In parallel, new design approaches are being explored that enable increased light output while maintaining a minimalistic, compact construction and relatively low power consumption. These solutions aim to enhance the performance and energy efficiency of lighting devices without compromising design simplicity.

Keywords: *Integrative modules; Electronic systems; Laser diodes; Light output; Diamond spheres; Ductile material; Composite material; Pseudo-porous structure; Optical cable; Laser radiation; Flat-emitter lamp*

Introduction

To eliminate energy losses and increase effective output – particularly in various lighting systems – active research is underway to develop integrative technical solutions that operate without additional structural components or extra energy consumption for cooling.

In parallel, new engineering approaches are being explored and refined to enable higher light output from lighting devices while maintaining a minimalistic and simplified design, operating at relatively low power and, consequently, low energy consumption.

The author of this publication considers the most effective solutions to be the integrative and comprehensive approaches proposed in the scientific and technological works and books of ***Rustam Mukhametov***, a well-known innovation specialist in this field.

What fundamentally distinguishes ***Rustam Mukhametov's*** proposals and developments from similar approaches by other authors is a broad platform for experimental

computer modelling, made possible by his deep and diverse expertise in the methods of systemic and combinatorial computational modelling across adjacent innovative processes, including at the intersections of fundamental disciplines.

Figure 1. *One of the innovative developments for converting laser radiation into light emission within familiar and standard spectral ranges is presented*

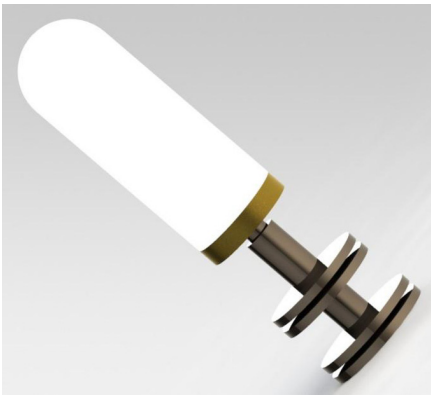

When analysing the advanced technologies presented in his innovative publications, ***Rustam Mukhametov*** formulates an exceptionally important thesis for solving the outlined problems – the combinatorial structure of each solution, meaning the harmonious integration and mutual reinforcement of traditional technologies and materials with innovative, primarily composite, technologies and materials.

A particularly significant aspect of ***Mukhametov's*** proposals is the consistent trend toward integrating and thoroughly adapting new materials and technological methods within the framework of established and proven technologies and materials. This creates a foundation for transforming properties and capabilities to a new, innovative level.

The next photo shows the axial cross-section of such a device, which is more convenient for detailed examination and analysis.

Figure 2.

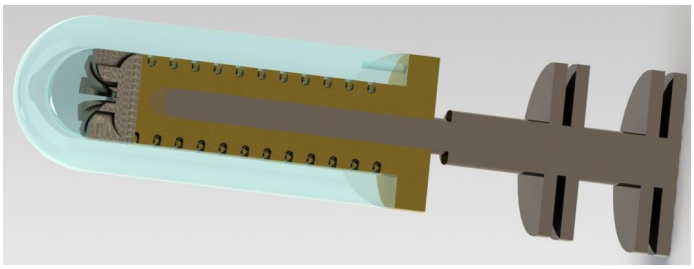

As can be seen, the design of the innovative lamp integrates the functions of several fundamental structural components.

The lamp holder incorporates a vortex radiator whose shaft and discs are made of a diamond–copper composite, which serves as the key element of the lamp's cooling system.

Each component of this system is multifunctional. In addition to pure heat-transfer and heat-accumulation properties, the structure of these parts – formed from numerous micro-globules of the composite – simultaneously performs a critically important function of dissipating thermal flows. This is achieved due to the pseudo-porous structure of the composite.

Let us focus on the innovative structure of the diamond–copper composite (Appendix 1).

The original process of manufacturing composite globules begins with the formation of synthetic diamond spheres 5–7 microns in diameter (the size may vary depending on the geometry of the component and its operating conditions).

These spheres are then coated with copper using a proprietary innovative technology (Appendix 2).

The coating thickness is selected to ensure that when the lamp component is formed in a mold, the diamond spheres retain sufficient ductile material for the metal to undergo liquid-flow deformation, filling the spaces between the synthetic diamond spheres.

As a result, a pseudo-porous structure is formed in which diamond spheres– the best known thermal conductor while being fully electrically non-conductive – are uniformly distributed. Such a structure allows heat to dissipate instantly and spread evenly across the cross-section of the radiator discs.

An optical cable is placed in the spiral grooves of the lamp body. A laser beam from the laser module is directed into this cable. The optical cable is wound in a spiral and placed within the grooves at a diameter that causes the cable to emit light across its entire cylindrical surface, which is significantly more efficient than end-face emission.

To separate the laser radiation from the lamp's output light, a layer of phosphor – calibrated for a specific emission spectrum – is applied to the optical cable.

Thus, the final emission of the lamp is completely non-toxic and, due to the emission area being thousands of times larger than the end face of an optical fiber, a laser diode operating at only 1–2 watts produces a light output equivalent to 60–75 watts.

The presented models demonstrate that, based on the general principles of innovative design proposed by **Rustam Mukhametov**, it is possible – within the framework of traditional geometries and structures, for example an ion-exchange filter – and using natural and completely safe materials, to achieve practically ideal results with unique parameters and properties, including:

- complete elimination of chemical reagents in the process;
- use of natural ion-exchange conditions;
- enormous potential for unique exchange capacity, including for the purification of liquids contaminated with radioactive substances.

Figure 3. *The presented models demonstrate that, based on the general principles of innovative design*

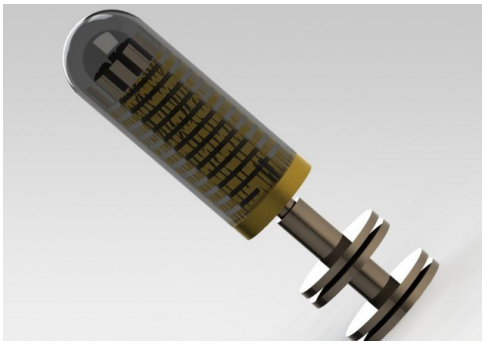

Under such design trends, the fundamental requirements for the design approach itself change, allowing extensive use of computer modelling methods and techniques to achieve an optimal and ideally calibrated final result.

Figure 4. *The presented models show that, when based on the general principles of innovative design*

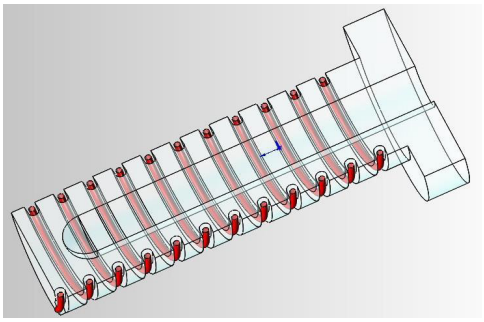

Figure 5.

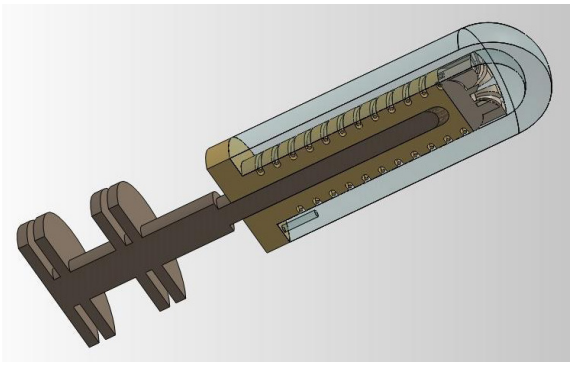

The generation of light from a curved optical cable – bent to a specific radius – has many possible alternatives. One such example is shown in the next photo: a cross-section of an emitter in which the cylindrical surface of the optical cable begins to emit light once a certain bend radius is reached.

Figure 6. *The next photo shows the structural layout of the lamp in a transverse longitudinal section*

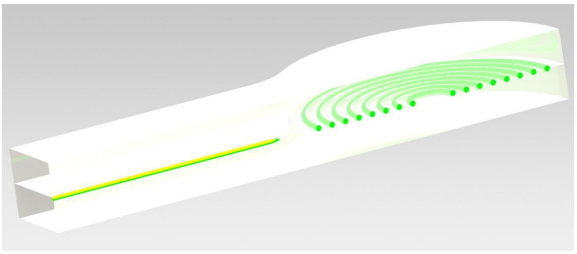

Here, the individual technical components are clearly visible, each carrying its own

functional and conceptual significance and performing specific technological and design-related roles.

Figure 7. *The design incorporates numerous innovative elements*

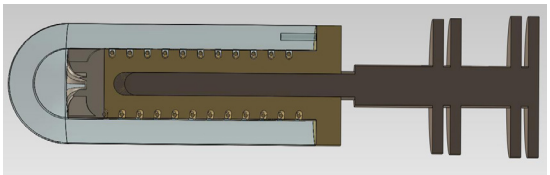

The proposed configuration contains many advanced features and, most importantly, is fully suitable for serial and large-scale production. Moreover, this lamp configuration – its combination of technological principles and structural materials – allows the integration of future technical solutions that may emerge as laser technologies, composite material engineering, and new energy-efficient cooling and control systems continue to evolve.

Figure 8. *The photo shows a mini-lamp in which a mixture of phosphors is applied to the end of an optical fiber according to a specific three-dimensional geometric pattern, providing white-spectrum light emission*

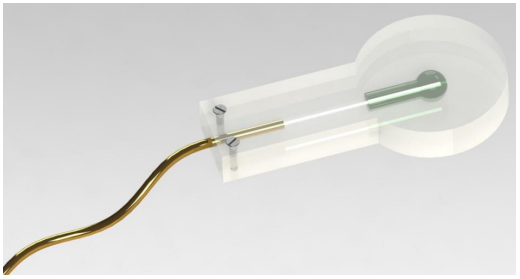

The diameter of the optical fiber is only 120 microns, which makes it possible to create micro-miniature light sources for use in highly compact optoelectronic systems.

Figure 9. *The photo shows a flat-emitter lamp connected to a single optical fiber*

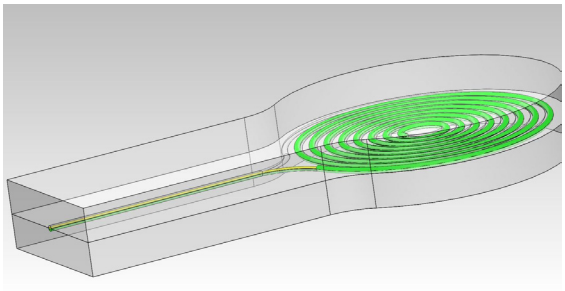

This system, in addition to its overall energy efficiency, makes it possible to achieve the required illumination level over a specified area with minimal cost and maximum simplicity.

The same configuration also allows for applying virtually any combination or mixture of phosphors to the spiral (flat spiral) section at the end of the optical fiber, enabling the generation of precisely defined light-emission parameters.

Figure 10. *The photo shows a laser-diode module based on the principles of active cooling achieved through the dissipative effect of components manufactured from a pseudo-porous diamond–copper composite*

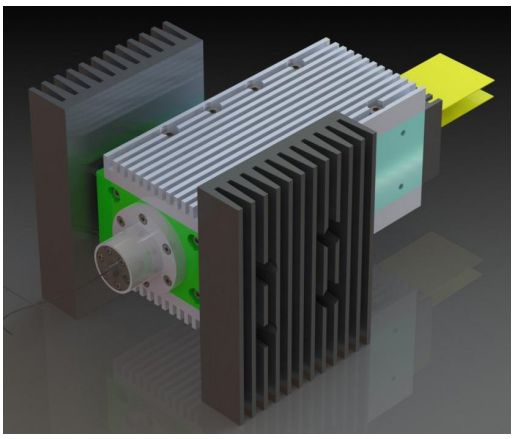

One of the innovative integrative features of the presented design is the use of thermoelectric coolers in combination with heat-conducting and heat-dissipating structural elements of the module housing.

The thermoelectric coolers are positioned between the external radiators and the module body. The heat-conducting elements direct thermal flows from the printed circuit board to the walls of the housing, where the thermoelectric coolers are mounted. The base surfaces of the radiators are pressed against these coolers, and additional module components requiring constant cooling may be mounted on the radiators when necessary.

Practical results have shown that reliable cooling ensures maximum stability of the laser output parameters, which in turn significantly expands the range of possible output configurations of the module. When required, this also enables the division of the

laser beam among several optical fibers, each supplying a separate lighting device.

Figure 11. *The models of such devices are shown in the photo*

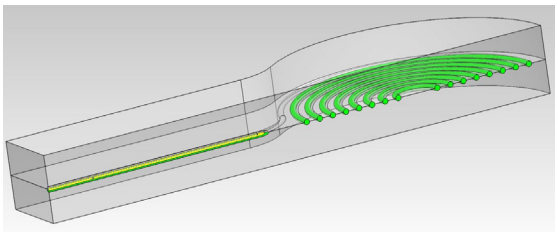

As can be seen from the models, despite their simplicity and manufacturability, the supporting disc of the laser diode (highlighted in red in the models) provides complete protection of the diode from overheating due to multiple contributing factors. As noted earlier, this significantly increases the operational stability of the module and reduces overall energy consumption for illumination.

The models also illustrate the coding and decoding system, which enables identification of the optical fibers connected to the module and the corresponding lighting devices.

Figure 12.

This system provides additional functional capacity for implementing and monitoring various computational models of energy control and distribution. These functions fully depend on the purpose and operating conditions of the module, and the possibility of embedding the software component precisely at the most critical point is of particular importance for further development of the technology.

Moreover, this fundamental approach to applying new composite materials in new applications – materials with completely unique properties and characteristics – makes it possible to create advanced lighting devices and instruments with parameters required by modern technologies.

Figure 13. *The presented three-dimensional models show the heat-conducting elements, which simultaneously serve as the structural mounting components for the laser diode inside the module housing*

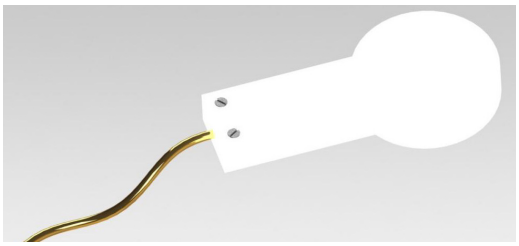

It is also important to note that, alongside the latest composite materials, nature provides exceptionally valuable natural materials.

The design principles described in the publications of **Rustam Mukhametov** allow the creation of a harmonious combination of long-established natural materials with proven engineering and manufacturing techniques.

The conceptual solutions proposed by **Rustam Mukhametov** enable further technological development – for example, transforming carbon – carbon composite fabrics into compressed solid components with entirely new properties, which open new innovative possibilities in lighting engineering and related technological fields.

Figure 14. *The photo shows the actual structural components of the innovative laser-diode module featuring a cooling system and a laser-diode holder made of a diamond – copper composite*

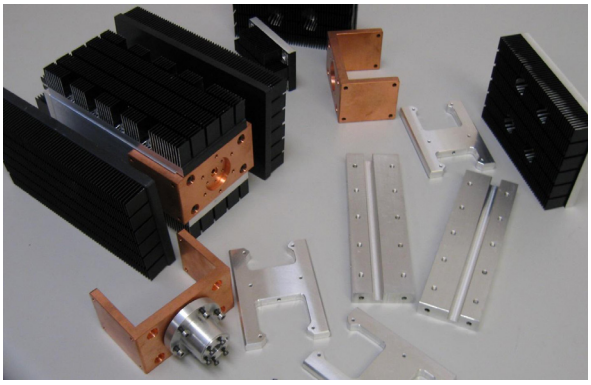

As can be seen in the photo, all other housing elements and components of the cooling system are manufactured from standard profiles and materials and do not require any special materials or specialised technological equipment; everything is produced using conventional cutting and measuring tools.

This may be considered an example of the integration and combination of innovative solutions for the efficient and safe conversion of laser-diode radiation into safe, high-intensity phosphor emission, with virtually complete heat dissipation and without thermal or optical losses.

All key output parameters of this integrated lighting system fully comply with current safety standards and regulations.

Appendices, references, patent and licensing information:

Appendix 1
United States Patent Application
20120040166
Kind Code: A1
Date: February 16, 2012
Title: Composite Material, Method of Manufacturing and Device for Moldable Calibration
Abstract:
Composite materials and methods and systems for their manufacture are provided. According to one aspect, a composite material includes a collection of molded-together multilayer capsules, each capsule originally formed of a core and a shell. After a plastic deformation process, the shell forms a pseudo-porous structure, with pore locations containing the capsule cores. The cores are made of a material – e.g., synthetic diamond – harder than the external shell, which may be formed of a ductile metal such as copper. The composite material exhibits high thermal and/or electrical conductivity and/or dissipation.

Appendix 2
United States Patent Application
20100224497
Kind Code: A1
Date: September 9, 2010
Title: *Device and Method for the Extraction of Metals from Liquids*
Abstract:
A volume-porous electrode is provided that increases the effectiveness and productivity of electrochemical processes. The electrode is formed of carbon, graphitic cotton wool, or carbon composites configured to permit fluid flow through the electrode volume in three orthogonal directions. The electrode conducts an electrical charge directly from a power source and also includes a conductive band connected to the surface of the electrode volume, ensuring a uniformly distributed high charge density. Apparatuses and methods employing the volume-porous electrode are disclosed for removing metals from liquid solutions using electroextraction and electrocoagulation techniques, as well as for electrochemical modification of a liquid's pH level.

submitted 14.11.2025;
accepted for publication 28.11.2025;
published 30.12.2025

Contact: sedova.alina7810@gmail.com

The European Journal of Technical and Natural Sciences 2025, No 6
ISSN 2414-2352

PREMIER Publishing
ppublishing.org

DOI:10.29013/EJHSS-25-6-108-113

BRIEF DESCRIPTION OF THE IMPEDANCE-RESONANCE METHOD – ELECTROMAGNETIC RESONANCE SPECTROSCOPY

Aleksandr Mikhalevich [1]

[1] Russia Saint Petersburg State University of Film and Television Saint Petersburg, Russia

Cite: *Mikhalevich A. (2025). Brief description of the impedance-resonance method - electromagnetic resonance spectroscopy. European Journal of Technical and Natural Sciences 2025, No 6.* https://doi.org/10.29013/EJHSS-25-6-108-113

Abstract:

This work examines the operating principle of the impedance resonance sensor, which is based on generating an alternating electromagnetic field in the area where the test sample is located. The electromagnetic field acts as an intermediary between the resonant circuit and the sample, capturing changes caused by the sample's physical properties. Under the influence of the external alternating field, the sample generates linear and eddy conduction currents, displacement currents, and ionic currents, which distort the original electromagnetic field. These distortions are detected by the solenoid of the resonant circuit, enabling the identification of the electrical characteristics of the material under study. The described principle provides a non-contact method of analysis and expands the functional capabilities of impedance resonance sensors.

Keywords: *Technological integration; Composite technical solutions; Innovative integration tool; Traditionally accepted production methods; Various technical and technological cultures; Psychological barriers; Technological breakthrough; Initiated innovation process; Main instrument of technological integration; Thermodynamic cycle; Optimization of the thermodynamic cycle*

Operating principle of the impedance resonance sensor

In accordance with the principle of superposition of fields, these electrical phenomena distort the external alternating electromagnetic field. These distortions are sensed by the solenoid of the impedance resonance sensor (IR sensor).

The resonant circuit, which includes this solenoid, changes its behavior in the same way as if additional elements were added to its composition: a capacitor, an inductor and a resistor.

The combination of additional capacitive, inductive and active resistances is an additional impedance introduced into the system by the test sample; this attribute will be measured by the IR sensor.

Changes in the parameters of the resonant circuit are reflected in the change in its amplitude-frequency characteristic, namely, the resonant frequency and amplitude of the circuit change.

By examining these changes, one can judge the impedance of the sample under

study. As it is clear from the above description of the principle of operation, the impedance resonance sensor is a complex response from the measured object and can be applied in all applications where the Eddy current sensors are used, as well as in all applications where the contact as, for example, in the case of RF impedance / material analyzers or non-contact (through an insulating material or an air gap), measurement of the impedance of an object placed between the electrodes.

The advantage that the IR sensor has over the above methods lies in the higher (at least ten times) sensitivity, which is provided by the use of the resonant circuit in its extremely reduced form, namely, consisting only of an inductance coil, which is used to create an oscillatory contour its interturn capacity.

One- and two-component applications

This includes all applications in which it is sufficient to use one impedance-resonance sensor, which provides two parameters as an indication: the resonant frequency and the resonant amplitude.

These applications include all flaw detection applications and all applications that track changes in one or two parameters, such as chemical-mechanical planarization processes, film and coating processes, determination of object moisture, determination of water salinity, etc.

Building an analytical system For tasks where it is necessary to measure and / or track changes in complex, multicomponent systems, it becomes necessary to build an analytical system consisting of many sensors, each of which operates at its own unique operating frequency.

The initial data for constructing such a system used for the chemical and / or physical analysis of the object under study are the spectra obtained by the methods of Electrochemical impedance spectroscopy (EIS) and / or Dielectric relaxation spectroscopy (DLS) on the measuring equipment used by these methods: radio frequency impedance / material analyzers, potentiostats, etc.

To construct the spectra, reference samples of the object under study with a known variation of chemical components or with a known variation in the physical properties of the object are used.

The accuracy of measurements using an impedance-resonant analytical system will depend on how these reference samples fully cover all possible states of the object under study. Further, using the chemometric * approach, on the basis of the obtained spectra, the operating frequencies for the impedance-resonance sensors that are part of the analytical system are determined.

The number of sensors in the system must be greater than or equal to the number of investigated components. The main criteria for choosing an operating frequency is the maximum change in impedance in accordance with a change in the concentration of the investigated component or physical property and the contrast of this response against the background of changes in other components or physical properties.

Proposed research project Evaluation of the fundamental possibility of creating a measuring device for contactless monitoring of specific components in water in real time A measuring device for monitoring the concentrations of measured components in water makes it possible to determine their slightest changes and determine whether the measured concentrations are within certain specified limits.

If not, an audible or visual signal is generated. The liquid monitoring system includes at least one IR sensor, which is located on the tube with the test liquid, and its readings are used to determine the concentrations of the monitored components in the water.

The sensor readings are displayed on the screen of the device itself or transmitted via a cable to an external monitor. The device interprets the sensor readings by comparing them with calibration values to quantify the concentration values of the monitored components.

Thus, the current concentrations of the components are determined, the data obtained is processed and stored (for history creation or long-term storage) and can also be displayed on the display in an easy-to-read form. Information on changes in the concentration (tendency) of the measured components in water can also be displayed in numerical or graphical form.

To date, we have carried out a number of experiments to determine the frequencies with

which it is possible to determine the various concentrations of sodium chloride in water.

We also performed experiments to detect the minimum amount of mercury in the water, and to determine the sensor's ability to detect the difference between different samples of bottled drinking water and distilled water. All experiments were successful – the results are shown below.

Example 1: Measurement of various concentrations of NaCl in water

To determine the optimal operating frequencies for measuring the concentration of sodium chloride (NaCl) dissolved in water, preliminary studies were carried out by probing solution samples with different concentrations of NaCl with a harmonic electromagnetic field in a wide range of operating frequencies: from 1 MHz to 500 MHz.

Frequencies of the order of 20 MHz showed the best results. The frequency range for scanning by the IR sensor was selected within the following limits: from 17 to 20 MHz.

In this range, the amplitude-frequency characteristics (AFC) were plotted for various NaCl concentrations.

Diagram 1.

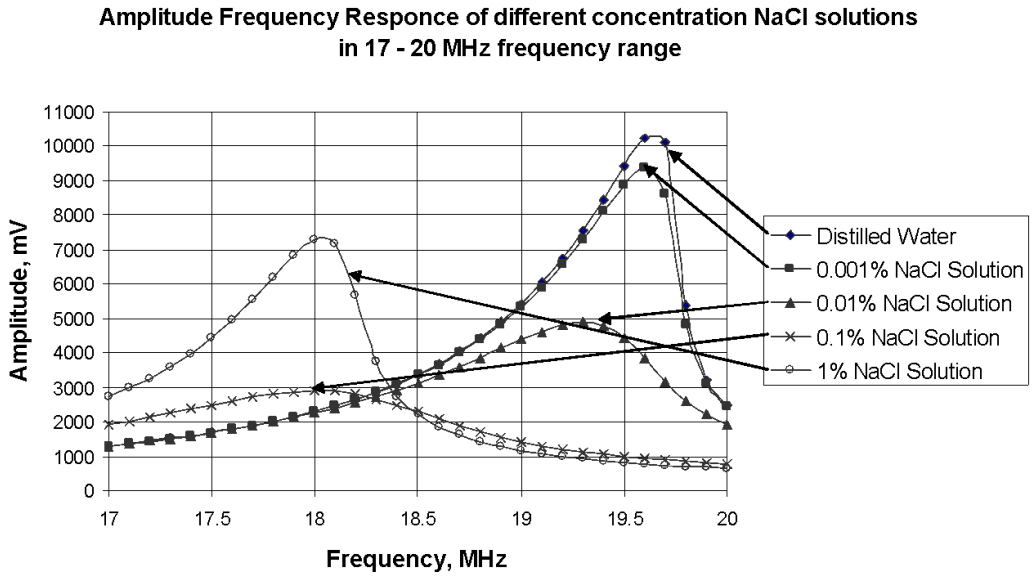

Diagram 2.

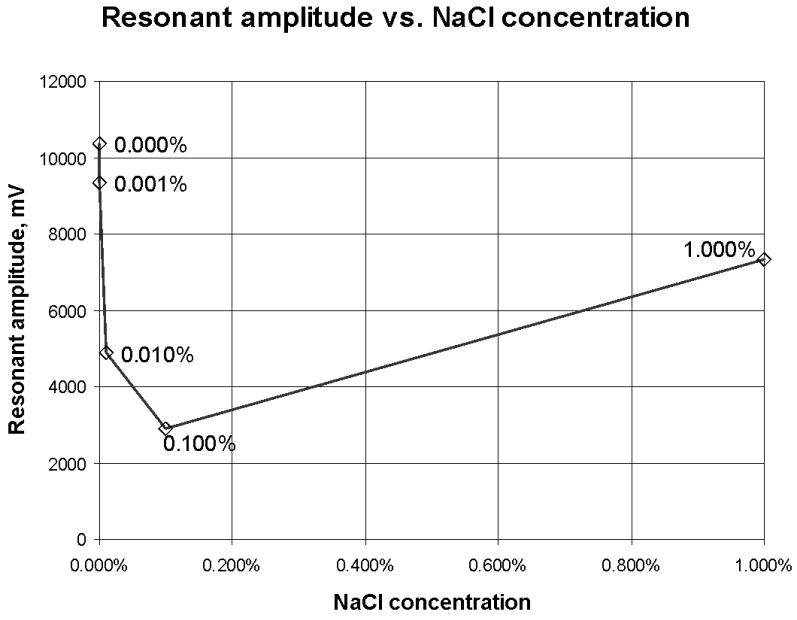

Diagram 2 shows the results of these constructions.

From the amplitude-frequency characteristics, it can be seen that solutions containing different concentrations of NaCl clearly differ from each other.

Distilled water (shaded diamonds) showed the highest maximum amplitude of the frequency response at a resonance frequency of about 19.6 MHz.

With an increase in NaCl concentration to 0.1%, the maximum amplitude of the frequency response decreased, and the resonance frequency also decreased.

Further, with an increase in the concentration of NaCl to 1%, the maximum amplitude of the frequency response increased, with a further decrease in the resonance frequency.

These results demonstrate the capabilities of the proposed innovative impedance system for measuring concentrations of various solutions in a wide range with the highest resolution.

Rice. 3 shows the change in the maximum value of the amplitude of the frequency response depending on the change in the concentration of NaCl, presented in a logarithmic scale.

Example 2: Measurement of various concentrations of mercury in water. This is another example that demonstrates the capabilities of IR sensor technology

Applied MRS has conducted a series of experiments to measure the concentration of mercury (Hg) in water.

To determine the frequency at which a change in the concentration of mercury ions (Hg +) in distilled water causes the maximum change in the electrochemical impedance of this solution, we used a potentiostat.

The resulting frequency was chosen as the operating frequency for the designed IR sensor, which is the reference point for the design of the resonance circuit.

Thereafter, the measuring resonant circuit can be built according to well-known design rules, taking into account the specific task.

Figure 4 shows the amplitude-frequency characteristics (AFC) for samples of solutions with different concentrations of Hg + in distilled water.

These results clearly demonstrate the ability to measure Hg + concentrations in distilled water at very low levels of the order of 1 ppb.

Diagram 3.

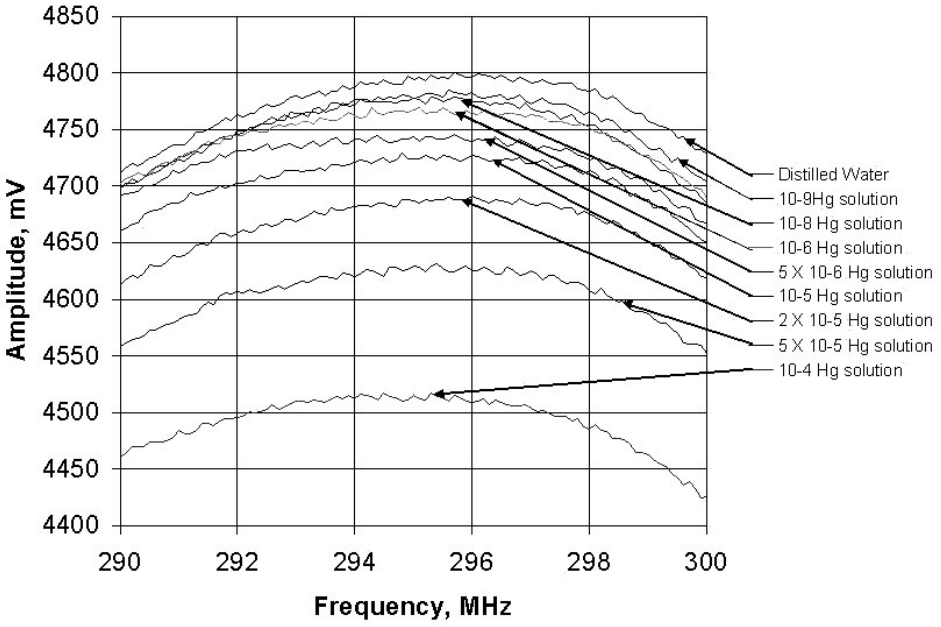

Example 3: Testing Samples of Distilled and Tap Water

Figure 5 shows a graph of test results under various conditions: 1 – no liquid in the sampler, 2 – when

the sampler was filled with distilled water, and 3 – when the sampler was filled with tap water.

Compared to an empty sampler, distilled water showed only a relatively small change in sensor amplitude.

At the resonant frequency, a large shift is observed from 12.5 MHz for an empty vessel to 11 MHz for the same vessel filled with distilled water.

The tap water drastically changed the amplitude and resonance frequency.

This result is understandable and expected since the electrical resistance of distilled water at 25 °C is about 18.2–40 MΩ-cm and tap water, as a rule, is below 0.1 MΩ-cm.

This example demonstrates the very high sensitivity of the innovative impedance sensing method and shows that even small contaminants in liquids can be detected and measured accurately.

Diagram 4.

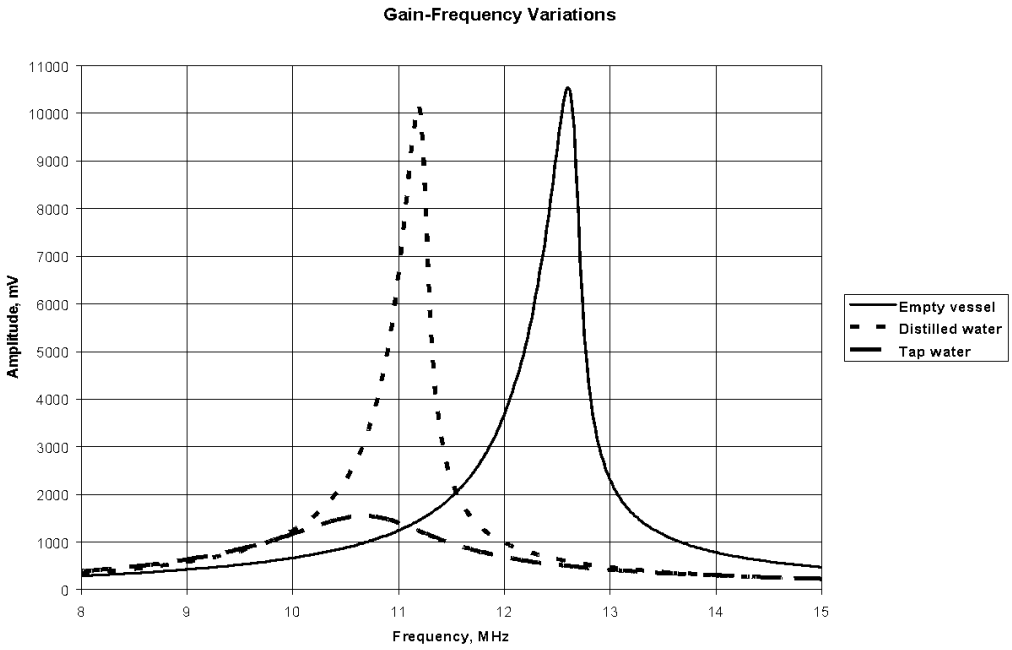

Example 4: Determining the Difference Between Water Samples

Table 1. Provides the values of resonance amplitudes and frequencies for the tested water samples

Table 1.

No.	Name	Frequency, MHz	Amplitude, y.e.	pH
0	Empty	4.212	865	
1	Alhambra	4.201	832	6.7
2	Aquafina	4.2012	822	–
3	Rain water	4.201	758	–
4	Dasani	4.2015	750	–
5	Arrowhead	4.201	694	6.9
6	Crystal Geyser	4.2009	648	7.1
7	Trader Joe's water	4.1998	579	–
8	Crystal Lake	4.199	528	7.9
9	Tap Water	4.1974	380	–

The frequency response with the name "Empty" was used for the situation when there are no water samples in the test vessel.

The rest of the frequency response are numbered in accordance with Table 1 (see above).

Diagram 5.

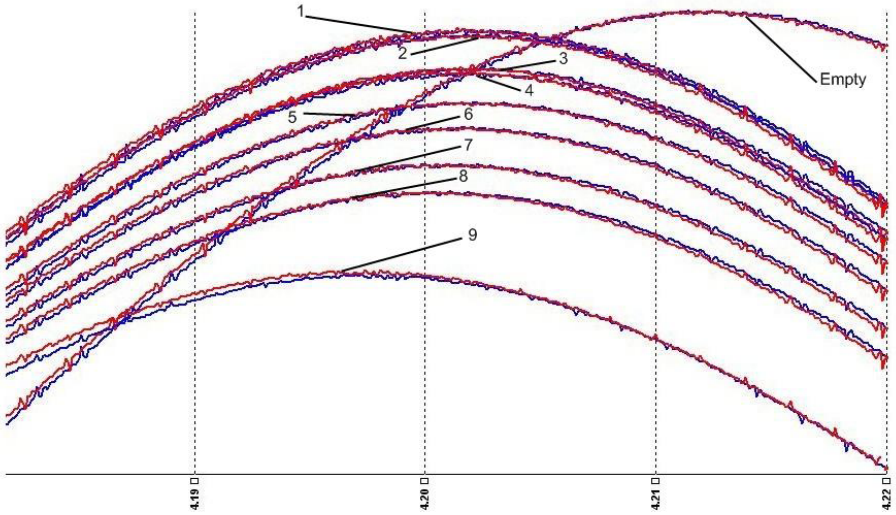

Figure 6 shows the amplitude-frequency characteristics for all tested samples.

Conclusions

Based on the experiments carried out to date, we – Applied MRS can confidently assume that non-contact detection of various elements in water in real time is quite possible using IR sensors due to their extremely high sensitivity and due to the fact that Each element dissolved in water has its own unique electrochemical impedance spectrum ("electronic signature"), which allows, when using several IR sensors with different operating frequencies, to distinguish one element dissolved in water from another.

We propose to conduct an evaluative study that will focus on the design and tuning of IR sensors that will be able to discriminate between different concentration levels of individual constituents in water.

To carry out this study, we need to obtain sets of samples of aqueous solutions from the customer, with different concentrations of the required elements, for the development of IR sensors and further to demonstrate that we can distinguish samples in real time without direct contact with liquids. Any suggestions you make will be considered. By the end of this evaluation study, we will manufacture a test device that will be able to fairly accurately distinguish samples with different concentrations of individual elements in water, while other parameters / components of the water remain unchanged.

References

United States Patent Application US20060250934A1. *Three-dimensional optical information carrier and a method of manufacturing thereof*. Publication Date: November 9, 2006.

United States Patent Application US20070288947A1. *Swing arm optical disc drive*. Publication Date: December 13, 2007.

submitted 04.11.2025;
accepted for publication 18.11.2025;
published 30.12.2025

Contact: sedova.alina7810@gmail.com

The European Journal of Technical and Natural Sciences 2025, No 6
ISSN 2414-2352

PREMIER Publishing
ppublishing.org

DOI:10.29013/EJHSS-25-6-114-118

APPLICATION OF DYNAMIC AND AERODYNAMIC FOAM GENERATORS. (The use of dynamic foam generators in integrated technologies for water purification, regeneration, and recirculation, including their application in greenhouse facilities and hydroponic systems)

Eduard Natanovich Milman [1]

[1] Academician of the International Academy of Sciences for Ecology and Life Safety

Cite: *Milman E.N. (2025). Application of Dynamic and Aerodynamic Foam Generators. (The use of dynamic foam generators in integrated technologies for water purification, regeneration, and recirculation, including their application in greenhouse facilities and hydroponic systems). European Journal of Technical and Natural Sciences 2025, No 6.* https://doi.org/10.29013/EJHSS-25-6-114-118

Abstract

This work examines modern technologies for water purification and regeneration, as well as the range of materials, including composite ones, used in these processes. It highlights that selecting the optimal technological solution is complicated by scale-dependent factors and varying operational conditions. Special attention is given to recent engineering findings: studies have revealed unique properties of gripping mechanisms in specialized robotics. The injection of compressed air from a vacuum gripping device operating on the Bernoulli principle into a liquid enables effective foaming, opening new prospects for applying such mechanisms in innovative water treatment methods.

Keywords: *Foam generator; Aerodynamic foam generator; Optimal compressed gas pressure; Scale factor; Foam load-bearing capacity; Technical specifications; Vacuum level; Required purification quality level*

Introduction

There are many different basic technologies for the purification and regeneration of water and aqueous process solutions. The market offers a wide variety of materials, including composite ones, for the same purpose. However, when it comes to making a final decision on the selection of a specific technology and material for a particular case, difficulties arise in performing a comparative analysis.

The latest technological concepts in this and related fields encounter significant challenges during implementation due to the substantial influence of the scale factor on the results of various water treatment, purification, and regeneration operations.

During the initial experiments, it was discovered that the prototype of the future foam generator, due to the fact that the air flow thickness does not exceed a few microns, can control the diameter of air bubbles in the

foam by adjusting the gap between the membrane and the housing.

This indicator and technical parameter turned out to be particularly important, as it provided flexibility and a wide range of possibilities for foam generation processes based on a new principle.

In addition, the load-bearing capacity of the foam obtained in this way turned out to be significantly higher than that of conventional foam.

Figure 1. *Dynamic foam generator*

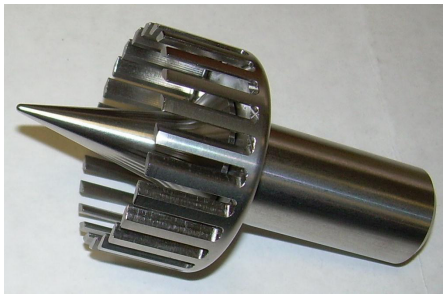

Figure 2. *Foam produced using a dynamic foam generator*

The ease and precision of adjusting the diameter of air bubbles in the foam are demonstrated in the following photograph. It shows how the structure of the foam within the same liquid and the same container can change when the gap between the membrane and the housing is adjusted.

It is necessary to emphasize the exceptional importance of applying the innovative developments and publications of the well-known specialist and highly qualified expert **Nikolai Seriukov**. In his research and designs, he successfully integrated the most effective technical solutions, enabling confident achievement of the ideal final result in accordance with the **Theory of Inventive Problem Solving (TRIZ)** and the **Algorithm for Inventive Problem Solving (ARIZ)**, which he masters to perfection. At the same time, the required level of structural simplicity is maintained – positively influencing the reliability of the system.

Figure 3. *Foam generator*

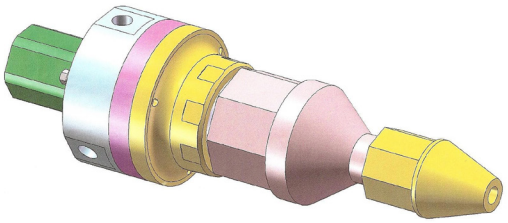

This simplicity is achieved through the exceptionally simple design of the foam generator.

Figure 4. *Composition of the foam generator*

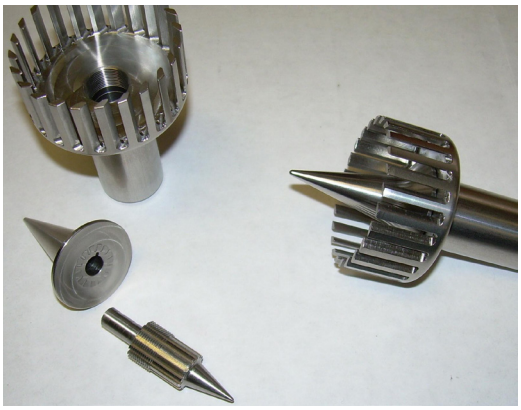

As shown in the photograph, the dynamic foam generator consists of three parts, none of which are movable.

Additional technical conditions for planning water treatment equipment using foam generators based on the aerodynamic effect

Several variants of the foam generator's scale factor and design features are considered. Foam generator with optimal dimensions and optimally selected compressed gas pressure. The overall dimensions of the foam generator and the compressed gas pressure determine the quantity and size of the bubbles that form the foam, which accumulates contaminants and carries them to the surface of the liquid within the module. In addition, as mentioned earlier, the most critical factor determining the foam type and the overall efficiency of the foam generator is the thickness of the gap between the membrane and the generator housing.

Foam generator with optimal dimensions and reduced compressed gas pressure relative to the optimal level

A reduction in compressed gas pressure relative to the nominal or optimal pressure (8 atmospheres) decreases the rate of bubble formation, reduces the number of bubbles, and lowers the efficiency of contaminant fraction separation in the water. Proportional enlargement of the foam generator dimensions, while maintaining the compressed gas pressure and key operational characteristics, leads to increased gas consumption and a greater number of generated bubbles.

At this point, the author proposes to pause the description of technical conditions and turn to one of the practical applications of the foam generator.

Figure 5. *Foam layer obtained using a foam generator on wastewater from modern butter production*

All major contaminants of fatty and organic origin are present in this foam layer, which forms a relatively isolated layer that can be easily separated from the remaining liquid. The liquid, once freed from fats and other organic impurities, can then be effectively treated using electrochemical technologies.

To form and generate the foam, only a foam generator and a compressor are required – no additional chemical reagents are needed.

It should be noted that in current industrial practice, similar processes typically rely on chemical reagents, the cost of which can reach hundreds of thousands of dollars per month, not to mention the need to protect the final products from the harmful effects of these chemicals. Eliminating the adverse impact of chemical reagents and their residues in process water used for food and dairy production is both complex and extremely expensive. Therefore, achieving the same technological effect through aerodynamic action – using only compressed air – provides the technology of aerodynamic foam formation with significant **economic** and **environmental** advantages.

Figure 6. *Liquid treated using an aerodynamic foam generator*

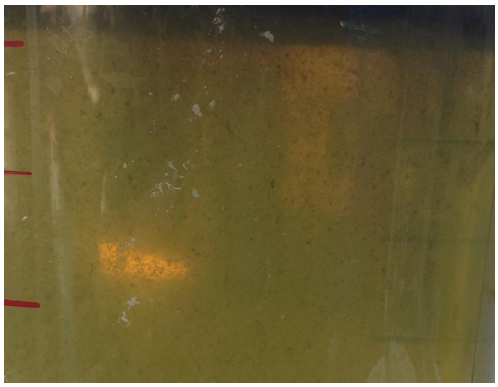

Liquid treatment using aerodynamic foam generators makes it possible to achieve the required level of purification quality at relatively low process costs, without the need for investments in the development of soy graphene production. After this brief digression, it is appropriate to return to the discussion of additional technical conditions.

Foam generator with reduced dimensions and optimal compressed gas pressure

Reducing the dimensions of the foam generator while maintaining optimal pressure leads to lower compressed gas consumption and a reduction in the number of generated bubbles.

Foam generator with increased dimensions and increased compressed gas pressure relative to the optimal level

In this case, if the increase is proportional across all parameters, there is a linear rise in compressed gas consumption and, accordingly, in the number of formed bubbles, while maintaining their energy characteristics.

Foam generator with reduced dimensions and increased compressed gas pressure relative to the optimal level

Here, the amount of compressed gas and the number of generated bubbles do not decrease, but their energy intensity increases.

Variants and parameter ratios of the module for aerodynamic flotation

Increased module column capacity with a constant optimal number of foam generators

Increasing the column capacity while maintaining the optimal number of foam generators reduces the flotation module's productivity.

Increased module column capacity with an increased number of foam generators

In this case, the productivity of the module increases, but so do the energy costs of its operation.The design of the foam generator is so universal and simple that it can be manufactured from a wide variety of structural materials, including all types of plastics and composite materials.The following photographs show foam generators made of aluminum alloys and stainless steel. The author draws attention to the **shape of the membrane combined with the conical reflector**, which allows the establishment of a minimal gap regardless of the construction material and its rigidity.

Figure 8. *Shape of the membrane combined with the conical reflector*

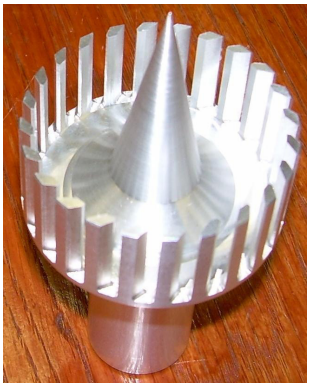

Applications of Foam Generators

There are many known applications of foam generators, two of which are worth discussing in detail for comparison – one in **greenhouse environments**, and the other in **systems designed for cleaning oil from the sea surface**.

System for Cleaning Oil from the Sea Surface

The device for separating oil from seawater is mounted on a specially equipped vessel. This separation apparatus must be installed on a ship equipped with all necessary systems and modules where oil is separated from seawater through **aerodynamic treatment** using foam generators. The ship must also include diesel generators (powered by the same oil-water mixture), compressors (powered by those diesel generators), pipelines, pumps, tanks for contaminated water, oil collectors, and reservoirs for purified seawater.

General Specifications of the Apparatus

- **Productivity**
- **Occupied operational area**
- **Compressed air consumption**
- **Duration of one purification cycle**
- **Number of modules per ship**

The **expected purification efficiency** of seawater should be **at least 99.97%**, with a **residual oil concentration** not exceeding **3 mg per liter** of purified seawater.

- Compressed air consumption at 4 bar: no more than **0.8 liters per second per foam generator**.
- Productivity per module: at least **20 gallons of water per minute**.

- Total compressed air consumption for one module: **19.2 liters per second (1152 liters/min, or 40.7 cubic feet/min at 4 bar)**.
- Power consumption per module (using screw compressors): not more than **5 kW (6.7 horsepower)**.

Advantages of the Proposed Method and Apparatus

- The system has a **modular design**, enhancing overall reliability.
- **Productivity** can be increased by adding more modules (each occupying ≤ 6 m²). A full-scale system of 125 modules occupies about **750 m²**.
- The entire purification complex, including all cleaning stages, can be installed on a ship with a **deck area of 1000 m²**.
- Modules can be arranged in **two or more tiers**, allowing capacity to double or triple without changing ship type.
- The system can be expanded with additional purification units.
- The ship and its purification modules are **fully autonomous**, generating energy from the oil–water mixture itself, eliminating the need for external fuel deliveries to spill zones.
- Thanks to its modular architecture, the system offers **high flexibility, interchangeability, reliability, and maintainability**.

Conclusion

As evident from the above, the proposed **dynamic foam generation technology** has a **wide range of applications**, offering **significant technical and economic advantages** while maintaining **low investment costs**.

References

United States Patent Application US20100193445A1. *Foaming of liquids*. Publication Date: August 5, 2010.
United States Patent Application US20150130091A1. *Foaming of liquids*. Publication Date: May 14, 2015.
United States Patent Application US20160207013A1. *Device for mixing fluids*. Publication Date: July 21, 2016.
United States Patent Application US20100224506A1. *Process and apparatus for complex treatment of liquids*. Publication Date: September 9, 2010.
United States Patent Application US20100224497A1. *Device and method for the extraction of metals from liquids*. Publication Date: September 9, 2010.

submitted 03.11.2025;
accepted for publication 17.11.2025;
published 30.12.2025

Contact: 9545482482usa@gmail.com

The European Journal of Technical and Natural Sciences 2025, No 6
ISSN 2414-2352

PREMIER Publishing
ppublishing.org

DOI:10.29013/EJHSS-25-6-119-126

MODULAR ARCHITECTURE OF SYSTEMS FOR THE REGENERATION AND RECIRCULATION OF PROCESS LIQUIDS, INCLUDING WATER AND AQUEOUS SOLUTIONS

Petrovych Volodymyr Vasylovych [1]

[1] Department of Transport Construction and Asset Management, National Transport University

Cite: *Petrovych V.V. (2025). Modular architecture of systems for the regeneration and recirculation of process liquids, including water and aqueous solutions. European Journal of Technical and Natural Sciences 2025, No 6.* https://doi.org/10.29013/EJHSS-25-6-119-126

Abstract

Modern industrial sectors that use water in technological processes face significant limitations imposed by traditional water treatment methods. Currently, three main groups of technologies are employed: reagent-based chemical treatment (over 70% of the market), non-reagent treatment methods (less than 20%), and combined technologies (approximately 10%). However, these existing solutions no longer meet contemporary industrial demands, as partial purification or localized improvements in water quality are insufficient for modern production requirements.

Given the inability of established methods to effectively address current challenges, the author-drawing on recent innovative concepts advanced by specialists such as Illia Beda – proposes a comprehensive water-treatment technology. This approach is based on the use of complete, autonomous, and standardized technological modules that ensure scalability, adaptability, and seamless integration into various industrial environments.

Keywords: *Modular Structure; Structure of Systems for the Regeneration of Technological Liquids; Structure of Systems for the Recirculation of Technological Liquids; Regeneration of Water and Aqueous Solutions; Recirculation of Water and Aqueous Solutions; Unified Technological Modules; Reagent-Based Chemical Treatment Method; Additional Technological Procedures; Reagent-Free Method of Water Treatment and Purification*

Comprehensive Technology for the Treatment of Industrial Wastewater Using Sequential Autonomous Processing Modules.

At present, in various industrial sectors that use water for technological purposes, the following methods of treatment and purification of water contaminated by products and by-products of technological processes are commonly applied:

- Reagent-based chemical treatment, which includes several modifications

of this method as well as combinations with other technologies; this method and its variations are the most widespread, accounting for more than 70% of the water treatment market;
- Non-reagent water treatment methods, which also include several main modifications differing in their operational ranges and performance characteristics; these methods cover less than 20% of the water treatment market;
- Various combined methods, typically consisting of the first two approaches supplemented with additional technological procedures dictated by local conditions specific to each user of the technology; these methods account for approximately 10% of the market and show a tendency toward expansion.

The challenges of water purification and conditioning identified to date cannot be effectively solved using known methods and technologies alone. The solution must be comprehensive, as partial solutions are not sufficient for any modern industrial process. Therefore, applying individual methods or their combinations does not address all new and continuously emerging requirements.

Considering the above and taking into account recent innovative concepts, the author proposes a comprehensive technology for the treatment of industrial wastewater, which consists of a series of sequential but functionally independent operations.

More precisely, all stages of water treatment can be viewed as consecutive modes of influence on the water, each based on different physical and chemical operating principles.

In combination with the latest innovative ideas presented and published by advanced specialists – primarily Illia Beda – the author proposes a complete technology that can be implemented through finished, autonomous, standardized technological modules arranged in the following configuration:

Figure – Diagram 1. *Nine primary technological modular compositions that incorporate all processing stages and operations required for the formation of a modular technological equipment complex intended for the purification, regeneration, and recirculation of process liquids, including water and aqueous solutions*

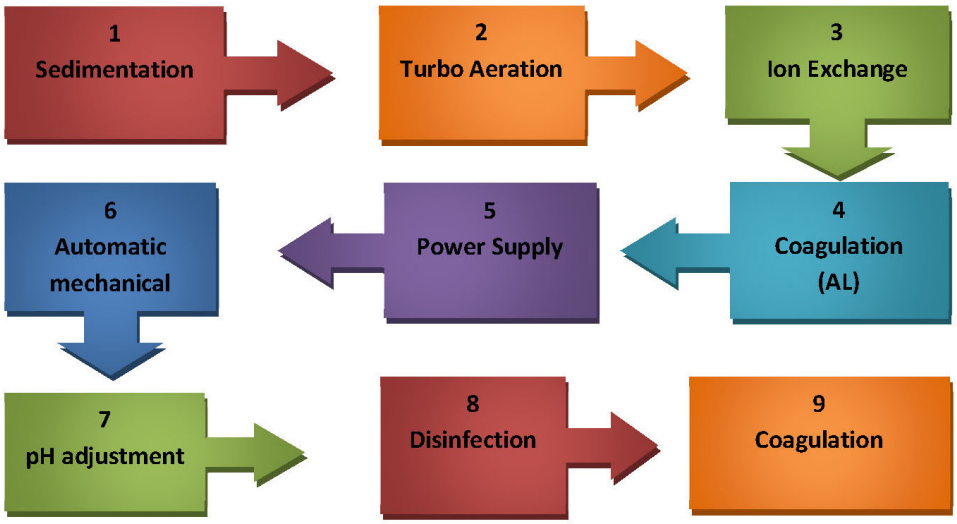

Of all the presented modules, Module 5 – the power supply unit – is relatively universal, while the remaining eight modules have a more specialized field of application:

Module 1 – Sedimentation Module, which may be implemented as either a sedimentation column or a sedimentation tank with a parallelepiped geometry.

Module 2 – Turbo-Aeration Module, which may have at least two configurations: one using foam generators and another employing a mixing device with real-time (online) homogenization.

Module 3 – Ion-Exchange Treatment Module, which can have numerous configurations, one of the most efficient being ion-exchange

columns equipped with capsules for ion-exchange resins made from carbon–carbon composite fabrics.

Module 4 – Coagulation Module, which uses aluminum ions as a coagulant, generated in electrochemical reactors with aluminum anodes.

Module 6 – Automatic Mechanical Filtration Module, equipped with automatic cleaning for filtration sections and real-time (online) regeneration of filter elements.

Module 7 – Acidity and Alkalinity Adjustment Module.

Module 8 – Electrochemical Reagent-Free Disinfection Module.

Module 9 – Final Electrochemical Coagulation Module.

Figure 2. *Example of a Modular Composition: System for the Regeneration of Process Liquids, including Water and Aqueous Solutions*

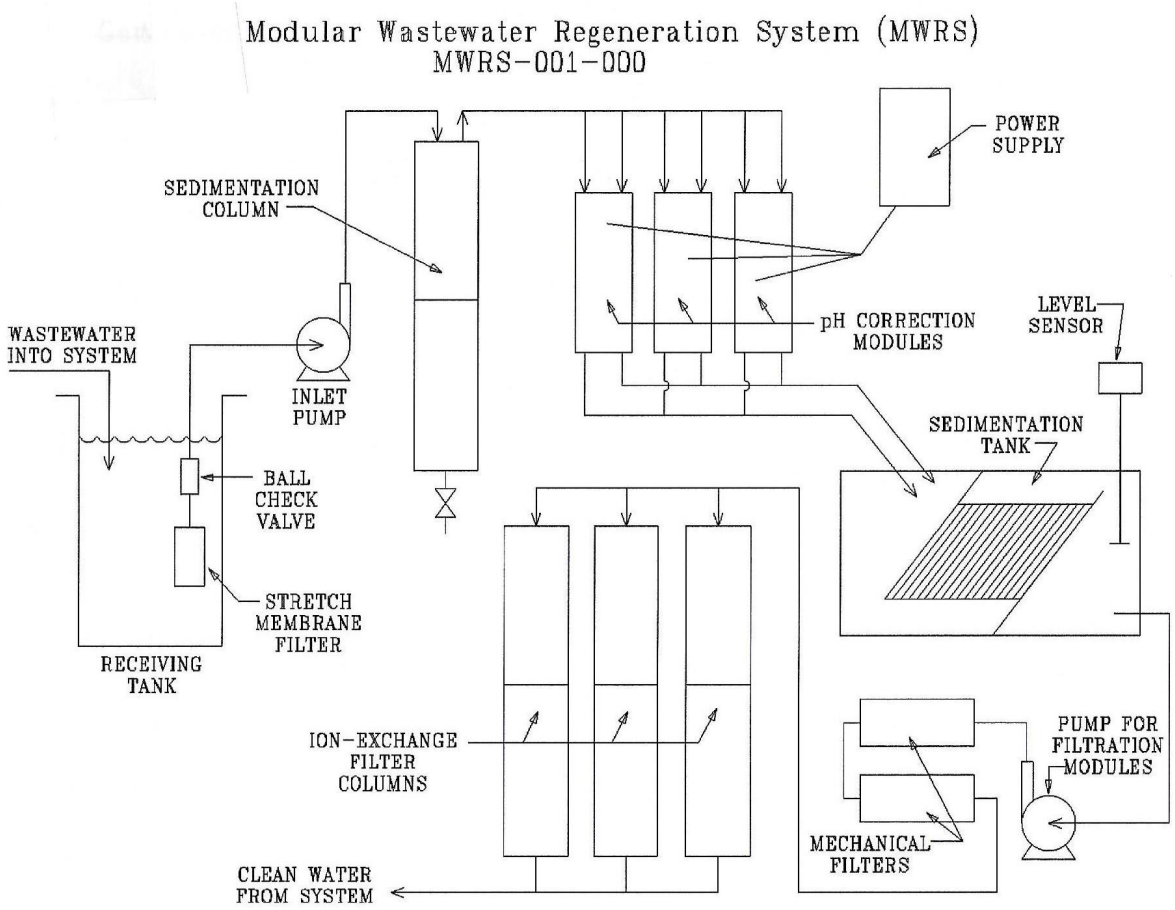

As illustrated in the diagram, the system includes an intake tank equipped with several elements that enable the initial treatment of the spent process liquid. The liquid undergoes primary processing through a membrane filter connected via a check valve to the inlet pump, which delivers the regenerating liquid to the sedimentation column. Depending on the required flow rate, the sedimentation column may consist of one, two, or three sections.

After the first sedimentation stage, the liquid is directed to electrochemical reactors used for acidity and alkalinity correction. These reactors are controlled and powered by a multifunctional power supply source.

Once acidity is adjusted to ensure an alkaline state that provides optimal conditions for sedimentation, the liquid enters a specialized sedimentation module with a unique geometry that enables the separation of formed sediment conglomerates within the upward flow.

After the sedimentation process is completed, a level sensor activates a centrifugal pump that transfers the liquid to mechanical filtration modules, where remaining conglomerate particles that did not enter the sediment layers are retained.

Since the mechanical filters operate in an online mode, the pressure generated by the filtration pumps is sufficient to supply the filtered liquid to the ion-exchange columns.

Based on the conclusions and proposals outlined in the publications and patent applications of Illia Beda, as well as his multifunctional foresight regarding the development of eco-friendly technologies and advanced processing systems, the author of the present publication has significantly expanded the technical capabilities of the ion-exchange columns – a subject that merits more detailed consideration.

It is particularly important to emphasize that, in addition to synthetic ion-exchange resins, natural materials such as zeolite can also be effectively used for ion-exchange treatment.

Under the modular scheme proposed by Illia Beda – where an ion-exchange column consists of at least two modules (sections) – it becomes possible to use several ion-exchange materials of different exchange capacities within a single column. For example, the upper section may contain zeolite, while the lower section may contain ion-exchange resin.

The combination of these materials provides the most optimal conditions for purification, regeneration, and recirculation.

This modular configuration is based on the technological principles described in the inventions of Illia Beda, a well-known innovator in reagent-free real-time intensive liquid-processing technologies, including systems for water and aqueous solutions in directed flows.

Figure 3. *A modular system featuring an intermediate module equipped with a preliminary inlet filter and a set of sequential mechanical filters located at the outlet of the intermediate module and before the inlet to the electrochemical reactors for acidity and alkalinity correction*

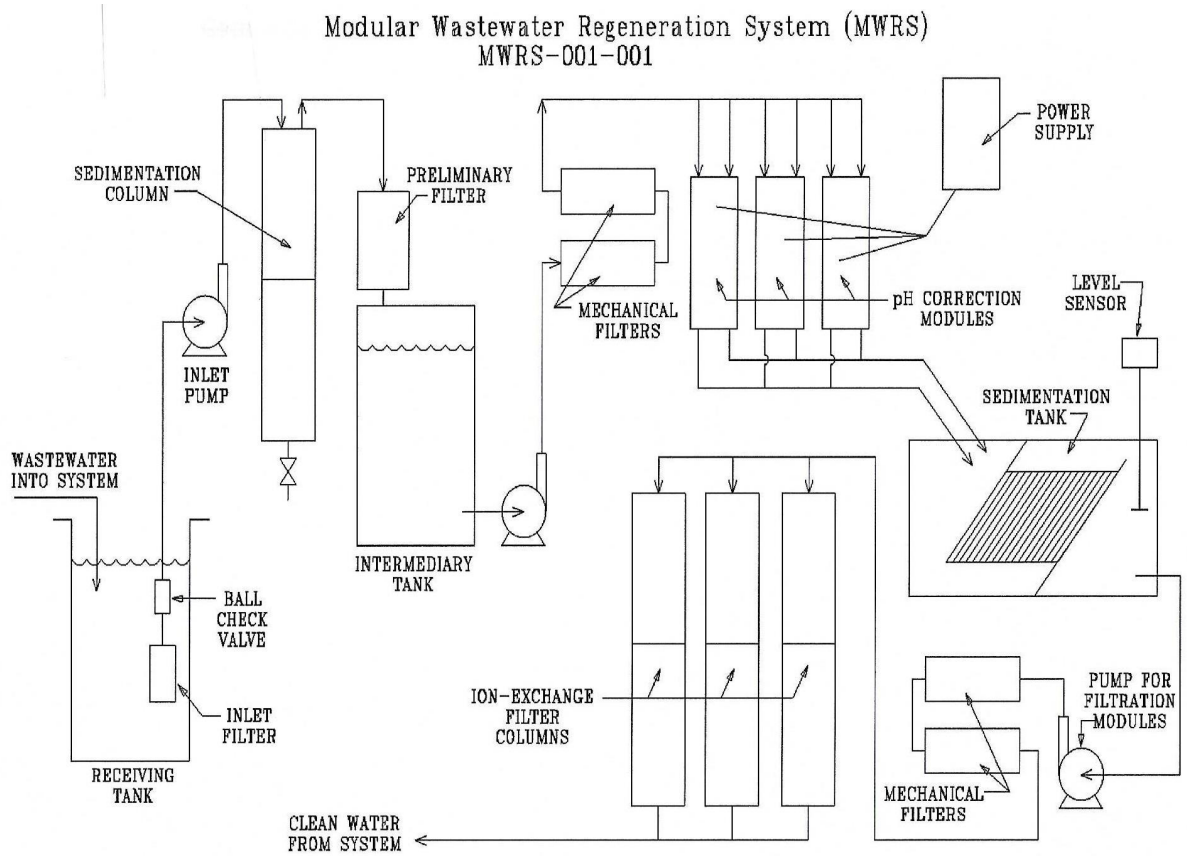

Practical implementation has shown that the hierarchical modular systems invented by Illia Beda – despite having a narrow technological

specialization – are sufficiently autonomous and operate within independent production – technological cycles without the use of chemical reagents or activating synthetic additives. This allows lower – level modules in the hierarchy to be effectively combined into higher-level modules while maintaining full economic and technological efficiency.

Furthermore, the absence of chemical reagents introduced into the process makes it possible to initiate and successfully carry out online recirculation immediately after the completion of the regeneration cycle, while preserving the high quality of process liquids and solutions.

Figure 4. *The most compact modular system without intermediate technological or structural elements*

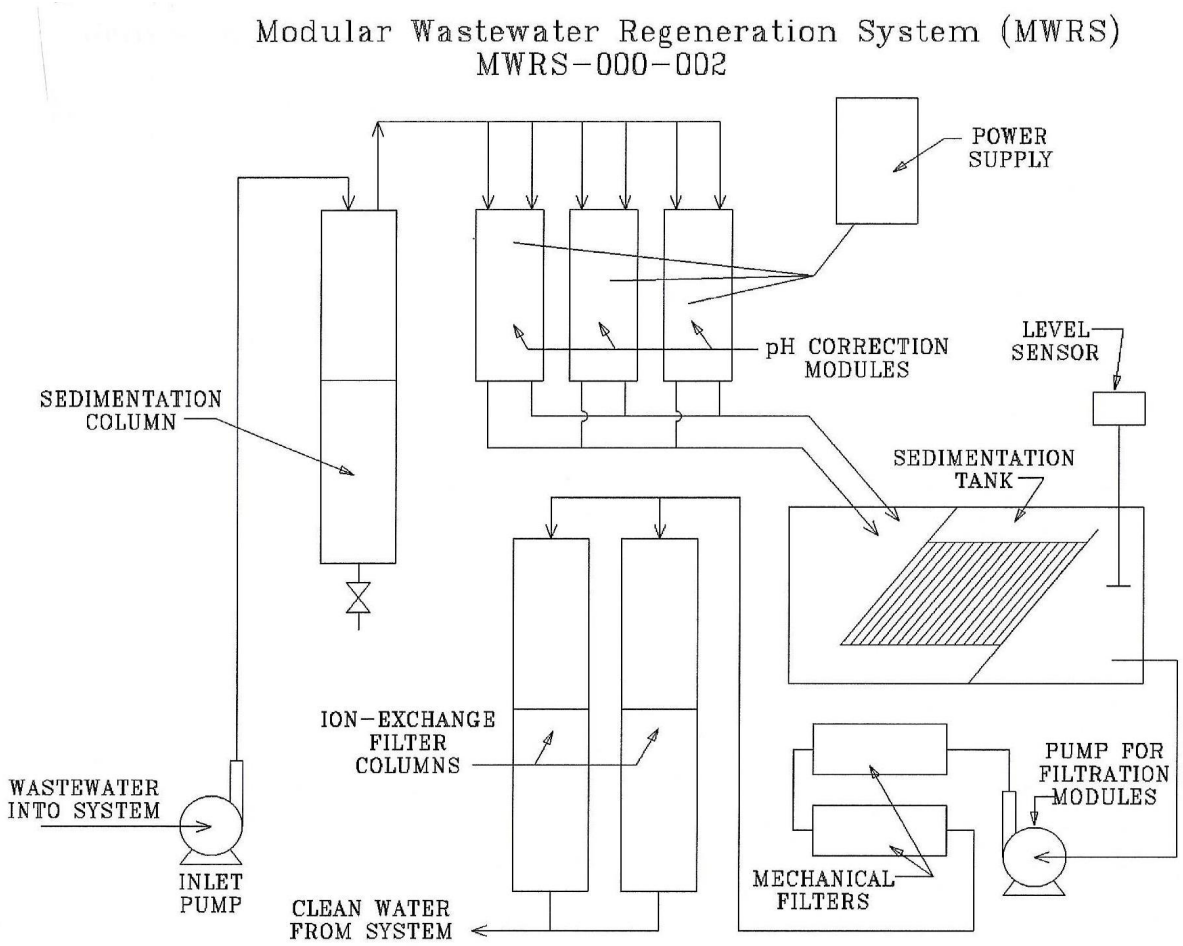

Thus, the presented figures and diagrams clearly demonstrate that the hierarchical structure of vertically integrated modular systems makes it possible to fully resolve both technological and environmental challenges while simultaneously meeting the needs of industrial facilities of any profile and any level of waste contamination, ensuring complete regeneration and subsequent recirculation of process effluents.

In this way, the approach also addresses the broader objective of gradually transforming industrial facilities of all types and levels of organizational flexibility into so-called "smart production" systems.

As shown in the presented algorithmic diagram – developed with consideration of innovative ideas and proposals derived from the inventions and publications of Illia Beda – a total of 14 objects are examined and represented in the diagram. Each of these objects is itself a complex of modules composed of autonomous modules of a lower combinatorial level.

Figure 5. *Basic IP*

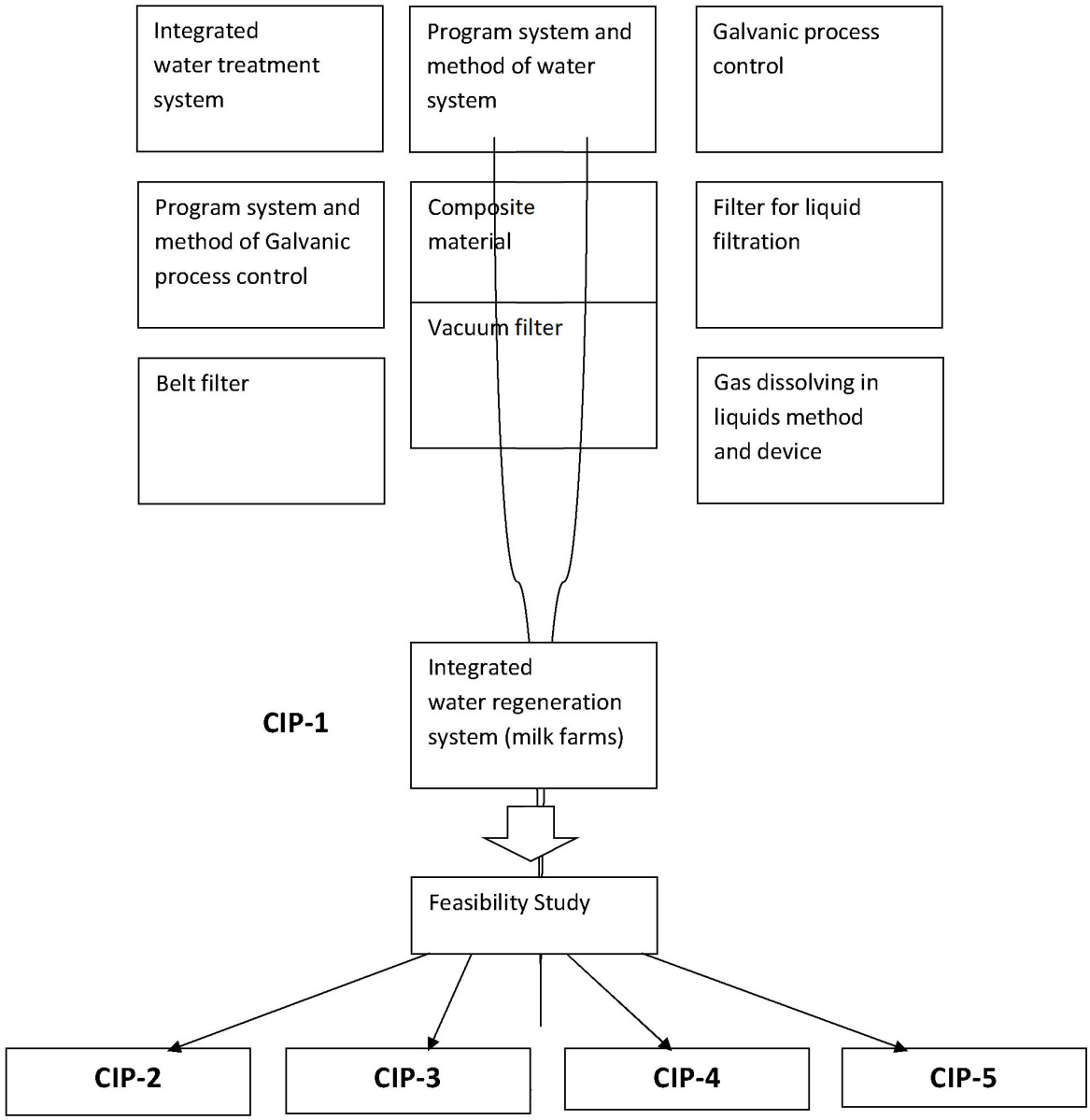

Each module presented in the diagram qualifies as a subject of patent protection, and all possible combinations of these modules likewise constitute fully eligible patentable subject matter, including objects suitable for further patent continuation (in accordance with current U.S. patent legislation).

As of today, users of water-treatment technologies face a range of issues that prevent the auxiliary stages of water purification from achieving the same level of efficiency as the main technological processes. The major challenges include:

- continuous limitations on the availability of water resources that can be used in technological processes;
- ongoing deterioration in the quality of natural water resources suitable for industrial use;
- a constant increase in the cost of water resources;
- steadily tightening standards for wastewater discharge, which raise the cost of wastewater treatment;
- increasing requirements for the quality parameters of water used in technological processes;
- the emergence of new synthetic and organic materials due to the development of new and improved technological processes, which necessitates constant modernization of water-

treatment facilities or extremely broad functional capabilities, resulting in increased cost of both equipment and technological operations;

- the existence of numerous industrial facilities operating with outdated traditional equipment that has exhausted its service life, replacement of which requires significant investment or is not feasible at all.

Patent and Licensing Landscape for the Proposed Technologies Patentability of the Proposed Technological Methods

Based on preliminary studies and a patent search, the following topics have been identified for patent applications related to the proposed water-treatment methods:

- a module complex for advanced processing of water and aqueous solutions, and the associated method of its use;

Figure 6.

Integrated water treatment technology

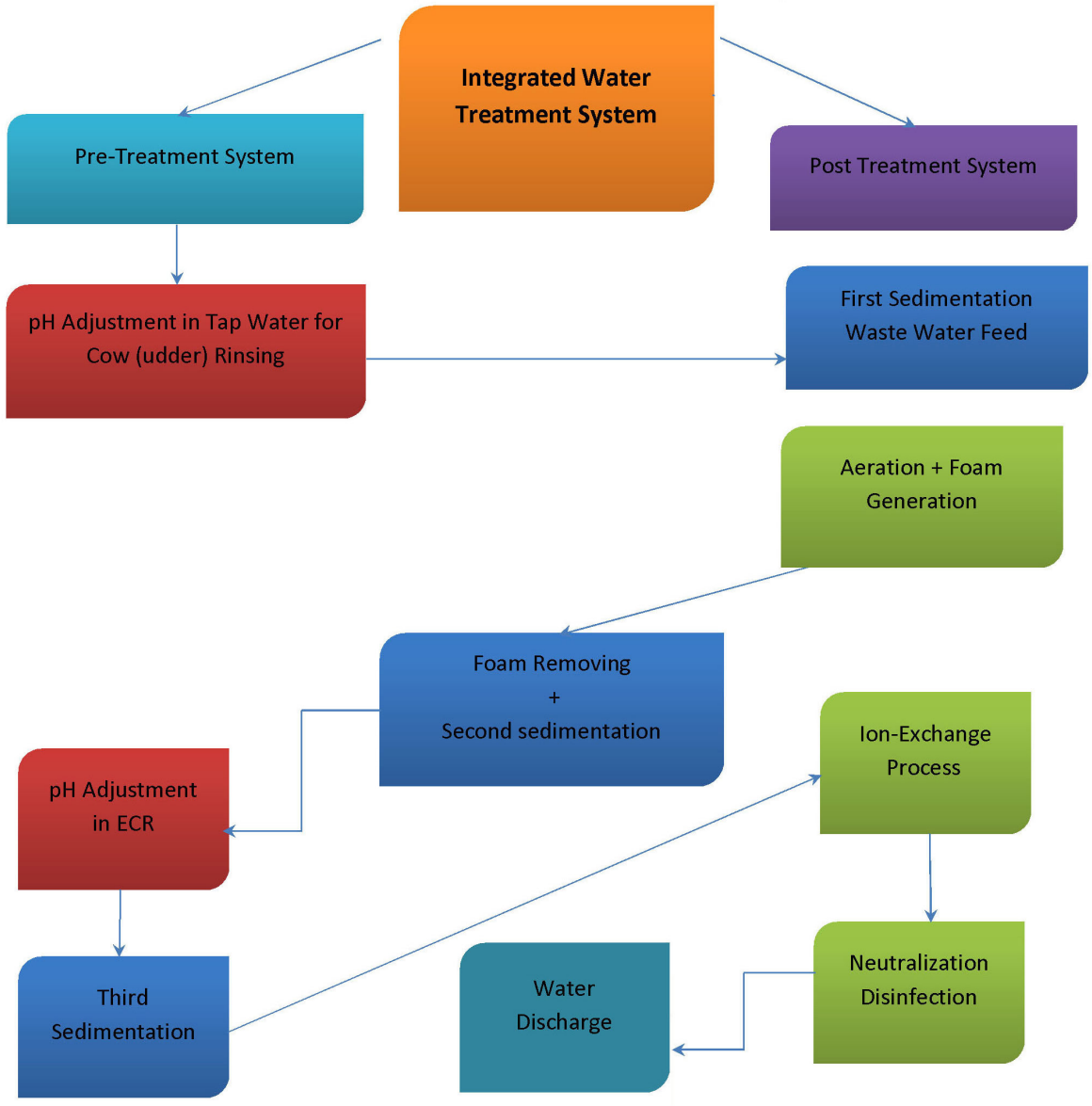

- a method of comprehensive water treatment and the technological modules required for its implementation;
- a method for electrolytic extraction of metals from a water or aqueous-solution stream and electrode cells for implementing this method;

- a method of aerodynamic water foaming in a continuously flowing stream and a foam generator for this method;
- an integrated method of combined filtration with ion-exchange treatment and biosorption;
- an electrode cell for electrocoagulation with coaxial electrodes;
- an electrode cell for electrocoagulation with a continuously moving strip cathode;
- an electrode cell for acidity or alkalinity correction using blocks of polarizable soluble electrodes;
- an electrode cell for acidity or alkalinity correction with volumetric porous electrodes;
- an electrode cell for acidity or alkalinity correction with continuously moving strip electrodes;
- an electrode cell for electrochemical disinfection and associated electrode configurations for implementing the method.

For each patent application, prototypes and analogs have been identified among the inventions of Illia Beda – the originator of the proposed new methods. According to the results of preliminary patent searches and structural analysis, all listed technological solutions demonstrate full patentability.

Based on the above, it becomes possible – through vertical integration and modular composition – to develop a block diagram of an integrative technological complex in which flexibility and selectivity of each process are achieved within every module at the lowest hierarchical level.

References

United States Patent Application US 2010/0224506 A1. Livshits, David, et al. *Process and Apparatus for Complex Treatment of Liquids* September 9, 2010.

United States Patent Application US 2010/0224497 A1. Livshits, David, et al. *Device and Method for the Extraction of Metals from Liquids* September 9, 2010.

United States Patent Application US 2011/0069579 A1. Livshits, David, et al. *Fluid Mixer with Internal Vortex* March 24, 2011.

United States Patent Application US 2010/0193445 A1. Livshits, David, et al. *Foaming of Liquids*.August 5, 2010.

United States Patent Application US 2015/0130091 A1. Livshits, David, et al. *Foaming of Liquids*. May 14, 2015.

United States Patent US 6,139,714. Livshits *Method and Apparatus for Adjusting the pH of a Liquid*.October 31, 2000.

United States Patent US 9, 144, 774. Livshits, David, et al. *Fluid Mixer with Internal Vortex*. September 29, 2015.

submitted 09.11.2025;
accepted for publication 23.11.2025;
published 30.12.2025

Contact: sedova.alina7810@gmail.com

The European Journal of Technical and Natural Sciences 2025, No 6
ISSN 2414-2352

PREMIER Publishing
ppublishing.org

DOI:10.29013/EJHSS-25-6-127-133

WATER REGENERATION IN SMART HOME INFRASTRUCTURE

Volodymyr Savenko [1]

[1] Department of Construction Organization and Management (Kyiv National University of Construction and Architecture)

Cite: *Savenko V. (2025). Water Regeneration in Smart Home Infrastructure. European Journal of Technical and Natural Sciences 2025, No 6.* https://doi.org/10.29013/EJHSS-25-6-127-133

Abstract

Water supply represents one of the fundamental components of smart home life-support systems, determining both the technological level and the overall economic efficiency of the smart home infrastructure. This publication summarizes a set of innovative technologies developed by engineer and innovation specialist Bohdan Vitiv, aimed at meeting the core technical requirements for modern smart home water systems. The author emphasizes the importance of these developments for advanced educational programs and professional training in the field of smart home technologies. The article provides an overview of the key technological solutions proposed by Vitiv and outlines their potential for improving the quality and effectiveness of specialist preparation in this rapidly evolving domain.

Keywords: *Water in smart home infrastructure; Electrochemical water regeneration in smart home infrastructure; Chemical-free water regeneration; Comprehensive water recirculation; Compact modules for electrochemical water regeneration; Integrated water supply system within smart home infrastructure and ecosystems; Input control and pre-treatment modules within smart home infrastructure; Used-water storage modules; Separation systems with vortex foam generators; Final control systems without direct contact; Control and processing unit for remote real-time management and monitoring*

Electrochemical regeneration of tap water in smart home infrastructure for recirculation and comprehensive disinfection using real-time online control lines based on electromagnetic resonance spectroscopy principles, operated by artificial intelligence and artificial neural network elements

Integrated Water Supply System within Smart Home Infrastructure

An integrated water supply system within the smart home infrastructure typically includes four groups of modules interconnected by their operating principles and functional interaction:

1. **Input control and pre-treatment modules**, including inlet water tanks and reserve tanks for peak loads. Pre-treatment includes

electrochemical disinfection, aeration, and increasing oxygen concentration to the level of full saturation. Input control modules operate using a non-contact method based on the principles of electromagnetic resonance spectroscopy.

2. **Local modules for electrochemical processing**, installed separately for each residential unit and including water consumption metering units with real-time monitoring sections at the inlet (non-contact, working on the principles of electromagnetic resonance spectroscopy).
3. **Used-water storage modules**, dividing the water into at least two groups: water containing toilet waste and general greywater.
4. **Water regeneration modules**, consisting of at least two sections: one for water with fecal content and one for all other water. These modules include separation systems with vortex foam generators and final non-contact control systems based on the principles of electromagnetic resonance spectroscopy. In addition to the operational modules, the integrated water supply system includes a control and processing unit with artificial intelligence and artificial neural network elements, enabling remote management and real-time monitoring.

Water Consumption Parameters

Water volume is calculated in full accordance with the standards for supplying residential units.

Number of residential units: 100

Estimated number of residents: 150

System Structure Overview

The integrated water supply system includes four groups of interrelated modules:

1. Input control and pre-treatment modules, including inlet water tanks and reserve water tanks for peak loads. Pre-treatment includes electrochemical disinfection, aeration, and increasing oxygen concentration to the level of full saturation. These modules operate via non-contact methods based on electromagnetic resonance spectroscopy.
2. Local electrochemical treatment modules for each residential unit, including inlet water consumption metering blocks with real-time control sections (non-contact, using electromagnetic resonance spectroscopy).
3. Used-water storage modules with separation into at least two groups: water containing toilet waste and general greywater.
4. Water regeneration modules with at least two sections-one for water with fecal particles and one for remaining water. These modules incorporate separation systems with vortex foam generators and final non-contact control systems based on electromagnetic resonance spectroscopy.

The system also includes a central control and processing unit equipped with artificial intelligence and artificial neural network elements, enabling remote control and real-time monitoring.

Carbon–Carbon Composite Fabric

A carbon–carbon composite fabric has the following functions:

(When you provide the functions, I will translate and format this section in the same style.)

Carbon-Carbon Composite Fabric: Functional Application

In the anode block of a water desalination unit, the functions of this fabric consist in significantly increasing the contact surface between the anode (the fabric itself) and the stream of saline water. As the saline water passes through the openings in the fabric-anode, it receives the maximum possible amount of positive electrical charge.

In an electrochemical cell for disinfection (an electrochemical reactor of any type), this fabric (not connected to the power supply) is positioned as a spacer between the electrodes – the anode and the cathode. This spacer equalizes and stabilizes the flow of liquid, which, in the electric field between the electrodes, migrates and separates: the positively charged liquid contacts the cathode, while the negatively charged liquid contacts the anode.

After passing through the inter-electrode zone, the charged liquid exits in an upward flow: on the cathode side, the liquid carries a negative charge (a flow with an acidic background), and on the anode side, the liquid carries a positive charge (a flow with an alkaline background).

Innovations Opening a New Scientific and Technical Service Direction

Augmented reality in consumer and personal optics is still in its early development, yet it is expected to have significant future potential. Such headsets remain expensive, and continuous daily use is not yet convenient. Nevertheless, several high-quality devices are already available on the market or at the final stages of development. This review aims to provide an analytical overview of these products.

More than ten years have passed since the release of the first successful augmented reality headset, Oculus Rift. These glasses produced an immediate "wow effect," but after some time, once users were sufficiently familiar with the novelty, interest decreased. The key issue is that developers have not yet succeeded in transforming augmented reality glasses into a device as commonplace as a smartphone, game console, or smartwatch.

According to the author of this publication, one of the reasons for this situation lies in the state of service technologies, which are not yet sufficiently developed to support such complex devices in conditions of mass production and, consequently, mass consumption.

The state of patent protection for these new technologies also raises numerous questions.

It is noteworthy that, despite expectations of rapid market growth for augmented reality visualization projects and technologies, the dynamics of patent filings remain slow and inactive.

A patent search conducted by the author using key terms in the United States Patent Office database identified only 133 patent applications and no patent grants related to this topic.

An initial analysis of the published patent applications revealed that all such applications are exploratory in nature and do not focus on the construction or systems of augmented reality glasses as finalized products. In addition, the examples provided in these applications refer to devices at the final stages of development.

Figure 1. *Model of a system for bidirectional correction of acidity and alkalinity in deionized water*

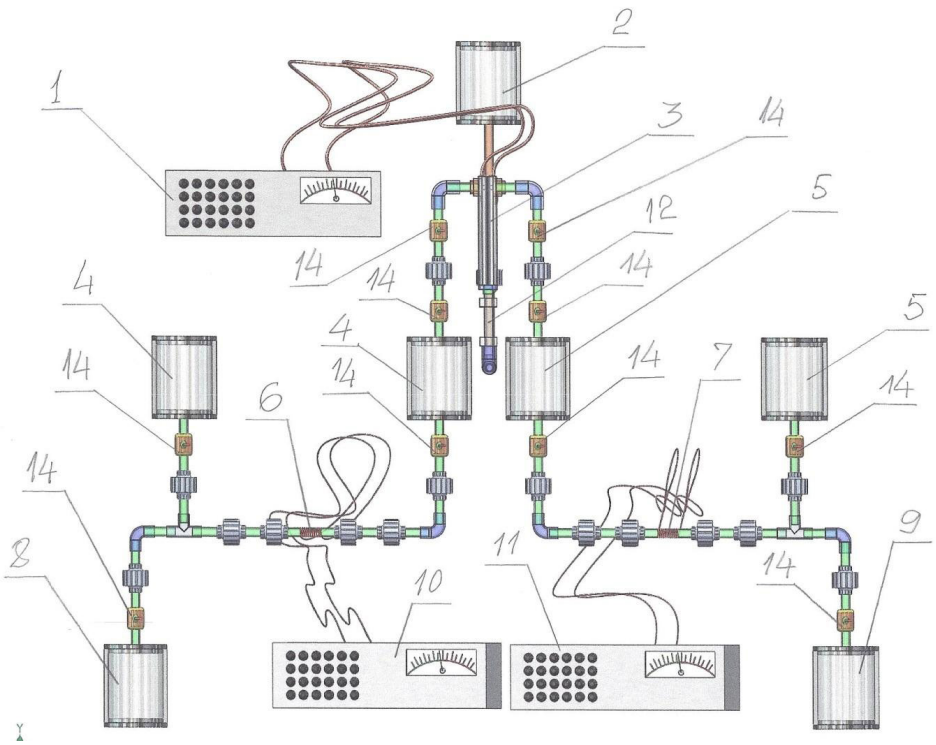

1 – power supply unit for the electrochemical reactor

2 – tank with deionized water for feeding into the electrochemical reactor

3 – electrochemical reactor with an interelectrode space in which processing is carried out in two parallel upward flows

4 – collector of water with a reduced acidity level

5 – collector of water with an increased alkalinity level

6 – sensor module for measuring the reduced acidity level

7 – sensor module for measuring the increased alkalinity level

8 – reservoir for water with a reduced acidity level

9 – reservoir for water with an increased alkalinity level

10 – pulse generator for the impedance-resonance sensor

11 – pulse generator for the impedance-resonance sensor

Since the author of this series of articles is engaged in the practical implementation of such devices for a specific market, it is noted that a significant number of technical solutions are currently lacking-both for the devices themselves and for the accompanying tools and products necessary for their everyday use. One of the primary needs is the development of technical solutions and products designed to support augmented reality glasses in daily operation, including cleaning the lenses from inevitable contamination of both organic and inorganic origin.

As the lenses of augmented reality glasses become dirty just as easily as those of standard glasses, the first practical requirement is the creation of an integrated technology for producing a cleaning and disinfecting liquid from water that does not contain high concentrations of salts, including hardness salts.

However, this proved insufficient. As required by practical conditions, the liquid used for rinsing must be an insulator in order to eliminate any possible local current impulses. An analysis of potential water sources for processing within the system led to manufacturing complexes of photolithography, where deionized water is used. This water demonstrates properties closely matching the characteristics considered most necessary and suitable for servicing the optical lenses of augmented reality glasses.

Figure 2. *Model of a system for bidirectional correction of acidity and alkalinity in deionized water*

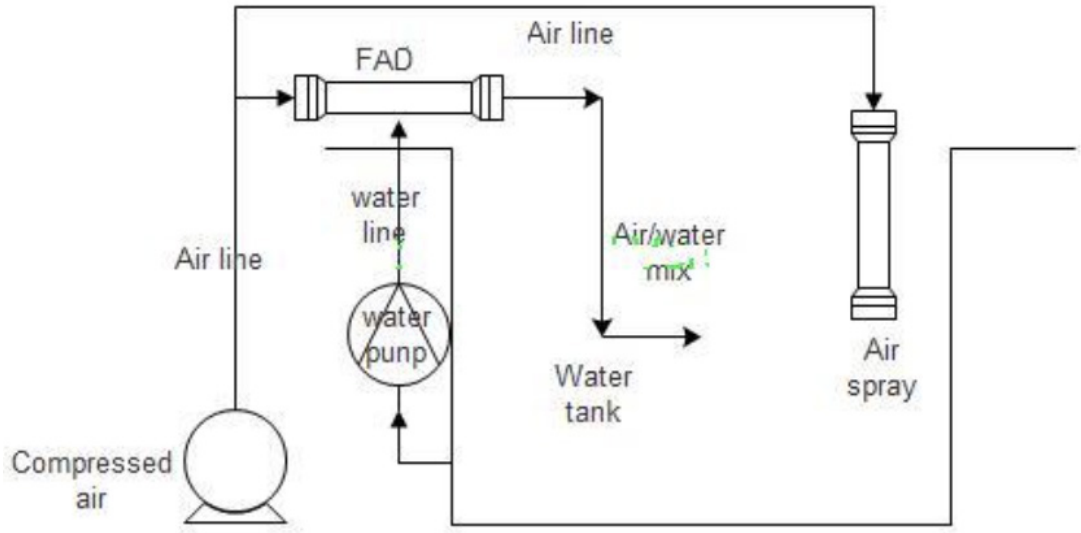

12 – inlet pipeline to the electrochemical reactor

14 – regulating and control valves

15, 16 – flow meters

17 – current-carrying cables

For comparison, variants using distilled water and deeply purified water were also examined and analyzed. Nevertheless, the properties and performance characteristics of deionized water proved superior. Special

attention was given to the possibility of using deionized water in the future, both after treatment in an electrochemical reactor and before treatment, for preparing various emulsions intended for subsequent service operations on augmented reality glasses.

Experimental evaluations confirmed the feasibility of producing high-quality emulsions both with deionized water before treatment and with water after modification of its neutral acidity or alkalinity level.

Figure 3. *Model of an electrochemical reactor with a power supply*

Since this technology was recommended for use for the first time, it became necessary to produce a basic prototype to verify, under real operating conditions, the feasibility of implementing several innovative technologies, the first of which was the technique and technology of the electrochemical reactor.

In the described reactor, the electrode cells have working zones separated by a neutral membrane positioned symmetrically between two electrodes. One of the important operating principles in the electrode cells is that the processing of deionized water takes place in an intensified upward flow. The distance between the active surfaces of the electrodes is only 3 millimetres, of which the membrane thickness accounts for 1 millimetre. Thus, the thickness of the liquid stream in such an electrode cell is only 1 millimetre.

This small stream thickness made it possible to sharply increase the current density to 100 amperes per square decimetre, which in turn enabled the electrochemical correction of acidity and alkalinity in water that is very similar in its parameters and properties to a dielectric liquid. Because the processed liquid forms two separate outlet streams, it becomes possible to use either the highly alkaline water or the highly acidic water for treating the optics of augmented-reality glasses.

This approach made it possible to disinfect the surface of optical lenses from microorganisms and bacteria using the acidic stream, and to remove fatty contaminants using the alkaline stream. It must also be emphasized that because the system for preparing and treating deionized water is structurally simple and uses the most widely available engineering materials and components, it can be installed in any small retail enterprise that sells optical instruments and glasses, including augmented-reality glasses-both current and future models. Another important factor relates not only to the specific requirements of augmented-reality glasses, but to optical devices in general. This concerns the anti-allergenic effect. Since the electrode cell of the electrochemical reactor is powered from a single power source, and the electrodes have identical active surface areas, the correction of liquid parameters in two opposite directions proceeds proportionally. As a result, the acidic stream and the alkaline stream do not cause any allergic reactions when used simultaneously. This phenomenon fundamentally changes the consumer properties of the system, not only for augmented-reality glasses but also for any other optical devices. As in any system for dynamic electrochemical treatment of liquids-especially liquids with a low level of electrical conductivity-the design of the electrode cell becomes critically important. All structural features of the cell must be considered: the materials used for electrode fabrication, the materials and design of the neutral membrane, and the materials and design of the cell housing. It was found that a particularly high efficiency

potential is associated with the use of electrodes made of carbon–carbon composite materials (the phenomenon associated with these materials will be described in subsequent publications).

Figure 4. *Model of the electrode cell of the electrochemical reactor. Photograph of the system for real-time correction of acidity and alkalinity in deionized water*

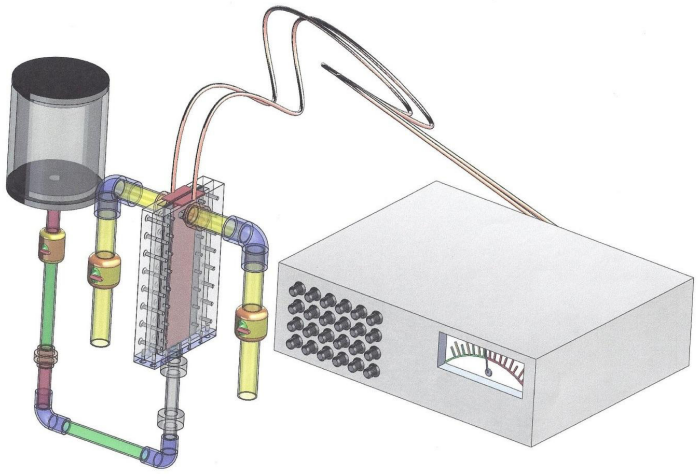

Photographs of the actual prototype system demonstrate the intentionally designed structural simplicity and, as a result, the low cost combined with sufficiently convenient operation. Such a system can be installed and operated in virtually any retail facility without significant expenses, and through the products generated by this system, it becomes possible to raise the level of servicing such devices to the standard of technological refinement required for all current and future optical instruments. To present the broader situation within the technological field-which, in addition to traditional optical technologies and materials, includes a wide range of processes, technological groups, and materials-the author intends to provide, in subsequent publications, an analysis of the overall state of innovation development in this area. The search for an open and unoccupied niche within this technological field continues with exceptional intensity. However, the actual degree of this intensity remains unclear, as the level of patent protection for these solutions does not correspond to the publicly stated degree of development of these projects, nor to the declared breadth of efforts aimed at identifying new technical solutions.

References

Appendix 1. Johnson, L. E., et al. *Smart Glasses Having Interfering Light Filtering*. United States Patent Application US 2018/0031836 A1, February 1, 2018.

Appendix 2. Kawamura, T. *Head Mounted Apparatus and Gripping Apparatus*. United States Patent Application US 2017/0307787 A1, October 26, 2017.

Appendix 3. Kuehne, M., et al. *Method for Operating Virtual Reality Glasses and Systems with Virtual Reality Glasses*. United States Patent Application US 2015/0378155 A1, December 31, 2015.

Appendix 4. Joo, G.-h. *Wearable Glasses and Method of Providing Content Using the Same*. United States Patent Application US 2016/0034042 A1, February 4, 2016.

Appendix 5. Park, J., et al. *Glasses-Type Mobile Terminal and Method of Operating the Same*. United States Patent Application US 2018/0005421 A1, January 4, 2018.

Appendix 6. Sevostianov, P. V. *Method and System for Displaying Three-Dimensional Objects*. United States Patent Application US 2017/0366805 A1, December 21, 2017.

Appendix 7. Liao, C. *Wearable Smart Glasses*. United States Patent Application US 2017/0371164 A1, December 28, 2017.

Appendix 8. Park, S. W. *Wearable Glasses, Control Method Thereof, and Vehicle Control System*. United States Patent Application US 2016/0173865 A1, June 16, 2016.

Technical Report. TEI Company. *Technical Report – Water Aeration: Increasing the Oxygen Concentration in Water*. Test installation conducted at the Dor Chemicals maintenance site, including a 1000-liter tank system with two FAD devices, a circulation pump, and compressed air supply (7–8 bar). Experimental results demonstrated an increase of water saturation level from 40% to 96% after 10–15 minutes of operation.

Technical Report. TEI Company. *Technical Report - Water Aeration: Increasing the Oxygen Concentration in Water*. Test installation conducted at the Dor Chemicals maintenance site, including a 1000-liter tank system with two FAD devices, a circulation pump, and compressed air supply (7-8 bar). Experimental results demonstrated an increase of water saturation level from 40% to 96% after 10–15 minutes of operation

submitted 09.11.2025;
accepted for publication 23.11.2025;
published 30.12.2025

Contact: sedova.alina7810@gmail.com

The European Journal of Technical and Natural Sciences 2025, No 6
ISSN 2414-2352

PREMIER Publishing
ppublishing.org

DOI:10.29013/EJHSS-25-6-134-141

SMART MANUFACTURING ECOSYSTEM

Shabaev Renat [1]

[1] Owner of the Investment Fund "HOOVER"

Cite: *Shabaev R. (2025). Smart Manufacturing Ecosystem. European Journal of Technical and Natural Sciences 2025, No 6.* https://doi.org/10.29013/EJHSS-25-6-134-141

Abstract

Transformation and upgrading (Gentrification) of smart industrial spaces with simultaneous revitalization and reconstruction. The article examines methods and techniques for the sequential adaptation and transformation of the properties and characteristics of elements in the infrastructure of a smart production facility. This includes startups in the brownfield category, transitioning in the first stage to the smart brownfield category, with subsequent adjustments to all ecosystem characteristics as a whole to align with the greenfield stage. Finally, in the third stage, a transition is made to align with the smart greenfield category.

Keywords: *transformation of premises, startup ecosystems, stabilization of the psychological climate, psychological climate of startups, visual stabilizers of the psychological climate, infrastructural stabilizers of the psychological climate, combined systems of psychological climate stabilizers*

Purpose

The sections of this publication provide definitions, explanations, and characteristics that outline the criteria for compliance with all categories of characteristics and parameters of smart production facilities across the following classes:

- Brownfield;
- Smart Brownfield;
- Greenfield;
- Smart Greenfield.

In relation to the additional conditions, characteristics, and requirements that have arisen and continue to arise in the context of creating and accommodating innovative projects with their entire ecosystem and specific features, designers and builders are constantly engaged in creative exploration.

Introduction

Of course, all of this represents approximate content for documents, and for each project, depending on its specifics and market implementation conditions, as well as the requirements of potential investors, this list may vary significantly.

Particular attention should be paid to projects in the fields of biotechnology and genetic engineering. For such projects, a special expert, technological, and commercial review is likely required.

To ensure the descriptions are as close to reality as possible when constructing smart facilities, the author of this publication exclusively referenced effective and popular projects developed by the renowned specialist in this field, Bohdan Vitiv.

Revitalization

Revitalization of industrial buildings differs from reconstruction as it involves changing the functional purpose of the building while preserving it as a valuable historical and cultural asset, without altering its exterior. Virtually all changes to the building itself are confined to the interiors.

After revitalization, buildings can serve various purposes: cultural or recreational (museums, art centers, creative spaces), commercial (shops, shopping centers), or economic (office centers). A distinctive feature of revitalization is that the above-mentioned purposes can be successfully combined while preserving historical buildings.

Economic support for revitalization processes may vary. American urbanist Brent Ryan identifies two types of revitalization depending on the source of initiative and funding: "top-down" (initiated from above) and "bottom-up" (initiated from below).

- Top-down projects are typically costly and initiated by municipal authorities, who often provide financial support;
- Bottom-up projects are less expensive, with initiatives originating from local entrepreneurs, cultural communities, etc.

The concept of a smart production building and a smart production space, as part of a specialized ecosystem for the development of new innovative projects, is much broader. It also includes the introduction of psychological climate stabilizers at all levels of the ecosystem infrastructure. These include:

- Visual stabilizers of the psychological climate;
- Infrastructural stabilizers of the psychological climate

All types and variations of such stabilization create and foster a psychological environment conducive to the brainstorming process so critical for the development of startups.

The Essence of Revitalization

The primary principle of revitalization lies in uncovering new opportunities for old territories and buildings.

A comprehensive approach is used in the revitalization process to preserve the uniqueness, authenticity, identity, and historical resources of the urban environment and industrial zones, while also considering the specifics of startups.

Revitalization originated in industrialized nations during the second half of the last century, significantly impacting the appearance, infrastructure, and demographic situation of many cities.

Revitalization may involve relocating industrial enterprises, resettling people, and changing the functional purpose of certain urban spaces and buildings.

Figure 1. *The figure shows the view of an innovation corridor as part of the ecosystem of a smart production facility in a restored industrial building designed for startups*

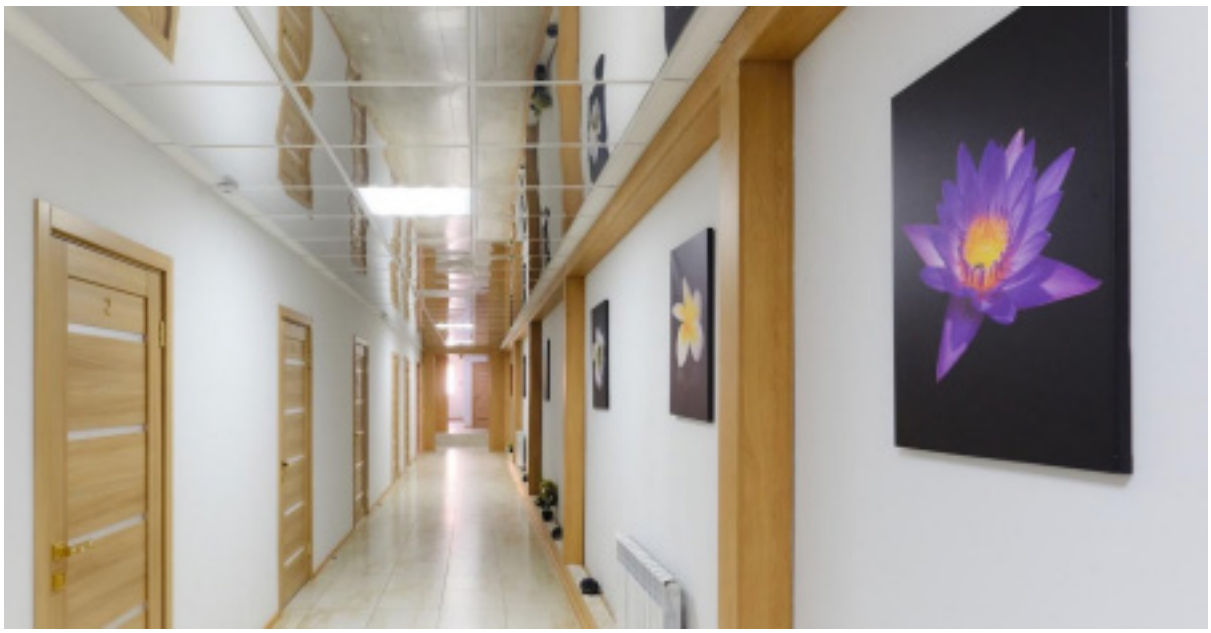

Gentrification

Gentrification refers to the improvement of previously unattractive areas in terms of infrastructure. Typically, this process involves industrial zones, urban outskirts, or neighborhoods built during the Soviet era for workers. These areas are transformed into comfortable urban spaces and business centers. As a result, the reputation of the old neighborhood changes, and gradually, people begin to seek quality new housing in these areas. Dilapidated buildings are demolished and replaced with modern homes.

For developers, gentrification is a way to implement their projects even in parts of the city where no free land remains. For the city, it is an opportunity to revitalize abandoned areas.

Perhaps one of the most well-known examples of gentrification is the High Line elevated park in New York City. Previously, this space was a railway for freight trains; today, it is a park spanning over two kilometers, visited annually by several million people. The High Line is not only a recreational area but also a venue for contemporary art exhibitions. Thanks to the creation of this new public space, real estate prices in the surrounding areas have significantly increased. Old, low-budget buildings have been replaced by higher-class complexes. Currently, around 30 development projects have been completed near the park.

The primary residents of such clusters include representatives of creative industries, architectural studios, art galleries, shops, offices, and coworking spaces. An important feature of the space is the availability of numerous locations for photo shoots.

Similar projects can be found in provincial areas. For example, the “Art Square” district in Ufa. The investor set an ambitious goal to create a beautiful creative center in the city. This space was once a regular factory, but today it has become a favorite leisure spot for locals and visitors. Shops, showrooms, cafes, bars, smart offices, craft workshops, and art salons have opened here.

A key part of the project was the restoration of historic buildings, abandoned factories, and other structures, which have now turned into tourist attractions. Naturally, the implementation of this project increased the capitalization of the district and nearby land.

A noteworthy example of gentrification is the transformation of the Polish city of Lodz. Once a major industrial and wealthy center of the textile industry, production declined, as did the factory buildings. This occurred between 1989 and 1993, following the fall of the communist regime in Eastern Europe.

Over time, the red-brick factory buildings, mansions, and Art Nouveau style houses located in the city center began to attract tourists. The city’s industrial heritage and examples of Polish modernism became some of the first tourist attractions.

The interest of travelers and the efforts of local authorities resulted in the creation of remarkable projects involving the repurposing of factories into cultural centers, museums, and residential spaces. Projects of gentrification and revitalization of former seaport areas have become widespread in Northern Europe. For instance, in Amsterdam, Copenhagen, and Hamburg, former industrial zones located in port areas, often connected to historical locations, have been transformed by developers. These projects take quite a long time to complete, but the results exceed all expectations. In Copenhagen, for example, a sandy beach with a reservoir for paddleboarding and swimming was created on the site of a former industrial zone. Naturally, housing and commercial spaces also emerge, revitalizing the area and integrating it into the city’s life.

In Russia, a notable project for reorganizing an industrial zone is “Sevkabel” in St. Petersburg. The territory of former enterprises was converted into a large creative cluster. With the growing number of visitors, infrastructure is also expanding, which is expected to increase the status and value of the residential sector.

Brownfield: An industrial park created on previously developed land. Such sites, often already equipped with infrastructure, are transformed through reconstruction or renovation. Greenfield: An industrial park created on a specially allocated plot of land that lacks infrastructure.

The conditions for technical creativity that have developed in recent times are largely shaped by the global division of labor between countries and regions with varying levels of development and fundamentally different mental and technocratic traditions.

Historically, the foundational ideas for the development of technology and engineering (with rare exceptions) were born in Europe and the United States. This trend has largely persisted to this day. However, it must be acknowledged that the entire process from the inception, formulation, and crystallization of an innovative idea to the production of a new product or any other type of practical realization has undergone significant fundamental changes. It seems that the innovative community has not entirely adapted to these changes. These fundamentally altered conditions – or even the "changed rules of the game" in the innovation field – force inventors to seek new approaches to organizing the innovation process and to develop new foundations for relationships between inventors, investors, manufacturers, and sellers of innovative products.

Naturally, the innovation and expansion of these newly created productions does not stop at the component market but increasingly encroaches on the markets of finished products of various kinds and purposes. It is now evident that re establishing the production of basic components in countries where they were previously manufactured is neither physically nor economically feasible. Developers of cutting-edge innovative products must take into account the uncomfortable reality that component manufacturers can easily seize the initiative. Leveraging their significant advantage in production costs, they could independently develop and manufacture new innovative products, potentially pushing established companies that invest colossal resources into advancing innovative technologies to the margins of the market.

How can individual inventors navigate situations where even large corporations cannot fully protect their interests in intellectual property? As the author sees it, the idea must first be properly formulated and, as much as possible, protected using scientific and technical methods rather than solely legal measures. Naturally, many options exist, each of which accounts for key nuances and details that pave the way for the successful implementation of an innovative idea.

On the path to implementing progressive and innovative ideas, authors often face numerous systemic traps. These traps may be exploited by patent specialists in large and medium-sized companies to identify, appropriate, or simply steal the idea. Stabilizing the Psychological Climate is one of the tools to protect the innovative products being developed in a startup.

Since the primary idea and its patent protection may significantly change during this process, the initial version of the agreement for testing feasibility may also undergo substantial revisions. In such situations, psychological rehabilitation for startup employees becomes critically important and necessary.

In these circumstances, it is challenging for authors to independently define the limits of what is possible and formulate their demands and claims toward investors. Furthermore, the technical situation may necessitate involving specialists with profiles and capabilities that the authors of the innovative idea do not possess.

In this case, a comprehensive solution is necessary, both in technical and commercial-patent aspects. Again, if the investor is interested in the further continuation of the project, the most appropriate and effective decision might be joint ownership of intellectual property and joint execution of the project.

As convincingly demonstrated in the characteristics of his innovative developments by Vitiv Bohdan, the conditions for technical creativity that have emerged recently are largely influenced by new directions in the development of building and architectural technologies. These, in turn, arose based on the requirements and new standards of smart homes, and are also connected to the global division of labor between countries and regions with varying levels of development, as well as fundamentally different mental and technocratic traditions.

A new interpretation of finishing elements of the structural components of a smart home is proposed in the new projects by Vitiv Bohdan as visual and design tools that contribute to stabilizing the psychological climate and, most importantly and valuably, ensuring the reliability and convenience of operating a smart building in the context of brainstorming sessions and the intense work of a startup team and also ensuring similar stabilizing effects for other startups located in the same space.

Figure 2, 3. *The figures show fragments of the working corridor in a renovated industrial building*

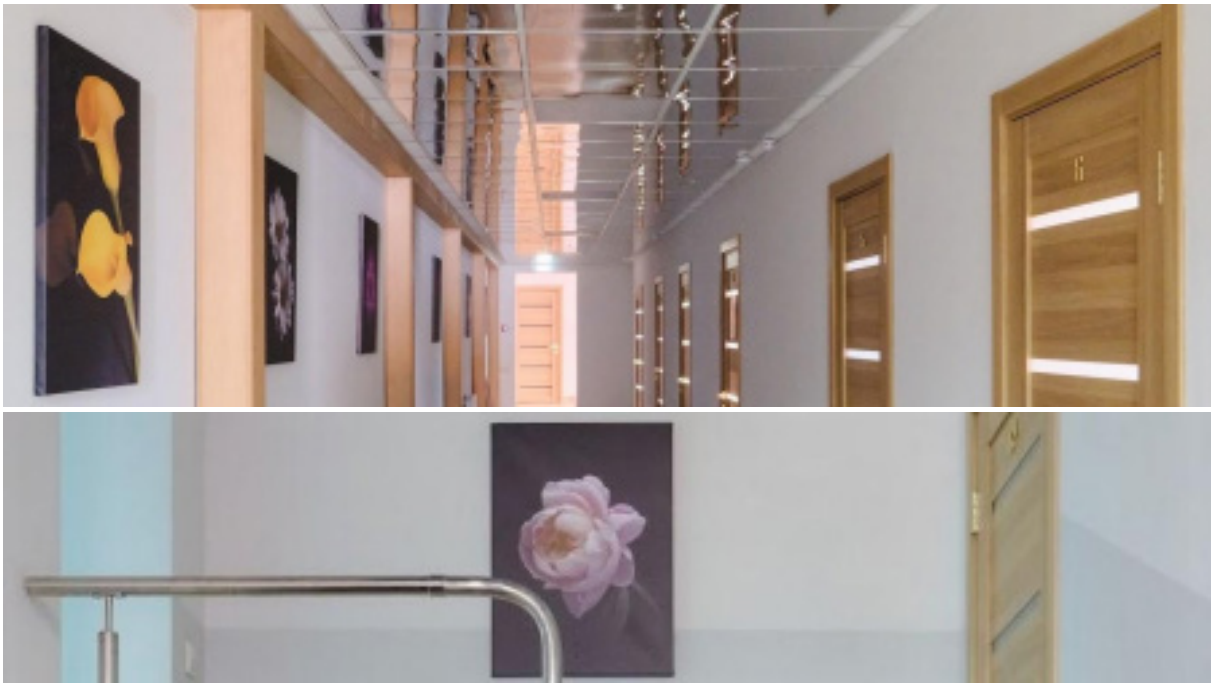

Figure 4. *The figure also shows a lawn with flowers planted on a surface covered with ceramic particles, with the color of the ceramics harmonizing with the flowers and the structural elements of the walls of the industrial building*

This space design concept between buildings, also developed and proposed by Bogdan Vityv in his projects, helps to accommodate technological incubator projects or even multiple technological incubators in such modernized smart spaces.

These opportunities allowed Vitiv Bohdan to develop conditions and proposals for organizing new technological incubators in Ukraine, utilizing the advantages that Ukraine possesses.

Figure 5. *The figure also shows a lawn with flowers planted on a surface covered with ceramic particles, where the color of the ceramics harmonizes with the flowers and the structural elements of the walls of the industrial building*

The entire interior space between the production buildings is occupied by unique lawns with flowers in various tones, and the entire surface of the lawn is covered with fine gravel that matches the color of the restored walls of the production buildings after gentrification and revitalization.

Requirements for projects developed in technological incubators. The materials of the project, when presented to the intermediary company, should contain or are recommended to include the following documents and materials:

Composition and structure of intellectual property objects owned by the company or initiative group applying for the project. Typically, all technological directions at various stages of development within the applicant company are comprehensive intellectual property objects. Each technological direction should be represented by a systematic structure of components, which includes the following key documents:

- Forecast of technological development for the near and distant future;
- Patent and licensing strategy for all products in the direction, covering all stages of the project, production, and marketing;
- Principal and basic patents for inventions that form the foundation of the technological direction;
- Patents for applications arising from the development of the technological direction;
- Inventions created by the employees and partners of the applicant company before the establishment of the company, which have author certificates or other legal documents;
- Reports on scientific research and experimental design work carried out by employees and partners of the applicant company outside of the company for this technological direction;
- SolidWorks models for all modifications of the products in the technological direction, including all assembly, node, part variants, and models for digital and virtual simulation of product performance;
- Basic principles of technology for manufacturing components and assemblies of the products in the technological direction;
- Complete set of working design and technological documentation for manufacturing the products in the technological direction;
- Corrected CNC machine programs for manufacturing experimental product samples in this technological direction;
- Programs and methods for all necessary types of testing of experimental samples and products in the technological direction at all stages of production;
- Working models of innovative products in the technological direction and results of field testing of technological agricultural products;
- Operational and accompanying documentation for products in the technological direction, including technological instructions for installation, conservation, storage, repair, and transportation;
- Working experimental product samples in the technological direction;
- Technical descriptions of the principles and devices of special technological equipment for manufacturing basic parts and assembling products in the technological direction;
- Materials for patent applications for the aforementioned special technological equipment.

Of course, this is a general outline of the documents, and depending on the project's specifics, its conditions for implementation in the market, and the requirements of potential investors, this list can change significantly.

Projects in biotechnology and genetic engineering should especially be noted; such projects likely require special expert-technical and commercial analysis.

Proposal for organizing technological incubators in Ukraine There are all the necessary conditions and prerequisites for establishing technological incubators in Ukraine: Thousands of qualified specialists are working, and over the years of stable operations in defense enterprises, enormous industrial and technical experience has been

accumulated. Engineering personnel, trained over many years, possess a high level of professional expertise required for initiating innovative technical solutions.

In Ukrainian enterprises and rural areas, there is unique agricultural production experience, combined with special, unrivaled natural conditions (such as the famous Ukrainian black soil), which create prerequisites for establishing highly efficient and profitable agricultural enterprises. Of course, covering the entire country with technological incubators is impossible and unwise because, despite their technical and commercial revolutionary potential, the creation of highly effective technological incubators remains an evolutionary process.

The organization of the first steps in the development of technological incubators in Ukraine or any other region can be carried out in the following sequence:

1. Based on the expertise of Ukrainian specialists, it is necessary to determine the area of technology where the country's combined scientific, commercial, and historically established potential is the highest and most competitive.

2. It makes no sense to make premature predictions. As the author of this publication believes, it is most appropriate to announce a competition for the best technological project in all production sectors, especially agriculture, in all regions of Ukraine. To evaluate the technical and commercial level of proposed projects, it is advisable to form competition conditions and an expert group, inviting commercialization specialists from the USA (who have already expressed interest) for the first stage of evaluation. In the second evaluation stage, when the most promising projects are selected, investment fund representatives with experience working in Ukraine should be involved. Many of these representatives are already familiar with the idea of organizing technological incubators in Ukraine and have shown interest.

The activity area of a technological incubator in one of Ukraine's regions is divided into work in Ukraine and international cooperation. The following sequence of organizational-technical stages is proposed for the formation of the project (assuming the incubator has already been opened):

1. The project initiator or author prepares the necessary information and technical documents and finds an initial private or other investor of at least $50,000. If the authors or initiators struggle то find one, it makes sense to contact a company that specializes in this.

2. Upon receiving the first private investor, the authors of the innovation, possibly with the investor or the investor's representative, come to the technological incubator, where, under specific standard conditions developed by the incubator, the project is organized, and a new innovative company is created.

Now, it makes sense to briefly outline the standard (for this technological incubator) conditions.

Investments in the new company should include private investments (around $50,000 minimum, but private investments can be higher if the investor is confident in the project).

The rest of the required funds (approximately $400,000) are provided by the technological incubator.

Both the private investor and the incubator do not contribute all the funds at once; the company initially receives an advance of 10% of the total investment, and further funds are allocated as the project progresses, subject to the completion of each phase. Thus, investors protect themselves from any technological mistakes or failures during the project, as the next financial tranche is made only after errors are corrected and phase results are positive.

How are company shares distributed?

When the company is established, the project authors receive 50% of the shares, the private investor who contributed $50,000 receives 15%, and the remaining 35% is divided between the technological incubator (25%) and the employees of the company who contributed the most to the project's implementation (10%).

Repayment of funds is made after the first profit is received from the project, and no more than 5% of the profit annually. In case of failure and the inability to generate commercial profit from the project, the invested funds are not returned. Naturally, to attract

investors, government and state structures should find appropriate incentives, the most significant of which should be exempting the new company from profit taxes for at least 10 years after receiving the first profit.

All of the above are just assumptions, and in reality, other options for organizing and implementing an innovative project may arise.

Now, let's assume the project was successful and economically efficient. In this case, there will be additional opportunities for its commercial realization. This concerns options for entering foreign markets and, again, if circumstances are favorable, the possibility of listing the company on stock markets in the US or European countries.

References

United States Patent Application US 2010/0193445 A1. (2010, August 5). *Foaming of liquids*. Methods and systems for processing liquids using compressed gases or compressed air.

United States Patent Application US 2010/0224497 A1. (2010, September 9). *Device and method for the extraction of metals from liquids*. A volume-porous electrode for electro-extraction, electro-coagulation, and electrochemical pH modification.

United States Patent Application US 2010/0224506 A1. (2010, September 9). *Process and apparatus for complex treatment of liquids*. Methods and apparatus for multi-stage treatment of contaminated liquids using filtration, separation, and electroextraction.

United States Patent Application US 2011/0069579 A1. (2011, March 24). *Fluid mixer with internal vortex*. A compact static mixer for combining fluids using vortex dynamics without moving parts.

United States Patent Application US 2012/0102736 A1. (2012, May 3). *Micro-injector and method of assembly and mounting thereof*. A compact device for producing composite fluid mixtures and injecting them into a target volume.

submitted 03.11.2025;
accepted for publication 17.11.2025;
published 30.12.2025

Contact: bogdan.vstsv@gmail.com

The European Journal of Technical and Natural Sciences 2025, No 6
ISSN 2414-2352

PREMIER Publishing
ppublishing.org

DOI:10.29013/EJHSS-25-6-142-149

MULTIFUNCTIONAL SENSOR TECHNOLOGY. (Potential application areas of methods, approaches, and technologies of electromagnetic resonance spectroscopy)

Denis Slivka [1]

[1] Brest CAD Project LLC Brest, Republic of Belarus

Cite: *Slivka D. (2025). Multifunctional Sensor Technology. (Potential application areas of methods, approaches, and technologies of electromagnetic resonance spectroscopy). European Journal of Technical and Natural Sciences 2025, No 6.* https://doi.org/10.29013/EJHSS-25-6-142-149

Abstract

The classical and standardized methodology for measuring acidity levels requires mandatory calibration of the measuring instrument using reference solutions with acidity values of pH 4 and pH 7 prior to any measurement. Accordingly, the proposed experimental measurement system also necessitates calibration mechanisms before performing control measurements, which significantly increases the overall measurement time.

During the study, various types and designs of sensors (solenoids) were tested, including a planar sensor configuration used at the final stage of the experiments. A comprehensive global patent search confirmed that this type of sensor, its application for acidity measurement and monitoring, as well as its structural implementation, were employed for the first time. The term *biosensor* traditionally refers to a device in which biological materials – such as enzymes, tissues, bacteria, yeasts, antigens/antibodies, liposomes, organelles, receptors, DNA, and viruses (including coronaviruses)—directly respond to signals generated by the proposed sensor, producing a resonant output functionally linked to the presence and concentration of the target component.

Keywords: *Electromagnetic resonance spectroscopy; electromagnetic resonance measurement; measurement of electromagnetic resonance in biological tissues; influence of membrane presence on the electromagnetic properties of a planar inductive coil*

Potential Application Areas of Electromagnetic Spectroscopy in Multifunctional Sensor Technology in Medicine and Biology Measurement of the concentration and composition of components in liquids

This category includes mixtures such as solutions and dispersed systems: emulsions, suspensions, and biological fluids (blood, milk, lymph, urine, etc.). Owing to the high sensitivity of the proposed sensor design variants, the technology can be widely applied in:

- the pharmaceutical industry within technological processes for the production of medicinal products;
- laboratory and point-of-care analysis of biological fluids such as blood, milk, urine, etc.;

- medical, technical, and food microbiology for monitoring the concentration of microorganisms and the presence of viruses, including coronaviruses.

Measurement of the electromagnetic impedance of biological tissues

At present, impedance measurement of biological tissues at various alternating-current frequencies is widely used in diagnostics as well as in biological and medical research.

For example, a significant increase in tissue impedance at low frequencies allows detection of inflammation at its earliest stages. Certain thyroid disorders are diagnosed by changes in the phase shift angle between current and voltage.

Electromagnetic resonance mammography is an effective method for early detection of breast cancer. Measurement of skin impedance assists in diagnosing dermatological conditions, for example, in identifying non-pigmented malignant melanoma, as well as locating areas of skin contamination with coronaviruses.

Endoscopic impedance measurements may be used to detect pathologies of internal organs. This also includes non-invasive blood analysis – for example, to determine elevated glucose levels- and assessment of lymphatic fluid condition.

In all the above application areas of resonance measurements, electromagnetic spectroscopy technology can make a significant contribution by substantially increasing measurement sensitivity.

In addition, the use of the proposed sensors may enable detection of coronavirus presence in the human throat at early stages of infection.

Application of electromagnetic spectroscopy methods and technologies in biosensors

The term “biosensor” typically refers to a device in which biological materials (enzymes, tissues, bacteria, yeasts, antigens/antibodies, liposomes, organelles, receptors, DNA, viruses – including coronaviruses) directly respond to the signal from the proposed sensor and generate a resonant signal functionally associated with the presence and concentration of the target component.

In this case, the proposed device implements a fundamentally new method of obtaining information about the chemical composition of a solution.

The presence of biological material with unique properties in the solution enables highly selective identification of required compounds in a complex mixture without the need for additional operations involving other reagents, concentration procedures, etc. (hence the term “methods of analysis without the use of chemical and biological reagents”).

Influence of a membrane on the electromagnetic properties of a planar inductive coil

To evaluate the influence of the membrane on the ability of a planar inductive coil to generate a probing electromagnetic field, a dedicated software tool was used, developed on the basis of artificial intelligence and artificial neural networks. This program is capable of calculating and visualizing the electromagnetic field emitted by various inductive coils when electric current flows through their turns.

Three scenarios were simulated:

- absence of a membrane, Gap = 0;
- presence of a membrane, Gap = 1 mm;
- presence of a membrane and an additional gap between the membrane and the coil, Gap = 1.5 mm.

The simulations were performed for a planar single-layer coil with a diameter of 16.24 mm and 29 turns of wire, corresponding to the planar inductive coil currently used for evaluating the possibility of pH measurement in liquids.

The images presented above clearly illustrate the attenuation of the probing electromagnetic field as the distance from the inductive coil increases. The key characteristic of this field – Max (relative maximum induction)—decreases from 8.70 (Gap = 0 mm) to 2.95 (Gap = 1.5 mm).

In the classical and standardized methodology for measuring acidity levels, prior to the direct measurement of the acidity of the test sample, calibration of the measuring instrument is mandatory. This calibration is performed using standard buffer solutions with acidity levels of pH 4 and pH 7.

Figure 1.

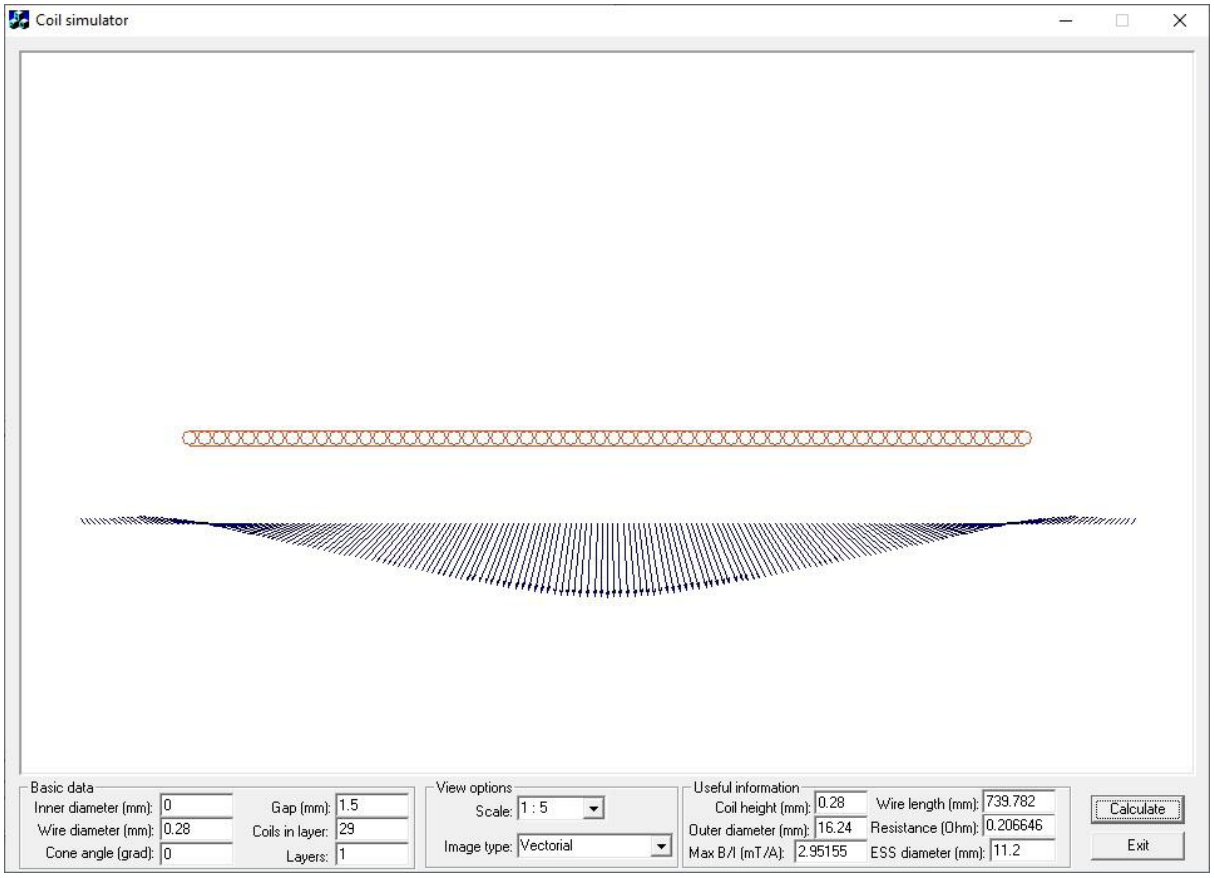

In accordance with this standard methodology, the proposed experimental measurement system also requires calibration mechanisms prior to performing control acidity measurements. This significantly increases the total time required to carry out the measurement process.

For testing and comparative analysis of measurement results, two basic types of liquids were used: distilled water and regular tap water. To adjust the acidity levels of the test samples, concentrated hydrochloric acid prepared specifically by a chemical laboratory was added.

Various types and designs of sensors (solenoids) were used during the experiments, including a planar sensor (solenoid), which was employed at the final stage of testing.

Based on the results of an extensive global patent search, this type of sensor, its application for such measurements and monitoring, as well as its structural implementation, were used for the first time.

Below is the electrical connection diagram for the planar sensor integrated with the instruments of the test equipment set.

During preparation of this publication, the author conducted a patent search covering a period of 50 years, using as a reference point the systems operating online in real time for contactless monitoring of parameters of industrial processes interacting with the technology and equipment complex for electromagnetic resonance spectroscopy.

Search results:

The well-known inventor **Aliaksandr Vitun**, author of comprehensive integrative inventions developed according to the scheme “device – system (consisting of a control and supervisory super-system with functionally embedded subsystems) – software – associated method”, created three advanced interconnected integrative technical solutions. Using active artificial intelligence components and artificial neural networks, these solutions have the potential to complete the full measurement cycle in strict accordance with metrological standards in just 10 milliseconds.

This is a unique performance indicator and may be considered one of **Aliaksandr Vitun’s** significant achievements.

According to metrology experts, the comprehensive methodology invented by Alexander Vitun can not only ensure exceptional measurement speed but will also reliably introduce into technical and technological measurement processes the operational parameters required for the more active use of artificial intelligence and artificial neural networks in industrial workflows.

Furthermore, his (**Aliaksandr Vitun's**) creative multifunctional design developments and original inventions in real-time monitoring and control systems, based on the principles of electromagnetic resonance spectroscopy, make it possible to incorporate into classical innovative technologies elements of quantum superiority, quantum neural networks, advanced quantum neural architectures exhibiting the properties of ultra-precise neural networks with enhanced sensitivity of machine-learning algorithms and new types of artificial synapses for transmitting information between neurons.

Figure 2.

Schematic of planar Impedance Resonance Sensor connection

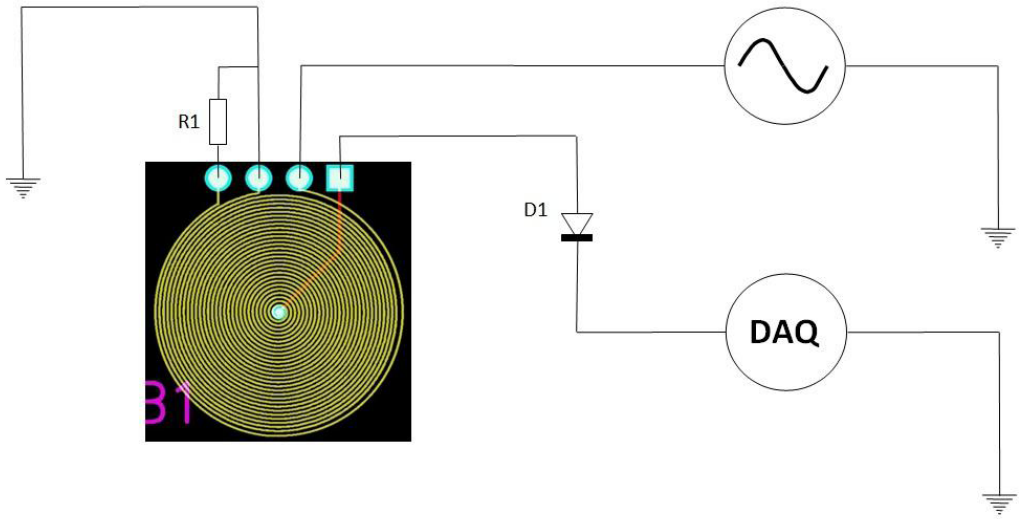

Excitation coil is connected to generator with frequency sweep. Resistance of R1 depends on output resistance of the generator and length of line between the sensor and the generator. If the length of line is less then ¼ of wavelength, the resistor can be omitted. Sensing coil is connected to Data Acquisition (DAQ). If operating frequency of the sensor is more than frequency capability of the DAQ, then the diode can solve that problem.
Both the generator and the DAQ are connected to personal computer and work under control of computer program. The program calculates resonant frequency and amplitude of the sensor and measure their changes caused by presence of analyte under test.

The following diagram presents the measurement results of the resonance levels in samples of distilled water and regular tap water obtained using the planar sensor.

All versions of the tests and measurements demonstrated that the planar sensor has the highest potential for further use, including in the final product – a capsule for autonomous monitoring of gastric acidity in a cow.

Moreover, the planar sensor provides the best conditions for all adjacent components of the capsule. This is largely due to the fact that, while offering higher sensitivity and measurement accuracy, the sensor has significantly smaller overall dimensions.

Therefore, the goal and objectives of this stage of the project are defined as a comparative preliminary verification of all acidity-measurement results using synthetic gastric juice with detailed analytical evaluation of the following parameters:

- sensitivity of the test system to changes in the electrical conductivity of gastric juice samples;
- sensitivity of the test system to changes in the temperature of gastric juice samples;

Figure 3.

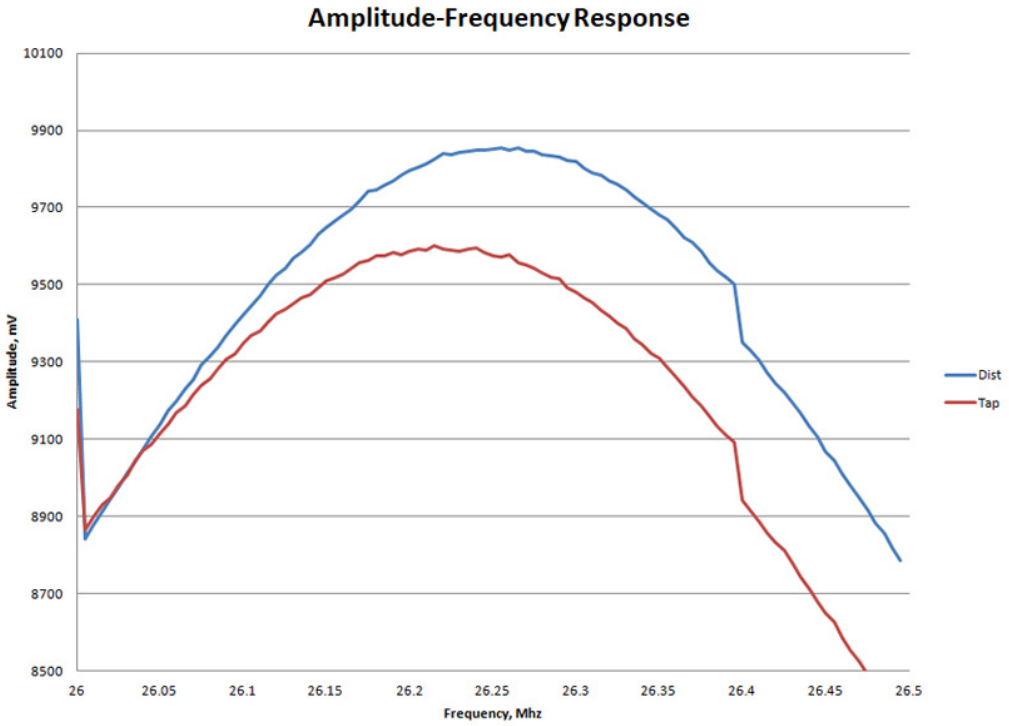

- sensitivity of the test system to changes in the chemical composition of gastric juice samples;
- sensitivity of the test system to changes in the acidity of gastric juice samples when additional hydrochloric acid is introduced into their chemical composition;
- sensitivity of the test system to the introduction of organic particles into gastric juice samples;
- repeatability of measurement results across all test variants;
- comparison of measurement results for each case with calibration of the control instrument and with subsequent measurements obtained from this control instrument, which simultaneously monitors:
  - the acidity level of the sample,
  - electrical conductivity of the sample,
  - temperature of the sample,
  - presence and calorimetric content of the sample;
- determination of maximum and minimum permissible deviations when measuring the parameters of gastric juice;
- determination of permissible maximum and minimum limits of acidity deviation when measuring the acidity of gastric juice.

This stage, by its nature, may be executed in at least two versions:

First version:

Carrying out all required measurements using the planar-solenoid sensor on gastric juice samples with different fillers and impurities, in accordance with the table of 22 variants that form the structure of the final report (this version is implemented if no additional funding is provided).

Second version:

Carrying out all required measurements using the planar-solenoid sensor on gastric juice samples for the purpose of calibrating measurement indicators and entering these results into the measurement program and model according to points 3 and 4 (this version is implemented if additional funding is obtained).

Given the superiority of the planar sensor (solenoid) over all other tested variants, a design proposal was made for two types of planar sensors:

– as a single-layer printed circuit board, and

– as a multilayer printed circuit board (with fully identical external dimensions, overall size, and the same number of connection points to the other instruments of the testing module).

The project developer proposed to create these PCB variants using a specialized computer program developed within the company.

According to the conditions set by the PCB manufacturer, the board contour must be square, and before final assembly, the contour may be transformed into a circular shape – or a rectangular pocket must be created in the body of the testing module.

This stage includes an extended cycle of all required calibration measurements and all necessary control measurements using at least two variants of the planar-solenoid sensor: a two-layer working design and a three-layer working design, tested on gastric juice samples with different chemical compositions and with various added particles of organic cow feed, for the purpose of calibrating measurement indicators and entering these results into the measurement program and model according to points 3 and 4.

One of the innovative objectives of the stage is to provide program-level functionality enabling the use of artificial intelligence and artificial neural networks during the processing and evaluation of sensor-based measurement data.

Products manufactured by leading companies specializing in artificial intelligence technologies are already functioning successfully: their inference processors, produced as interface cards, are capable of transmitting approximately one and a half thousand statements per second when solving linguistic tasks, with nearly zero probability of information loss. These companies have recently introduced an even more advanced processor.

Such technologies are in high demand – many individuals and organizations worldwide are attempting to teach computers to solve tasks not easily formalized by conventional methods, meaning tasks that are accessible to humans yet practically impossible to reduce to algorithms. Creating and training neural networks capable of collecting and processing numerous features – on the basis of which a computer can make decisions about the outcome of such non-formalizable tasks – requires sophisticated machine-level solutions.

Therefore, the development of such networks, which in some ways imitate the functioning of the human brain, became possible only with the advent of powerful graphics processors, although the underlying ideas date back to the cybernetics theories of the 1970 s. According to their developers, processors produced by the Israeli company surpass graphics processors in power, efficiency, and suitability for neural-network training.

Repeated Sensitivity Analysis Parameters

(The following repeated list is translated consistently and preserved exactly as in the original.)

- sensitivity of the test system to changes in the temperature of gastric juice samples;
- sensitivity of the test system to changes in the chemical composition of gastric juice samples;
- sensitivity of the test system to changes in the acidity of gastric juice samples when additional hydrochloric acid is introduced;
- sensitivity of the test system to the introduction of organic particles into gastric juice samples;
- repeatability of measurement results across all test variants;
- comparison of measurement results for each case with calibration of the control instrument and with subsequent measurements obtained from the instrument monitoring simultaneously:
- acidity level of the sample,
- electrical conductivity of the sample,
- temperature of the sample,
- presence and calorimetric content of the sample;
- determination of maximum and minimum permissible deviations when measuring gastric juice parameters;
- determination of maximum and minimum permissible deviations of acidity when measuring the acidity of gastric juice.

Use of Resonance Sensor Technology (RIST) in Investigating the Causes of Industrial Accidents

There is no need to prove the necessity of rapid on-site analysis of industrial accident causes. Such express-analysis can be conducted using a RIST sensor or a system of such sensors.

These sensors may be applied, for example, to investigate fractured structures for signs of material fatigue or violations of manufacturing technology or composition.

To enable such express-analysis, certain organizational measures must be undertaken – specifically, establishing a bank of "electronic signatures" (resonance responses of standard reference materials when measured using a RIST sensor or sensor system at a set of operating frequencies).

Once such a database is available, express-analysis consists of measuring the damaged material using a RIST sensor or sensor system and comparing the results with data from the electronic-signature database.

Naturally, before measurement, the surface of the investigated material must be smoothed or cleaned to ensure identical measurement conditions to those used for reference samples.

Of course, the availability of such express-analysis does not eliminate the need for further detailed laboratory investigations.

The express-analysis technology described above – applicable to both electrically conductive and non-conductive materials – can currently be implemented only using Resonance Sensor Technology (RIST).

Existing methods of non-destructive testing based on probing the material with an alternating electromagnetic field are limited in application.

These methods include:

Non-destructive testing based on analyzing the interaction of the electromagnetic field of the transducer with the electromagnetic field of eddy currents induced in the test object.

The method is used to inspect objects made of electrically conductive materials.

Eddy currents are induced in the object by a transducer in the form of an inductive coil supplied with alternating or pulsed current.

The receiving transducer (detector) may be the same or another coil. The transmitting and receiving coils can be placed on the same side or on opposite sides of the test object.

The intensity and distribution of eddy currents in the object depend on its dimensions, electrical and magnetic properties of the material, the presence of discontinuities or structural defects, the relative positioning of the transducer and the test object, and many other parameters.

List of References, Patent and Licensing Information:

1. United States Patent Application
US 2009/0245066 A1
October 1, 2009
Optical Data Carrier, and Method for Reading/Recording Data Therein
Abstract:
An optical data carrier is presented. The carrier includes at least one recording layer composed of a material whose fluorescent properties vary upon multi-photon absorption induced by an optical beam. The recording layer has a thickness that enables the formation of multiple recording planes. At least one non-recording layer is positioned on either the upper or lower surface of the recording layer and differs from it in fluorescent properties. The carrier also includes at least one reference layer with a reflective surface formed at the interface between the recording and non-recording layers.

2. United States Patent Application
US 2008/0285396 A1
November 20, 2008
Method and Apparatus of Formatting a Three-Dimensional Optical Information Carrier

Abstract:
A method is provided for formatting an optical information carrier by creating a sequence of formatting marks for subsequent addressing during data reading/recording. The method records these marks in an interleaved order within the carrier volume, reducing delays associated with writing adjacent marks and significantly decreasing overall formatting time.

3. United States Patent Application
US 2008/0182060 A1
July 31, 2008
Manufacturing of Multi-Plate for Improved Optical Storage
Abstract:
A new optical data carrier and production methods are disclosed. The carrier is characterized by plates with differing material concentrations, providing improved optical storage performance.

4. United States Patent Application
US 2006/0250934 A1
November 9, 2006
Three-Dimensional Optical Information Carrier and a Method of Manufacturing Thereof
Abstract:
A three-dimensional optical information carrier is described, comprising formatting marks located at the nodes of a three-dimensional lattice formed by intersections of equally angled radial planes, equidistant cylindrical spiral tracks, and virtual recording planes.

5. United States Patent Application
US 2007/0288947 A1
December 13, 2007
Swing Arm Optical Disc Drive
Abstract:
A swing-type optical disc drive is disclosed. The drive includes a rotating disc and a swing arm pivoted at one end, with its distal end connected to an encoder. The pivot point and distal point define the swing axis. An optical system is mounted on the arm such that its optical axis is parallel to the swing axis and lies within the same plane. A cam actuator induces swinging motion, positioning the plane so that it remains tangent to the disc's reading/recording track.

submitted 09.11.2025;
accepted for publication 23.11.2025;
published 30.12.2025

Contact: sedova.alina7810@gmail.com

The European Journal of Technical and Natural Sciences 2025, No 6
ISSN 2414-2352

PREMIER Publishing
ppublishing.org

DOI:10.29013/EJHSS-25-6-150-153

WATER TREATMENT IN A SMART HOME ECOSYSTEM

Vitiv Bohdan [1]

[1] Kiev National University everyday life and architecture Head of the development company

Cite: *Vitiv B. (2025). Water Treatment in a Smart Home Ecosystem. European Journal of Technical and Natural Sciences 2025, No 6.* https://doi.org/10.29013/EJHSS-25-6-150-153

Abstract

This article describes the design and economic characteristics of a modular water purification system built from standardized column segments. Each column can include up to three quickly interchangeable segments, each holding up to three disposable ion-exchange cartridges filled with OZOLA sorbent. The cartridges, based on mass-produced polymer fiber sleeves, ensure low consumable costs. The modular system is mounted on a dedicated platform equipped with pumps, mechanical self-cleaning filters, and measurement and control devices. A complete purification unit with a capacity of 1 m³/hour – comprising three three-segment columns, a pump, and a two-stage inlet and outlet filtration cascade – has a total cost of 35,000 USD. The modular design supports rapid maintenance, scalability, and cost-efficient operation.

Keywords: *Smart Home Ecosystem, Smart Home Infrastructure, Modular Purification Systems, Ion Exchange Purification Process, Application for Purification of Dried Biomass, Symmetrical Electrochemical Electrode Cell, Active Working Surface*

A comprehensive water supply system consists of 4 groups of interconnected modules, based on their principles and interactions:

Modules for input control and pre-treatment, including water storage tanks at the system's entry point and reserve water tanks for peak loads. Pre-treatment includes electrochemical disinfection, aeration, and oxygen concentration enhancement to full saturation levels. The input control modules operate on a contactless method based on the principles of electromagnetic resonance spectroscopy.

Local modules for electrochemical treatment, specific to each residential unit, including flow meter blocks at the entry point with a real-time monitoring section (contactless, operating on the principles of electromagnetic resonance spectroscopy).

Used water storage modules, which separate water into at least two categories: wastewater containing toilet residues and general wastewater.

Used water regeneration modules, with at least two sections: one for water containing fecal particles and one for other water. These modules include separation systems with vortex foam generators and final control systems that work without direct contact, operating on the principles of electromagnetic resonance spectroscopy.

In addition to the operational modules, the comprehensive water supply system includes a control and processor section with

elements of artificial intelligence and artificial neural networks, enabling remote control and real-time monitoring.

Figure 1. *The diagram presents the model of an electrochemical reactor with two electrode cells*

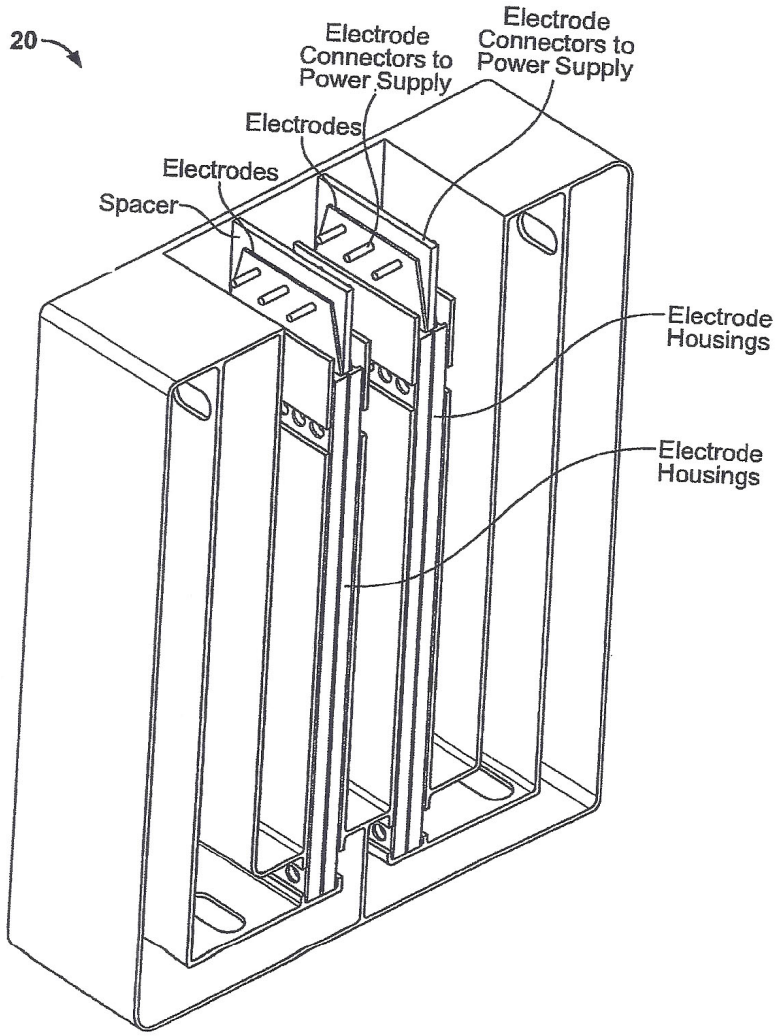

Water Purification from Radioactive Isotopes and Heavy Metals Using Biomass Obtained From Algae of the Type – Ozola

Ion Exchange Purification Process

As practice has shown, dried biomass of algae of the type – OZOLA has the ability to undergo ion exchange reactions for the absorption of heavy metal ions and radioactive isotope ions. To achieve purification, water must pass through the biomass volume, where, during the contact time, ion exchange occurs, and the biomass absorbs radioactive metal isotopes and associated heavy metal ions.

As tests and industrial operation of water purification systems at nuclear reactors have shown, the level of purification using algae of the type OZOLA can be reduced to residual concentrations of 0.000001 milligrams per liter, which exceeds the requirements of current environmental standards.

Design of the modular purification system

The modular purification system consists of one or more columns, each of which is made up of standardized segments. Typically, a column may have one, two, or three segments connected by a special element made of nylon and polyvinyl chloride, with a silicone rubber seal.

It takes no more than 1 minute to connect or disconnect a segment. Each segment accommodates up to three ion-exchange

cartridges. Each ion-exchange cartridge consists of a knitted sleeve made of fibers, into which OZOLA is poured.

The ion-exchange cartridges are single-use. The knitted sleeves made of polymer fibers are mass-produced, and their cost does not exceed 5 USD each.

The columns and necessary piping are assembled and mounted on a special stand, which includes pumps, mechanical self-cleaning filters, and measurement and control instruments.

The cost of one modular purification system, designed for a capacity of 1 cubic meter per hour, which includes three columns (each with three segments), a pump, a cascade of two mechanical filters at the inlet, and a cascade of two automatic mechanical filters at the outlet, is 35,000 USD.

The cost of OZOLA for one ion-exchange cartridge is 50 USD.

Principle of Operation of a Symmetrical Electrochemical Electrode Cell in Water Treatment in Hospitals

The liquid, and in the case of hospitals, water, under the influence of gravitational forces, enters the inlet of the device housing for water treatment according to the principle of communicating vessels. The flow of liquid or water, in a laminar regime, penetrates inside the electrode volume through a permeable contact.

The electrode and its entire internal volume are under the influence of a positive electrical potential due to the connection of the contact and the electrode to a positive electrical potential source. Depending on the water flow rate or the device's performance, the power of the power supply can vary.

For a device with a flow rate of 5 gallons per hour, the power supply can be 3 kilowatts, with three possible combinations of current and voltage:

- Current: 50 amperes, Voltage: 60 volts;
- Current: 30 amperes, Voltage: 100 volts;
- Current: 100 amperes, Voltage: 30 volts.

For a device with a flow rate of 150 gallons per hour, the power supply may be 10 kilowatts, achieved by forming an integrated power supply from at least 3 modules, each with 3 kilowatts, with combinations of current and voltage similar to those for the 5-gallon-per-hour device.

Under the influence of gravitational forces, the liquid or water rises through the electrode volume and, spreading across it, seeps through the membrane and contact into the internal volume of the second electrode, which is connected to the negative electrical potential source. The distance between the electrodes is determined only by the thickness of the membrane, and since this distance is a maximum of 0.8 mm, the efficiency of the electrode pair, the entire volume of which has an active electrochemical function, is very high.

From the moment the liquid or water enters the volume of the electrode connected to the negative electrical potential source, an active, rapid electrochemical processing of the materials contained in the liquid begins inside the electrode cell.

After passing through the cathode volume, the liquid exits the device housing through the outlet window.

Since significant areas of active working surface are involved in the electrochemical process, thanks to the three-dimensional structure of the electrodes, it is possible, in combination with an increase in current density, to achieve a significant enhancement in the effect of changing the properties of the materials contained in the water on the surface of carbon fibers that make up the volume of the electrodes

References

Emery, N., et al. (2022, May 26). *Apparatus and method for providing purified water*. United States Patent Application US 20220162108 A1.

Katragadda, R. R. (2022, May 19). *Ultra-high alkaline electrolyzed water generation system*. United States Patent Application US 20220153613 A1.

Slack, J., et al. (2022, April 28). *Systems, methods, and devices for cation-associating fuel cell components*. United States Patent Application US 20220131170 A1.
Jennings, J. W. (2022, April 28). *Integrated power system*. United States Patent Application US 20220127168 A1.
Friesen, G., et al. (2022, April 28). *Systems and methods for water treatment and storage*. United States Patent Application US 20220127172 A1.
Nakashima, N., et al. (2022, June 2). *Catalyst, electrode, membrane electrode assembly, and air battery*. United States Patent Application US 20220173457 A1.
bogdan.vstsv@gmail.com

submitted 04.11.2025;
accepted for publication 18.11.2025;
published 30.12.2025

Contact: bogdan.vstsv@gmail.com

The European Journal of Technical and Natural Sciences 2025, No 6
ISSN 2414-2352

PREMIER Publishing
ppublishing.org

DOI:10.29013/EJHSS-25-6-154-157

NEW SMART MANUFACTURING TECHNOLOGIES IN THE SMART HOME INFRASTRUCTURE

Vitiv Bohdan [1]

[1] Kiev National University everyday life and architecture Head of the development company

Cite: *Vitiv B. (2025). New Smart Manufacturing Technologies in the Smart Home Infrastructure. European Journal of Technical and Natural Sciences 2025, No 6.* https://doi.org/10.29013/EJHSS-25-6-154-157

Abstract

Ensuring environmental safety in smart manufacturing technologies in accordance with current standards is an essential prerequisite for establishing and maintaining such production processes. This requirement is particularly relevant within the infrastructure and ecosystem of the smart home.

Before the widespread adoption of environmental standards with stricter limits on the concentration of substances polluting industrial waste, it was generally sufficient to perform waste treatment before disposal at designated facilities.

Today, due to the sharp tightening of environmental regulations and the emergence of smart technologies-especially within the smart home infrastructure-such treatment has become extremely costly, significantly reducing the overall economic efficiency of any production process.

Keywords: *Waste utilization; regeneration of process waste; etching process solutions; recirculation of etching solutions and other process liquids; toxic exhaust gases; transformation of toxic exhaust gases into harmless liquid; smart home ecosystem; smart home infrastructure; technologies for extracting heavy metals from waste; continuous recirculation of process solutions to extend their operational production cycle*

The need to build interconnections within the smart home infrastructure has introduced entirely new concepts and approaches into the production cycle:

- search for methods of waste regeneration within the production process, enabling subsequent recirculation and repeated reuse;
- implementation of technologies for extracting heavy metals from waste to return them to the production cycle, ensuring continuous recirculation of process solutions and extending their operational lifespan.

For example, continuous extraction of copper from etching solutions used in automatic etching lines for printed circuit boards and thin-film microassemblies allows for the permanent recirculation of the etching solution, eliminates environmental contamination by toxic copper ions, and significantly increases the economic efficiency of the etching processes:

- modification of waste structure aimed at changing the properties of polluting materials and transforming these materials and their chemical compounds into harmless or significantly less harmful substances.

This process has become highly relevant in complex technologies, where the waste products are exhaust gases that cannot be purified to the desired level within acceptable cost limits, even with the most advanced filtration systems currently available.

The author proposes, within the framework of the smart home infrastructure, the consideration of a system designed for this purpose – an alternative solution for reducing the toxicity level of atmospheric emissions generated by a standard diesel generator used as a backup power source in the smart home.

Figure 1. *The figure shows a fragment of a three-dimensional model of a vortex generator as part of a system designed for the condensation of liquid from an exhaust gas stream*

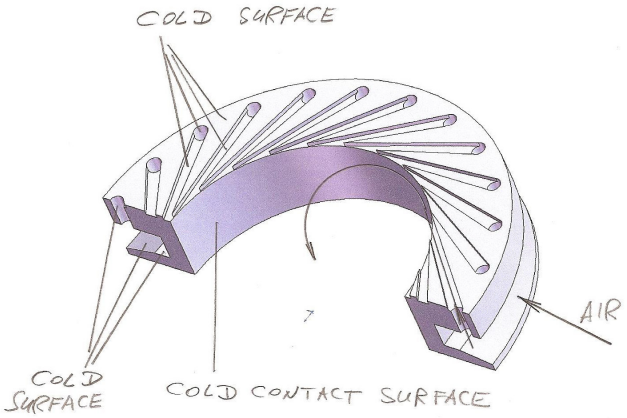

Figure 2. *The figure shows the connection diagram of vortex generators to a unit consisting of an inlet filter, a compressor, and a receiver*

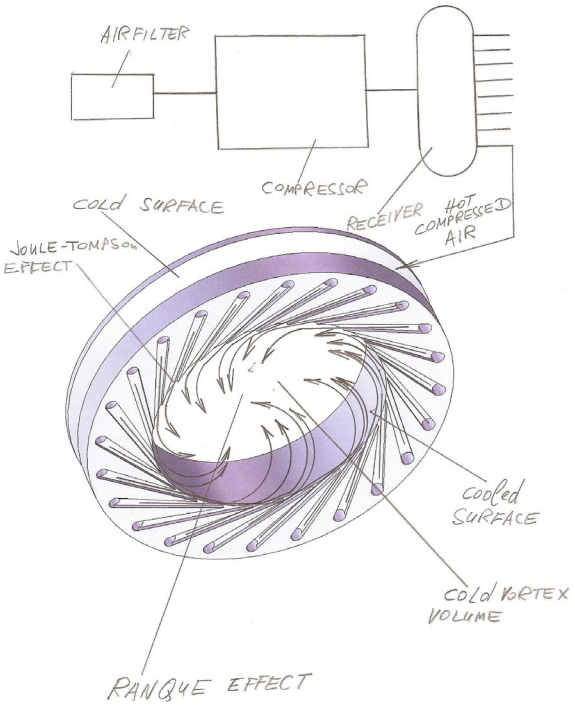

For further explanation, let us assume that the discussion concerns a liquid condensation system for the exhaust gases of a diesel generator operating on Diesel Fuel No. 5 (equivalent to purified and homogenized fuel oil).

First, it is necessary to establish the condition under which condensation occurs – namely, cooling the gas to its dew point.

The following figure presents the connection diagram and model of the vortex generator, which enables efficient cooling of compressed gas (air) used in the condensation process.

Due to the fact that the vortex generator initiates the formation of a vortex tube, a significant cooling effect arises within it, in accordance with the Joule-Thomson and Ranque–Hilsch laws. This cooling occurs both at the periphery of the vortex tube (at the outlet of the injection channels of the vortex generator) and at the center of the vortex tube-known as the Ranque-Hilsch effect.

This mechanism stimulates moisture (liquid) condensation and induces structural transformation of pollutants, thereby neutralizing their harmful effects. As a result, the technology becomes more efficient, less costly, and produces an unconventional (innovative) outcome.

Figure 3. *The figure shows a fragment of the vortex generator, revealing details of its operating principle. As can be seen from the model, during the first stage of condensation, all surfaces that come into contact with the hot compressed gas (air) are cold, and upon contact with the heated gas flow, they initiate the initial phase of condensation*

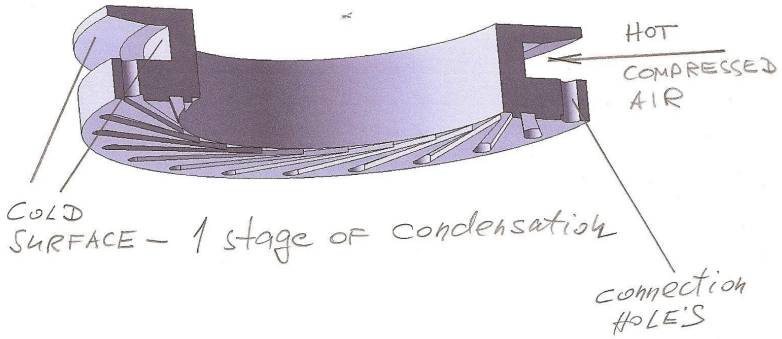

As demonstrated in the following models, the liquid condensed during the first stage flows into a collection chamber, from which it can be easily removed and disposed of without causing any harm to the environment or to the technological equipment.

Figure 4. *The figure shows the reverse side of the vortex generator, where the cold surfaces are indicated. These surfaces stimulate micro-condensation, which, in combination with the vortex tube effects, transitions into an intensive condensation phase*

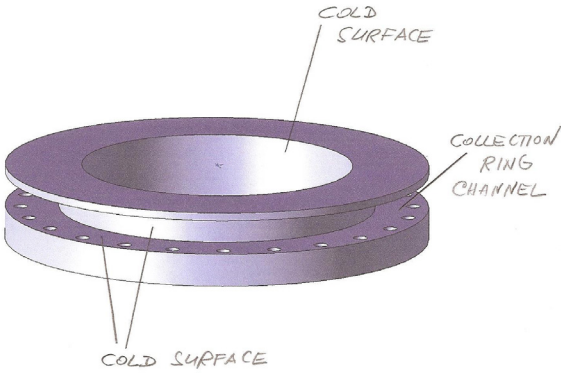

As can be seen from the model, the vortex generator-despite its seemingly simple design-contains several elements that can be considered innovative in many respects and embody a significant degree of fundamental novelty.

For the first time, the design of the vortex generator employs the principle of an accumulation channel-ring, into which the condensing gas is introduced. The gas then passes through transit openings into tangential channels, from which it is directed at high velocity into the central channel formed by the internal openings of all vortex generators in the system. Within this channel, a vortex tube is formed, consisting of spiral flows, the number of which corresponds to the number of tangential openings.

Such an aerodynamic structure of the vortex tube enables a significant intensification of heat exchange processes and ensures an active surface condensation process on all planes and surfaces with which the vortex spirals come into contact.

The same design and fundamental structural principles are applied both in stationary systems, such as those installed on diesel generators, and in mobile systems, which can be used on diesel engines of heavy-duty vehicles.

When discussing smart manufacturing technologies, it is important to emphasize the efficiency of the technical principle of condensing liquid from exhaust gases instead of performing deep exhaust gas purification.

This method provides significant advantages: in addition to purifying exhaust gases and drastically reducing their toxicity, it allows all pollutants to be bound within the condensed liquid, thereby reducing disposal costs by an order of magnitude.

Moreover, the energy consumption required for liquid condensation is much lower than that needed for deep filtration. Furthermore, the disposal of used filters is a far more complex and resource-intensive process than the safe disposal of condensed liquid.

Figure 5. *The figure illustrates the principle of interaction between the system components in cases where pure compressed air is used for additional cooling. This air moves through separate channels and does not mix with the exhaust gases at any stage of the cooling or condensation process*

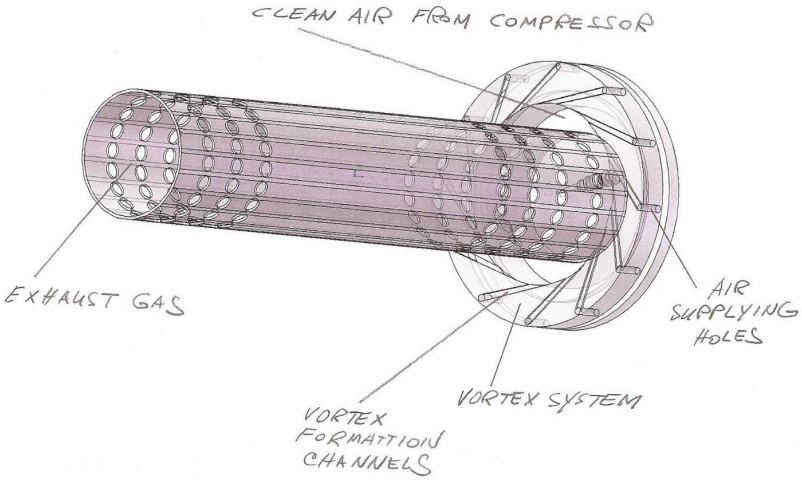

References

United States Patent Application US20110056457 A1. *System and Apparatus for Condensation of Liquid from Gas and Method of Collection of Liquid.* – March 10, 2011.
United States Patent Application US20110126462 A1. *Device for Producing a Gaseous Fuel Composite and System of Production Thereof.* – June 2, 2011.
United States Patent Application US20170184055 A9. *Device for Producing a Gaseous Fuel Composite and System of Production Thereof.* – June 29, 2017.
United States Patent Application US20110048353 A1. *Engine with Integrated Mixing Technology.* – March 3, 2011.
United States Patent Application US20120103306 A1. *Engine with Integrated Mixing Technology.* – May 3, 2012.

submitted 03.11.2025;
accepted for publication 17.11.2025;
published 30.12.2025

Contact: bogdan.vstsv@gmail.com

The European Journal of Technical and Natural Sciences 2025, No 6
ISSN 2414-2352

PREMIER Publishing
ppublishing.org

DOI:10.29013/EJHSS-25-6-158-162

FORECASTING STATE MACROECONOMIC INDICATORS WITH ARTIFICIAL INTELLIGENCE TOOLS

Zurab Tuskia [1]

[1] Georgian Technical University

Cite: *Tuskia, Z. (2023). Forecasting State Macroeconomic Indicators with Artificial Intelligence Tools. European Journal of Technical and Natural Sciences 2025, No 6.* https://doi.org/10.29013/EJHSS-25-6-158-162

Abstract

In an era of rapid advances in artificial intelligence (AI), innovation increasingly shapes many domains of human activity. Public administration is no exception: across the world, governments are adopting AI for forecasting and planning-from the Baltic states' e-Governance platforms to Southeast Asia's "smart state" initiatives (e.g., Singapore) and national AI programs in the Middle East. The shared goal is to raise the quality of forecasts and to make planning, crisis management, and economic policy more responsive to change.

This paper presents a practical, step-by-step methodology for producing targeted, one-year forecasts of state macroeconomic indicators. The approach combines time-series analysis and neural networks with deep learning (BiLSTM + Attention), using efficient, iterative procedures that systematically increase forecast accuracy.

Kywords: *Time Series; Deep Learning (BiLSTM-Attention); ETS; ARIMA; Deep Learning*

Methodology

Data – We use primary data from Georgia's National Statistics Office covering 17 key macroeconomic indicators. For this study, we selected eight: GDP, GDP per capita, imports, state revenues, broad money (M3), average USD/GEL exchange rate, number of employees, and agricultural production output.

$$x_f^{\min} = \min_t x_{t,f}, \quad x_f^{\max} = \max_t x_{t,f},$$

$$R_f = \max(x_f^{\max} - x_f^{\min}, \varepsilon)$$

$$\tilde{x}_{t,f} = \frac{x_{t,f} - x_f^{\min}}{R_f} \in [0,1],$$

The sample spans 2008–2023 with quarterly observations (Q1–Q4). The task was to produce a 2024 forecast achieving an average accuracy above 90% for the chosen indicators, F=Ffull={All quarters 2008–2023}. All 2008–2023 quarterly data were preprocessed using Min–Max normalization, then split into TRAIN (2008–2022) and TARGET (2023). We formed sliding windows and targets for a four-quarter horizon: the previous four quarters as inputs and the subsequent four as targets (for each admissible index within TRAIN).

$$X_i = [\tilde{z}_i, \tilde{z}_{i+1}, ..., \tilde{z}_{i+W-1}] \in \mathbb{R}^{W \times F}.$$

First pass (global model) – We remove a strong stationary component via a naïve "hold-last" baseline and train a global, multi-output model on the residuals. We then construct a *teacher* for future quarters and run quarter-level models with warm starts. In brief: Full matrix, normalized by Min–Max-(2008–2023). Window width W, last index $t = i + W - 1$

$$\hat{Z} \in [0,1]^{T \times P}, \quad \text{naive}_{i,h,k} = \tilde{z}_{i+W-1,\,p_k}.$$

$$\text{resid}_{i,h,k} = Y_i[h,k] - \text{naive}_{i,h,k}$$

Baseline & residuals – The "hold-last" (naive) forecast serves as a baseline; the model learns to predict residuals. p_k – **colum index in** matrix $\hat{Z}$.

Deep model (BiLSTM + Attention, multi-output)

$$e_t = V^T \tanh(\mathrm{W}\, h_t), \quad \alpha_t = \frac{\exp(e_t)}{\sum_{j=1}^{W} \exp(e_j)},$$

$$c = \sum_{t=1}^{W} \alpha_t h_t.$$

Encoder: BiLSTM(64) → Dropout(0.2) → BiLSTM(32, return_sequences) Head: Dense(64, ReLU) → Dropout(0.2) → Dense → reshape (multi-horizon outputs). Loss: horizon-weighted MAE.

$$L = \frac{1}{N} \sum_i \frac{1}{HT} \sum_{h=0}^{H-1} \sum_{k=1}^{T} w_h \left| \widehat{\text{resid}}_{i,h,k} - \text{resid}_{i,h,k} \right|,$$

$$\sum_h w_h = 1.$$

Ensembling-Train multiple replicas with different random seeds and average the predictions.

$$\widehat{\text{resid}}^{(\text{ens})}_{h,k} = \frac{1}{M} \sum_{m=1}^{M} \widehat{\text{resid}}^{(m)}_{i,h,k}.$$

$$\widehat{\text{resid}}^{\text{future}}_{h,k} = \tilde{z}_{\text{last}}, p_k$$

Seasonal profile & teacher (grid-search)- We assume a seasonal profile based on average quarterly values on TRAIN; combine it with the residual model to create a stable *teacher* for the TARGET quarters.

Composition – Choose among candidate compositions by minimizing MAE on TRAIN windows. **Warm-start quarterly heads –** Transfer the encoder to compact scalar heads (per target and quarter) and calibrate only the output bias to align with the teacher at initialization.

$$Y^{\text{tech}}_{h,k} = \gamma \left(\text{native}^{\text{future}}_{h,k} + \alpha \cdot \widehat{\text{resid}}^{(\text{ens})}_{h,k} \right) +$$

$$+ (1-\gamma) S[h,k],$$

$$\hat{y}_{k,q}(X_{\text{future}}) = \hat{Y}^{\text{teach}}_{q,k}.$$

The global model learns residual structure; blending with the seasonal component stabilizes the teacher; quarterly heads start from a well-calibrated bias.

Figure 1. *DL Model (BiLSTM + Attention)*

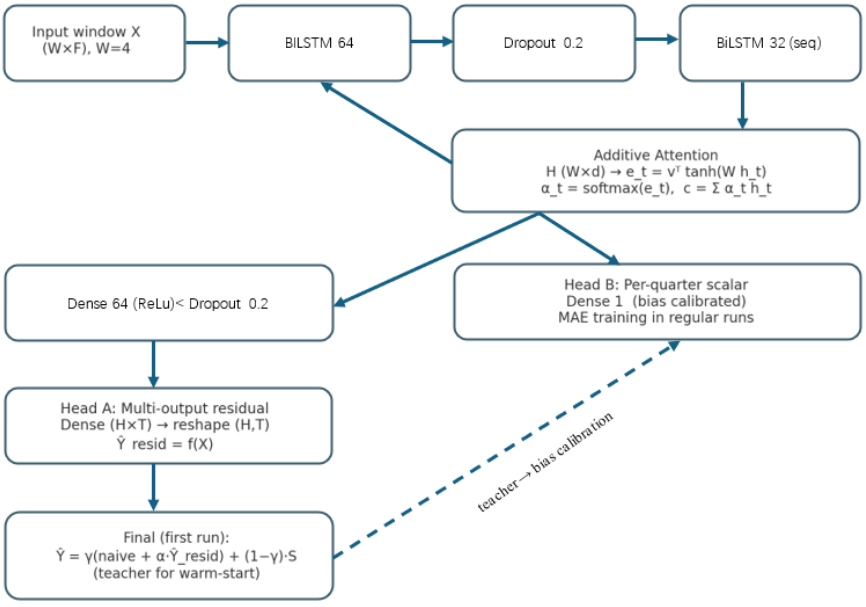

Regular reruns with feedback and a nudge-controller – For each (target, quarter) pair:

- If feedback is **GOOD**, the quarter's head is *locked* and excluded from further training.
- If **BADUP/BADDOWN**, perform local adaptation with controlled step size and a trust region.

$$\text{acc} = 1 - \left|\hat{y} - y\right|.$$

Feedback classification – Threshold θ is set to 0.99 (i.e., 99%).

$$\text{GOOD} \Leftrightarrow \text{acc} \geq \theta, \quad \text{BADUP} \Leftrightarrow \hat{y} < y,$$

$$\text{BADDOWN} \Leftrightarrow \hat{y} > y,$$

Local reinforcement- For BADUP/BADDOWN, increase the weight of the last TRAIN window and perform a small, bounded update.

$$y^{\star}_{last} = \begin{cases} y_{last}(1+\delta), & \text{BADUP} \\ y_{last}(1-\delta), & \text{BADDOWN} \end{cases},$$

$$\delta = \text{FEEDBACK\_SHIFT},$$

Bounded nudge without TARGET leakage – Use an adaptive base push; a seasonal *anchor*; a minimal step; and a trust corridor around the planned target. In the late *POLISH* phase, updates are one-sided (BADUP only upward; BADDOWN only downward).

$$\text{BADUP}: p_{\text{nudget}} = p + k(1-p),$$

$$\text{BADDOWN}: p_{\text{nudged}} = p - kp,$$

$$p_{\text{anch}} = (1-\lambda)p_{\text{nudged}} + \lambda S_q, \quad \lambda \in [0,1].$$

Using the controlled sequence of steps "push → anchor → minimal step → confidence corridor," and **without** training on the current TARGET year's data (2023 in this case), we achieved **GOOD** values of the feedback metric for all quarters and saved the stable models into a single model file. Using the stored quarterly weights ("GOOD-locks"), we built the forecast for the next year (2024 in this case) in **RAW** units. We formed X_{future} from the last $W = 4$ quarters of the full history (TRAIN + TARGET). For each target k and quarter q, we loaded the weights and computed the normalized forecast $\hat{y}^{\text{norm}}_{(k,q)}$. Transition to the RAW space: $\hat{y}^{\text{raw}}_{(k,q)} = \hat{y}^{\text{norm}}_{(k,q)} \cdot R_{p_k} + x^{\min}_{p_k}$, where R_{p_k} and $x^{\min}_{p_k}$ are the min–max normalization parameters for the corresponding target column p_k.

Results

With the proposed methodology, the **average forecast accuracy for 2024 reached 93.22%**. To benchmark, we uploaded the same macro data to emulated models on several platforms (ChatGPT, Amazon AWS, Microsoft Azure) to obtain their 2024 forecasts. We then compared quarterly accuracies per indicator and the overall average:

Feature	Year	Quarter	Forecast Accuracy GPT CHAT %	Forecast Accuracy AMAZON AWS %	Forecast Accuracy MS AZURE %	Forecast Accuracy Our Project %
GDP (MILLION $)	2024	I	73.61	92.01	92.01	97.88
GDP (MILLION $)	2024	II	71.27	91.37	91.37	97.37
GDP PER CAPITA $	2024	IV	70.15	89.85	89.85	90.57
IMPORTS (MILLION $)	2024	I	82.23	98.58	98.58	92.02
IMPORTS (MILLION $)	2024	II	73.37	92.21	92.21	97.44
IMPORTS (MILLION $)	2024	III	73.09	92.15	92.15	95.57

Feature	Year	Quarter	Forecast Accuracy GPT CHAT %	Forecast Accuracy AMAZON AWS %	Forecast Accuracy MS AZURE %	Forecast Accuracy Our Project %
IMPORTS (MILLION $)	2024	IV	71.70	84.23	84.23	85.33
STATE REVENUES (MILLION $)	2024	I	60.12	82.50	82.50	84.32
STATE REVENUES (MILLION $)	2024	II	63.36	92.03	92.03	97.36
STATE REVENUES (MILLION $)	2024	III	66.22	88.55	88.55	92.45
BROAD MONEY M3 (MILLION $)	2024	IV	72.68	89.64	89.64	90.56
AVERAGE EXCHANGE RATE USD-$	2024	I	82.75	95.88	97.81	92.25
AVERAGE EXCHANGE RATE USD-$	2024	IV	84.19	97.46	98.06	98.99
NUMBER OF EMPLOYEES	2024	I	96.18	95.56	95.56	98.21
NUMBER OF EMPLOYEES	2024	II	96.98	95.82	95.82	96.85
NUMBER OF EMPLOYEES	2024	III	98.17	96.14	96.14	97.10
NUMBER OF EMPLOYEES	2024	IV	99.48	96.36	96.36	96.72
AGRICULTURAL PRODUCTION OUTPUT (MILLION $)	2024	I	86.54	95.90	95.89	89.29
AGRICULTURAL PRODUCTION OUTPUT (MILLION $)	2024	IV	83.96	90.28	90.28	95.45
Average Forecast Accuracy			77.83	91.94	92.04	93.22

This methodology blends several practices known from classical modeling, but using them as a unified ensemble yields distinctive advantages:

1. ***Two-stage architecture ("global encoder → quarterly heads").***

Rather than training "one big network," we train a single multi-task (BiLSTM + Attention) model on residuals, transfer its encoder into small quarterly heads (per target and quarter), and then perform calibration with reinforcement-style updates.

2. ***Controlled, monotonic correction without data leakage.***

In reruns we do *not* feed TARGET-year data to the network. Instead, we adjust only the output bias of the quarterly head with small, controlled steps toward the planned point. Modes (TURBO/AGGR/POLISH) adapt automatically based on the shortfall to the GOOD threshold; the nudge intensity and trust interval width are adjusted accordingly. Once a (target, quarter) crosses the threshold, we lock that head, preventing later degradation.

3. ***Micro-models ("quarter × target") instead of a monolithic head.***

Quarters behave differently in practice. Splitting heads by quarter yields natural localization and faster convergence to accurate forecasts.

Conclusion

In today's environment-where economic stability and well-targeted investment decisions are prerequisites for national development-forecasting plays a crucial role. Using macroeconomic data from 2008–2023, we set out to build a model capable of rationally predicting 2024 indicators (we chose 2024 specifically to allow straightforward accuracy verification). The challenge required not only

capturing historical trends but also uncovering the internal logic and interrelations among those trends. Our streamlined, practical pipeline couples time-series analysis with a neural baseline and then refines it through carefully controlled deep-learning adjustments, reaching 90–95% accuracy. The resulting next-year forecasts achieved **93.22%** average accuracy in this study-useful for planning and for optimizing the management of public resources.

References

Hyndman & Athanasopoulos (2021) “Forecasting: Principles and Practice (FPP3)”.
Defu Cao, Yixiang Zheng, Parisa Hassanzadeh… (2023) “Large Scale Financial Time Series Forecasting with Multi-faceted Model”.
– Bahdanau, Cho, Bengio (2014) “Neural Machine Translation by Jointly Learning to Align and Translate”.
Hyndman, R. J., Koehler, A. B., Ord, J. K., & Snyder, R. D. (2002) A state space framework for automatic forecasting using exponential smoothing.
Box, G. E. P., Jenkins, G. M., Reinsel, G. C., & Ljung, G. M. (2015) Time Series Analysis: Forecasting and Control.

submitted 15.11.2025;
accepted for publication 29.11.2025;
published 30.12.2025

Contact: zurabtuskia@gmail.com

Contents

Section 6. Medical science

Section 7. Physics

Section 8. Technical sciences in general